

REPORT DOCUMENTATION PAGE

AFRL-SR-BL-TR-98-

0786

Public reporting burden for this collection of information is estimated to average 1 hour per response, including the time for and maintaining the data needed, and completing and reviewing the collection of information. Send comments regarding information, including suggestions for reducing this burden, to Washington Headquarters Services, Directorate for information, including suggestions for reducing this burden, to Washington Headquarters Services, Directorate for information 1204, Arlington, VA 22202-4302, and to the Office of management and Budget, Paperwork Reduction Project (0704-0188) 1

1. AGENCY USE ONLY (Leave Blank)		2. REPORT DATE December, 1994	3. REPORT TYF. Final
4. TITLE AND SUBTITLE USAF Summer Research Program - 1994 High School Apprenticeship Program Final Reports, Volume 15B, Wright Laboratory			5. FUNDING NUMBERS
6. AUTHORS Gary Moore			
7. PERFORMING ORGANIZATION NAME(S) AND ADDRESS(ES) Research and Development Labs, Culver City, CA			8. PERFORMING ORGANIZATION REPORT NUMBER
9. SPONSORING/MONITORING AGENCY NAME(S) AND ADDRESS(ES) AFOSR/NI 4040 Fairfax Dr, Suite 500 Arlington, VA 22203-1613			10. SPONSORING/MONITORING AGENCY REPORT NUMBER
11. SUPPLEMENTARY NOTES Contract Number: F49620-93-C-0063			
12a. DISTRIBUTION AVAILABILITY STATEMENT Approved for Public Release			12b. DISTRIBUTION CODE
13. ABSTRACT (Maximum 200 words) The United States Air Force High School Apprenticeship Program's (USAF- HSAP) purpose is to place outstanding high school students whose interests are in the areas of mathematics, engineering, and science to work in a laboratory environment. The students selected to participate in the program work in an Air Force Laboratory for a duration of 8 weeks during their summer vacation.			
14. SUBJECT TERMS AIR FORCE HIGH SCHOOL APPRENTICESHIP PROGRAM, APPRENTICEDHIP, AIR FORCE RESEARCH, AIR FORCE, ENGINEERING, LABORATORIES, REPORTS, SCHOOL, STUDENT, SUMMER, UNIVERSITIES			15. NUMBER OF PAGES
			16. PRICE CODE
17. SECURITY CLASSIFICATION OF REPORT Unclassified	18. SECURITY CLASSIFICATION OF THIS PAGE Unclassified	19. SECURITY CLASSIFICATION OF ABSTRACT Unclassified	20. LIMITATION OF ABSTRACT UL

UNITED STATES AIR FORCE
SUMMER RESEARCH PROGRAM -- 1994
HIGH SCHOOL APPRENTICESHIP PROGRAM FINAL REPORTS

VOLUME 15B
WRIGHT LABORATORY

RESEARCH & DEVELOPMENT LABORATORIES
5800 Uplander Way
Culver City, CA 90230-6608

Program Director, RDL
Gary Moore

Program Manager, AFOSR
Major David Hart

Program Manager, RDL
Scott Licoscas

Program Administrator, RDL
Gwendolyn Smith

Program Administrator, RDL
Johnetta Thompson

Submitted to:

AIR FORCE OFFICE OF SCIENTIFIC RESEARCH

Bolling Air Force Base

Washington, D.C.

December 1994

DTIC QUALITY INSPECTED 4

19981204 029

PREFACE

Reports in this volume are numbered consecutively beginning with number 1. Each report is paginated with the report number followed by consecutive page numbers, e.g., 1-1, 1-2, 1-3; 2-1, 2-2, 2-3.

Due to its length, Volume 15 is bound in two parts, 15A and 15B. Volume 15A contains #1-26. Volume 15B contains reports #27-52. The Table of Contents for Volume 15 is included in both parts.

This document is one of a set of 16 volumes describing the 1994 AFOSR Summer Research Program. The following volumes comprise the set:

<u>VOLUME</u>	<u>TITLE</u>
1	Program Management Report
	<i>Summer Faculty Research Program (SFRP) Reports</i>
2A & 2B	Armstrong Laboratory
3A & 3B	Phillips Laboratory
4	Rome Laboratory
5A & 5B	Wright Laboratory
6	Arnold Engineering Development Center, Frank J. Seiler Research Laboratory, and Wilford Hall Medical Center
	<i>Graduate Student Research Program (GSRP) Reports</i>
7	Armstrong Laboratory
8	Phillips Laboratory
9	Rome Laboratory
10	Wright Laboratory
11	Arnold Engineering Development Center, Frank J. Seiler Research Laboratory, and Wilford Hall Medical Center
	<i>High School Apprenticeship Program (HSAP) Reports</i>
12A & 12B	Armstrong Laboratory
13	Phillips Laboratory
14	Rome Laboratory
15A&15B	Wright Laboratory
16	Arnold Engineering Development Center

HSAP FINAL REPORT TABLE OF CONTENTS

i-xiv

1. INTRODUCTION	1
2. PARTICIPATION IN THE SUMMER RESEARCH PROGRAM	2
3. RECRUITING AND SELECTION	3
4. SITE VISITS	4
5. HBCU/MI PARTICIPATION	4
6. SRP FUNDING SOURCES	5
7. COMPENSATION FOR PARTICIPANTS	5
8. CONTENTS OF THE 1994 REPORT	6

APPENDICIES:

A. PROGRAM STATISTICAL SUMMARY	A-1
B. SRP EVALUATION RESPONSES	B-1

HSAP FINAL REPORTS

SRP Final Report Table of Contents

Author	University/Institution Report Title	Armstrong Laboratory Directorate	Vol-Page
Eugenia D Baker	A. Crawford Mosley High School , Lynn Haven , FL Reinventory of the Technical Information Center of	AL/EQP	12 - 1
Sara E Berty	Carroll High School , Dayton , OH The Biological Effects of an ADN on Hepatocytes:	AL/OET	12 - 2
Michael J Bruggeman	Archbishop Alter High School , Kettering , OH Cardiac Measures of Pilot Workload: The Wright-Pa	AL/CFHP	12 - 3
Heather E Castellano	East Central High School , San Antonio , TX The Directive Role of Statistics in Medicine	AL/AOCR	12 - 4
Christopher J Chadwell	James Madison High School , San antonio , TX A Pascal Program for a PC-Based Data Acquisition S	AL/CFT	12 - 5
Eleanore J Chuang	Beavercreek High School , Beavercreek , OH Evaluation of Head Scans From the HGU-53/P Helmet	AL/CFHD	12 - 6
Clayton J Ciomperlik	East Central High School , San Antonio , TX Concentrations of Radionuclides	AL/OEB	12 - 7
Kara L Ciomperlik	East Central High School , San Antonio , TX Analysis of Various Samples for the Presence of Me	AL/OEA	12 - 8
Joseph A Croswell	A Crawford Mosley High , Lynn Haven , FL Network Applications	AL/EQ	12 - 9
Timothy O Dickson	Rutherford High School , Springfield , FL Study, Design, and Modification of the Dynamic Con	AL/EQP	12 - 10
Maureen D Finke	New Braunfels High School , New Braunfels , TX An Optimization Study on a 99% Purity Molecular Si	AL/CFTS	12 - 11

SRP Final Report Table of Contents

Author	University/Institution Report Title	Armstrong Laboratory Directorate	Vol-Page
Angela D Foth	A. Crawford Mosley High School , Lynn Haven , FL Physical and Chemical Characterization of Columbus	AL/EQC	12 - 12
Andrea L Freeman	Judson High School , Converse , TX A Study of the Mortality Rate of the Test Organisms	AL/OEM	12 - 13
Jeffrey P Gavornik	Roosevelt High School , San Antonio , TX A Study on the Effects of Chronic Intermittent Exposure	AL/CFT	12 - 14
Mark W Giles	Bay High School , Panama City , FL Environmental Restoration Technologies Research	AL/EQW	12 - 15
Michael L Gunzburger	Kettering High School , Kettering , OH Programming Filtering Routines in the C Program	AL/CFBV	12 - 16
Brian C Harmon	A. Crawford Mosley High , Lynn Haven , FL A Study of the Nitrobenzene Reductase and its Reaction	AL/EQC	12 - 17
Wesley R Hunt	James Madison High School , San Antonio , TX The Knowledge Survey and Assessment (KSA) Project	AL/HRM	12 - 18
Karen M Johnson	James Madison High School , San Antonio , TX Hyperbaric Medicine	AL/AOH	12 - 19
Damian A Kemper	Winston Churchill High School , San Antonio , TX Perception of the Spoken Stimuli in the S.C.O.N.E.	AL/AOCF	12 - 20
Nathan R Large	Northwestern High School , Springfield , OH A Paradigm for Studying Mutually Advantageous Trade	AL/CFHD	12 - 21
Trang D Le	Brackenridge High School , San Antonio , TX The Spacecraft Charging and Discharging Problem	AL/OEM	12 - 22

SRP Final Report Table of Contents

Author	University/Institution Report Title	Armstrong Laboratory Directorate	Vol-Page
Adriana Y Lopez	East Central High School , San Antonio , TX An Analysis of Oil/Grease in Water and Soil	AL/OEA	12 - 23
Steve J Mattingley	Mosley High School , Lynn Haven , FL A Study of the Practicality of an Automated Airfie	AL/EQ	12 - 24
Elizabeth A McKinley	Tecumseh High School , New Carlisle , OH Digitizing of Technical Illustrations	AL/HRG	12 - 25
David P McManamon	Carroll High School , Dayton , OH REPORT NOT AVAILABLE AT PRESS TIME	AL/CFBA	12 - 26
Amanda L Olson	Rutherford High School , Panama City , FL Physical and Chemical Characterization of Columbus	AL/EQC	12 - 27
Christopher S Protz	A. Crawford Mosley High School , Lynn Haven , FL Network Considerations	AL/EQP	12 - 28
Sarah E Schanding	East Central High School , San Antonio , TX REPORT NOT AVAILABLE AT PRESS TIME	AL/CFTF	12 - 29
Rebecca J Scheel	James Madison High School , San Antonio , TX The Learning of Hyperbaric Medicine	AL/AOH	12 - 30
Tina K Schuster	Southwest High School , San Antonio , TX The Determination of Lead in Paint Chips	AL/OEA	12 - 31
Kirk M Sexton	Northside Hlth Careers HS , San Antonio , TX Predicting Performance in Real-Time Tasks	AL/HRM	12 - 32
Ryan Q Simon	Beavercreek High School , Beavercreek , OH The Combustion of Advanced Composite Materials	AL/OET	12 - 33

SRP Final Report Table of Contents

Author	University/Institution Report Title	Armstrong Laboratory Directorate	Vol-Page
Kenneth B Spears	Highlands High School , San Antonio , TX Molecular Modeling and Editing of Dalm Halides	AL/OER	12 - 34
Courtney A Sprague	Southwest High School , San Antonio , TX A Study of the Visual Tests Performed on Air Force	AL/AOCO	12 - 35
Jonathan S Vinarskai	Castle Hls First Baptist Schoo , San Antonio , TX Which is a Better Sleep Scoring Device for Operati	AL/CFTO	12 - 36
Zac J Westbrook	Somerset High School , Somerset , TX The Effectiveness of Hyperbaric Oxygen Therapy in	AL/AOH	12 - 37
Thomas E Whalen	Carroll High School , Dayton , OH Utility of Internet Based Information Systems in A	AL/CFBE	12 - 38

SRP Final Report Table of Contents

Author	University/Institution Report Title	Phillips Laboratory Directorate	Vol-Page
Christopher D Amos	Desert High School , Edwards , CA Thermal Analysis of HADN and S-HAN-5	PL/RKAP	13- 1
Rhianna S DaSalla	West Mesa High School , Albuquerque , NM Reflected Laser Communication Systems	PL/SXO	13- 2
Alexander E Duff	La Cueva High School , Albuquerque , NM Construction and Testing of a Dual Photodiode Rece	PL/LIMI	13- 3
Bridget C Engelhardt	Paraclete High School , Lancaster , CA A Study of Liner Compositions for Solution Propell	PL/RKAP	13- 4
Daniel C Ghiglia	Sandia Prep High School , Albuquerque , NM The Construction of a Model Solar Powered Car	PL/VTPC	13- 5
Tad Goetz	Sandia Preparatory High School , Albuquerque , NM Theoretical Study of Radiation and Heating Effects	PL/VTET	13- 6
DeLesley S Hutchins	Albuquerque High School , Albuquerque , NM Programming Data Classification Procedures, Time M	PL/LIAE	13- 7
Caroline H Lee	Lexington Sr. High School , Lexington , MA The Spacecraft Charging and Discharging Problem	PL/WSSI	13- 8
David P Mirabal	West Mesa High School , Albuquerque , NM High Altitude Ballon Capabilities and Options	PL/SXO	13- 9
Nicholas P Mitchell	Belen High School , Belen , NM Development of the PICLL (Particle in Cell Linked	PL/WSP	13- 10
Julie A Niemeyer	Valley High School , Albuquerque , NM Nickel-Cadmium Batteries	PL/VTSI	13- 11

SRP Final Report Table of Contents

Author	University/Institution Report Title	Phillips Laboratory Directorate	Vol-Page
Krista M Nuttall	La Cueva High School , Albuquerque , NM The Characterization of an Atmospheric Turbulence	PL/LIMI	13 - 12
Matthew J Pepper	St. Pius X High School , Albuquerque , NM The PSPH Computer Code an the WSCD Reference Datab	PL/WSCE	13 - 13
Jeremy G Pepper	St. Pius X High School , Albuquerque , NM A Study of the CIV Phenomenon and the Secondary an	PL/WSCD	13 - 14
Paul A Rodriguez	Santa Fe High School , Santa Fe , NM Using Image Processing Programs to Aid Space to Gr	PL/LIMI	13 - 15
Alok J Saldanha	Philips Academy , Andover , MA REPORT NOT AVAILABLE AT PRESS TIME	PL/GPSG	13 - 16
David M Schindler	Los Lunas High School , Los Lunas , NM Projects in the Nonlinear Optics Branch of the Phi	PL/LIDN	13 - 17
Min Shao	Arlington High School , Arlington , MA A Study of the Ionsphere	PL/GPIA	13 - 18
Raul Torrez	Sandia Preparatory School , Albuquerque , NM A Study of Infrared Devices and RADIometric Measur	PL/VTRP	13 - 19
Christian G Warden	Rosamond High School , Rosamond , CA Introduction to Electric Propulsion	PL/RKCO	13 - 20

SRP Final Report Table of Contents

Author	University/Institution Report Title	Rome Laboratory Directorate	Vol-Page
Thomas J Angell	Camden Central High , Camden , NY A Comparison Between Relational Databases and Obj	RL/C3AA	14 - 1
Jonathan C Bakert	Sauquoit Valley Central High S , Sauquoit , NY C Programming for Digital Analysis and the Unix Op	RL/ERDA	14 - 2
Craig M Belusar	Oneida High School , Oneida , NY A Study in the Development of Specialized Software	RL/IRAP	14 - 3
Shawn H Bisgrove	Rome Free Academy , Rome , NY Arc-Second Raster Chart/Map Digitized Raster Grap	RL/IRRP	14 - 4
Stacy R Fitzsimmons	Vernon Verona Sherrill Cen Sch , Verona , NY An Implementation of the Multiple Signal Classific	RL/IRAA	14 - 5
David W Gurecki	Rome Catholic High School , Rome , NY The Information Superhighway: Still Under Constr	RL/C3B	14 - 6
Eric J Hayduk	Rome Catholic High School , Rome , NY Developing a Software Environment for a High Perfo	RL/OCTS	14 - 7
Justin D O'Brien	Bishop Guertin High School , Nashua , NH REPORT NOT AVAILABLE AT PRESS TIME	RL/ERMH	14 - 8
Michael J Panara	Rome Free Academy , Rome , NY Multi-Media-Creation and Uses (Using the MacroMind	RL/C3CA	14 - 9
Anne E Pletl	Notre Dame , Utica , NY Study of Global Hypermedia Networks	RL/C3BC	14 - 10
Richard A Schneible	Trivium School , Lancaster , MA Developing a Software Environment for a High Perfo	RL/OCTS	14 - 11

SRP Final Report Table of Contents

Author	University/Institution Report Title	Rome Laboratory Directorate	Vol-Page
Nathan B Terry	Clinton High School , Clinton , NY ADESH as a Sample Generator for mdem	RL/ERDR	14- 12
Brian P Testa	Oxford Road , New Hartford , NY The Physical Significance of the Eigenvalues in Ad	RL/OCTS	14- 13

SRP Final Report Table of Contents

Author	University/Institution Report Title	Wright Laboratory Directorate	Vol-Page
Christine M Baker	Norhmont High School , Cayton , OH Thermal Stresses in Composite Materials	WL/FIOP	15- 1
Jennifer Bautista	Fort Walton Beach High , Fort Walton Beach , FL Analysis of a Three-Penetrator Concrete Penetratio	WL/MNOE	15- 2
Jessica M Behm	Kettering Fairmont High School , Kettering , OH A Study of Silk Coatings on Thin Films	WL/MLPJ	15- 3
Tim B Booher	Tippecanoe High School , Tipp City , OH Analysis of Spectrum Loading of SCS-6/Timetal 21s	WL/MLLM	15- 4
Kim Cabral	Choctawhatchee High School , Ft. Walton Beach , FL Chemical Decomposition Using Non-Thermal Discharge	WL/MNOE	15- 5
Robyn M Carley	Ft. Walton Beach High School , Ft. Walton Beach , FL Accuracy Verification Exercise for the Composite H	WL/MNOE	15- 6
Jason P Carranza	Chaminade-Julienne High School , Dayton , OH The Adams Project	WL/AAAF-	15- 7
George P Choung	Beavercreek High School , Beavercreek , OH Development of Astros, Version II for a Personal C	WL/FIOP	15- 8
Nick D DeBrosse	Kettering Fairmont High School , Kettering , OH Advanced Gas Turbine Engine Compressor Design	WL/POTF	15- 9
Nancy H Deibler	Choctawhatchee High School , Ft. Walton Beach , FL Characterization of Core Soil Samples and Plants F	WL/MNOE	15- 10
Timothy G Donohue	Carroll High School , Dayton , OH The Building of Computer Programs and Inexpensive	WL/FIOP	15- 11

SRP Final Report Table of Contents

Author	University/Institution Report Title	Wright Laboratory Directorate	Vol-Page
Michael J Dooley	Niceville High School , Niceville , FL Investigation of Programming and UNIX Applications	WL/MNOE _____	15- 12
Ajay Goel	Centerville High School , Centerville , OH A Study of Polymer Dispersed Liquid Crystals	WL/MLPJ _____	15- 13
Christie Gooden	Fort Walton Beach High School , Fort Walton Beach , FL Automated Integration of LADAR Imagery and TIFF St	WL/MNOE _____	15- 14
Gary L Grogg	Carroll High School , Dayton , OH Heat Pipe Compatibility with Aircraft	WL/POOS _____	15- 15
Matthew T Gudorf	Carroll High School , Dayton , OH The Analog Systems in Test Cell 22	WL/POPT _____	15- 16
Brian J Guilfoos	Kettering High School , Kettering , OH CAD: A Testing of the Effectiveness of Process De	WL/MLIM _____	15- 17
Douglas J Heil	Vandalia-Butler , Vandalia , OH Projects in Pattern Theory	WL/AART- _____	15- 18
Laura L Hemmer	Choctawhatchee High School , Ft. Walton Beach , FL High Surface Area Conductive Polymer Films Using A	WL/MNOE _____	15- 19
David B Hernandez	Freeport High School , Freeport , FL Preliminary Study for Application of IRMA Syntheti	WL/MNOE _____	15- 20
Melanie L Hodges	W.Carrollton Sr. High School , West Carrollton , OH Parallel Gaseous Fuel Injecton into a Mach 2 Frees	WL/POPT _____	15- 21
Venessa L Hurst	Walton Senior High School , DeFuniak Springs , FL Fluorodenitration of Aromatic Substrates	WL/MNOE _____	15- 22

SRP Final Report Table of Contents

Author	University/Institution Report Title	Wright Laboratory Directorate	Vol-Page
Ryan A Jasper	Carroll High School , Dayton , OH Experiments in Fuel Research	WL/POSF	15- 23
Mark E Jeffcoat	Choctawhatchee High School , Ft. Walton Beach , FL Segmentation of an M-60 Tank from a High-Clutter B	WL/MNOE	15- 24
Andrew J Konicki	Kettering Fairmont High School , Kettering , OH Carbon-Carbon Structures Test	WL/FIOP	15- 25
Barry Kress	Niceville High , Niceville , FL The Effectiveness and Accuracy of Cadra Software	WL/MNOE	15- 26
Sandra R McPherson	Bishop Brossart High School , Alexandria , KY A Study of KTA	WL/MLPO	15- 27
Benjamin J Merrill	Bellbrook High School , Bellbrook , OH Visual Instrumentation Development	WL/FIOP	15- 28
Gary W Midkiff	Kettering Fairmont High School , Kettering , OH Porting Spice 2G.6 to UNIX	WL/ELED	15- 29
Karthik Natarajan	Beavercreek High School , Beavercreek , OH A Study of the Organic Reactions of Phthalocyanine	WL/MLPJ	15- 30
Christina L Noll	Tritwood-Madison High , Trotwood , OH A Study of the Viscosity of Lubricating Oils	WL/POSL	15- 31
Joanna E Odella	Kettering Fairmont High School , Kettering , OH Starting Here and Going Beyond	WL/AAAI-	15- 32
Alexander Penn	Niceville High School , Niceville , FL Design and Construction of a Fluorescence	WL/MNOE	15- 33

SRP Final Report Table of Contents

Author	University/Institution Report Title	Wright Laboratory Directorate	Vol-Page
Kyle Perry	Crestview High School , Crestview , FL Validation of Synthetic Imagery	WL/MNOE	15- 34
Daniel R Pfunder	Centerville High School , Centerville , OH Integrated Generator Technology	WL/POOS	15- 35
Mary Pletcher	Niceville High School , Niceville , FL Chemical Characteristics of the Rocky Creek System	WL/MNOE	15- 36
Scott E Sadowski	Centerville High School , Centerville , OH PAC vs. Area Methods of Determining "Learnability"	WL/AART-	15- 37
Raul H Sanchez	Centerville High School , Centerville , OH Quantum Well Infrared Detector Research	WL/ELOD	15- 38
Jill M Schlotterbeck	Kettering Fairmont High School , Kettering , OH A Study of Single Tube Catalyzed Heat Exchange	WL/POPT	15- 39
Robert J Skebo	Beavercreek High School , Beavercreek , OH The Effect of Humidity on Friction and Wear for M5	WL/MLBT	15- 40
Jennifer A Starr	Trotwood Madison Sr. High Scho , Trotwood , OH My Introduction to the Internet	WL/AAAF-	15- 41
Todd D Stockert	Centerville High School , Centerville , OH The Effect of Temperature Upon Ho:YA1O3 Fluorescen	WL/ELOS	15- 41
David B Storch	Beavercreek High School , Beavercreek , OH High Temperature/High Speed Laser Project	WL/ELR	15- 41
Christopher J Sutton	Jefferson High School , Dayton , OH Dynamic Testing of Composites	WL/FIVS	15- 41

SRP Final Report Table of Contents

Author	University/Institution Report Title	Wright Laboratory Directorate	Vol-Page
Thomas R Sutton	Sauquoit Valley High , Sauquoit , NY Dynamic Testing of Composites	WL/FIVS	15- 45
Randy Thomson	Choctawhatchee High , Fort Walton Beach , FL Development and Testing of a Two-Dimensional Finit	WL/MNOE	15- 46
John W Vest	Niceville High School , Niceville , FL Characterization of Optical Filters Built Using Sy	WL/MNOE	15- 47
MR Jon R Ward	Walton High School , DeFuniak Springs , FL Data Acquisition, Reduction, and Storage Using Lab	WL/MNOE	15- 48
Jeffrey D Warren	Fairborn High School , Fairborn , OH Computer Resource Team	WL/FIOP	15- 49
Joshua A Weaver	Niceville High School , Niceville , FL Moments and Other PC Utilities	WL/MNOE	15- 50
Gerad M Welch	Beavercreek High School , Beavercreek , OH Software Assisted Component Testing for the Antenn	WL/AAAI-	15- 51
Gabrielle W WhiteWolf	Choctawhatchee High Schoo , Chcotawhatchee , FL Laser Speckle MTF Test Automation and Characteriza	WL/MNOE	15- 52

SRP Final Report Table of Contents

Author	University/Institution Report Title	Arnold Engineering Development Center Directorate	Vol-Page
Ryan B Bond	Tullahoma High School , Tullahoma , TN Modeling Engine Test Facility Cells in Vissim	Sverdrup	16 - 1
Robert B Cassady	Coffee County Cen High School , Manchester , TN Mach-Flow Angularity Probe Calibration	Calspan	16 - 2
Thomas L Clouse	Coffee County Central HS , Manchester , TN Workstation Inventory Control Program	Sverdrup	16 - 3
Michael L Fann	Tullahoma High School , Tullahoma , TN The Conversion of Millivolts Measured from Thermoc	Sverdrup	16 - 4
Derek E Geeting	Shelbyville Central High , Shelbyville , TN Lighting Calculation Study and Software Evaluation	SSI	16 - 5
Jennifer A Groff	Franklin County Sr High School , Winchester , TN The Use of Labview for Serial Data Transmission	Sverdrup	16 - 6
James J Lemmons	Coffee County Central HS , Manchester , TN Out of Band Filter Calibration Technology Project	Bionetics	16 - 7
Lana L Matthews	Coffee County Central HS , Manchester , TN A Study of Hydrocarbon Combustion: Stoichiometry	Sverdrup	16 - 8
Steve G Pugh	Shelbyville Central HS , Shelbyville , TN An Analytic Capability for Predicting Sability of	Sverdrup	16 - 9
Kristopher S Ray	Shelbyville Central High Schoo , Shelbyville , TN Power Systems Analysis	SSI	16 - 10

1. INTRODUCTION

The Summer Research Program (SRP), sponsored by the Air Force Office of Scientific Research (AFOSR), offers paid opportunities for university faculty, graduate students, and high school students to conduct research in U.S. Air Force research laboratories nationwide during the summer.

Introduced by AFOSR in 1978, this innovative program is based on the concept of teaming academic researchers with Air Force scientists in the same disciplines using laboratory facilities and equipment not often available at associates' institutions.

AFOSR also offers its research associates an opportunity, under the Summer Research Extension Program (SREP), to continue their AFOSR-sponsored research at their home institutions through the award of research grants. In 1994 the maximum amount of each grant was increased from \$20,000 to \$25,000, and the number of AFOSR-sponsored grants decreased from 75 to 60. A separate annual report is compiled on the SREP.

The Summer Faculty Research Program (SFRP) is open annually to approximately 150 faculty members with at least two years of teaching and/or research experience in accredited U.S. colleges, universities, or technical institutions. SFRP associates must be either U.S. citizens or permanent residents.

The Graduate Student Research Program (GSRP) is open annually to approximately 100 graduate students holding a bachelor's or a master's degree; GSRP associates must be U.S. citizens enrolled full time at an accredited institution.

The High School Apprentice Program (HSAP) annually selects about 125 high school students located within a twenty mile commuting distance of participating Air Force laboratories.

The numbers of projected summer research participants in each of the three categories are usually increased through direct sponsorship by participating laboratories.

AFOSR's SRP has well served its objectives of building critical links between Air Force research laboratories and the academic community, opening avenues of communications and forging new research relationships between Air Force and academic technical experts in areas of national interest; and strengthening the nation's efforts to sustain careers in science and engineering. The success of the SRP can be gauged from its growth from inception (see Table 1) and from the favorable responses the 1994 participants expressed in end-of-tour SRP evaluations (Appendix B).

AFOSR contracts for administration of the SRP by civilian contractors. The contract was first awarded to Research & Development Laboratories (RDL) in September 1990. After completion of the 1990 contract, RDL won the recompetition for the basic year and four 1-year options.

2. PARTICIPATION IN THE SUMMER RESEARCH PROGRAM

The SRP began with faculty associates in 1979; graduate students were added in 1982 and high school students in 1986. The following table shows the number of associates in the program each year.

Table 1: SRP Participation, by Year

YEAR	Number of Participants			TOTAL
	SFRP	GSRP	HSAP	
1979	70			70
1980	87			87
1981	87			87
1982	91	17		108
1983	101	53		154
1984	152	84		236
1985	154	92		246
1986	158	100	42	300
1987	159	101	73	333
1988	153	107	101	361
1989	168	102	103	373
1990	165	121	132	418
1991	170	142	132	444
1992	185	121	159	464
1993	187	117	136	440
1994	192	117	133	442

Beginning in 1993, due to budget cuts, some of the laboratories weren't able to afford to fund as many associates as in previous years; in one case a laboratory did not fund any additional associates. However, the table shows that, overall, the number of participating associates increased this year because two laboratories funded more associates than they had in previous years.

3. RECRUITING AND SELECTION

The SRP is conducted on a nationally advertised and competitive-selection basis. The advertising for faculty and graduate students consisted primarily of the mailing of 8,000 44-page SRP brochures to chairpersons of departments relevant to AFOSR research and to administrators of grants in accredited universities, colleges, and technical institutions. Historically Black Colleges and Universities (HBCUs) and Minority Institutions (MIs) were included. Brochures also went to all participating USAF laboratories, the previous year's participants, and numerous (over 600 annually) individual requesters.

Due to a delay in awarding the new contract, RDL was not able to place advertisements in any of the following publications in which the SRP is normally advertised: *Black Issues in Higher Education*, *Chemical & Engineering News*, *IEEE Spectrum* and *Physics Today*.

High school applicants can participate only in laboratories located no more than 20 miles from their residence. Tailored brochures on the HSAP were sent to the head counselors of 180 high schools in the vicinity of participating laboratories, with instructions for publicizing the program in their schools. High school students selected to serve at Wright Laboratory's Armament Directorate (Eglin Air Force Base, Florida) serve eleven weeks as opposed to the eight weeks normally worked by high school students at all other participating laboratories.

Each SFRP or GSRP applicant is given a first, second, and third choice of laboratory. High school students who have more than one laboratory or directorate near their homes are also given first, second, and third choices.

Laboratories make their selections and prioritize their nominees. AFOSR then determines the number to be funded at each laboratory and approves laboratories' selections.

Subsequently, laboratories use their own funds to sponsor additional candidates. Some selectees do not accept the appointment, so alternate candidates are chosen. This multi-step selection procedure results in some candidates being notified of their acceptance after scheduled deadlines. The total applicants and participants for 1994 are shown in this table.

Table 2: 1994 Applicants and Participants

PARTICIPANT CATEGORY	TOTAL APPLICANTS	SELECTEES	DECLINING SELECTEES
SFRP	600	192	30
(HBCU/MI)	(90)	(16)	(7)
GSRP	322	117	11
(HBCU/MI)	(11)	(6)	(0)
HSAP	562	133	14
TOTAL	1484	442	55

4. SITE VISITS

During June and July of 1994, representatives of both AFOSR/NI and RDL visited each participating laboratory to provide briefings, answer questions, and resolve problems for both laboratory personnel and participants. The objective was to ensure that the SRP would be as constructive as possible for all participants. Both SRP participants and RDL representatives found these visits beneficial. At many of the laboratories, this was the only opportunity for all participants to meet at one time to share their experiences and exchange ideas.

5. HISTORICALLY BLACK COLLEGES AND UNIVERSITIES AND MINORITY INSTITUTIONS (HBCU/MI)s

In previous years, an RDL program representative visited from seven to ten different HBCU/MI's to promote interest in the SRP among the faculty and graduate students. Due to the late contract award date (January 1994) no time was available to visit HBCU/MI's this past year.

In addition to RDL's special recruiting efforts, AFOSR attempts each year to obtain additional funding or use leftover funding from cancellations the past year to fund HBCU/MI associates. This year, seven HBCU/MI SFRPs declined after they were selected. The following table records HBCU/MI participation in this program.

Table 3: SRP HBCU/MI Participation, by Year

YEAR	SFRP		GSRP	
	Applicants	Participants	Applicants	Participants
1985	76	23	15	11
1986	70	18	20	10
1987	82	32	32	10
1988	53	17	23	14
1989	39	15	13	4
1990	43	14	17	3
1991	42	13	8	5
1992	70	13	9	5
1993	60	13	6	2
1994	90	16	11	6

6. SRP FUNDING SOURCES

Funding sources for the 1994 SRP were the AFOSR-provided slots for the basic contract and laboratory funds. Funding sources by category for the 1994 SRP selected participants are shown here.

Table 4: 1994 SRP Associate Funding

FUNDING CATEGORY	SFRP	GSRP	HSAP
AFOSR Basic Allocation Funds	150	98 ^{*1}	121 ^{*2}
USAF Laboratory Funds	37	19	12
HBCU/MI By AFOSR (Using Procured Addn'l Funds)	5	0	0
TOTAL	192	117	133

*1 - 100 were selected, but two canceled too late to be replaced.

*2 - 125 were selected, but four canceled too late to be replaced.

7. COMPENSATION FOR PARTICIPANTS

Compensation for SRP participants, per five-day work week, is shown in this table.

Table 5: 1994 SRP Associate Compensation

PARTICIPANT CATEGORY	1991	1992	1993	1994
Faculty Members	\$690	\$718	\$740	\$740
Graduate Student (Master's Degree)	\$425	\$442	\$455	\$455
Graduate Student (Bachelor's Degree)	\$365	\$380	\$391	\$391
High School Student (First Year)	\$200	\$200	\$200	\$200
High School Student (Subsequent Years)	\$240	\$240	\$240	\$240

APPENDIX A – PROGRAM STATISTICAL SUMMARY

A. Colleges/Universities Represented

Selected SFRP and GSRP associates represent 158 different colleges, universities, and institutions.

B. States Represented

SFRP - Applicants came from 46 states plus Washington D.C. and Puerto Rico. Selectees represent 40 states.

GSRP - Applicants came from 46 states and Puerto Rico. Selectees represent 34 states.

HSAP - Applicants came from fifteen states. Selectees represent ten states.

C. Academic Disciplines Represented

The academic disciplines of the combined 192 SFRP associates are as follows:

Electrical Engineering	22.4%
Mechanical Engineering	14.0%
Physics: General, Nuclear & Plasma	12.2%
Chemistry & Chemical Engineering	11.2%
Mathematics & Statistics	8.1%
Psychology	7.0%
Computer Science	6.4%
Aerospace & Aeronautical Engineering	4.8%
Engineering Science	2.7%
Biology & Inorganic Chemistry	2.2%
Physics: Electro-Optics & Photonics	2.2%
Communication	1.6%
Industrial & Civil Engineering	1.6%
Physiology	1.1%
Polymer Science	1.1%
Education	0.5%
Pharmaceutics	0.5%
Veterinary Medicine	0.5%
TOTAL	100%

Table A-1. Total Participants

Number of Participants	
SFRP	192
GSRP	117
HSAP	133
TOTAL	442

Table A-2. Degrees Represented

Degrees Represented			
	SFRP	GSRP	TOTAL
Doctoral	189	0	189
Master's	3	47	50
Bachelor's	0	70	70
TOTAL	192	117	309

Table A-3. SFRP Academic Titles

Academic Titles	
Assistant Professor	74
Associate Professor	63
Professor	44
Instructor	5
Chairman	1
Visiting Professor	1
Visiting Assoc. Prof.	1
Research Associate	3
TOTAL	192

Table A-4. Source of Learning About SRP

SOURCE	SFRP		GSRP	
	Applicants	Selectees	Applicants	Selectees
Applied/participated in prior years	26%	37%	10%	13%
Colleague familiar with SRP	19%	17%	12%	12%
Brochure mailed to institution	32%	18%	19%	12%
Contact with Air Force laboratory	15%	24%	9%	12%
Faculty Advisor (GSRPs Only)	--	--	39%	43%
Other source	8%	4%	11%	8%
TOTAL	100%	100%	100%	100%

Table A-5. Ethnic Background of Applicants and Selectees

	SFRP		GSRP		HSAP	
	Applicants	Selectees	Applicants	Selectees	Applicants	Selectees
American Indian or Native Alaskan	0.2%	0%	1%	0%	0.4%	0%
Asian/Pacific Islander	30%	20%	6%	8%	7%	10%
Black	4%	1.5%	3%	3%	7%	2%
Hispanic	3%	1.9%	4%	4.5%	11%	8%
Caucasian	51%	63%	77%	77%	70%	75%
Preferred not to answer	12%	14%	9%	7%	4%	5%
TOTAL	100%	100%	100%	100%	99%	100%

Table A-6. Percentages of Selectees receiving their 1st, 2nd, or 3rd Choices of Directorate

	1st Choice	2nd Choice	3rd Choice	Other Than Their Choice
SFRP	70%	7%	3%	20%
GSRP	76%	2%	2%	20%

APPENDIX B -- SRP EVALUATION RESPONSES

1. OVERVIEW

Evaluations were completed and returned to RDL by four groups at the completion of the SRP. The number of respondents in each group is shown below.

Table B-1. Total SRP Evaluations Received

Evaluation Group	Responses
SFRP & GSRPs	275
HSAPs	116
USAF Laboratory Focal Points	109
USAF Laboratory HSAP Mentors	54

All groups indicate near-unanimous enthusiasm for the SRP experience.

Typical comments from 1994 SRP associates are:

"[The SRP was an] excellent opportunity to work in state-of-the-art facility with top-notch people."

"[The SRP experience] enabled exposure to interesting scientific application problems; enhancement of knowledge and insight into 'real-world' problems."

"[The SRP] was a great opportunity for resourceful and independent faculty [members] from small colleges to obtain research credentials."

"The laboratory personnel I worked with are tremendous, both personally and scientifically. I cannot emphasize how wonderful they are."

"The one-on-one relationship with my mentor and the hands on research experience improved [my] understanding of physics in addition to improving my library research skills. Very valuable for [both] college and career!"

Typical comments from laboratory focal points and mentors are:

"This program [AFOSR - SFRP] has been a 'God Send' for us. Ties established with summer faculty have proven invaluable."

"Program was excellent from our perspective. So much was accomplished that new options became viable "

"This program managed to get around most of the red tape and 'BS' associated with most Air Force programs. Good Job!"

"Great program for high school students to be introduced to the research environment. Highly educational for others [at laboratory]."

"This is an excellent program to introduce students to technology and give them a feel for [science/engineering] career fields. I view any return benefit to the government to be 'icing on the cake' and have usually benefitted."

The summarized recommendations for program improvement from both associates and laboratory personnel are listed below (Note: basically the same as in previous years.)

- A. Better preparation on the labs' part prior to associates' arrival (i.e., office space, computer assets, clearly defined scope of work).
- B. Laboratory sponsor seminar presentations of work conducted by associates, and/or organized social functions for associates to collectively meet and share SRP experiences.
- C. Laboratory focal points collectively suggest more AFOSR allocated associate positions, so that more people may share in the experience.
- D. Associates collectively suggest higher stipends for SRP associates.
- E. Both HSAP Air Force laboratory mentors and associates would like the summer tour extended from the current 8 weeks to either 10 or 11 weeks; the groups state it takes 4-6 weeks just to get high school students up-to-speed on what's going on at laboratory. (Note: this same argument was used to raise the faculty and graduate student participation time a few years ago.)

2. 1994 USAF LABORATORY FOCAL POINT (LFP) EVALUATION RESPONSES

The summarized results listed below are from the 109 LFP evaluations received.

1. LFP evaluations received and associate preferences:

Table B-2. Air Force LFP Evaluation Responses (By Type)

Lab	Evals Recv'd	How Many Associates Would You Prefer To Get ?								(% Response)			
		SFRP				GSRP (w/Univ Professor)				GSRP (w/o Univ Professor)			
		0	1	2	3+	0	1	2	3+	0	1	2	3+
AEDC	10	30	50	0	20	50	40	0	10	40	60	0	0
AL	44	34	50	6	9	54	34	12	0	56	31	12	0
FJSRL	3	33	33	33	0	67	33	0	0	33	67	0	0
PL	14	28	43	28	0	57	21	21	0	71	28	0	0
RL	3	33	67	0	0	67	0	33	0	100	0	0	0
WHMC	1	0	0	100	0	0	100	0	0	0	100	0	0
WL	46	15	61	24	0	56	30	13	0	76	17	6	0
Total	121	25%	43%	27%	4%	50%	37%	11%	1%	54%	43%	3%	0%

LFP Evaluation Summary. The summarized responses, by laboratory, are listed on the following page. LFPs were asked to rate the following questions on a scale from 1 (below average) to 5 (above average).

2. LFPs involved in SRP associate application evaluation process:
 - a. Time available for evaluation of applications:
 - b. Adequacy of applications for selection process:
3. Value of orientation trips:
4. Length of research tour:
5.
 - a. Benefits of associate's work to laboratory:
 - b. Benefits of associate's work to Air Force:
6.
 - a. Enhancement of research qualifications for LFP and staff:
 - b. Enhancement of research qualifications for SFRP associate:
 - c. Enhancement of research qualifications for GSRP associate:
7.
 - a. Enhancement of knowledge for LFP and staff:
 - b. Enhancement of knowledge for SFRP associate:
 - c. Enhancement of knowledge for GSRP associate:
8. Value of Air Force and university links:
9. Potential for future collaboration:
10.
 - a. Your working relationship with SFRP:
 - b. Your working relationship with GSRP:
11. Expenditure of your time worthwhile:

(Continued on next page)

12. Quality of program literature for associate:
 13. a. Quality of RDL's communications with you:
 b. Quality of RDL's communications with associates:
 14. Overall assessment of SRP:

Laboratory Focal Point Reponses to above questions

	<i>AEDC</i>	<i>AL</i>	<i>FJSRL</i>	<i>PL</i>	<i>RL</i>	<i>WHMC</i>	<i>WL</i>
<i># Evals Recv'd</i>	10	32	3	14	3	1	46
<i>Question #</i>							
2	90 %	62 %	100 %	64 %	100 %	100 %	83 %
2a	3.5	3.5	4.7	4.4	4.0	4.0	3.7
2b	4.0	3.8	4.0	4.3	4.3	4.0	3.9
3	4.2	3.6	4.3	3.8	4.7	4.0	4.0
4	3.8	3.9	4.0	4.2	4.3	NO ENTRY	4.0
5a	4.1	4.4	4.7	4.9	4.3	3.0	4.6
5b	4.0	4.2	4.7	4.7	4.3	3.0	4.5
6a	3.6	4.1	3.7	4.5	4.3	3.0	4.1
6b	3.6	4.0	4.0	4.4	4.7	3.0	4.2
6c	3.3	4.2	4.0	4.5	4.5	3.0	4.2
7a	3.9	4.3	4.0	4.6	4.0	3.0	4.2
7b	4.1	4.3	4.3	4.6	4.7	3.0	4.3
7c	3.3	4.1	4.5	4.5	4.5	5.0	4.3
8	4.2	4.3	5.0	4.9	4.3	5.0	4.7
9	3.8	4.1	4.7	5.0	4.7	5.0	4.6
10a	4.6	4.5	5.0	4.9	4.7	5.0	4.7
10b	4.3	4.2	5.0	4.3	5.0	5.0	4.5
11	4.1	4.5	4.3	4.9	4.7	4.0	4.4
12	4.1	3.9	4.0	4.4	4.7	3.0	4.1
13a	3.8	2.9	4.0	4.0	4.7	3.0	3.6
13b	3.8	2.9	4.0	4.3	4.7	3.0	3.8
14	4.5	4.4	5.0	4.9	4.7	4.0	4.5

3. 1994 SFRP & GSRP EVALUATION RESPONSES

The summarized results listed below are from the 275 SFRP/GSRP evaluations received.

Associates were asked to rate the following questions on a scale from
1 (below average) to 5 (above average)

1. The match between the laboratories research and your field:	4.6
2. Your working relationship with your LFP:	4.8
3. Enhancement of your academic qualifications:	4.4
4. Enhancement of your research qualifications:	4.5
5. Lab readiness for you: LFP, task, plan:	4.3
6. Lab readiness for you: equipment, supplies, facilities:	4.1
7. Lab resources:	4.3
8. Lab research and administrative support:	4.5
9. Adequacy of brochure and associate handbook:	4.3
10. RDL communications with you:	4.3
11. Overall payment procedures:	3.8
12. Overall assessment of the SRP:	4.7
13. a. Would you apply again?	Yes: 85%
b. Will you continue this or related research?	Yes: 95%
14. Was length of your tour satisfactory?	Yes: 86%
15. Percentage of associates who engaged in:	
a. Seminar presentation:	52%
b. Technical meetings:	32%
c. Social functions:	03%
d. Other	01%

16. Percentage of associates who experienced difficulties in:

- | | |
|---------------------|-----|
| a. Finding housing: | 12% |
| b. Check Cashing: | 03% |

17. Where did you stay during your SRP tour?

- | | |
|----------------------|-----|
| a. At Home: | 20% |
| b. With Friend: | 06% |
| c. On Local Economy: | 47% |
| d. Base Quarters: | 10% |

THIS SECTION FACULTY ONLY:

18. Were graduate students working with you? Yes: 23%

19. Would you bring graduate students next year? Yes: 56%

20. Value of orientation visit:

- | | |
|-----------------|-----|
| Essential: | 29% |
| Convenient: | 20% |
| Not Worth Cost: | 01% |
| Not Used: | 34% |

THIS SECTION GRADUATE STUDENTS ONLY:

21. Who did you work with:

- | | |
|-----------------------|-----|
| University Professor: | 18% |
| Laboratory Scientist: | 54% |

4. 1994 USAF LABORATORY HSAP MENTOR EVALUATION RESPONSES

The summarized results listed below are from the 54 mentor evaluations received.

1. Mentor apprentice preferences:

Table B-3. Air Force Mentor Responses

		How Many Apprentices Would You Prefer To Get ?			
		<i>HSAP Apprentices Preferred</i>			
<i>Laboratory</i>	<i># Evals Recv'd</i>	<i>0</i>	<i>1</i>	<i>2</i>	<i>3+</i>
AEDC	6	0	100	0	0
AL	17	29	47	6	18
PL	9	22	78	0	0
RL	4	25	75	0	0
WL	18	22	55	17	6
Total	54	20%	71%	5%	5%

Mentors were asked to rate the following questions on a scale from 1 (below average) to 5 (above average)

2. Mentors involved in SRP apprentice application evaluation process:
 - a. Time available for evaluation of applications:
 - b. Adequacy of applications for selection process:
3. Laboratory's preparation for apprentice:
4. Mentor's preparation for apprentice:
5. Length of research tour:
6. Benefits of apprentice's work to U.S. Air force:
7. Enhancement of academic qualifications for apprentice:
8. Enhancement of research skills for apprentice:
9. Value of U.S. Air Force/high school links:
10. Mentor's working relationship with apprentice:
11. Expenditure of mentor's time worthwhile:
12. Quality of program literature for apprentice:
13.
 - a. Quality of RDL's communications with mentors:
 - b. Quality of RDL's communication with apprentices:
14. Overall assessment of SRP:

	<i>AEDC</i>	<i>AL</i>	<i>PL</i>	<i>RL</i>	<i>WL</i>
# Evals Recv'd	6	17	9	4	18
<i>Question #</i>					
2	100 %	76 %	56 %	75 %	61 %
2a	4.2	4.0	3.1	3.7	3.5
2b	4.0	4.5	4.0	4.0	3.8
3	4.3	3.8	3.9	3.8	3.8
4	4.5	3.7	3.4	4.2	3.9
5	3.5	4.1	3.1	3.7	3.6
6	4.3	3.9	4.0	4.0	4.2
7	4.0	4.4	4.3	4.2	3.9
8	4.7	4.4	4.4	4.2	4.0
9	4.7	4.2	3.7	4.5	4.0
10	4.7	4.5	4.4	4.5	4.2
11	4.8	4.3	4.0	4.5	4.1
12	4.2	4.1	4.1	4.8	3.4
13a	3.5	3.9	3.7	4.0	3.1
13b	4.0	4.1	3.4	4.0	3.5
14	4.3	4.5	3.8	4.5	4.1

5. 1994 HSAP EVALUATION RESPONSES

The summarized results listed below are from the 116 HSAP evaluations received.

HSAP apprentices were asked to rate the following questions on a scale from 1 (below average) to 5 (above average)

1. Match of lab research to you interest:	3.9
2. Apprentices working relationship with their mentor and other lab scientists:	4.6
3. Enhancement of your academic qualifications:	4.4
4. Enhancement of your research qualifications:	4.1
5. Lab readiness for you: mentor, task, work plan	3.7
6. Lab readiness for you: equipment supplies facilities	4.3
7. Lab resources: availability	4.3
8. Lab research and administrative support:	4.4
9. Adequacy of RDL's apprentice handbook and administrative materials:	4.0
10. Responsiveness of RDL's communications:	3.5
11. Overall payment procedures:	3.3
12. Overall assessment of SRP value to you:	4.5
13. Would you apply again next year?	Yes: 88%
14. Was length of SRP tour satisfactory?	Yes: 78%
15. Percentages of apprentices who engaged in:	
a. Seminar presentation:	48%
b. Technical meetings:	23%
c. Social functions:	18%

A Study of KTA

Sandra R. McPherson

Bishop Brossart High School
Jefferson and Grove Streets
Alexandria, Ky 41011

Final Report for:
High School Apprentice Program
Wright Laboratory

Sponsored by:
Air Force Office of Scientific Research
Bolling Air Force Base, DC

and

Wright Laboratory

August 1994

27-1

A Study of KTA

Sandra R. McPherson
Bishop Brossart High School

Abstract

KTA was studied in order to determine if it can be used in advancing the world of nonlinear crystals. The index of refraction, which is a measure of how light travels through a substance, is a basic characterization done by scientists after a new material is created. A spectrometer is used to record the data and we discuss how the data is taken and analyzed. The index of refraction was measured up to 1.4 microns. Due to mechanical difficulties, it was not possible, to go higher, however, it will be in the near future to enable complete characterization of the material. This research was supported by Air Force Office of Scientific Research, Research and Development Laboratories.

Acknowledgements

The author acknowledges Ms. Angela McPherson of Wright-Patterson Air Force Base and Dr. Uma Ramabadran of the University of Dayton Research Institute for their guidance and support of this project. The Nonlinear Optics Group of Wright Laboratory, Materials Directorate, Wright-Patterson Air Force Base is acknowledged for use of their equipment. Crystal Associates, in Waldwick, New Jersey is recognized for supplying the KTA prisms. Captain Dale Fenimore is credited for initiating the study of KTA.

TABLE OF CONTENTS

<u>Section</u>	<u>Page Number</u>
Abstract	2
Acknowledgements	3
List of Figures	5
Introduction	6
Discussion	6
Methods	8
Results	12
Conclusion	15
References	16

LIST OF FIGURES

<u>FIGURE</u>	<u>Page Number</u>
FIGURE 1, 3D drawing showing prism axes for bi-axial materials	6
FIGURE 2, Gaertner L124 spectrometer	8
FIGURE 3, Depicts Index of Refraction for KTP:Na	10
FIGURE 4, Refractive Index Data for KTA	11

A Study of KTA

Sandra R. McPherson

Introduction

One of the best nonlinear optical crystals known today is KTiOPO_4 (KTP)¹. The KTP used in this experiment was grown by the high temperature flux method at Crystal Associates, Waldwick, New Jersey. KTP is the standard for frequency doubling of the Nd:YAG laser at 1064 nm². 1064 nm is currently the standard wavelength used, however, as index is determined at longer wavelengths, this may change². Scientists are hard at work to improve KTP, improve meaning to change the indices to what they need. They have tried doping it with various materials and substituting elements. In this paper we discuss a sodium doped KTP crystal designated KTP:Na and KTiOAsO_4 (KTA)¹. This new material is reported to have many of the same properties of its predecessor, KTP. Distinct measurements on KTA itself must therefore be completed to determine if it will be of use in the scientific community¹.

Discussion

The materials to be studied, KTA and KTP, are bi-axial². Two prisms are used for this measurement. They are labeled x and y according to Figure 1.

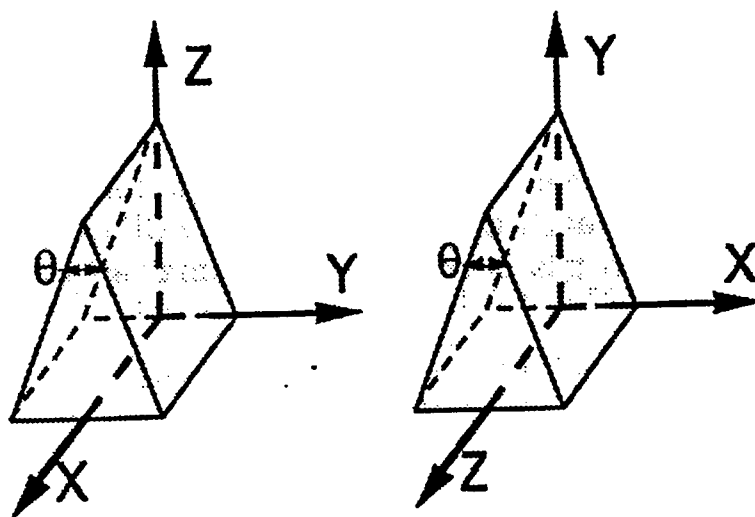


FIGURE 1

3D drawing showing prism axes for bi-axial materials (In this case, the prisms would be labeled x and y according to which axes is parallel to the prism angle).

Methods

We measure the index of refraction by minimum deviation method with a Gaertner L124 spectrometer. An Oriel Hg-Xe high intensity white light is used as a source of light and it is directed through a Digikrom 240 monochromator to separate the colors using a diffraction grating. A polarizer is placed at the output of the monochromator. All wavelengths in the visible spectrum can be used, and near infrared (NIR) measurements are possible with an Electrophysics handheld electroviewer which converts NIR radiation to a visible image. Also, a UV detection plate can be placed in front of the eyepiece to make UV measurements possible. A specific wavelength enters the collimator which spreads out the input light so it is larger than the sample. The sample, cut into the shape of a prism so that light can

pass through it and be refracted, is sitting on a table that swivels at the base to allow it to move and has an adjustable height. The light is incident of one face of the prism and is refracted out the other face.

On the other side of the prism table is a telescope used to focus the light coming out of the prism. At the end of the telescope is an eyepiece that we look through to see the light. The prism table is then slowly twisted toward the inside until the light reverses its direction. This is the called minimum deviation.

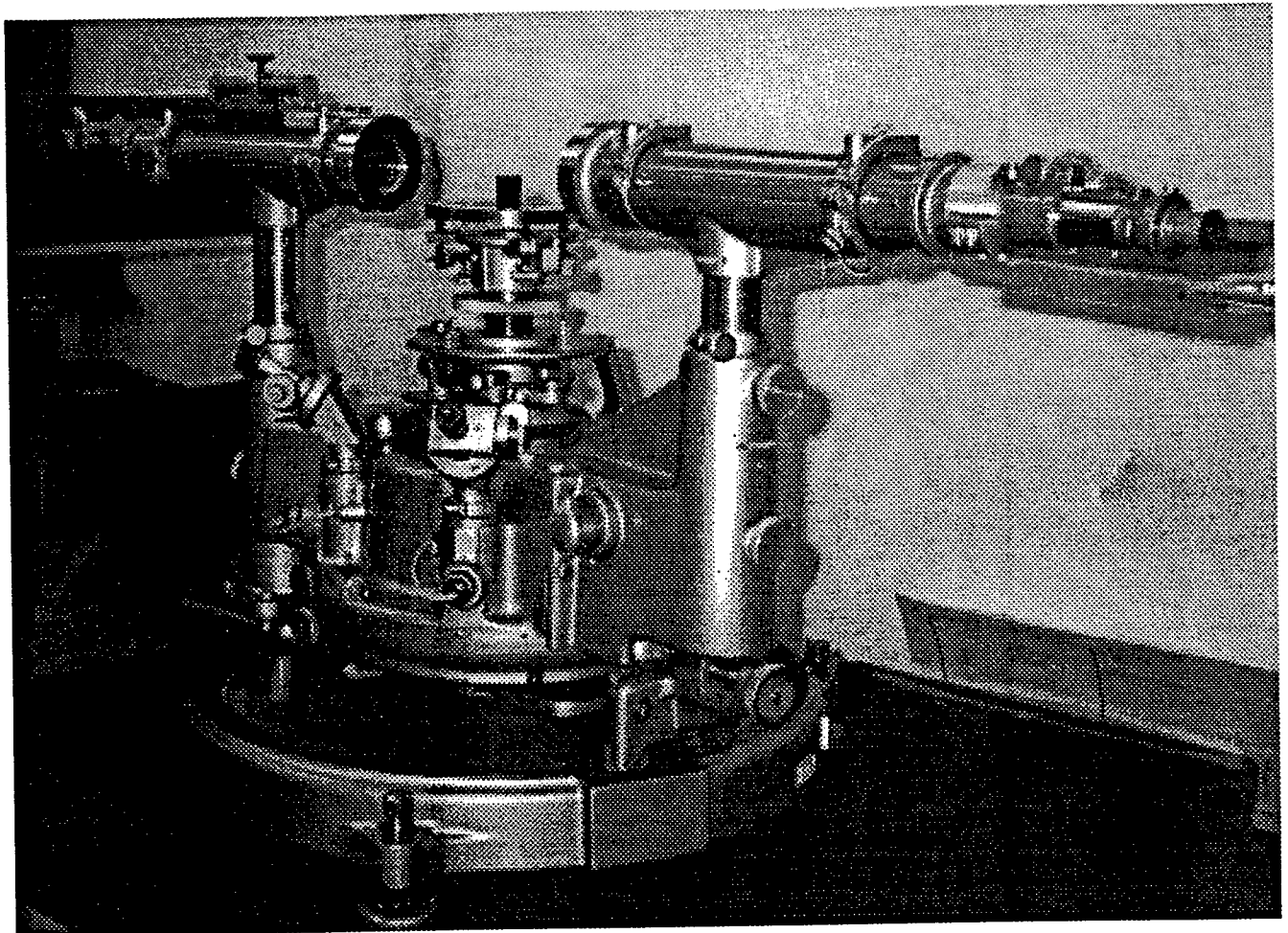


FIGURE 3
Gaertner L124 spectrometer

FIGURE 3 is the spectrometer used in this study to measure index using minimum deviation. To the right is the telescope with the eyepiece. The flat platform in the middle is the moveable prism table. To the right of the prism table is the collimator. The black box on the far left is the monochromator. Two of the microscopes used to measure the angle as described below are seen, one below the collimator, and the other to the left of the telescope.

To record data, the prism table is left at the point where the light is at its furthest position to the inside and the telescope is locked into place. It is important that the table be left at the point of minimum deviation, or the measurements will be incorrect. Also, the telescope is attached to a divided circle that angle measurements are taken from, so it is imperative that the telescope does not move. A fine adjust helps to center the beam on the crosshairs located inside the eyepiece. (These are merely a constant spot to place the beam for measuring.) Four microscopes are situated 90° apart around the bottom of the prism table so the graduated circle can be read down to half second arc. These numbers, which are in degrees, minutes and seconds, are used to determine the angle of the beam as it comes out.

An explanation of the method used in recording data can be found in reference number 4.

After recording the angle measurements, the wavelength is changed and a minimum deviation is found again. Each wavelength bends more at different wavelength, meaning the index varies with wavelength. This is known as dispersion³ and is the reason for the "rainbow" formed when white light goes through a prism.

This process is repeated over a pre-determined wavelength range, called a run, that varied between prisms. The standard number of runs was 5 for each axis.

All numbers recorded are entered into a program written by my mentor for the Software package *Mathematica* version 2.2 designed to calculate the index. Some modifications to the program were made based on the wavelength range used. All 5 runs on each sample are compared and a standard of deviation (STD) is calculated. How small the STD is determines the accuracy of the final index number. No number is accepted unless its STD is smaller than 10^{-3} .

Results

Figure 3 shows our index of refraction data for KTP:Na taken last year at Wright-Patterson Air Force Base, as sent to Crystal Associates⁴.

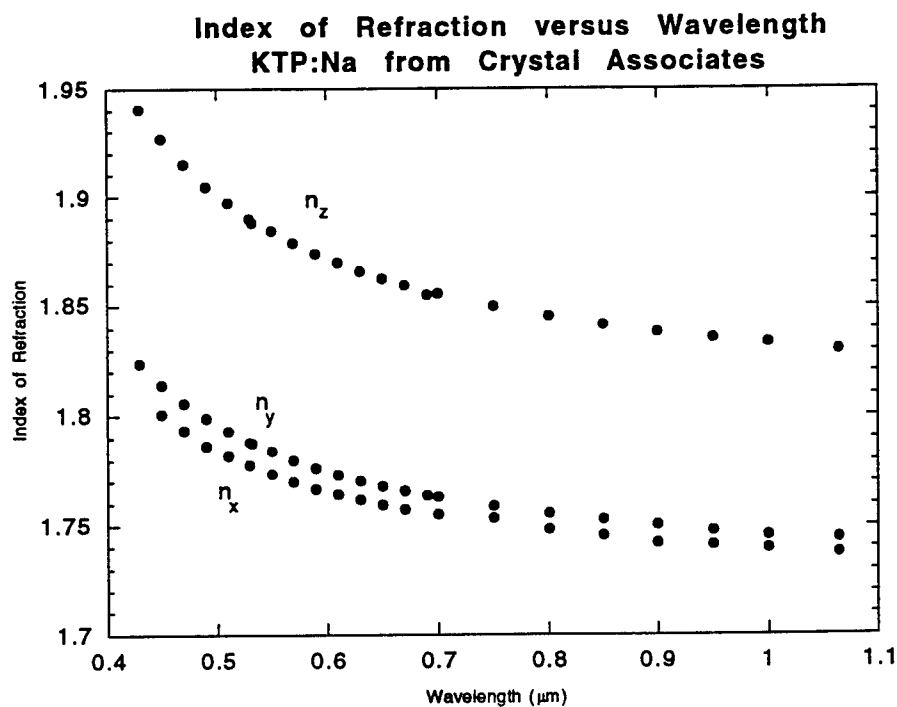


Figure 3
27-10

Depicts Index of Refraction for KTP:Na

KTA, the sample being measured in this study was also sent to Wright Labs from Crystal Associates, in Waldwick, New Jersey, to be measured. As stated previously, Crystal Associates determined KTA to be bi-axial so there would be three indices. Each prism was measured first doing 5 runs with vertically polarized light, and then 5 with the horizontally polarized light. We recorded measurements for both the visible and NIR range of 410-650 nm in increments of 20 nm, 700-1000 nm in steps of 50 nm and 1064 nm. The results are shown in Figure 4.

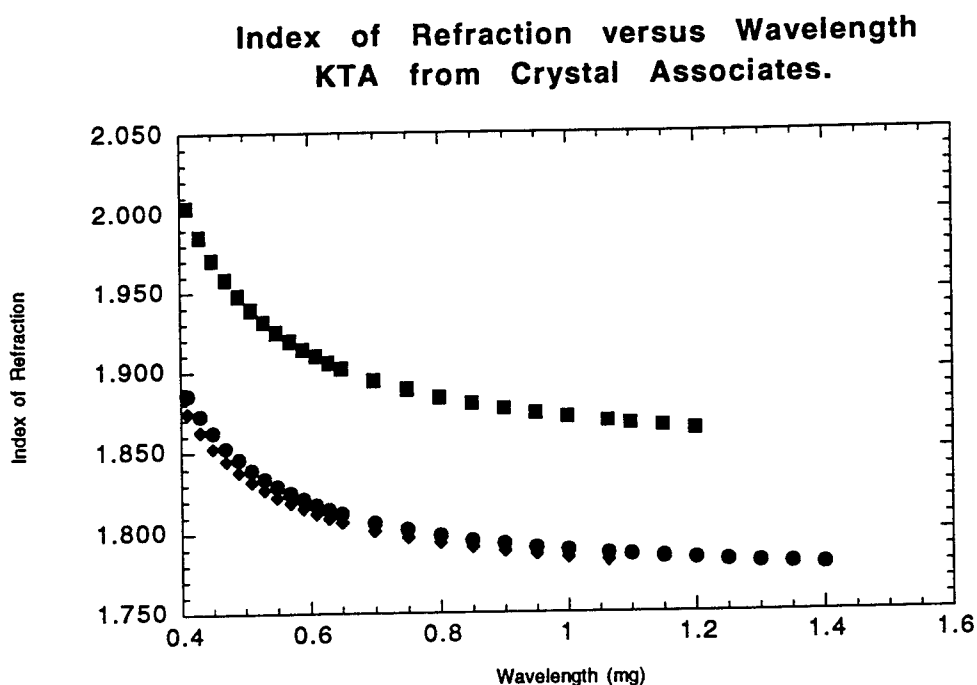


Figure 4
Refractive Index Data for KTA

An attempt was made to measure the index of refraction into the IR range. However, the detector used was for NIR measurements and did not provide a reliable

refractive index. Also, the transmission grating on the monochromator needed to be replaced in order to measure the higher wavelengths. On one of the indices, we were able to measure all the way up to 1.4 microns, however, due to the combined faults of the monochromator and the viewer, it was difficult to see. The index was measured to the highest wavelength that could be seen, and that varied on each axis.

In a previous paper written by Cheng et. al.¹, the index of refraction for each axis is measured to 1.4 microns. We find that it is necessary to study the index of refraction into the higher IR range in order to determine if KTA is usable in other applications. This will be accomplished in the very near future by one of the scientists at Wright Patterson Air Force Base once a new viewer is found and the monochromator is adjusted.

Plans to perform measurements in the UV are in order when the monochromator (which is out for upgrade) is returned. The 1994 Summer Research term ended before the monochromator was returned.

Conclusion

In conclusion, KTA is the latest attempt to improve on the world of nonlinear crystals. It is necessary to study the index of refraction of KTA into the IR range, much higher than has been completed in this study and by Cheng et. al. This will be done by another scientist at Wright Patterson Air Force Base. Then, the index of refraction data taken will be further analyzed to determine if this new crystalline material is an improvement on its predecessor, KTP, and in what ways.

References

1. L.K. Cheng, L.-T. Cheng, J.D. Bierlein, and F.C. Zumsteg, "Properties of doped and undoped crystals of single domain KTiOAsO_4 ," *Appl Phys. Lett.*, vol 62, pp. 346-348, 1993.
2. Tso Yee Fan, C.E. Huang, B.Q. Hu, R.C. Eckardt, Y.X. Fan, Robert L. Byer, and R.S. Feigelson, "Second harmonic generation and accurate index of refraction measurements in flux-grown KTiOPO_4 ," *Appl. Optics*, vol. 26, pp. 2390-2392, 1987.
3. Sears, Francis W., Mark W. Zemansky and Hugh D Young, *University Physics*, Sixth Edition, Addison-Wesley Publishing Company, Reading. 1982. p. 725.
4. "A Study of the Minimum Deviation Method for Refractive Index Measurements," Sandra McPherson, End of Summer Report, 1993 Summer Research Program.

VIRTUAL INSTRUMENTATION
DEVELOPEMENT

Benjamin J. Merrill

Bellbrook High School
3491 Upper Bellbrook Rd.
Bellbrook, OH 45305

Final Report for:
High School Apprenticeship Program
Wright Laboratory

Sponsored by:
Air Force Office of Scientific Research
Bolling Air Force Base, DC

and

Wright Laboratory

August 5, 1994

VISUAL INSTRUMENTATION DEVELOPMENT

Benjamin J. Merrill
Bellbrook High School

Abstract

I spent my summer apprenticeship with the Structural Dynamics Branch of the Flight Dynamics Directorate, Wright Laboratory, Wright Patterson AFB. During this time, I developed a data logging program that was needed to periodically sample up to eight channels of data during extended fatigue panel tests. The data was to be sampled, processed, displayed, and written to file. I used LabVIEW's (by National Instruments) graphical programming software package to develop a program that calculates the root mean square value for eight channels of data and displayed these values on real-time strip charts while it recorded this data to file to later be read into any standard spreadsheet software to be recalled and analyzed. This program was also designed and documented to be later modified in similar tests in this facility.

Benjamin J. Merrill

Introduction

This summer I worked in the Data Analysis Group of the Structural Dynamics Branch which is part of the Flight Dynamics Directorate, Wright Laboratories, WPAFB. The Structural Dynamics Branch is responsible for conducting experiments in vibration, acoustics, and structural dynamics. Many of these tests concern extending the life of existing aircraft by designing and testing new methods of reducing structural fatigue and harmful vibration. It is the Data Analysis Group's job to obtain the data taken in these tests and analyze it in a manner in which the engineers will be able to make use of it. My job was to develop a software program which could read in the data, display it in real-time, and write it to a file which could later be read by a spreadsheet.

Methodology

In particular, the task required reading in eight channels of data. Every thirty minutes, for an unlimited amount of time, the root mean square of each channel was to be calculated and displayed on a strip chart along with a measure of the frequency of one of the channels. The data was then to be stored in a data file where it could later be called and read into a spreadsheet file. The user was to supply the sample rate at which the program would take data in from each channel, the engineering units, the offset values,

and could give each channel a specific identification name. To do this I used the LabVIEW software package. This is a graphical programming package used to create virtual instruments (VI's) for personal computers. I was able to develop a program that displayed eight different strip charts, one for each channel. Controls were set up on the front panel of the VI (figure 1) to tell it which specific devices and channels from which to read in data. There were also controls to set the scan rate, seconds per update, and seconds between updates. When the program is first opened, it prompts the user for a file name and path to write the calculated data to. The program then reads in data for the user-specified amount of time (seconds per update) and calculates the root mean square of these values. Engineering units and offset values supplied by the user for each channel are figured in at this point. The calculated value for each channel is displayed on its appropriate strip chart, converted to a string value and written into an ASCII file. The program then waits for the specified amount of time (seconds between updates) until it repeats the procedure with a new set of data. The program is designed to run until the user presses a stop button on the front panel of the VI, after which the VI completes the current cycle it is on and quits. The file can then be read into any standard spreadsheet program (figure 2) making the data easy to extract and manipulate. The program is only restricted by the input device being used to read in data, and the amount of memory which is available for the program to use.

Conclusion

Currently, this program is being gradually implemented into panel fatigue testing. If it proves to be a more optimal convention of testing than the current methods, it will be used on a regular basis by the test engineers when performing tests of this sort. The program has also been documented and made available to other members of this branch. It was designed to be easily modified by others and can serve as a template for other programs of this sort.

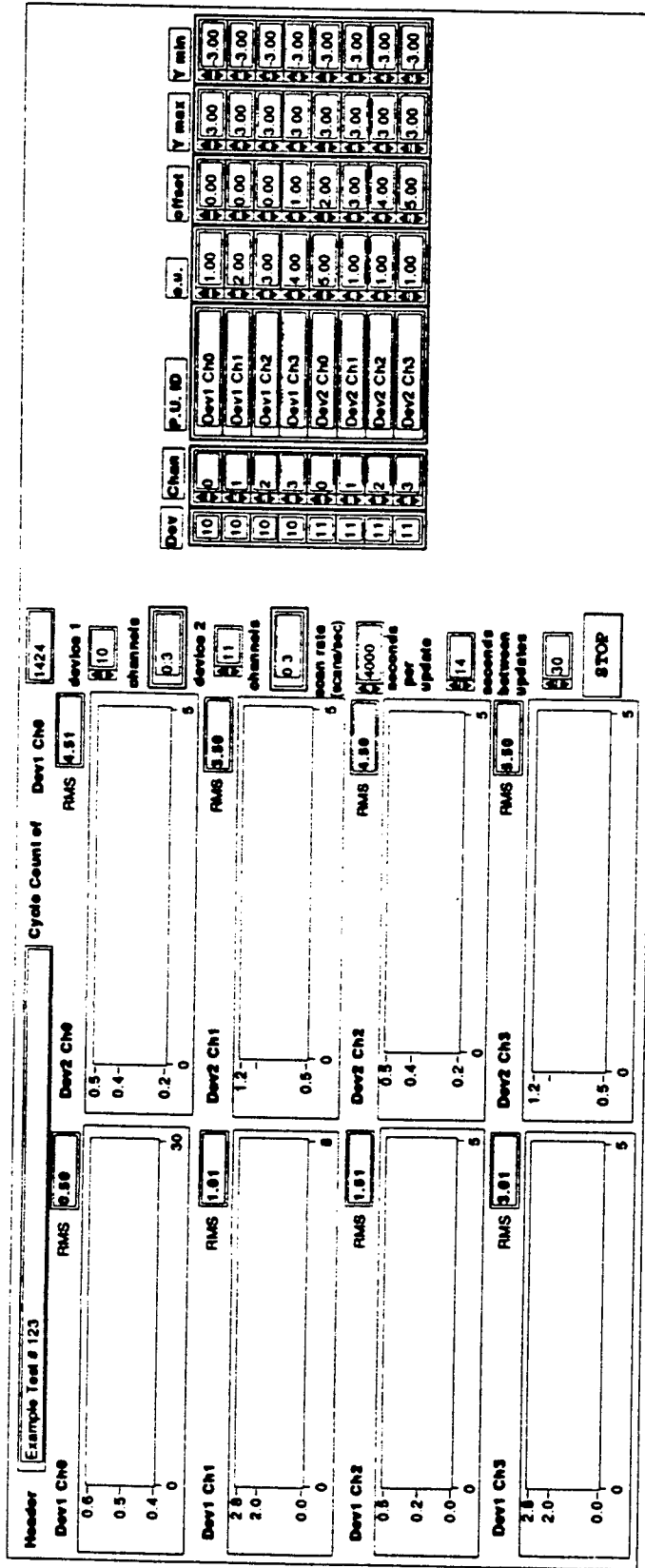


Fig. 1

Fig. 2

Example Test # 123										
Dev	Ch	PUID	E. U.	Offset	Ymax	Ymin				
10	0	Dev1	1	0	3	-3				
10	1	Dev1	2	0	3	-3				
10	2	Dev1	3	0	3	-3				
10	3	Dev1	4	1	3	-3				
11	0	Dev2	5	2	3	-3				
11	1	Dev2	1	3	3	-3				
11	2	Dev2	1	4	3	-3				
11	3	Dev2	1	5	3	-3				
Date	Time	Cycle Count	Dev1Ch0	Dev1Ch1	Dev1Ch2	Dev1Ch3	Dev2Ch0	Dev2Ch1	Dev2Ch2	Dev2Ch3
8/2/94	10:08:26	3352	0.48	0.97	1.45	2.94	3.53	3.29	4.27	5.3
8/2/94	10:09:09	1428	0.5	1.01	1.51	3.01	4.51	3.5	4.5	5.5
8/2/94	10:09:50	1425	0.5	1.01	1.51	3.01	4.51	3.5	4.5	5.5
8/2/94	10:10:32	1424	0.5	1	1.51	3.01	4.51	3.5	4.5	5.5
8/2/94	10:11:13	1426	0.5	1.01	1.51	3.01	4.51	3.5	4.5	5.5
8/2/94	10:11:54	1424	0.5	1.01	1.51	3.01	4.51	3.5	4.5	5.5
8/2/94	10:12:36	1426	0.5	1.01	1.51	3.01	4.51	3.5	4.5	5.5
8/2/94	10:13:17	1425	0.5	1.01	1.51	3.01	4.51	3.5	4.5	5.5
8/2/94	10:13:59	1426	0.5	1.01	1.51	3.01	4.51	3.5	4.5	5.5
8/2/94	10:14:40	1425	0.5	1.01	1.51	3.01	4.51	3.5	4.5	5.5
8/2/94	10:15:22	1425	0.5	1.01	1.51	3.01	4.51	3.5	4.5	5.5
8/2/94	10:16:03	1424	0.5	1.01	1.51	3.01	4.51	3.5	4.5	5.5

PORTING SPICE 2G.6 TO UNIX

Gary W. Midkiff

August 1994

Fairmont High School
3301 Shroyer Road
Kettering, OH 45429

Final Report for:
High School Apprenticeship Program
Wright Laboratories

Sponsored by:
Air Force Office of Scientific Research
Bolling Air Force Base, DC

and

Wright Laboratories

PORTING SPICE 2G.6 TO UNIX

Gary W. Midkiff

Fairmont High School

Abstract

Spice 2G.6 was originally written in fortran and assembly language for VAX-11/780 VMS operating system. However, the VMS operating systems are rapidly being replaced by Unix, and therefore Spice 2G.6 needed to be modified in order to run on Unix machines. Spice 2G.6 was not easily ported over because some of the original subroutines are compiled in VAX assembly language, which is not compatible between the different machines. These subroutines had to be rewritten into a higher level language that would be compatible with many different systems. The C language was chosen to replace the assembly language for the porting of Spice 2G.6 to the SPARC and HP Series 700 computers.

Acknowledgements

It is important to note that other people have contributed time and effort to this project also. Recognition should go to Robert Ewing, Scott Bilik, and Val Jogai for there help. It should also be noted that Othman Ahmad compiled a version for DOS and some of this C code influenced the C routine used in this version.

PORTING SPICE 2G.6 TO UNIX

Gary W. Midkiff

1 Introduction

Spice is a computer-aided simulation program that enables an engineer to design a circuit and then simulate the design on a computer. *Spice*, an acronym for a Simulation Program with Integrated Circuit Emphasis, was developed by the Electronics Research Laboratory of the University of California and has been available to the public since 1975^[1]. *Spice 2G.6* is a public domain software program originally compiled for VAX/VMS. *Spice 2G.6* is a very useful and effective tool for electrical engineering. However, the VAX machine at W.P.A.F.B. (Wright-Patterson Air Force Base) is soon to be eliminated, and replacing *Spice 2G.6* with a new registered version for Unix machines would be very expensive. To avoid this problem *Spice 2G.6* was modified so that it could be executed on the HP and Sparc workstations. This is the first known *porting* of the fortran code to Unix, where other *Spice* versions, such as *Spice 3.0*, were rewritten in C, and then *ported* to Unix.

2 Methodology

Spice 2G.6 was originally written for the VAX/VMS in about 18000 lines of fortran. At the time, fortran was still a popular programming language, but it was tedious and slow performing memory

to memory copies. Therefore, several of Spice's subroutines were compiled in assembly language. Assembly is much faster performing such tasks. The problem is that the assembly language for VAX/VMS is not the same as the assembly language for Unix machines. Assembly is a low level, hardware dependent language. These subroutines had to be rewritten in a higher level language. This makes Spice portable to many different machines because high level languages are not hardware dependent. If the assembly had merely been rewritten in assembly for the HP or Sparc, the new version would still not be portable to many different machines.

The first step in porting the code was to rewrite the following assembly subroutines: move, copy4, copy8, copy16, zero4, zero8, zero16 in fortran, and include them in the main program. I translated the routines one at a time, recompiled and ran several tests to check for errors along the way. When I came to copy4, the program failed. Copy4 appeared to be no more difficult than any of the other routines. Its purpose was to take a value in an array and copy it to a different position in the array. I ran different tests to find out where the routine failed. Copy4 is called several times during the execution of Spice. Each time copy4 was called, I had the program print out the source and destination locations and values in the array. The very first call for copy4 worked, but the next time it was called, the program failed.

At this point I began looking for other ways to get around this routine. I switched to the C programming language and tried working with that for a while. I also surfed the net for information on Spice and other solutions to my problem.

Eventually, by examining data I printed out as the program was running, I discovered that the parameters passed to copy4 were asking it to take x many values in the array and copy them to y number of locations farther in the array. However, x was bigger than y , so the routine was overwriting data that had not been copied yet.

Upon this discovery, and files retrieved from the internet, I was able to write a c program to handle all of the original assembly routines. The main program, and the c subroutine were compiled and linked. For simplicity, some timing and dating routines were eliminated as they are not necessary and were very difficult to include.

Upon completion of this project, I was able to run many different circuit analyses, such as the CMOS inverter in Figure 1^[2], with Spice on the HP and the Sparc. The Sparc was phenomenally faster than the old VAX/VMS machine despite the fact that the high level language is slower than assembly. The HP 700 series was even faster than the Sparc.

Appendix A (C Code)

The following is the C routines for the HP's and Sparc's.

```
HP: ANSI C
Compile: %cc -c -Aa hpcopy.c
Link: %f77 spice.o hpcopy.o

/* File   : copyhp.c
   Author : Robert Ewing, Scott Bilik, Val Jogai, Gary Midkiff
   Updated: JUL 21, 94
   Purpose: Replaces Copy4, Copy8, & Copy16
*/
#include <stdio.h>
#include <string.h>
#include <ctype.h>
#include <memory.h>
#include <stdlib.h>

#   define bcopy(s, d, l) memcpy(d, s, l)
#   define bzero(b, l) memset(b, 0, l)

static void
mcopy (register char *from, register char *to, register int size);

void
move(register char *array1, int *index1, register char *array2,
      int *index2, register int *length )
{
array1 += *index1 - 1;
```

```
array2 += *index2 - 1;
mcopy( array2, array1, *length );
}
```

```
void
copy4(char *from, char *to,int *length )
{
mcopy( from, to, *length * 4 );
}
```

```
void
copy8(char *from, char *to,int *length )
{
mcopy( from, to, *length * 8 );
}
```

```
void
copy16(char *from, char *to,int *length )
{
mcopy( from, to, *length * 8 );
}
```

```
void
zero4( char *array, unsigned *length )
{
bzero( array, *length * 4 );
}
```

```
void
zero8( char *array, unsigned *length )
{
bzero( array, *length * 8 );
}
```

```
void
zero16( char *array, unsigned *length )
{
bzero( array, *length * 8 );
}
```

```
/*
 * mcopy - copy memory.
 */
static void
mcopy( register char *from, register char *to, register int size)
{
```

```

    register char *frome, *toe;

    if (size <= 0) return;

    frome = from + size;
    if (from >= to || frome <= to) {
bcopy (from, to, size);
    }
    else {
/* Source and destination overlap with destination above source.
Therefore a forward copy will bash later source to be copied.
Use a backward copy instead. */
toe = to + size;
if (((unsigned)to ^ (unsigned)from) & 3) != 0 || size < 4) {
    /* alignment of source and destination not identical;
    use a simple byte copy. */
    do {
*--toe = *--frome;
    } while (frome != from);
    }
    else {
        while (((unsigned)toe & 3) != 0) {
*--toe = *--frome;
size -= 1;
        }
        size -= 16;
        while (size >= 0) {
toe -= 16;
frome -= 16;
((int*)toe)[3] = ((int*)frome)[3];
((int*)toe)[2] = ((int*)frome)[2];
((int*)toe)[1] = ((int*)frome)[1];
((int*)toe)[0] = ((int*)frome)[0];
size -= 16;
        }
        size += 16 - 4;
        while (size >= 0) {
toe -= 4;
frome -= 4;
((int*)toe)[0] = ((int*)frome)[0];
size -= 4;
        }
        size += 4;
        while (size > 0) {
*--toe = *--frome;
size -= 1;
        }
    }
}
}

```

Sparc: ANSI C++
Compile: %CC -c sparccopy.c
Link: %f77 spice.o sparccopy.o

```
/* File   : copy.c
   Author  : Robert Ewing, Scott Bilik, Val Jogai, Gary Midkiff
   Updated: JUL 21, 94
   Purpose: Replaces Copy4, Copy8, & Copy16
*/
#include <stdio.h>
#include <string.h>
#include <ctype.h>
#include <memory.h>
#include <stdlib.h>

#       define bcopy(s, d, l) memcpy(d, s, l)
#       define bzero(b, l) memset(b, 0, l)

extern "C" {
static void
mcopy (register char *from, register char *to, register int size);
void
move_(register char *array1, int *index1, register char *array2,
      int *index2, register int *length );
void
copy4_(char *from, char *to, int *length );
void
copy8_(char *from, char *to, int *length );
void
copy16_(char *from, char *to, int *length );
void
zero4_( char *array, unsigned *length );
void
zero8_( char *array, unsigned *length );
void
zero16_( char *array, unsigned *length );
}

void
move_(register char *array1, int *index1, register char *array2,
      int *index2, register int *length )
{
array1 += *index1 - 1;
array2 += *index2 - 1;
mcopy( array2, array1, *length );
}
```

```

void
copy4_(char *from, char *to,int *length )
{
mcopy( from, to, *length * 4 );
}

```

```

void
copy8_(char *from, char *to,int *length )
{
mcopy( from, to, *length * 8 );
}

```

```

void
copy16_(char *from, char *to,int *length )
{
mcopy( from, to, *length * 8 );
}

```

```

void
zero4_( char *array, unsigned *length )
{
bzero( array, *length * 4 );
}

```

```

void
zero8_( char *array, unsigned *length )
{
bzero( array, *length * 8 );
}

```

```

void
zero16_( char *array, unsigned *length )
{
bzero( array, *length * 8 );
}

```

```

/*
 * mcopy - copy memory.
 */
static void
mcopy (register char *from, register char *to, register int size)
{
    register char *frome, *toe;

    if (size <= 0) return;

```

```

    frome = from + size;
    if (from >= to || frome <= to) {
bcopy (from, to, size);
    }
    else {
/* Source and destination overlap with destination above source.
   Therefore a forward copy will bash later source to be copied.
   Use a backward copy instead. */
toe = to + size;
if (((unsigned)to ^ (unsigned)from) & 3) != 0 || size < 4) {
    /* alignment of source and destination not identical;
       use a simple byte copy. */
    do {
*--toe = *--frome;
    } while (frome != from);
    }
    else {
        while (((unsigned)toe & 3) != 0) {
*--toe = *--frome;
size -= 1;
        }
        size -= 16;
        while (size >= 0) {
toe -= 16;
frome -= 16;
*((int*)toe)[3] = *((int*)frome)[3];
*((int*)toe)[2] = *((int*)frome)[2];
*((int*)toe)[1] = *((int*)frome)[1];
*((int*)toe)[0] = *((int*)frome)[0];
size -= 16;
        }
        size += 16 - 4;
        while (size >= 0) {
toe -= 4;
frome -= 4;
*((int*)toe)[0] = *((int*)frome)[0];
size -= 4;
        }
        size += 4;
        while (size > 0) {
*--toe = *--frome;
size -= 1;
        }
    }
}
}

```

Note that there are some differences in the two routines.

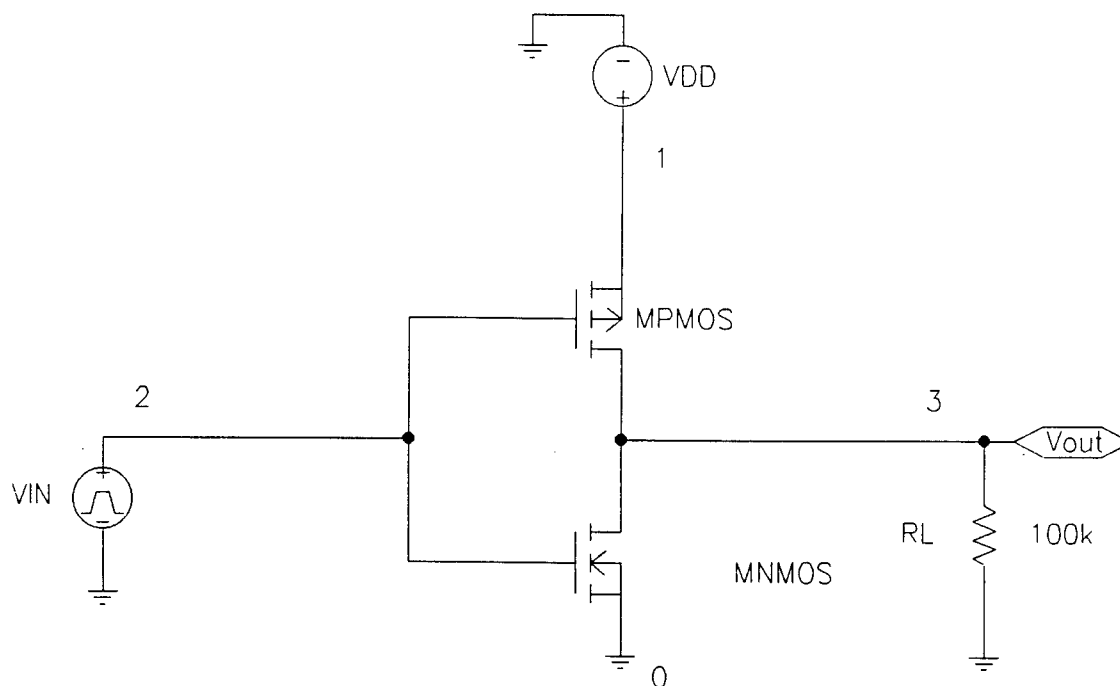


Figure 1: CMOS Inverter Circuit

Appendix B (Example of Output) The following pages includes the schematic circuit description file and results for the Spice2G.6 simulation of a CMOS inverter as shown in Figure 1.

```

****      INPUT LISTING      TEMPERATURE =      27.000 DEG C

VDD      1 0 DC 5V
VIN      2 0 DC 5V
+ PULSE 0 5 0 1NS 1NS 20US 40US
RL       3 0 100K
M1      3 2 1 1 MPMOS W=20U L=1U
M2      3 2 0 0 MNMOS W=5U L=1U

.MODEL MPMOS PMOS(VTO=-2 LEVEL=1 KP=450.00E-06 GAMMA=0 PHI=0.6
+ RD=5 RS=2 CBD=5.00E-12 CBS=2.00E-12
+ CGSO=1.00E-12 CGDO=1.00E-12 CGBO=1.00E-12 TOX=0)

.MODEL MNMOS NMOS(VTO=2 LEVEL=1 KP=45.00E-06 GAMMA=0 PHI=0.6
+ RD=5 RS=2 CBD=5.00E-12 CBS=2.00E-12
+ CGSO=1.00E-12 CGDO=1.00E-12 CGBO=1.00E-12 TOX=0)

.TRAN 1US 80US
.TF V(3) VIN
.PLOT TRAN V(3) V(2)
.END

```

**** MOSFET MODEL PARAMETERS TEMPERATURE = 27.000 DEG C

	MPMOS	MNMOS
TYPE	PMOS	NMOS
LEVEL	1.000	1.000
VTO	-2.000	2.000
KP	4.50D-04	4.50D-05
GAMMA	.000	.000
PHI	.600	.600
RD	5.000	5.000
RS	2.000	2.000
CBD	5.00D-12	5.00D-12
CBS	2.00D-12	2.00D-12
CGSO	1.00D-12	1.00D-12
CGDO	1.00D-12	1.00D-12
CGBO	1.00D-12	1.00D-12
TOX	.00D+00	.00D+00

**** SMALL SIGNAL BIAS SOLUTION TEMPERATURE = 27.000 DEG C

NODE	VOLTAGE	NODE	VOLTAGE	NODE	VOLTAGE
(1)	5.0000	(2)	.0000	(3)	4.9978

VOLTAGE SOURCE CURRENTS

NAME	CURRENT
VDD	-4.998D-05
VIN	.000D+00

TOTAL POWER DISSIPATION 2.50D-04 WATTS

**** OPERATING POINT INFORMATION TEMPERATURE = 27.000 DEG C

**** MOSFETS

	M1	M2
MODEL	MPMOS	MNMOS
ID	-5.00E-05	1.93E-12

```

VGS      -5.000      .000
VDS      -.002      4.998
VBS      .000      .000
VTH      -2.000      2.000
VDSAT    -3.000      .000
GM       1.67E-05     .00E+00
GDS      2.70E-02     .00E+00
GMB      .00E+00     .00E+00
CBD      4.99E-12     1.86E-12
CBS      2.00E-12     2.00E-12
CGSOVL   2.00E-17     5.00E-18
CGDOVL   2.00E-17     5.00E-18
CGBOVL   1.00E-18     1.00E-18
CGS      .00E+00     .00E+00
CGD      .00E+00     .00E+00
CGB      .00E+00     .00E+00

```

**** SMALL-SIGNAL CHARACTERISTICS

```

V(3)/VIN      = -6.174D-04
INPUT RESISTANCE AT VIN      = 1.000D+20
OUTPUT RESISTANCE AT V(3)    = 4.404D+01

```

**** INITIAL TRANSIENT SOLUTION TEMPERATURE = 27.000 DEG C

```

NODE   VOLTAGE   NODE   VOLTAGE   NODE   VOLTAGE
( 1)   5.0000   ( 2)   .0000   ( 3)   4.9978

```

VOLTAGE SOURCE CURRENTS

```

NAME      CURRENT
VDD       -4.998D-05
VIN        .000D+00

```

TOTAL POWER DISSIPATION 2.50D-04 WATTS

**** OPERATING POINT INFORMATION TEMPERATURE = 27.000 DEG C

**** MOSFETS

```

MODEL    M1      M2
          MPHOS  MNMOS
ID       -5.00E-05  1.93E-12
VGS      -5.000      .000

```



```

MOVAL  04(AP),R6      ; GET ADDRESS OF 'TO' ARGUMENT
MOVL   08(AP),R7      ; GET STARTING BYTE OF 'TO'
DECL   R7             ; SUBTRACT 1 TO GET DISPLACEMENT
ADDL2  R7,R6          ; ADD TO GET STARTING ADDRESS
MOVAL  012(AP),R8     ; GET ADDRESS OF 'FROM' ARGUMENT
MOVL   016(AP),R7     ; GET STARTING BYTE OF 'FROM'
DECL   R7             ; SUBTRACT 1 TO GET DISPLACEMENT
ADDL2  R7,R8          ; R8 IS STARTING BYTE ADDRESS
MOVC3  R9,(R8),(R6)   ; MOVE R9 CHARACTERS FROM (R8)
; TO (R6)
EXIT:  RET
.END

```

```

.TITLE COPY      BLOCK COPY ROUTINE
;-----*
;  ROUTINE:      COPY                                     *
;-----*
;  LANGUAGE:     VAX-11 MACRO                           *
;  SYSTEM:       VAX-11/780                             *
;-----*
;  DATE:        06-04-80                               *
;-----*
;  LAST CHANGE:                               BY        *
;-----*
;  PURPOSE:      THIS ROUTINE USES THE MOVC INSTRUCTION TO COPY *
;                BLOCKS OF MEMORY FROM ONE LOCATION TO ANOTHER *
;                IN AS EFFICIENT A MANNER AS POSSIBLE         *
;-----*
;  CALLED BY:    PRACTICALLY EVERY ROUTINE IN SPICE        *
;-----*
;  EXTERNALS:    NONE                                       *
;-----*
.PSECT $CODE,PIC,CON,REL,LCL,SHR,EXE,RD,NOWRT,LONG
.ENTRY COPY4r,~M<R2,R3,R4,R5,R6,R7,R8,R9,R10,R11>
ASHL  #2,012(AP),R6  ; CONVERT WORDS TO BYTES AND LOAD R6
JMP   COPY          ; GO TO SECTION THAT ACTUALLY COPIES
;
;
.ENTRY COPY8,~M<R2,R3,R4,R5,R6,R7,R8,R9,R10,R11>
ASHL  #3,012(AP),R6  ; CONVERT # OF R*8 WORDS TO BYTES, LOAD R6
JMP   COPY          ; GO TO SECTION THAT ACTUALLY COPIES
;
;
.ENTRY COPY16X,~M<R2,R3,R4,R5,R6,R7,R8,R9,R10,R11>
ASHL  #3,012(AP),R6  ; GET NUMBER OF COMPLEX WORDS TO COPY
; AND CONVERT TO BYTES, ASSUMING 8 BYTES

```

```

; PER COMPLEX PAIR.
JMP     COPY           ; LET'S GET THIS OVER WITH
;
;
.ENTRY COPYBX, ^M<R2,R3,R4,R5,R6,R7,R8,R9,R10,R11>
MOVL    012(AP),R6    ; GET NUMBER OF BYTES TO MOVE
;
;
COPY:   TSTL    R6           ; TEST FOR NUMBER OF BYTES LESS THAN OR
BLEQ   EXIT           ; EQUAL TO ZERO
MOVAL  04(AP),R7       ; GET ADDRESS OF 'FROM' ARGUMENT
MOVAL  08(AP),R8       ; GET ADDRESS OF 'TO' ARGUMENT
MOVL   #~X7FFF,R9      ; USEFUL CONSTANT
CMPL   R9,R6          ; COMPARE TO 2**15-1 (MAXIMUM FOR ONE MOV)
BGEQ   LASTMOVE       ; IF ONLY ONE MOVE REQUIRED, DO IT
CMPL   R7,R8          ; BRANCH IF FROM ADDRESS IS LESS THAN
BLSS   BACKWRDS       ; TO ADDRESS
;
;
FORWRDS:                ; COPY IN FORWARD DIRECTION IS OK
CMPL   R9,R6          ; COMPARE TO 2**15-1 (MAX FOR ONE MOV)
BGEQ   LASTMOVE       ; IF R6 IS LESS, ONE MOVE IS ALL IT TAKES
MOVC3  R9,(R7),(R8)   ; MOVE AS MANY AS YOU CAN WITH ONE MOV
ADDL2  R9,R7          ; UPDATE R7 ADDRESS
ADDL2  R9,R8          ; UPDATE R8 ADDRESS
SUBL2  R9,R6          ; ADJUST BYTES LEFT TO MOVE BY AMOUNT MOVED
JMP    FORWRDS       ; THEN DO IT AGAIN
;
;
BACKWRDS:                ; COPY IN REVERSE BLOCKS NECESSARY
MOVL   R7,R10         ; COPY REGISTER FOR FROM ADDRESS
MOVL   R8,R11         ; COPY REGISTER FOR TO ADDRESS
ADDL2  R6,R10         ; ADD LENGTH
ADDL2  R6,R11         ; ADD LENGTH
BACKLOOP:                ;
SUBL2  R9,R10         ; SUBTRACT LENGTH OF MOVE VECTOR
SUBL2  R9,R11         ; AND AGAIN
MOVC3  R9,(R10),(R11) ; MOVE BLOCK
SUBL2  R9,R6          ; ADJUST BYTES LEFT TO MOVE BY AMOUNT MOVED
CMPL   R9,R6          ; COMPARE TO 2**15-1 (MAX FOR ONE MOV)
BGEQ   LASTMOVE       ; IF R6 LESS THAN R9, DO LAST BLOCK
JMP    BACKLOOP       ; IF NOT, LOOP AND DO IT AGAIN
;
;
LASTMOVE:                ; LETS GET THIS OVER WITH
MOVC3  R6,(R7),(R8)   ; NOW WASN'T THAT EASY?
;
EXIT:   RET           ;
.END

```

```

.TITLE ZERO      BLOCK ZERO ROUTINE
;-----*
;   ROUTINE:     ZERO                                     *
;-----*
;   LANGUAGE:    VAX-11 MACRO                             *
;   SYSTEM:      VAX-11/780                               *
;-----*
;   DATE:        06-04-80                                 *
;-----*
;   LAST CHANGE:                BY                       *
;-----*
;   PURPOSE:     THIS ROUTINE USES THE MOVCL INSTRUCTION TO ZERO *
;                VERY LARGE (OR VERY SMALL) BLOCKS OF MEMORY *
;                IN AS EFFICIENT A MANNER AS POSSIBLE *
;-----*
;   CALLED BY:   PRACTICALLY EVERY ROUTINE IN SPICE *
;-----*
;   EXTERNALS:   NONE                                     *
;-----*
.PSECT $CODE,PIC,COM,REL,LCL,SHR,EXE,RD,NOWRT,LONG
.ENTRY ZERO4,~M<R2,R3,R4,R5,R6,R7,R9>
ASHL  #2,@8(AP),R6 ; CONVERT WORDS TO BYTES, LOAD R6
JMP   ZERO        ; GO TO SECTION THAT ACTUALLY ZEROS
;
;
.ENTRY ZERO8,~M<R2,R3,R4,R5,R6,R7,R9>
ASHL  #3,@8(AP),R6 ; CONVERT # OF R*8 WORDS TO BYTES
JMP   ZERO        ; GO TO SECTION THAT ACTUALLY ZEROES
;
;
.ENTRY ZERO16,~M<R2,R3,R4,R5,R6,R7,R9>
ASHL  #3,@8(AP),R6 ; THIS ASSUMES 8 BYTES PER COMPLEX PAIR
JMP   ZERO        ; LET'S GET THIS OVER WITH
;
;
.ENTRY ZEROB,~M<R2,R3,R4,R5,R6,R7,R9>
MOVL  @8(AP),R6    ; GET NUMBER OF BYTES TO ZERO
;
;
ZERO:  TSTL   R6          ; TEST FOR NUMBER OF BYTES LESS THAN OR
BLEQ  EXIT          ; EQUAL TO ZERO
MOVAL @4(AP),R7      ; GET ADDRESS OF ARGUMENT
MOVL  #~X7FFF,R9    ; USEFUL CONSTANT
;
;

```

```

LOOP:
CMPL R9,R6 ; COMPARE TO 2**15-1 (MAX FOR ONE MOV)
BGEQ LASTZERO ; IF R6 IS LESS, ONE MOV IS ALL IT TAKES
MOVCS #0,(R7),#0,R9,(R7)
; ZERO AS MANY AS YOU CAN WITH ONE MOV
ADDL2 R9,R7 ; UPDATE R7 ADDRESS
SUBL2 R9,R6 ; ADJUST BYTES LEFT TO MOVE BY AMOUNT MOVED
JMP LOOP ; THEN DO IT AGAIN
;
;
LASTZERO: ; LETS GET THIS OVER WITH
MOVCS #0,(R7),#0,R6,(R7)
; NOW WASH'T THAT SIMPLE?
;
EXIT: RET ;
.END

```

References

- [1] J. W. Nilsson, *Introduction to Spice*. Addison-Wesley Publishing Co., third ed., 1990.
- [2] "EE649 digital and pulse system." VHDL and SPICE Simulation of a Basic Inverter, Wright State University, 1994.

A STUDY OF THE ORGANIC REACTIONS OF PHTHALOCYANINES, ALLYLOXY GROUPS, AND
WAVEGUIDE MEASUREMENTS OF SPUN COATED SILOXANE-TOLUENE SOLUTIONS

Karthik Natarajan

Beavercreek High School
2660 Dayton-Xenia Road
Beavercreek, OH. 45434

Final Report for:
High School Apprentice Program
Wright-Patterson Air Force Base Materials Laboratory

Sponsored by:
Air Force Office of Scientific Research
Bolling Air Force Base, DC

and

Wright-Patterson Air Force Base Materials Laboratory

August 1994

30 - 1

A STUDY OF THE ORGANIC REACTIONS OF PHTHALOCYANINES, ALLYLOXY GROUPS, AND
WAVEGUIDE MEASUREMENTS OF SPUN COATED SILOXANE-TOLUENE SOLUTIONS

Karthik Natarajan
Beavercreek High School

(NOTE: Unlike most reports which deal with only one project, this report deals with three different projects that were performed this summer at Wright-Patterson Air Force Base Materials Laboratory. Therefore, there are presented here three different abstracts, and the report itself consists of three different introductions, methodologies, results, and conclusions.)

Abstract I

Phthalocyanines with sulfonic acid groups attached were always thought of and considered water-soluble, as a result of these groups. As a result, we attempted to perform a series of two reactions in solution, starting with copper phthalocyanine tetrasulfonic acid. Our first reaction would simply extract the copper out of the compound, leaving metal-free phthalocyanine tetrasulfonic acid, while our second would put lead into this metal-free compound. What we found out while performing our first reaction was that our copper compound was completely insoluble in water. Upon trying with a nonpolar solvent as well as an intermediate solution, we found similar results. Our conclusion from our analysis showed that in general, phthalocyanines are inert solutes, even with highly polar functional groups attached.

Abstract II

The allyloxy group is a special functional group in organic chemistry with the structural formula, $H_2C=CH-CH_2-O-$. We performed a series of three reactions, leading to the synthesis of 4-allyloxy-benzoic acid, 4-allyloxy-benzoyl chloride, and 4-allyloxy-1(4-nitrobenzene) piperidine. What we learned from these experiments was that although these reactions yielded low amounts of products, the ethanol we used in extracting our product almost completely

removed any impurities present; therefore, ethanol is a good solvent for obtaining purity, but a bad one for obtaining high yields.

Abstract III

The thickness of thin films is dependent upon a variety of factors. Two of these are the concentration of the solution and the speed at which a film is coated onto a material, in our case, glass microscope slides and silicon oxide wafers. This summer, we used Wacker-Blue siloxane dissolved in toluene as our solution. We varied each solution's concentration and its spin speed when making a film; then we used the instrument, *Dektak IIA* to measure each's thickness. We made graphs from these measurements. We found that a film's thickness is directly proportional to its concentration and inversely proportional to its spin speed. We also found that as a film's concentration increases, its overall homogeneity decreases.

A STUDY OF THE ORGANIC REACTIONS OF PHTHALOCYANINES, ALLYLOXY GROUPS AND WAVEGUIDE MEASUREMENTS OF SPUN COATED SILOXANE-TOLUENE SOLUTIONS

Karthik Natarajan

Introduction I

During the last thirty years, there has been an increasing demand in the production of phthalocyanine and its numerous derivatives. This has been primarily the result of their increasing number of applications, not only as dyes, but also as colorants, inks, paints, catalysts, xerography, and medicine, to name a few. Chemical and materials engineers have patented many different manufacturing processes for their production, but still need the information from chemists on different methods of laboratory synthesis so as to adjust it to a large-scale production. Copper phthalocyanine tetrasulfonic acid is one particular phthalocyanine derivative. However, theoretically, if we treat a solution of it with slightly concentrated sulfuric acid, and later with Lead (II) acetate, Lead phthalocyanine tetrasulfonic acid should form. A primary advantage of applying this technique is that it will produce another phthalocyanine derivative using an already made one, and can thereby avoid starting from scratch. Unfortunately, the above reaction works well only in solution, so if one of the materials is insoluble in solvents that the other reactants are soluble in, the reaction will not occur.

Methodology I

The theoretical method of producing Lead phthalocyanine tetrasulfonic acid from Copper phthalocyanine tetrasulfonic acid appeared simple, although in actuality, we encountered a significant obstacle that prevented us from attaining our goal. We first had to prepare 250 ml. of aqueous 50% sulfuric acid from concentrate, using dilution. Then, we had to add a few grams of our copper phthalocyanine derivative. Using a hot plate and a magnetic stirring bar, we heated the reaction mixture to about 60 degrees Celsius. Theoretically, what should have

happened was the formation of insoluble copper sulfate, which would eventually be filtered, and soluble metal-free phthalocyanine tetrasulfonic acid obtained. After letting it stir overnight, we used a syringe in order to filter out what we thought to be copper sulfate. However, the filtered liquid we got appeared clear in color; if the reaction did occur, the filtered liquid would have been light blue in color. This observation showed that no reaction occurred, and copper phthalocyanine tetrasulfonic acid was completely insoluble in water. We now faced a new problem: In what appropriate solvent could we carry out the reaction?

We next tried using a different solvent, this time testing the compound's solubility before reacting it. We used dimethylformamide, an aprotic organic solvent; Dimethylformamide, with its polar and non-polar ends, dissolves both polar and non-polar material, and if it dissolved our compound, we could carry the reaction out in it. Upon dissolving and syringing, we again discovered a clear liquid.

Last of all, we used a surfactant, X-100, and an ultraviolet spectrophotometer. We made nine mixtures using the same amount of water and surfactant, but varying the amount of our compound in each; in one sample, we added no phthalocyanine. In each case, a blue solution appeared to have formed. In order to check the validity of this, we used a UV spectrophotometer and the phthalocyanine-free water-surfactant solution as our background source, we analyzed each sample for its absorbance. What we discovered was that the places of absorbance were very precisely the same for each sample.

Results I

The first trial using water showed that no reaction between our compound and sulfuric acid had occurred, even though we heated the mixture to a high temperature and stirred it vigorously. This first showed that copper phthalocyanine tetrasulfonic acid was insoluble in highly polar solvents, such as water, as shown by its clearness. The second experiment showed that our phthalocyanine compound was insoluble even in an organic solvent, again because of the clearness of the solvent. The third experiment showed that although our compound appeared to go into solution, it actually did not, but instead, formed either a colloidal or suspended mixture. This was verified by the fact that our samples did not obey Beer's Law, whereby the absorbance

of light by a solution is directly proportional to its concentration; instead, our results showed the absorbances to be constant for all the samples.

Conclusion I

From all of our results, we could make one generalized conclusion: that phthalocyanine derivatives, with sulfonic acid groups attached, are completely insoluble in all types of solvents. Although it has been known for quite some time that phthalocyanines are inert solutes, it has always been known in organic chemistry that sulfonic acid groups (HSO_3^-) tend to make hydrophobic compounds more hydrophilic. With the addition of four of these groups on all four corners of the molecule, it was thought that it would be highly water-soluble. As a result of its insolubility and the fact that the metal atom in the center does not affect the solubility of the compound by much, we concluded that any phthalocyanine derivative, with sulfonic acid groups, would be completely insoluble in any type of solvent. As a result of this obstacle, we were unable to move on to synthesize our wanted lead phthalocyanine derivative from our copper phthalocyanine derivative.

Introduction II

Because of its vastness in the number of compounds and reactions, organic chemistry is constantly concerned with synthesizing either new or old compounds using different reactions. This summer, at WPAFB Materials Laboratory, the chemistry of allyloxy group compounds were studied. The allyloxy group has the formula of $\text{H}_2\text{C}=\text{CH}-\text{CH}_2-\text{O}-$. We synthesized three allyloxy based compounds, 4-allyloxy-benzoic acid ($\text{H}_2\text{C}=\text{CH}-\text{CH}_2-\text{O}-\text{C}_6\text{H}_4-\text{COOH}$), 4-allyloxy-benzoyl chloride ($\text{H}_2\text{C}=\text{CH}-\text{CH}_2-\text{O}-\text{C}_6\text{H}_4-\text{COCl}$), and 4-allyloxy-1(4-nitrobenzene) piperidine ($\text{CH}_2=\text{CH}-\text{CH}_2-\text{O}-\text{C}_5\text{H}_4\text{N}-\text{C}_6\text{H}_5\text{NO}_2$).

Methodology II

The synthesis of 4-allyloxy-benzoic acid was the simplest among the three. Preparing it took only one step. We mixed 7.75 grams of 4-hydroxy-benzoic acid ($\text{HO-C}_6\text{H}_4\text{-COOH}$) with 5.10 milliliters (7.13 grams) of allyl bromide ($\text{CH}_2=\text{CH-CH}_2\text{-Br}$) all in a methanol solution. We heated and stirred the reaction mixture. While heating and stirring, we slowly pipetted in 50 milliliters of 3.36 M KOH solution as a homogeneous catalyst. We let the reaction proceed overnight under the hot plate and magnetic stirrer. In the morning, we blew nitrogen to evaporate off any methanol or water remaining. Then we added water to our impure product to dissolve the KOH and some of our product. Using a separatory funnel, we added ethanol which would dissolve our product more than water, and then we separated the two liquids; we performed this procedure three times. Afterwards, we took our ethanol solution and refrigerated it to recrystallize our product. Two days later, we used vacuum filtration to obtain our product, and vacuum dried it in the oven. Since our entire reaction was in a 1 to 1 molar ratio, our theoretical yield was 10 grams; instead, we got only 3.03 grams to give us a 30.3% yield of our product. Using NMR and FTIR spectroscopy and previously obtained results of our product from these instruments, to check our results, we found that we did indeed obtain the desired product, 4-allyloxy-benzoic acid, and FTIR also showed that our product was almost 100% pure.

Our second reaction involved the synthesis of 4-allyloxy-benzoyl chloride. In this reaction, 4-allyloxy-benzoic acid reacts with liquid thionyl chloride (SOCl_2) in the presence of dimethylformamide ($\text{H-CO-N-(CH}_3)_2$) to produce our desired product as well as the by-products, HCl(g) and $\text{SO}_2\text{(g)}$. Into a 50 milliliter round-bottom flask with a condenser attached, we added 12.5 grams of 4-allyloxy-benzoic acid, 17 milliliters of thionyl chloride, and 2 to 5 drops of dimethylformamide. Because of thionyl chloride's violent reaction with water, we used an argon atmosphere to protect our mixture from water vapor in the air. Then, we heated our mixture at 60°C and let it stir for two hours. Afterwards, we removed the excess thionyl chloride using a vacuum; Later, we vacuum distilled our product at 100°C and 1 torr. As before, our reagents reacted in a one to one molar ratio, and we calculated our theoretical

yield to be 15 grams. We obtained 12.52 grams to get a percent yield of 83.5%.

In our third reaction, 4-allyloxy-1(4-nitrobenzene) piperidine was synthesized. This synthesis, unlike the previous two, was not a single step process, but involved two different steps. In the first, 0.6 grams of 4-hydroxy-1(4-nitrobenzene) piperidine ($\text{HO-C}_5\text{H}_4\text{-C}_6\text{H}_4\text{-NO}_2$) is mixed with the solvent, dimethylsulfoxide ($(\text{CH}_3)_2\text{S=O}$), in a round-bottom double neck 300 milliliter flask, along with a magnetic stir bar. Slowly, 0.065 grams of NaH(s) was added, and the reaction mixture was allowed to reflux in order to complete the first step; in this step, sodium 4-oxy-1(4-nitrobenzene) piperidine ($[\text{Na}^+[\text{O-C}_5\text{H}_4\text{-C}_6\text{H}_4\text{-NO}_2]^-]$) was formed. In the second step, 0.236 milliliters of allyl bromide was slowly added, and the reaction was allowed to proceed overnight. Afterwards, we extracted our product into ethanol through a separatory funnel. Then, we blew nitrogen onto our ethanol solution in order to blow off more of our solvent so that it would be easier to distill. Finally, we put our solution into a Rotary Evaporator low pressure distillator, and obtained our product. Although we did not exactly measure out the amount of product, we did observe that we got only a very small amount of our product.

Results II

In all three of our reactions, we used both nuclear magnetic resonance (NMR) and fourier transform infrared (FTIR) spectroscopy to check the results of our reactions. In each case, we used an already obtained spectra of each pure compound and compared its spectra to the one we obtained. What we found out in each case was that the product we obtained was very pure (almost 100%). We also found from our first and third reaction that extracting a compound from ethanol guarantees almost complete purity.

Conclusion II

The two main conclusions from these reactions are that first, on a small laboratory scale, the purity of products is almost 100%, while on a large scale, impurities are more. Secondly, ethanol is a good solvent for extracting and removing impurities from nonpolar compounds.

Introduction III

In modern chemistry, a field that is being explored is the study of thin films. The study of thin films has been greatly facilitated as a result of one instrument: the *Dektak IIA*. At the Wright-Patterson Materials Laboratory, thin films were studied using the *Dektak IIA* in order to perform waveguide measurements. By this, it is meant that in considering a film's thickness, we consider different factors responsible for it, in this case, concentration and spin speed (the speed at which a solution is spun onto a surface).

Methodology III

In performing our experiments, we coated our material on microscopic slides and silicon oxide wafers. Our material was composed of Wacker Blue Siloxane Liquid Crystal material dissolved in a varied amount of toluene. We made five different solutions, measuring each's concentration in grams of solute per volume of solvent; Our concentrations were 0.03 g/ml, 0.06 g/ml, 0.12 g/ml, 0.4 g/ml, and 0.8 g/ml. Using our laboratory's cleanroom, we syringed our material onto microscope slides and silicon oxide wafers. We then spun coat them at various speeds and let them dry in the vacuum oven. Then we used the *Dektak IIA* to measure each one's thickness. We used the computer to analyze our results.

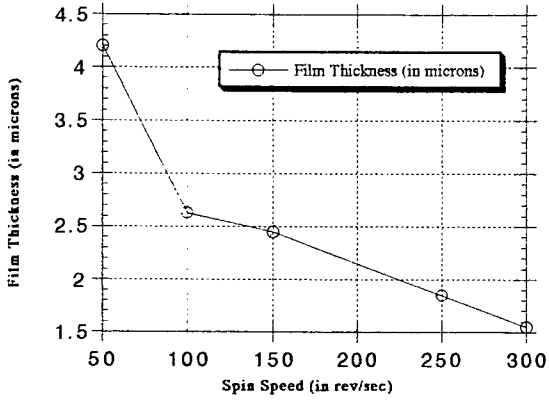
Results III

A graphical printout of our results is given on the next page. As one can clearly see, the thickness was directly proportional to the concentration. As we increased our concentration however, we also faced another problem: our films became less and less homogeneous. To overcome this problem, we employed another method: we would measure each film at three places, both opposite edges and the center, and took the average of the three.

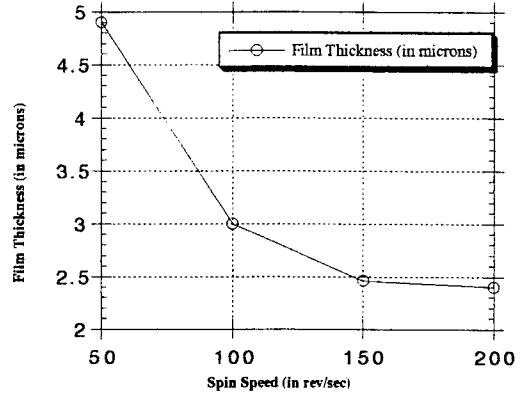
Conclusion III

Our conclusion from these graphs was that first, as concentration increases for a film, its thickness increases, and its overall homogeneity decreases. Second, as spin speed increases, the film's thickness decreased because its high speed made the films spread apart more.

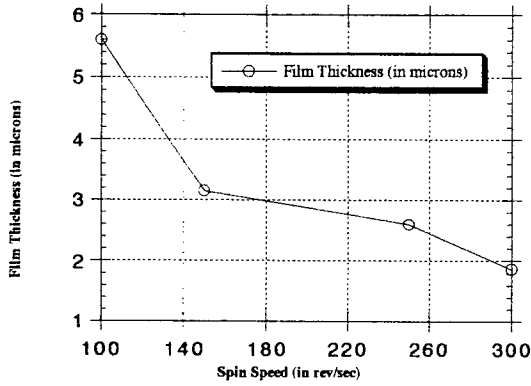
Thickness vs. Spin Speed in a 0.03 g/ml
Wacker Blue-Toluene Spun Coat Solution



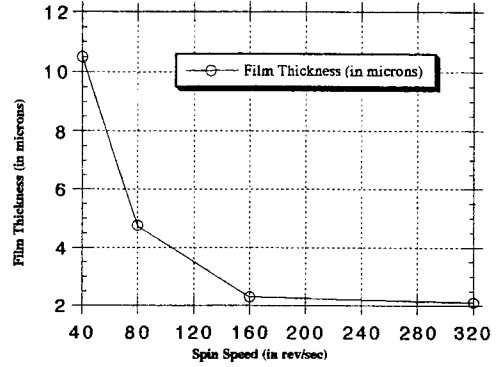
Thickness vs. Spin Speed in a 0.06 g/ml
Wacker Blue-Toluene Spun Coat Solution



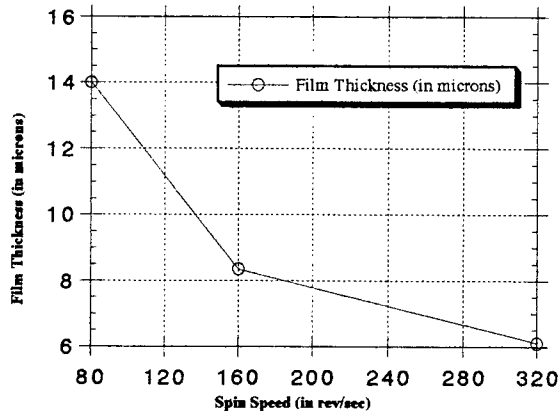
Thickness vs. Spin Speed in a 0.12 g/ml
Wacker Blue-Toluene Spun Coat Solution



Thickness vs. Spin Speed in a 0.4 g/ml
Wacker Blue-Toluene Spun Coat Solution



Thickness vs. Spin Speed in a 0.8 g/ml
Wacker Blue-Toluene Spun Coat Solution



WORKS CITED

Apfel, M.A.; Finkelmann, H; Janini, G.M.; Laub, R.J.; Luhmann, B.H.; Price, A.; Roberts, W.L.; Shaw, T.J.; Smith, C.A., Synthesis and Properties of High Temperature Mesomorphic Polysiloxane Solvents: Biphenyl- and Terphenyl-Based Nematic Systems , *Anal. Chem.* 1985, 57, 651-658.

Bunning, Timothy J., Structure and Properties of Siloxane Based Liquid Crystal Material , Ph.D Thesis, the University of Connecticut, May 1992, 109-136.

McHugh, Colin M., Synthesis and Characterization of Novel Steroidal-Based Liquid Crystals , Senior Research Thesis, the University of Dayton, December 1993.

Moser, Frank and Thomas, Arthur, Phthalocyanine Compounds , Reinhold Publishing Corporation, New York, 1963.

Moser, Frank, The Phthalocyanines, Volume I: Structure and Properties , Reinhold Publishing Corporation, New York, 1983.

Roberts, R.M.; Gilbert, J.C.; Rodewald, L.B.; Wingrove, A.S.; Modern Experimental Organic Chemistry , Holt, Rinehart, and Winston, New York, 1979.

A STUDY OF THE VISCOSITY OF
LUBRICATING OILS

Christina L. Noll

Trotwood-Madison High School
221 E. Trotwood Blvd.
Trotwood, OH 45426

Final Report for:
High School Apprenticeship Program
Wright Laboratory

Sponsored by:
Air Force Office of Scientific Research,
Bolling AFB, Washington DC

August 1994

A STUDY OF THE VISCOSITY OF LUBRICATING OILS

Christina L. Noll
Trotwood-Madison High School

Abstract

Lubrication is a very important issue when dealing with the durability of an engine. Lubricating oils, specifically, are studied because of their wide usage. When choosing a lubricating oil, its viscosity is the single most important factor. An oil's viscosity can aid in determining how well that oil will function under certain desired conditions. The viscosities of two separate engine oils are measured at 40°C and 100°C, and at different times (measured in hours). The object of this study is to determine the sustenance of the engine oils by comparing the increase in their viscosities over time.

A STUDY OF THE VISCOSITY OF LUBRICATING OILS

Christina L. Noll

Introduction

In order for an engine to function well, there are many factors to consider, such as which fuel has the proper octane level and energy content, maintaining the proper cooling functions, and which metal could sustain under severe conditions. Lubrication is also important in that it reduces friction, wear, and the heating of machine parts that move against one another. Lubrication is used in the form of a powder, a solid surface, or a liquid. When using oil as a liquid lubricant, viscosity plays an essential role in the prediction of its failure or success. In general terms, viscosity is the resistance of a liquid to flow. It is viscosity that determines the ability of the lubricant to maintain an oil film between the working parts of a machine. This film is what reduces friction, which in turn can reduce wear and over-heating.

When dealing with viscosity, you must consider the type of measurement required for use, the effect temperature has on the lubricant in use, and the thickening effects of an oil lubricant. These three factors must all be considered when putting the tested lubricants into use.

The word viscosity can refer to two slightly different physical properties. Dynamic viscosity refers to the physical quantity of a liquid, also called the absolute viscosity. However, when dealing with lubricants, the kinematic viscosity is traditionally used. The two measures of viscosity are related by the density as follows:

$$n = \nu \times \rho$$

where the dynamic viscosity (η) equals the kinematic viscosity (ν) multiplied by the density (ρ). Density has a significant effect on the gravitational flow of an oil, such as from a reservoir through a hose. In this case the driving force is proportional to the density of the oil. The result is that the kinematic viscosity becomes the controlling measure, and such is the reason why kinematic viscosity is used in the lubrication industry. The common technique for the measurement of the viscosity of an oil is to measure the flow rate of a certain volume of oil through a small capillary tube while under the force of gravity. The viscosity of lubricating oils is measured in centistokes (cSt).

Temperature has a definite effect on the viscosity of a lubricating oil. The viscosity of any fluid increases as the temperature decreases. The sensitivity of viscosity concerning temperature is an important property of lubricating oils, therefore their viscosities are typically reported at 40°C and 100°C (104°F and 212°F). Viscosity varies rapidly with temperature and the ratio of variation increases as the viscosity increases. At a very low temperature, the viscosity of an oil will usually double for every 5-degree decrease in temperature. However, at a typical working temperature in machinery (e.g. 40°C) where the viscosity is relatively low, the viscosity increase for every 5-degree decrease is only 25%.

There are other factors that cause thickening in an oil other than temperature. The viscosity of most oils increase slowly with use due to chemical reactions that occur in service, particularly when subjected to excessive heat. Some of the molecules in the oil react with oxygen to form oxygenated molecules which increase the viscosity. This is usually accompanied by a darkening of the oil. Additionally, exposure to strong light and the presence of clean metallic surfaces tend to accelerate this process. Plus, the individual molecules can combine to form larger molecules which also increase viscosity. In service, heat can be a very serious problem. To combat this, lubricants often contain antioxidant additives to control oxidative thickening.

Methodology

In order to determine the kinematic viscosity of a lubricating oil, a measurement is taken of the time for a certain volume of oil to flow under gravity through a calibrated glass capillary viscometer. The oil sample is first charged into the viscometer by way of suction. The viscometer is then placed in a high temperature bath (40°C and 100°C), and allowed twenty minutes for the sample to reach the test temperature. Using suction, the head level of the test sample is adjusted so that it reaches about 5 mm above the first timing mark on the capillary arm of the viscometer. With the sample flowing freely, measure in seconds the time required for the meniscus to pass from the first to the second timing mark. Repeat the steps taken to measure the efflux time twice. The kinematic viscosity is calculated, using the measured flow time and the instrument constant by means of the following equation:

$$v=Ct$$

where v is the kinematic viscosity in centistokes, C is the calibration constant of the viscometer, and t is the flow time in seconds.

Test Results

Tables 1 and 2 on page seven demonstrate the increase in viscosity of two different oils as time passes. Table 3 shows the measured viscosity versus the calculated viscosity using the following formula:

$$v=17.2292 + .050966t$$

where v is the viscosity at 40°C and t is the time in hours. The data is analyzed using linear regression analysis. The correlation coefficient is 0.999063 which is considered an excellent fit of the equation to the experimental data.

Pages eight and nine show the graph of the derived equation as it compares with the measured values. This graph can be used to determine the viscosity of that oil at a given temperature or vice versa.

Time	Viscosity at 40°C	Viscosity at 100°C
48 Hr	19.750 cSt	4.391 cSt
96 Hr	22.328 cSt	4.780 cSt
168 Hr	25.381 cSt	5.144 cSt
336 Hr	34.492 Cst	6.346 cSt

Table 1. TEL-93003: Squires, 205°C.

Time	Viscosity at 40°C	Viscosity at 100°C
8 Hr	17.492 cSt	4.056 cSt
16 Hr	17.482 cSt	4.065 cSt
24 Hr	17.597 cSt	4.065 cSt

Table 2. T-63 Engine oil.

Time	Measured Viscosity	Calculated Viscosity
48 Hr	19.750 cSt	19.676 cSt
96 Hr	22.328 cSt	22.122 cSt
168 Hr	25.381 cSt	25.791 cSt
336 Hr	34.492 cSt	34.354 cSt

Table 3. Measured viscosity versus Calculated viscosity of TEL-93003 using the following formula:

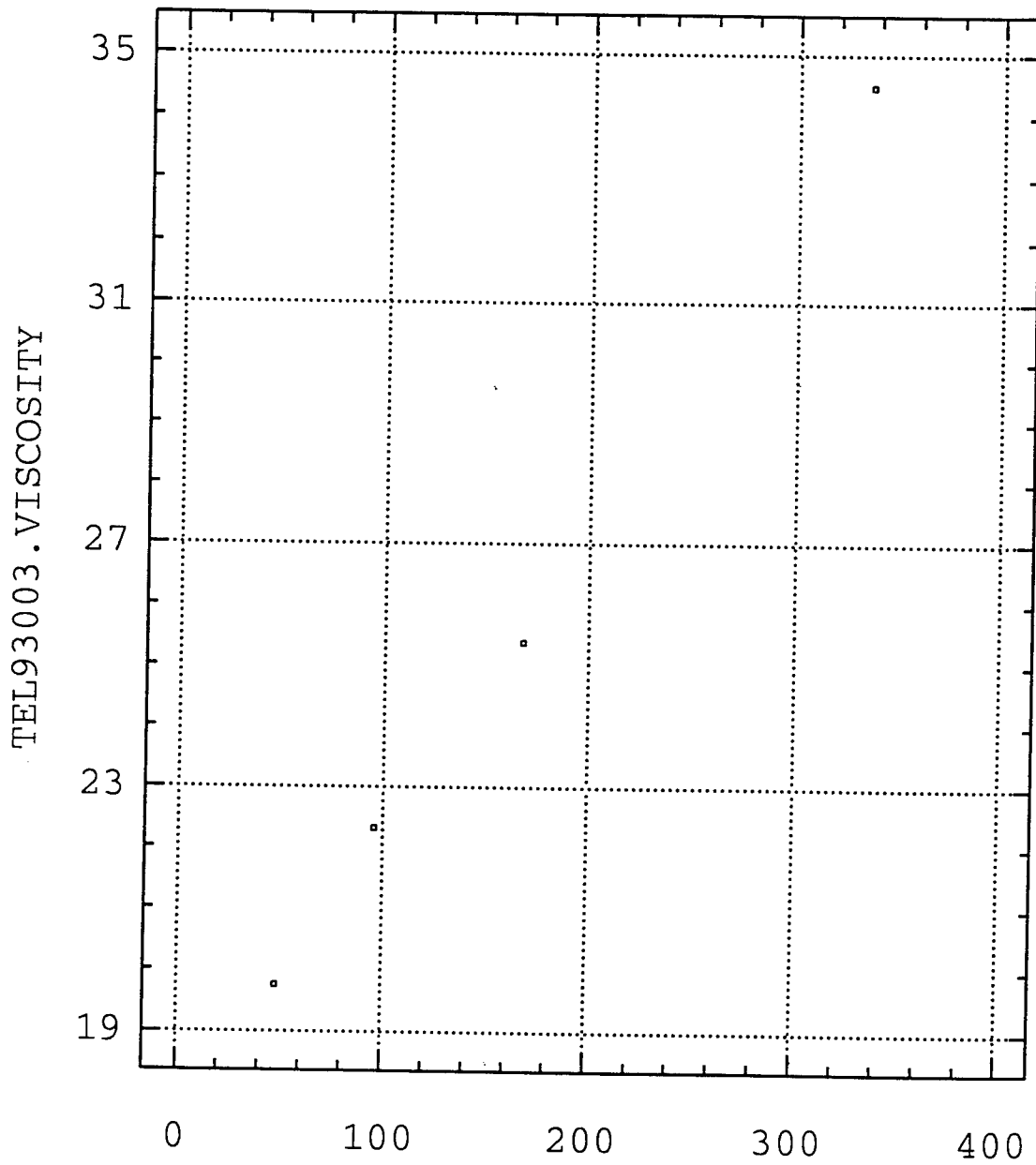
$$v = 17.2292 + .050966t$$

where v is the viscosity at 40°C and t is the time in hours.

* Using the above formula, at 1000 Hr v=68.2 cSt (1000 Hr is app. life of the oil).

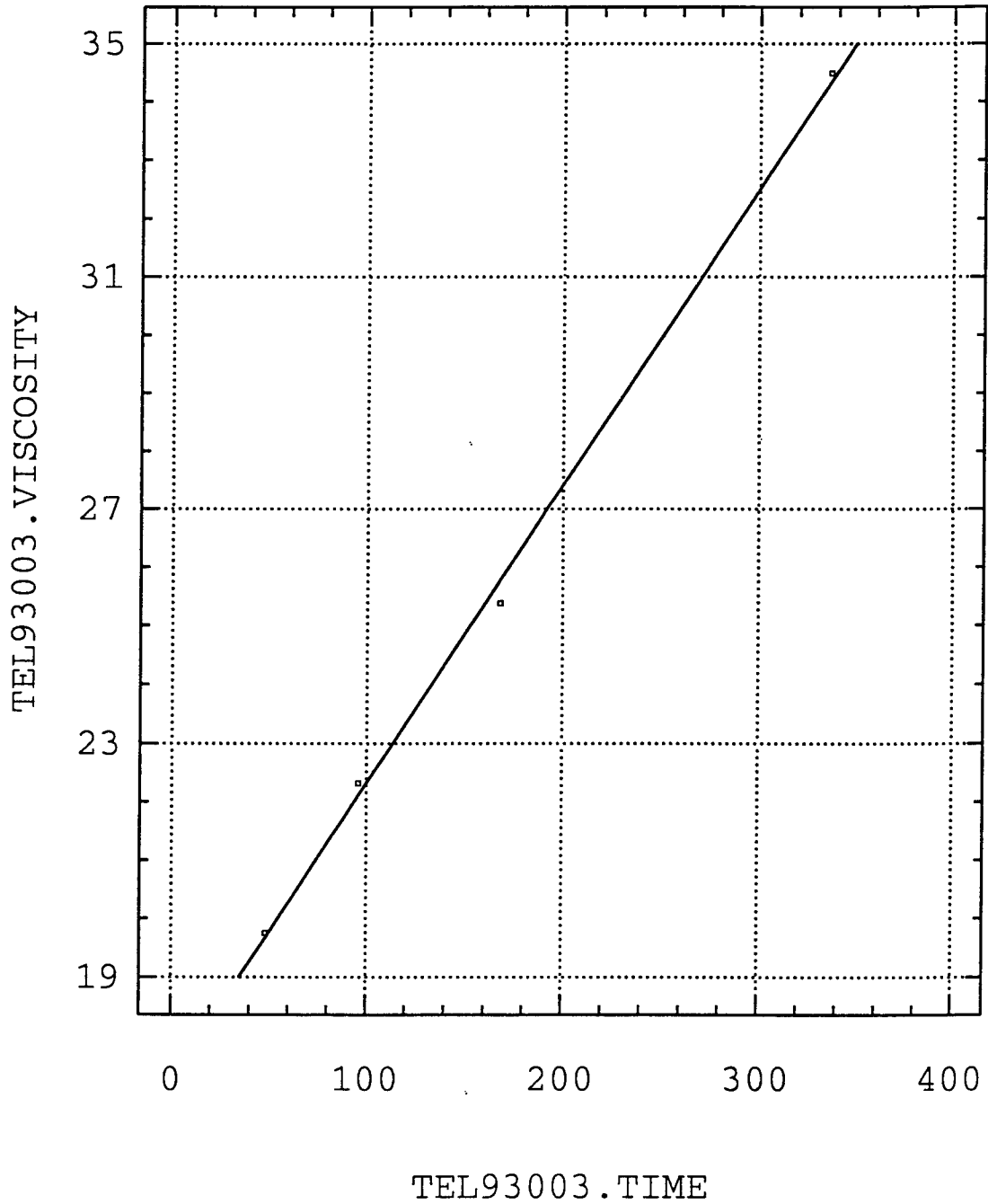
* The table indicates a 175% increase in viscosity over 288 Hr.

Plot of TEL93003.VISCOSITY vs TEL93003.TIME



TEL93003.TIME

Regression of TEL93003.VISCOSITY on TEL93003.TIME



Conclusion

From my test results, I found that the T-63 engine oil has little variation in viscosity as time in hours passes. Therefore, this particular oil sample should remain fairly stable and could be used efficiently as lubrication in an engine. However, the TEL-93003 Squires oil was very unstable and predicted to reach a viscosity of about 68.2 cSt at the end of its lifetime. This extremely high increase in viscosity over time is unacceptable for any engine oil.

Many petroleum products are used as lubricants in bearings, gears, and other machinery. The proper operation of such equipment depends upon the proper kinematic viscosity of the liquid. The above calculation proves how important the kinematic viscosity is when considering an oil for use as a lubricant in any piece of machinery.

REFERENCES

- 1) Shigley, Joseph Edward and Vesper, Karl H., "McGraw-Hill: Series in Mechanical Engineering", 2nd Edition. The Maple Press Company, 1972, pp. 410-423.
- 2) Weast, Robert C. and Selby, Samuel M., "Handbook of Chemistry and Physics", 47th Edition. The Chemical Rubber Co., 1966, pp. F31-F33.
- 3) Peters, Max S., "McGraw-Hill: Series in Chemical Engineering", 4th Edition. McGraw-Hill Book Company, Inc., 1963, pp. 5-15, 22-33, 3-228.
- 4) Alexander, David L., "Lubrication: The Viscosity of Lubricants". Texaco Inc., 1992, pp. 1-6, 12-14.
- 5) 1990 Annual Book of ASTM Standards, Section 5, Vol. 5.01 D56- D1947. "Standard Test Method for Kinematic Viscosity of Transparent and Opaque Liquids" pp. 170-174.

SARTING HERE AND GOING BEYOND

Joanna E. Odella

Kettering Fairmont High School
3301 Shroyer Road
Kettering, Ohio 45429

Final Report for:
High School Apprentice Program
Wright Laboratory

Sponsored by:
Air Force of Scientific Research
Bolling Air Force Base, DC

and

Wright Laboratory

August 1994

SARTING HERE AND GOING BEYOND

Joanna E. Odella
Kettering Fairmont High School

Abstract

I gained knowledge of engineering as a career. Working one on one with engineers of all levels helped me gain understanding of what engineering involves, and what I can expect out of college and my future. I studied the FORTRAN computer language. This knowledge will help me in my computer classes in college. The Antenna Wavefront Simulator was studied. Tests were done on phase shifters to control efficiency with the Antenna Wavefront Simulator. The Simulator is a device which uses GPS (Global Positioning System) technology for research and evaluation.

STARTING HERE AND GOING BEYOND

Joanna E. Odella

Electricians, that's what I thought electrical engineers were. I had no idea that electrical engineers not only work basically on computers, but program on computers also. I had it stuck in my head that programming was only a job for a computer science major, or a system analyst, but I was wrong. I had no concept what an electrical engineer did, that is why I never considered a career as an electrical engineer. During my internship, my eyes were not only opened wide to a different career aspect, but I realized that there are many career choices that I could make, but I simply just don't know about. The electrical engineers that I had an opportunity to work with relied heavily on their knowledge of different computer languages. I used to believe that computer languages were like foreign languages. If you know one, you can get around in life fine, but if you are exposed to many languages, you have an advantage that is admirable, but not necessary. If you only know one computer language, not only are you limited on the amount and quality of projects, you have a disadvantage in not making it accessible to all computers. Knowing more than one language is necessary in electrical engineering. I only had little training in BASIC, so this summer would be a challenge for me to become bilingual in computer languages.

My mentor, David Tsui, started me on FORTRAN. I had no experience with the FORTRAN language, so I started off very basic and simple. I would add two numbers together and print the sum, or I would enter a phrase and repeat the phrase 100 times. After some practice I went chapter by chapter through a problem solving and structured programming book in FORTRAN. I learned how it was possible to do many

different functions all with a simple do-loop, for example. It was very challenging for me to read a chapter and then program with what I just read. I would look at the program problem first, then I would go through and scan the chapter until I found what I need to complete my programs. I wrote a program to compute a magic square and a program that counts, gives the average overall grade, and an average of each grade level. (Found in appendix A). I really had no experience programming before I came to work at Wright Laboratory, so I had no idea if I wanted to think about programming as a possible career. Through these past months I have come to the conclusion that I was not meant to be a programmer. I enjoy working with people more than I do sitting at a desk with my computer all day. I am very grateful for having the opportunity to try this career. Without my experience at Wright Laboratory I would still be left in the cold with a lot of possibilities.

The section that I worked for this summer was CNI (Communications, Navigation, and Identification) Concepts Exploration Section which is located in the Avionics Division. One of the projects which is occupying this division is GPS (Global Positioning System). GPS is a spaced-based radio positioning and time-transfer system. There are three segments of GPS. Figure 1. The first segment is space. When it is able to be completely operated it will have a constellation of twenty-one Navstar satellites, in six planes, which will orbit the earth. Figure 2. shows that the satellites will be positioned so that atleast four satellites will be facing the earth at all times. The second segment, control, includes a Master Control Station (MCS), a number Monitor Stations (MS), and Ground Antennas (GA). The MS uses a GPS receiver that is specialized to track all satellites in view. Next, the MCS determines the satellite clock, the ephemeris values, and updates the navigation messages of every satellite from the information received by the MSs. Finally, the information that was updated is sent by the GAs to the satellites. The third and final segment, user, consists of UE (user equipment), SE (support equipment),

GPS SYSTEM

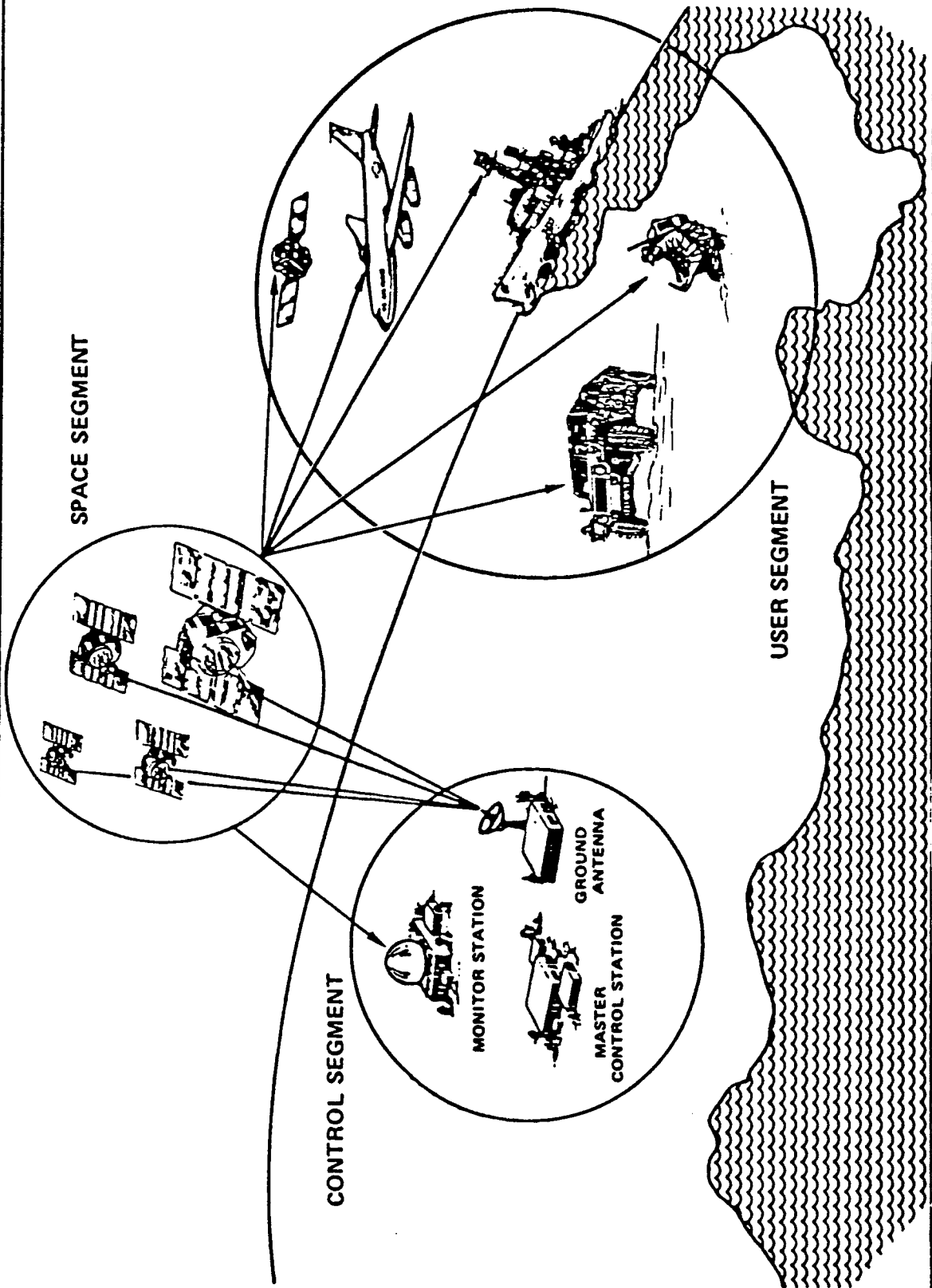
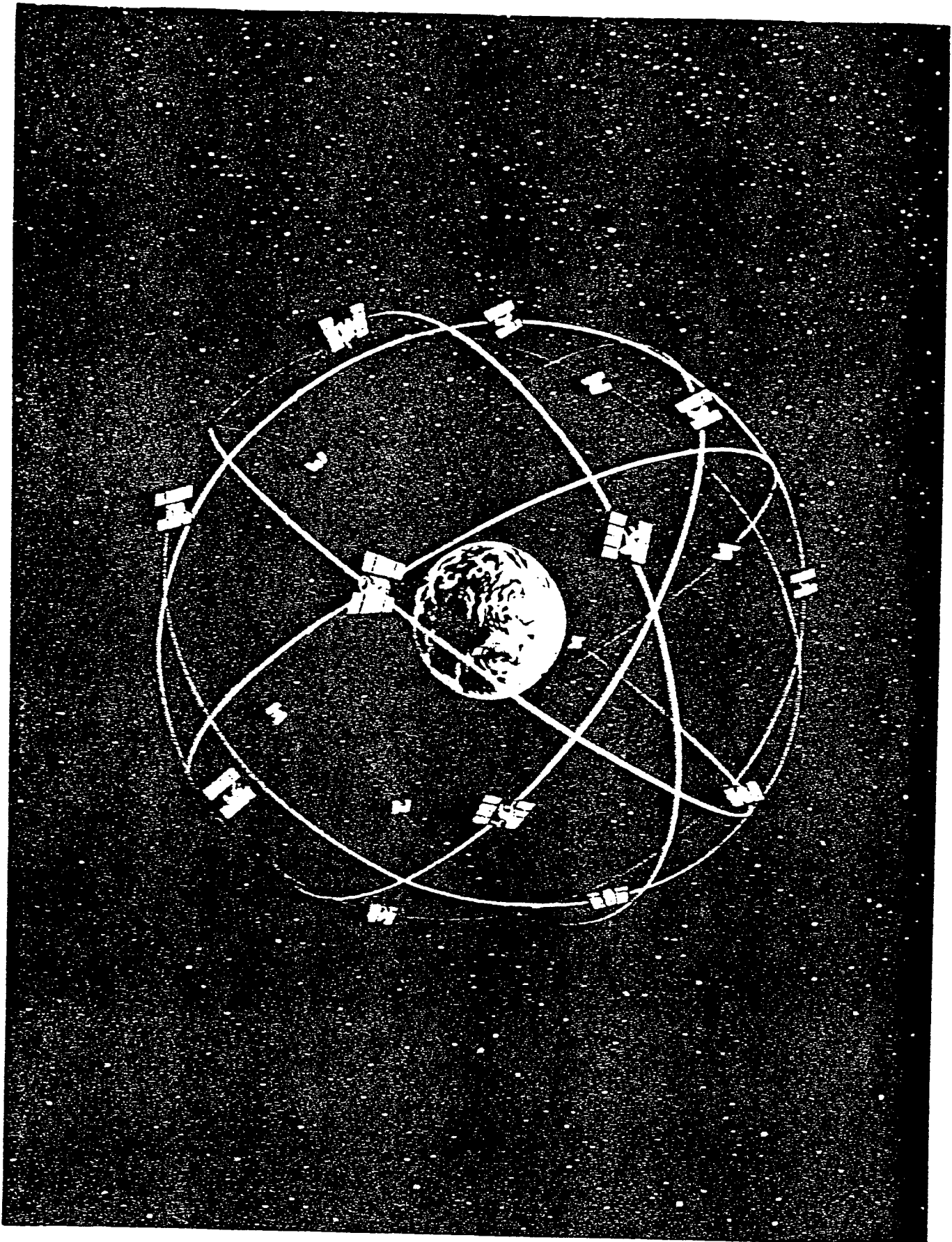


Figure 1
GPS system



Space segment of GPS

Figure 2

and many other items. The L-band RF (radio frequency) signals, received by the orbiting satellite constellation, operate with the UE sets to give appropriate users the PVT (position, velocity, and time) data with accuracies of about sixteen meters SEP (spherical error probable). All three segments play a vital role in order for GPS to be operated properly.

There are endless applications that GPS is useful for. Some examples include the following:

AIR NAVIGATION	LAND NAVIGATION	MARITIME NAVIGATION
-non precision approach landing -oceanic en route -domestic en route -terminal -remote areas -helicopter operations	-vehicle monitoring -schedule improvement -minimal improvement -law enforcement	-oceanic -coastal -harbor/approach -inland waterways
STATIC POSITIONING/TIMING	SPACE	SEARCH & RESCUE
-offshore resource exploration -hydrographic surveying -aids to navigation -time transfer -geographical surveying	-launch -orbit determination -re-entry/landing	-position & monitoring -rendezvous -repeatability of position -coordinated search -collision avoidance

**table 1.
applications of GPS**

Many people can and will benefit from GPS. Firefighters will not only be able to find water pumps in unfamiliar territories, but GPS will allow firefighters to be more efficient over all. During natural disasters GPS will allow authorities to locate

pipelines and storage tanks faster. GPS is an incredible necessity to NASA and their projects. For example, GPS was essential for the Voyager II fly-by of Neptune in 1989. There are quite a few systems accessible right now that can do some of the same tasks GPS can do, but without the quality. Some examples are Omega, STD INS, and Loran-C. Most positioning/navigation system comparisons are operational worldwide, with some few exceptions such as Loran-C. GPS is also operational worldwide, but with 24-hour all-weather coverage, which the comparisons are not. Many are limited by skywave interferences and degraded performance in polar areas.

The engineers that I worked with this summer are working on the Antenna Wavefront Simulator which is a device which uses GPS technology for research and evaluation. Figure 3. They are now on phase II of the project. There are many parts that go into making the wavefront simulator work. One of the main parts needed for the wavefront simulator is a voltage controlled phase shifter. There are two of these phase shifters in the antenna wavefront simulator. The phase shifters receive radio frequency signals which are lined up in all different directions. The phase shifters are in the simulator to line up all the signals to be used most efficiently. An intern from Wright State University and I tested these phase shifters on a machine called a network analyzer. The network analyzer is a voltage controlled machine which also tests the 10 dB ADJ. Attenuators. There are two of these attenuators along with one 10 dB fixed attenuator used in the Antenna Wavefront Simulator. Each phase shifter takes about 15 - 20 minutes to test. With the network analyzer it took forever to test a large amount of phase shifters. The other AFOSR student in my section cut the work load that would have taken 4 days, down to 4 hours. After we were done testing the phase shifters they were boxed up and sent to the next step of the assembly of the antenna wavefront simulator.

PHASE II

BLOCK DIAGRAM

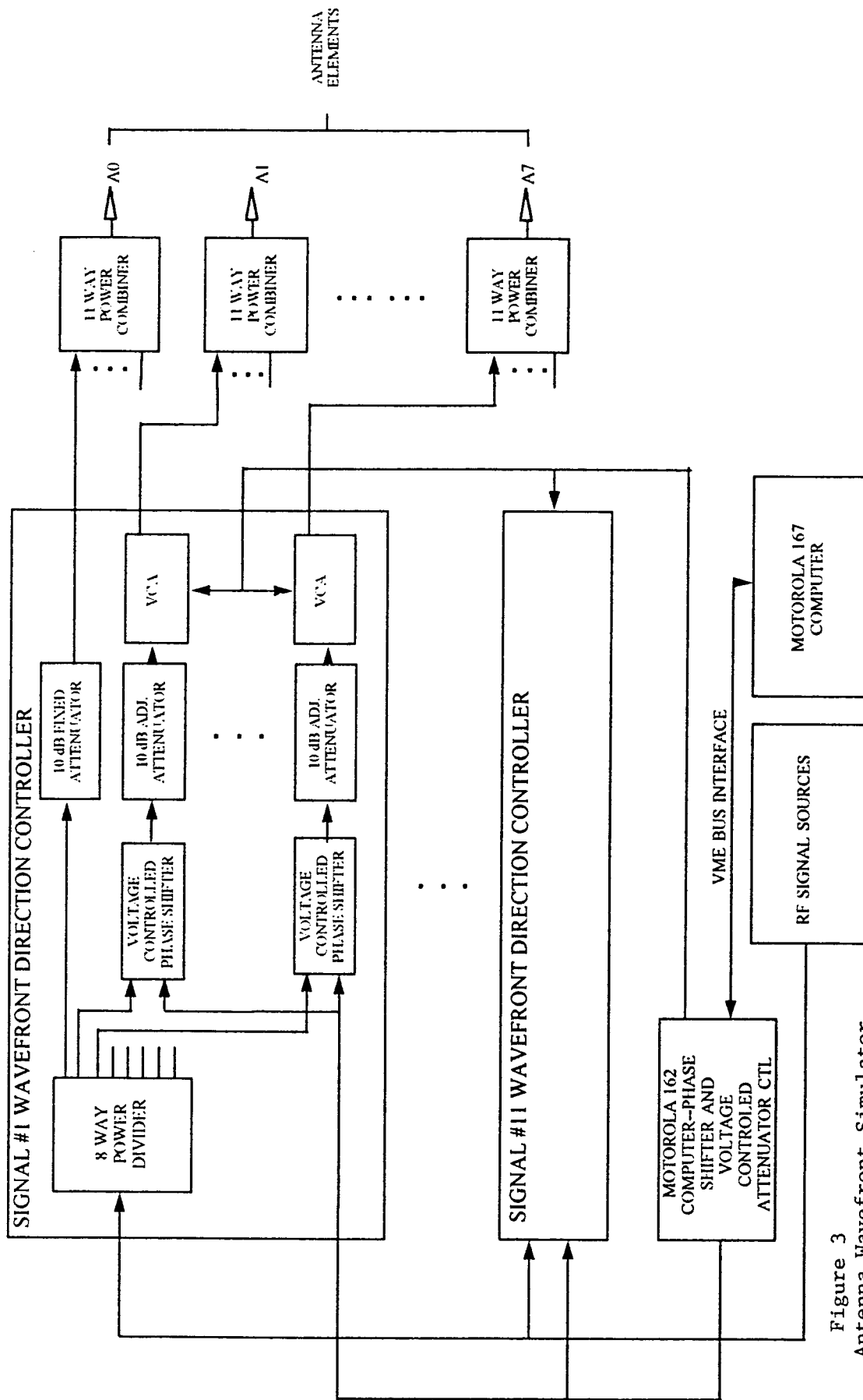


Figure 3
 Antenna Wavefront Simulator

Now that my internship is over at Wright Patterson Air Force Base, I look back on it as a very positive experience that will stick with me in my future. My internship taught me a lot more from the people that I worked with than just sitting at a computer ever could have. Before working at Wright Patterson, success was basically measured on how much money one made. That's not a part of the definition of success in my dictionary any more. One needs to be happy with what they are working on everyday. I am determined to find the career that will make me jump out of bed every morning. I may not find my dream career in 5 years, maybe not in 10, but I do believe it is out there. My co-workers this summer helped me realize that. I am going into Chemical Engineering this fall in college, and I am very determined to try my best in succeeding, but now I don't feel ashamed if I happen to change my major. My head use to be stuck just on Chemical Engineering, why? I believe it has something to do with society. I honestly never really knew what an engineer did before my intern, but I still wanted to become one because an engineer made a lot of money and sounded impressive. It does not means more to me now. It is a career that takes a lot of time, hard work, and perseverance. I feel I can take the challenge. I also believe if I am not happy, I should change. Success(often confused with money) is too much apart of acceptance in American society, where happiness should be the number priority.

```

Program lest
Author:Joanna Odella
July 12, 1994
Integer countr3, countr4, countr5, countr6
Integer I, countr, countr2,p,t,q,l,z,x
Integer f, u, y, k, d, w, n
p = 0
t = 0
q = 0
l = 0
z = 0
n = 0

```

counters for each grade (i.e. A,B,C etc.)

```

countr = 0
countr2 = 0
countr3 = 0
countr4 = 0
countr5 = 0
countr6 = 0

```

Do loop to read grade, catagorize grade, and keep a running total of how many in each grade level (ex. # of A's, # of B's)

```

Do I = 1,30
countr = countr + 1
print *, 'Please type in a grade: '
read *, n
if ( n .ge. 90) then
    countr2 = countr2 + 1
    p = p + n
else if ( n .ge. 80) then
    countr3 = countr3 + 1
    t = t + n
else if ( n .ge. 70) then
    countr4 = countr4 + 1
    q = q + n
else if ( n .ge. 60) then
    countr5 = countr5 + 1
    l = l + n
else if ( n .ge. 0) then
    countr6 = countr6 + 1
    z = z + n

```

```

end if
print *, ' Would you like to enter another
+ grade?(1 = yes, 2 = no)'

```

read if there is another grade, if no get the avg. of grades

```

read *, x
If ( x .eq. 2) then
    goto30
else
    continue
end if
end do

```

c formulas to get the avg. grade of each grade level

30 f = p / countr2
u = t / countr3
y = q / countr4
k = l / countr5
d = z / countr6

c finding the avg. grade over all

w = (p + t + q + l + z) /countr

```
print *, '# of As = ', countr2
print *, '# of Bs = ', countr3
print *, '# of Cs = ', countr4
print *, '# of Ds = ', countr5
print *, '# of Fs = ', countr6
print *, '# of grades = ', countr
print *, ' The average A is: ', f
print *, ' The average B is: ', u
print *, ' The average C is: ', y
print *, ' The average D is: ', k
print *, ' The average F is: ', d
print *, ' The average grade is: ', w
stop
end
```

# of As =	4		
# of Bs =	4		
# of Cs =	2		
# of Ds =	2		
# of Fs =	4		
# of grades =		16	
The average A is:			94
The average B is:			84
The average C is:			72
The average D is:			62
The average F is:			37
The average grade is:			70

Program magic
Author: Joanna Odella
June 20, 1994

```
Integer dir(5,5)
Integer I
Integer j
Integer factor
j = 3
I = 1
factor = 2
open(1,file = 'mag.dat' , status = 'unknown')
0 dir(I,j)= factor
```

making factor always be an even #

```
factor = factor + 2
```

placement of #'s

```
I = I - 1
if (I .eq. 0)then
  I = 5
end if
j = j + 1
if ( j .eq. 6)then
  j = 1
end if
if(dir(I,j) .ne. 0)then
  I = I + 2
  if (I .gt. 5) then
    I = I - 5
  end if
  j = j - 1
  if (j .lt. 1) then
    j = j + 5
  end if
end if
if(dir(I,j) .ne. 0)then
  goto 20
end if
goto 10
```

printing magic box

```
0 do 100 I = 1,5
  write(1,*) dir(I,1),dir(I,2),dir(I,3),dir(I,4),dir(I,5)
  write(6,*) dir(I,1),dir(I,2),dir(I,3),dir(I,4),dir(I,5)
00 continue
do 200 I = 1,5
  write(1,*) (dir(I,j), j = 1,5)
  write(6,*) (dir(I,j), j = 1,5)
00 continue
stop
end
```

34
46
8
20
22

48
10
12
24
36

2
14
26
38
50

16
28
40
42
4
16

30
32
44
6
18
30

DESIGN AND CONSTRUCTION OF A FLUORESCENCE
SPECTROSCOPY EXPERIMENT

Alexander H. Penn

Niceville High School
800 E John Sims Pky
Niceville, FL 32578

Final Report for: High School Apprenticeship Program
Wright Laboratories

Sponsored by:
Air Force Office of Scientific Research
Bolling Air Force Base, DC

and

Wright Laboratory, Eglin AFB

August 1995

DESIGN AND CONSTRUCTION OF A FLUORESCENCE SPECTROSCOPY EXPERIMENT

Alexander H. Penn
Niceville Senior High School

Abstract

Studied were the fluorescence spectra of Nd:YAG and Nd:YLF. The requirements for taking this spectral data were a working monochromator, a laser diode with all of its support equipment, optics, a chopper and lock-in amplifier, and computer control. The system was set up, calibrated, and succeeded in getting the correct data. Pieces designed for this experiment which may now be used for other experiments include optics for the monochromator and an easy-to-use software interface between it and the computer.

DESIGN AND CONSTRUCTION OF A FLUORESCENCE SPECTROSCOPY EXPERIMENT

Alexander H. Penn

Introduction

The project was to set up an experiment that could obtain fluorescence spectroscopy data. The materials measured were samples of Nd:YAG and of Nd:YLF. We decided that this would be a good experiment to do, despite the fact that this experiment has obviously been done before (Nd:YAG is perhaps the most popular laser used in laser radar work), because it would give me the opportunity to work an experiment not normally attempted until upper level college or graduate school and would provide the lab with new and working equipment (as the experiment would entail both the design and construction of new equipment and the fixing of old equipment).

Background

When light interacts with a material, it may be absorbed, transmitted, or reflected. What determines if the light will be absorbed or not is the wavelength of that light and the existence and availability of a corresponding energy transition in the substance. Every substance has its own set of energy levels that it may occupy and travel between. For instance, an electron in an atom has certain discrete energy bands which it may occupy, and, should an electron interact with a photon of the correct energy, there is a high probability that the photon will be absorbed by the electron and that the electron will then transition to a higher energy level. If there is no energy band available for the electron to move to, it will not absorb the photon.

The tendency of all substances is to occupy the lowest energy state possible. Thus, an excited substance will always seek to return to its ground state and divest itself of the extra energy absorbed. This is usually done in one of two fashions: either through spontaneous emission of radiation or stimulated emission of radiation. Spontaneous emission is, when an electron spontaneously makes an energy transition by emitting a photon equal in energy to the change of state. Stimulated emission occurs when a photon of the correct wavelength (usually the result of a spontaneous emission) interacts with an excited

ion causing it to also to drop in energy and emit a photon the twin of the first in frequency, phase, and direction. These three characteristics: monochromaticity, coherence, and unidirectionality, are the main features of the laser, which simply stands for *light amplification by stimulated emission of radiation*.

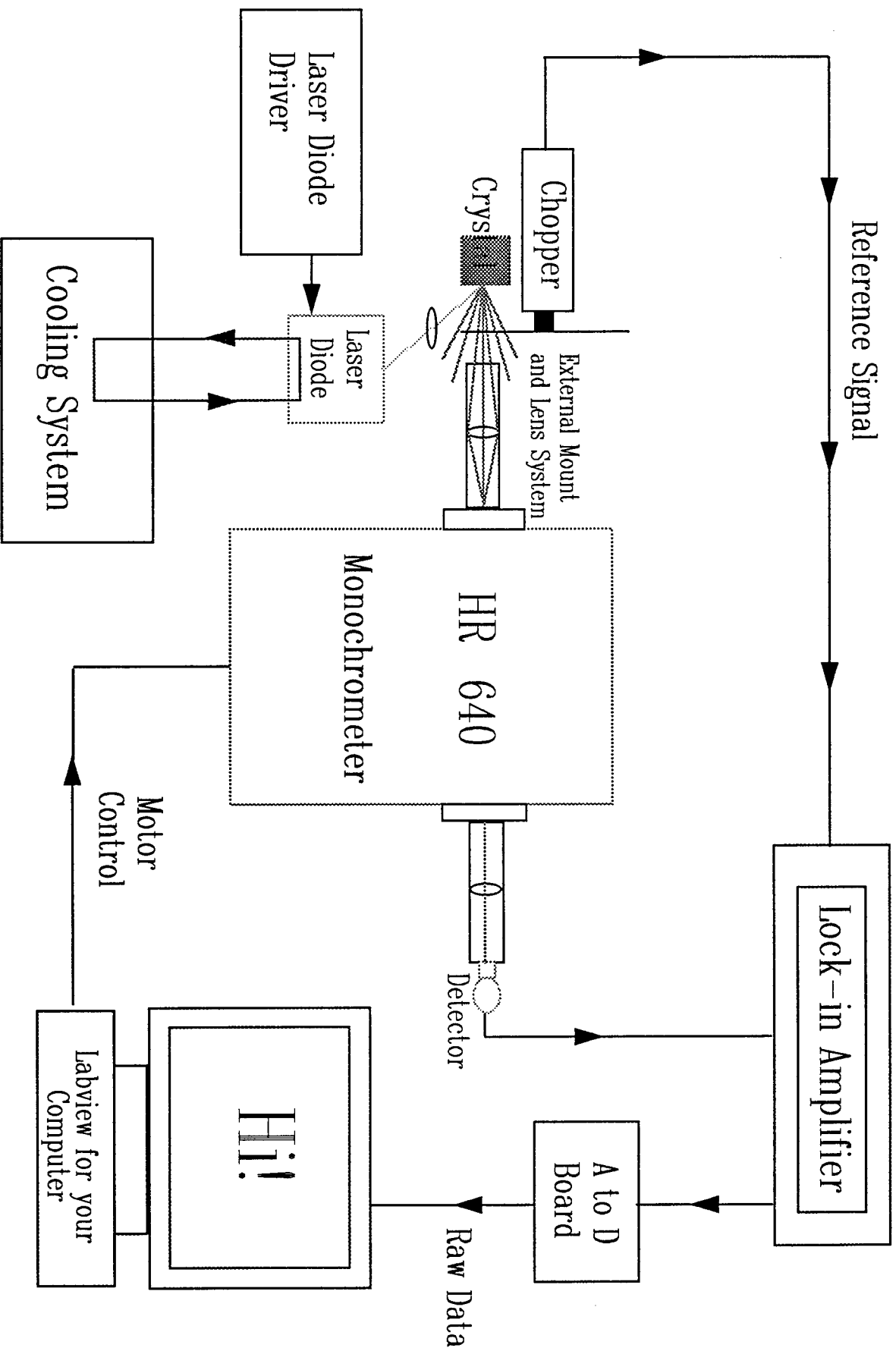
A laser is created when photons emitted by the substance are routed back through the substance. This is called feedback. The simplest example of a setup designed to accomplish this is an optical cavity consisting of a mirror 100% reflective at the desired wavelength for lasing and, on the other side of the fluorescing medium, facing the first mirror, another mirror partially reflective at that wavelength. A spontaneously emitted photon released along the cavity axis will begin to bounce back and forth through the medium. Each time it encounters an electron in the excited state it may cause the stimulated emission of a photon which will then also begin bouncing back and forth, causing more stimulated emission. Thus each pass causes an exponential growth in power, with the partially reflective mirror forming the output of the laser.

Laser operation can only occur when there is a population inversion, meaning there are more electrons in a higher energy state than in a lower energy state over the period of time that the laser is building up power and operating. This is achieved by pumping the material with an energy source. At what wavelengths the substance will lase can be determined from the gain curve which is based upon the fluorescence spectra and the population inversion. Without the fluorescence data the gain curve cannot be calculated. That is why fluorescence spectroscopy experiments are so important to laser research.

Methodology

On the following page can be seen the basic layout of my experiment. For the purposes of this paper, I have divided it into the following systems: the pump system, the monochromator, the optical systems, the chopper and lock-in amplifier, and the computer control.

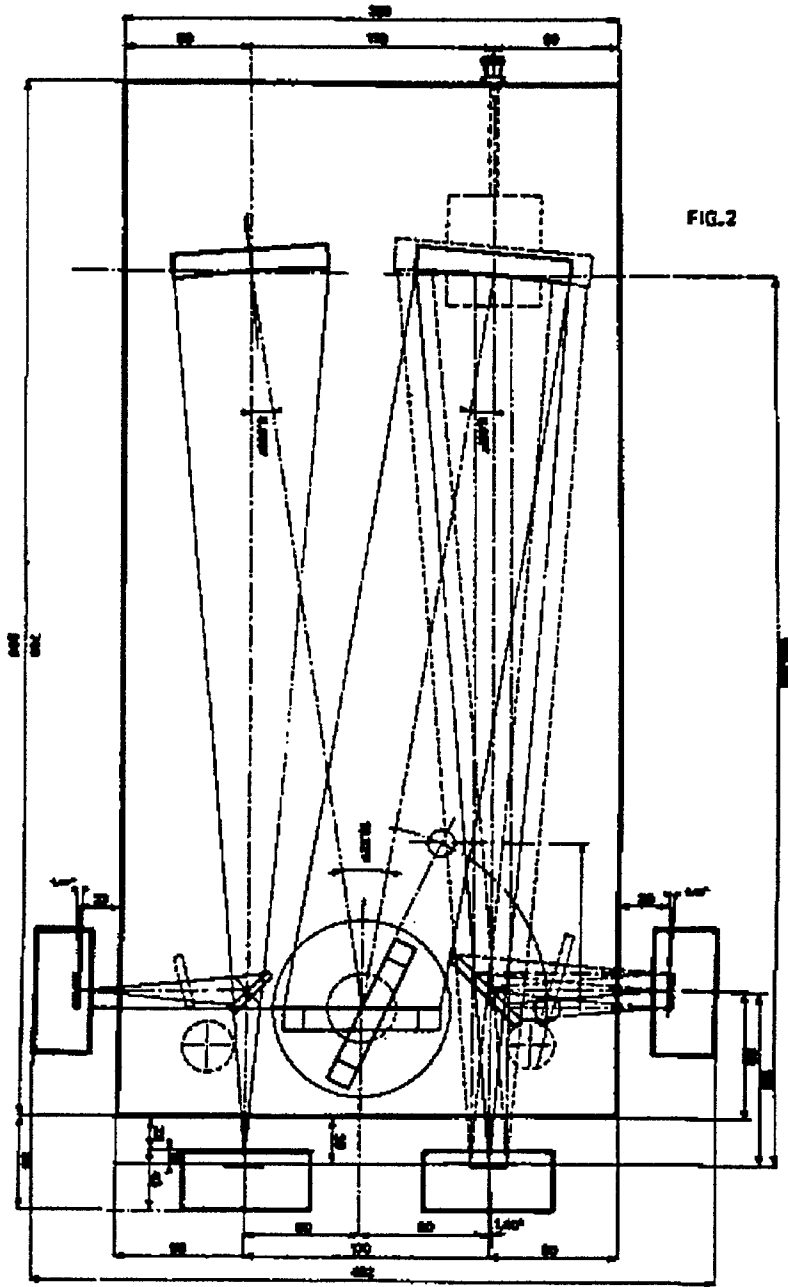
The pump system, responsible for pumping the crystal with energy, centered around a laser diode operating at approximately 805 nm. 805 was chosen because that is one of the absorption peaks for neodymium. The use of a diode as a pump source necessitated the use of other pieces of equipment such as focusing optics. Focusing is necessary because, unlike most other types of laser, laser diodes have a



high degree of beam divergence. The diode used in my experiment diverged forty-five degrees in the vertical direction and ten degrees in the horizontal. Another characteristic of laser diodes, namely that they are wavelength tunable by temperature, required the use of a two prong approach to temperature control. First was a water circulation system, making use of a water cooler and a "plumbing" system which I constructed, responsible for heat removal and coarse adjustment of temperature. Second was a thermo-electric, or TE, cooler, which was actually housed in the diode casing and which was responsible for fine temperature control and adjustment. Finally, a laser diode driver was used to control both the TE cooler and provide current to the diode (thus controlling the diode's power output).

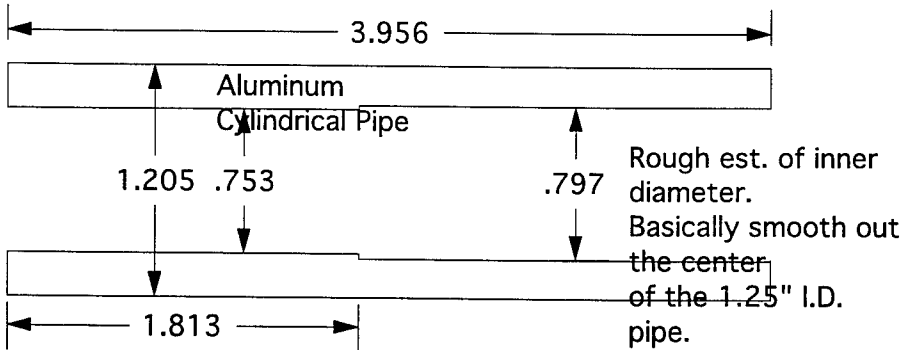
The monochromator itself acts basically like a prism. It takes the light entering at one slit and, by way of a diffraction grating, splits the light up into its various wavelengths, allowing only one of them to exit through the other slit (see diagram). The monochromator used was a Jobin\Yvon HR 640. The 640 refers to the optical cavity length in millimeters from the entrance slit to the first mirror. This long cavity plus the high quality diffraction grating and a small slit size combine to give this monochromator the resolution of one Angstrom. The cavity length, along with the mirror size, also contributes to give the $f\#$, or focal length to aperture ratio, of the device - in this case equal to $f/5.7$. This number is important when designing the optics. Though an excellent piece of equipment, this monochromator has been unusable for at least the past year because of the poor quality of the software interface. This problem was solved by writing a new interface which will be discussed later.

The purpose of the optical system is both to collect as much light as possible from the crystal into the monochromator and to act as a spatial filter. Light radiating from the crystal fluoresces in all directions. The optics gather as much of that light as possible guiding it through the entrance slit on the monochromator and causing it to fill the first mirror without overfilling it (as any excess causes scattering within the monochromator and leads to noise). This is done by matching the $f\#$ of the optical system to the $f\#$ of the monochromator. In designing the optics to be used, not only did the $f\#$'s have to match, but they also had to be mateable to existing equipment and be easily adaptable to experiments other than this one. After the design was complete, the drawings were sent to the Model Shop here at Eglin to be constructed (some of the many parts designed are shown in the drawing). While integrating the finished



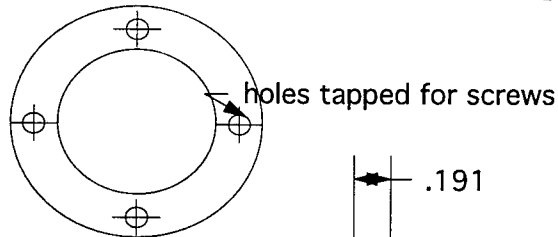
HR 640

Side View

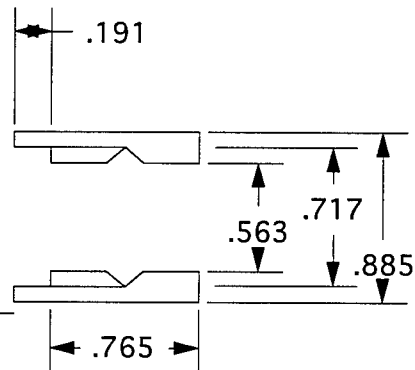
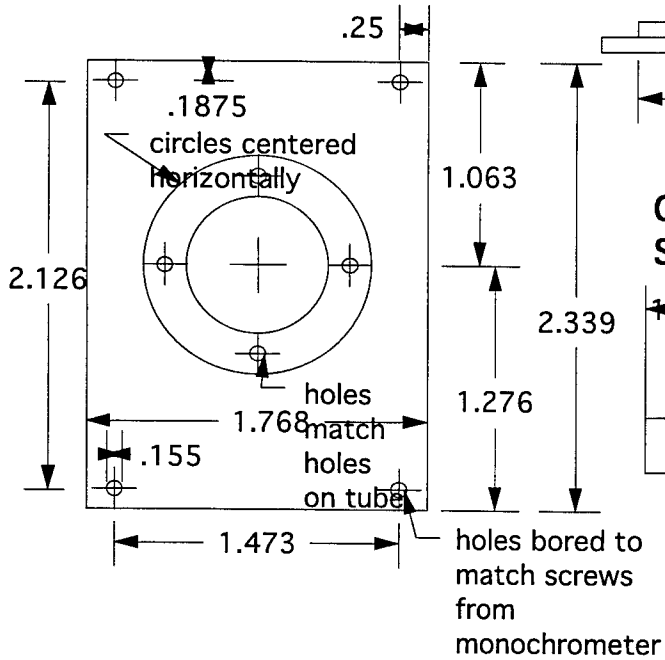


Collection Optics

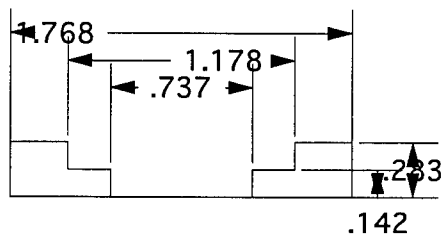
Back view



Back Plate

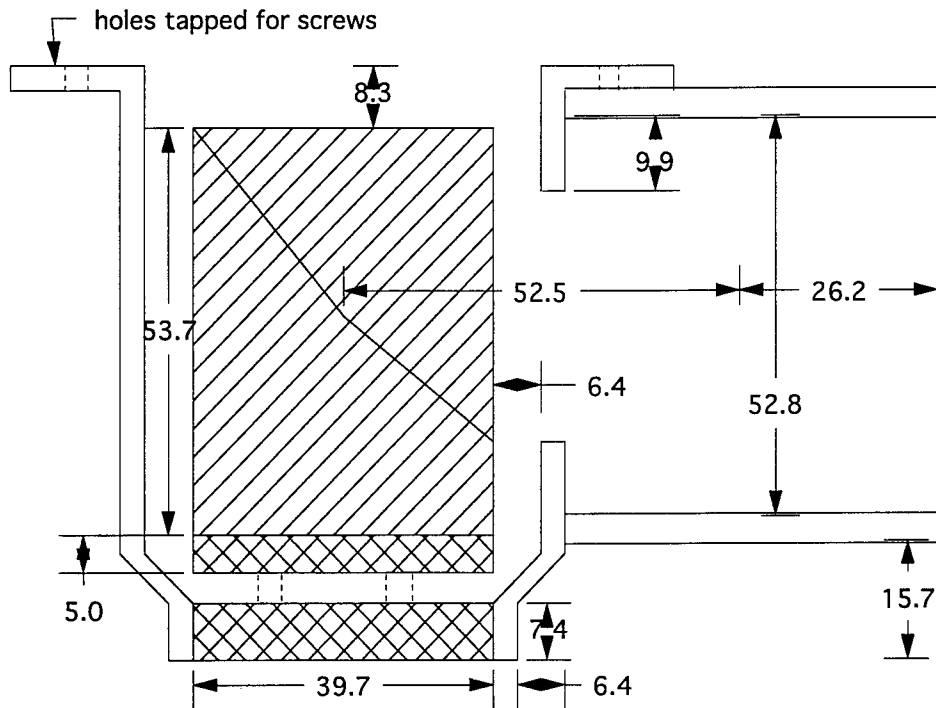


Cross-sectional Side View

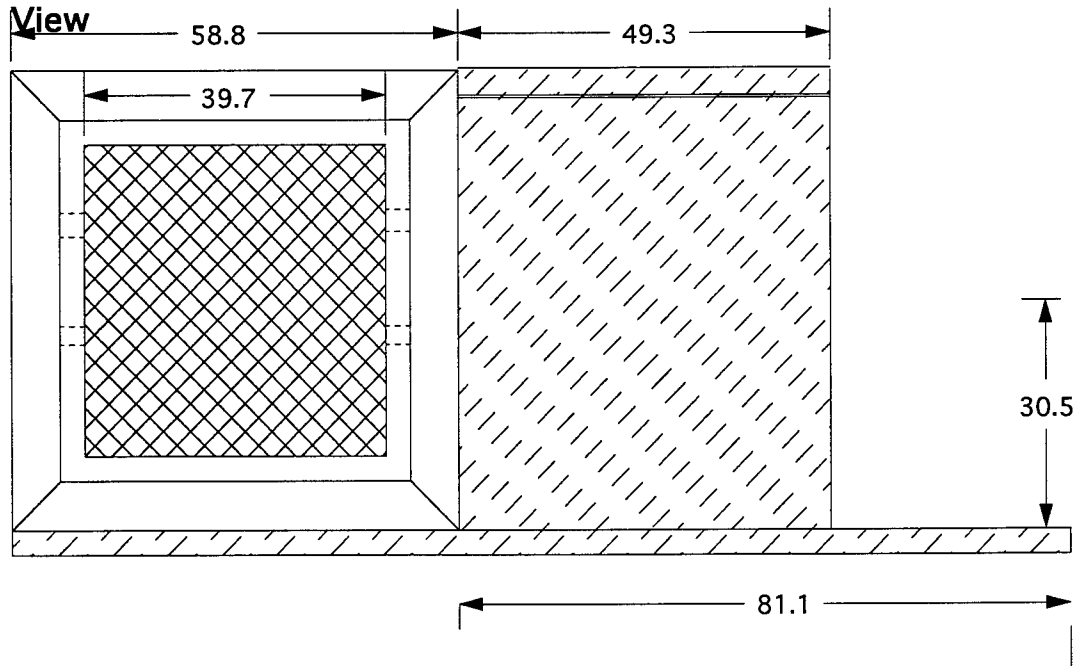


Detector optics

Cross-sectional View

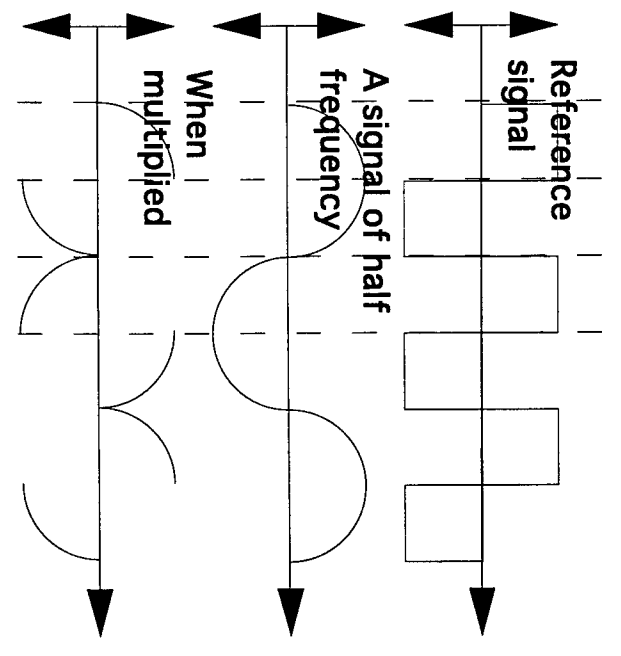
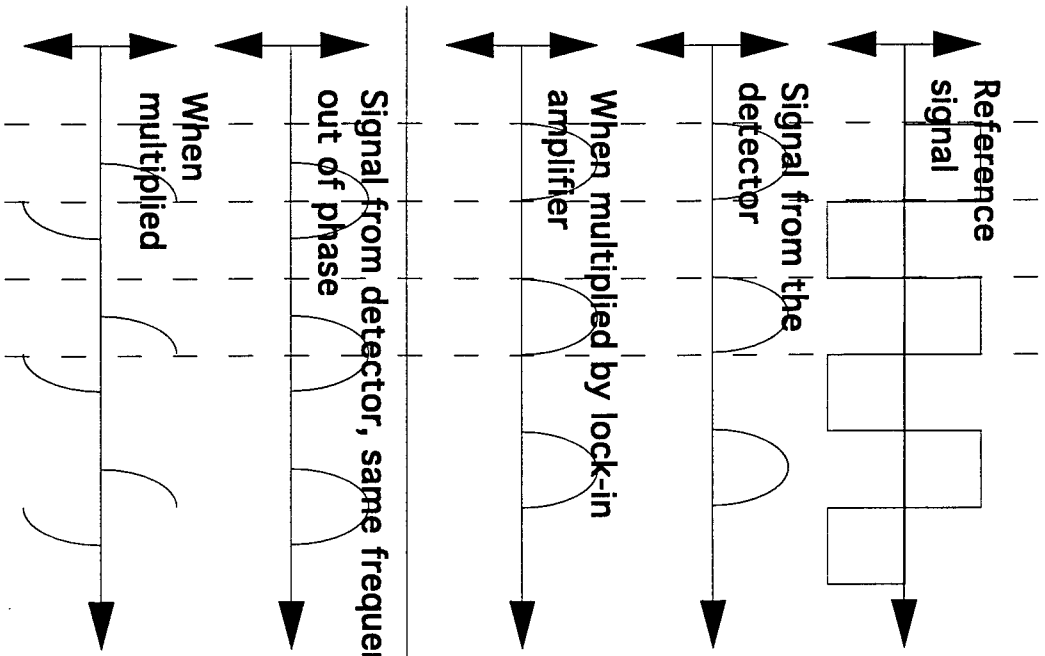


Side View



optics into my experiment, it became apparent that alignment is particularly crucial to the ability of the experiment to work. Because the image volume of the crystal was so small, the difference of a few tenths of a millimeter in any direction could mean the difference between maximum signal and no signal. By the same token, little extraneous light was allowed to enter the system.

The Chopper and lock-in amplifier work together as another type of filter. The chopper is basically a rapidly spinning disk with regularly spaced holes cut into it, located between the fluorescing crystal and the optics tube leading to the monochromator. It "chops" the light passing through it so that the signal coming through is pulsed at a set frequency. It also sends a reference signal of that frequency to the lock-in amplifier. This reference signal is a square wave, which is just an alternation of positive one and negative one at the same frequency that the light is being chopped. The lock-in amplifier takes this signal and the signal from the detector (like a square wave in that the signal alternates between the full intensity and zero but has rounded edges), multiplies them, and then integrates them over the set time period and displays this as the output. Thus, if the signal from the detector and the reference wave are of the same frequency and are in phase, the positive portion of the signal will be multiplied by positive one and the zero portion will be multiplied by negative one (and thus still come out to zero). Therefore, everything is positive before the lock-in integrates (takes the area under the curve) and divides by time giving the average signal for that period of integration (normally set to one second in my experiment). If the signal from the detector contains a signal whose frequency is other than that of the reference wave then parts of it will get multiplied by negative one. Thus, when the curve is multiplied and integrated, there will be a negative area to counter the positive area causing the incorrect signal to go to zero. This is how the lock-in amplifier works as a filter. Only the light that passes through the chopper will eventually be allowed through the lock-in. Thus the effect of extraneous light and electronic noise in the system is greatly reduced. Unfortunately, it is also possible for the correct frequency to go to zero if it is 90 degrees out of phase with the reference wave or completely negative if it is 180 degrees out of phase. Because of this, it is also important to make a phase adjustment as well to maximize the output. This must obviously be done at a wavelength where light is known to be, usually the wavelength of the laser diode.



The last system which had to be set up was the computer control of the monochromator. This was done on an IBM 486 and entailed writing a program in Lab-view. Lab-view is an icon-based, object-oriented programming language capable of, in most cases, better accommodating the human way of thinking and seeing a problem. Essentially, a function is represented as an icon to which inputs and outputs are "wired". In addition there are windows such as sequences which make certain functions are carried out in a certain order, case statements which check whether a condition is true or false and act accordingly, and the formula window which allows more difficult math to be worked without the simple arithmetic icons. After the program is written, it can all be run from the front panel which simulates the control area of a piece of equipment. The program, though it appears as just one page and the front panel, would actually take over 20 pages to print with frame after frame having been hidden by sequences or cases or as sub-programs. This is what actually turned the monochromator from a large paper weight into a high precision, user-friendly piece of lab equipment.

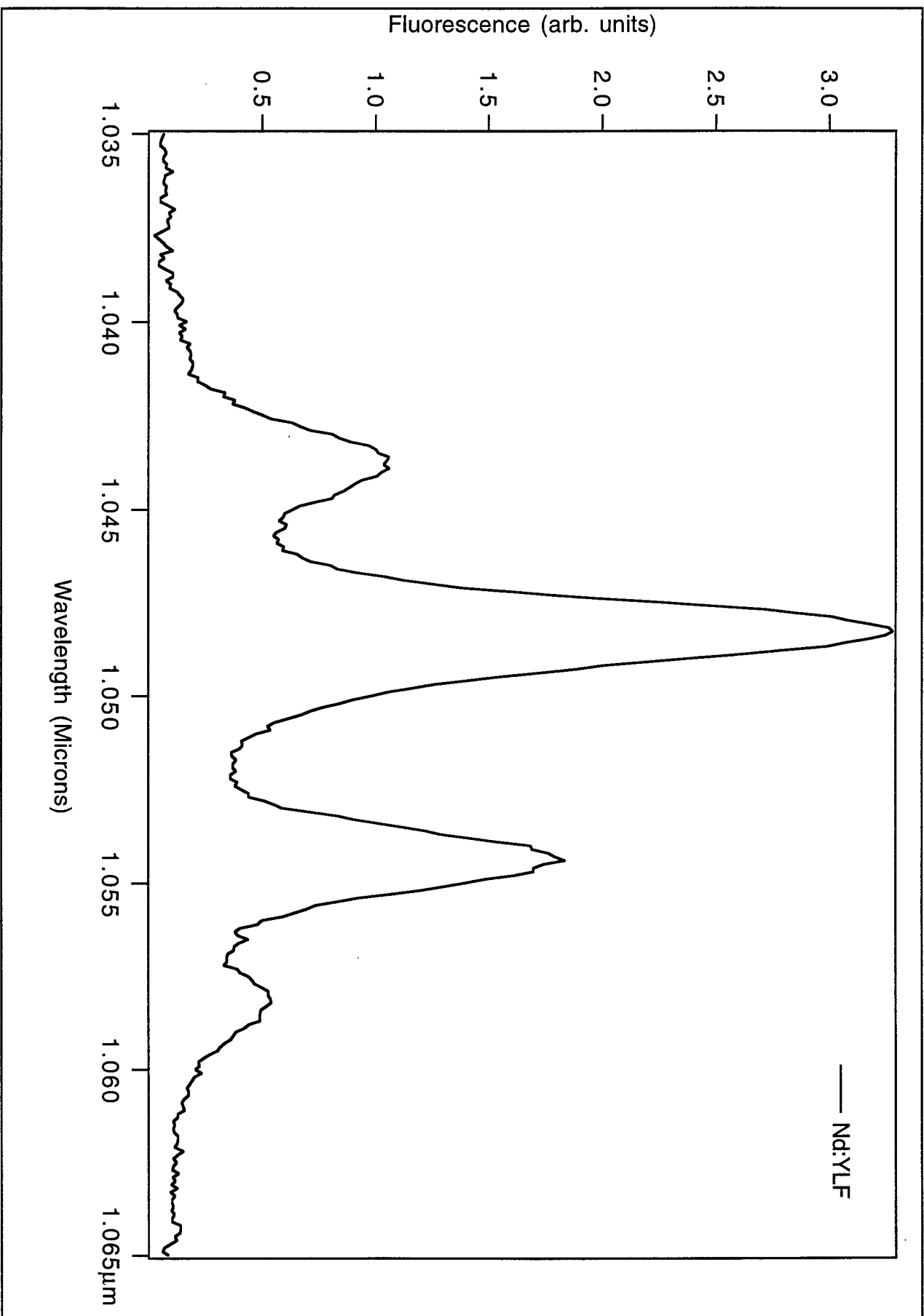
Results

With all the various systems up and working, it simply became a matter of calibration, alignment, adjustment of slit size, adjustment of sensitivity, adjustment of phase, etc., etc., the whole cycle repeated two or three times with occasional replacement of parts and the complete revamping of the optics (6 times) and, *voila!*...data. The graph included with this report is for Nd:YLF, but we also managed to find fluorescence in Nd:YAG, both corresponding to previously reported results. From this spectral data, it is possible to figure out the various energy levels of the two crystals and make a good guess as to where it will lase. To quantitatively figure out where it will lase and how much, a black body calibration for the system is also required and, in the case of the Nd:YLF, a polarizer is also need because Nd:YLF fluoresces at different wavelengths depending on which polarization you look at.

Conclusion

So, at the end of it all, I'm happy because my experiment worked and I actually got data not to mention a lot of practical experience and the lab is happy because they got a working high-res monochromator and great new optical equipment to go with it.

Unpolarized Nd:YLF Fluorescence



References

- Giancoli, Douglas C. Physics for Scientists and Engineers with Modern Physics. Prentice Hall. Englewood Cliffs, New Jersey. 1989. Second Ed.
- Hecht, Jeff. The Laser Guidebook. McGraw-Hill, Inc. New York, 1992. Second Ed.
- Melle Griot. Optics Guide 5. 1990

VALIDATION OF SYNTHETIC IMAGERY

Kyle D. Perry

Crestview High School
1304 North Ferdon Boulevard
Crestview, FL 32536

Final Report for:
High School Apprentice Program
Armstrong Laboratory

Sponsored by:
Air Force Office of Scientific Research
Bollin Air Force Base, DC

and

Wright Laboratory

August 1994

VALIDATION OF SYNTHETIC IMAGERY

Kyle D. Perry
Crestview High School

Abstract

The purpose of this research project was to produce graphs of real imagery comparing total attenuation(x axis) to the ratio of good pixels to total pixels(y axis). The graphs of the real images would then be compared to the graphs of the synthetic images to assess the similarity between the two. By proving the similarity by calculation, this would encourage use of synthetic imagery by research scientist involved in LADAR. In order to calculate total attenuation separate attentions had to be measured and entered into a formula on a spreadsheet. Average range, cosine factor, and good pixels to total pixels were taken using the Scoretool program. Weather attenuation at the 10.59102 micron wavelength was determined by using the Hitran PC program to graph total attenuation at that range and then transferring the graph to a text file. Reflectance was obtained from by using a table of values produced from prior research. Rain attenuation was found by looking up weather conditions for the test flights and entering the rain intensity during the flight into a formula. All these factors were entered into a spreadsheet and then into the total attenuation formula. The relationship of total attenuation to pixel percentages was charted and labeled for future use.

VALIDATION OF SYNTHETIC IMAGERY

Kyle D. Perry

Introduction

As the need for greater sensor capability increases, Ladar is becoming more and more of an asset to the Air Force. Ladar reflects a beam off an object and then produces an image of the target by use measuring delay and angle of reflectance. In order for a Ladar guidance system to identify a target, however, it must match the Ladar image it receives with a stored Ladar image of the target taken previously. The Ladar image that is taken of the target previously is called the real image. In order for scientist to obtain a real image for comparison they must go out and take an image manually using the Ladar system. This costs a substantial amount of time and money for the laboratory to do.

Recently an alternate method of producing a Ladar image for comparison has been found. A geometric figure of the target desired is drawn and stored in a computer. A computer program called IRMA then takes this geometric figure and generates a picture of what the Ladar image would look like. The picture produced is called the synthetic image. Synthetic images cost the laboratory less time and money than real images would.

Discussion of the Problem

The problem with using this method, however, is that synthetic imagery has not been proven similar to real imagery. The synthetic image just has the appearance of a real image by observation. This has made researchers wary of using synthetic imagery in their research. If synthetic imagery could be proven similar to real imagery by calculation, the researcher would be much more likely to utilize synthetic imagery in his work. The objective of this project was to perform a large amount of these calculations in order to prove the similarity between synthetic and real imagery.

Methodology

The first part of the project was spent finding separate attenuation factors that were present in one or both of the flight images that were received. These attenuation factors were range, cosine factor, reflectance, rain attenuation, and weather attenuation. These values were then placed onto a spreadsheet where a formula was applied to calculate total attenuation. The formula used to assess total attenuation was $(\text{total attenuation}) = \text{reflectance} * \text{cosine factor} * e^{(-2 * \text{range} * \text{weather attenuation})} / \text{range}^2$. After total attenuation was found, a graph was made comparing total attenuation(x axis) to the ratio of good pixels to total pixels(y axis). The graphs of the real images will be compared to graphs of the synthetic images so that similarity can easily be determined.

Using the Scoretool program, measurements of the range, cosine factor, and pixel percentage were taken. Range is the average distance from the object to the sensor while cosine factor is the angle of return for the laser to the sensor. Pixel percentage is the ratio of good pixels to total pixel in the area are measured and is equivalent to the quality of the image. This measurement will be used as the y axis for the graphs comparing real imagery to synthetic imagery. All three of these measurements were take for both flights f3-14 and f3-16 with 15 passes for each flight. Each pass was divided up into a series of frames where measurements were taken for frames 3-6 in order to conserve time. These measurements were recorded and entered into a spreadsheet program.

After taking these measurements, it was necessary to find weather attenuation. Weather conditions for both flights were found and transferred into units that the Hitran PC database program could work with. The Hitran program was instructed to chart all absorbance peaks in the 10.5 to 10.6 micron range in Voigt profile. These separate attenuation peaks were combined to form a composite absorption line that graphed the actual attenuation in that range. A text file of the graph was generated and entered into a word processing program so that the exact attenuation could be found at 10.59102 micron wavelength. This attenuation factor for both flights was then entered into the spreadsheet.

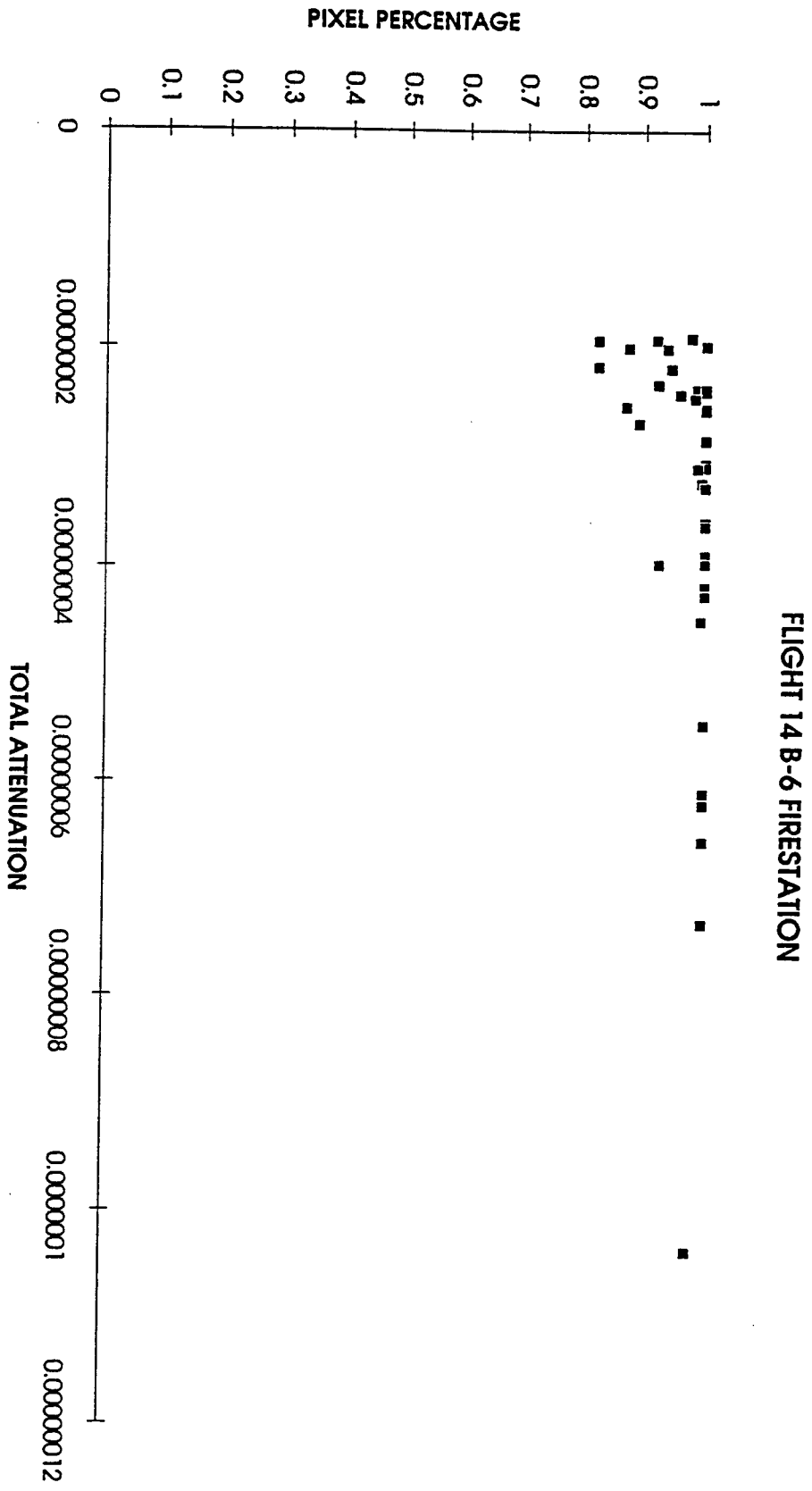
Due to some precipitation in Flight 3-16, rain attenuation was calculated by first finding the rain intensity for the time of the flight. This data was entered into a formula($\text{rain attenuation} = .21 * \text{rain intensity}(\text{mm/hr})^{.74}$) and rain attenuation was found. This measurement was then entered into the spreadsheet.

The last attenuation factor was the reflectance of the objects that were measured. A table of reflectance values was used to calculate the amount of attenuation that reflectance caused on the image. These values were also recorded onto the spreadsheet.

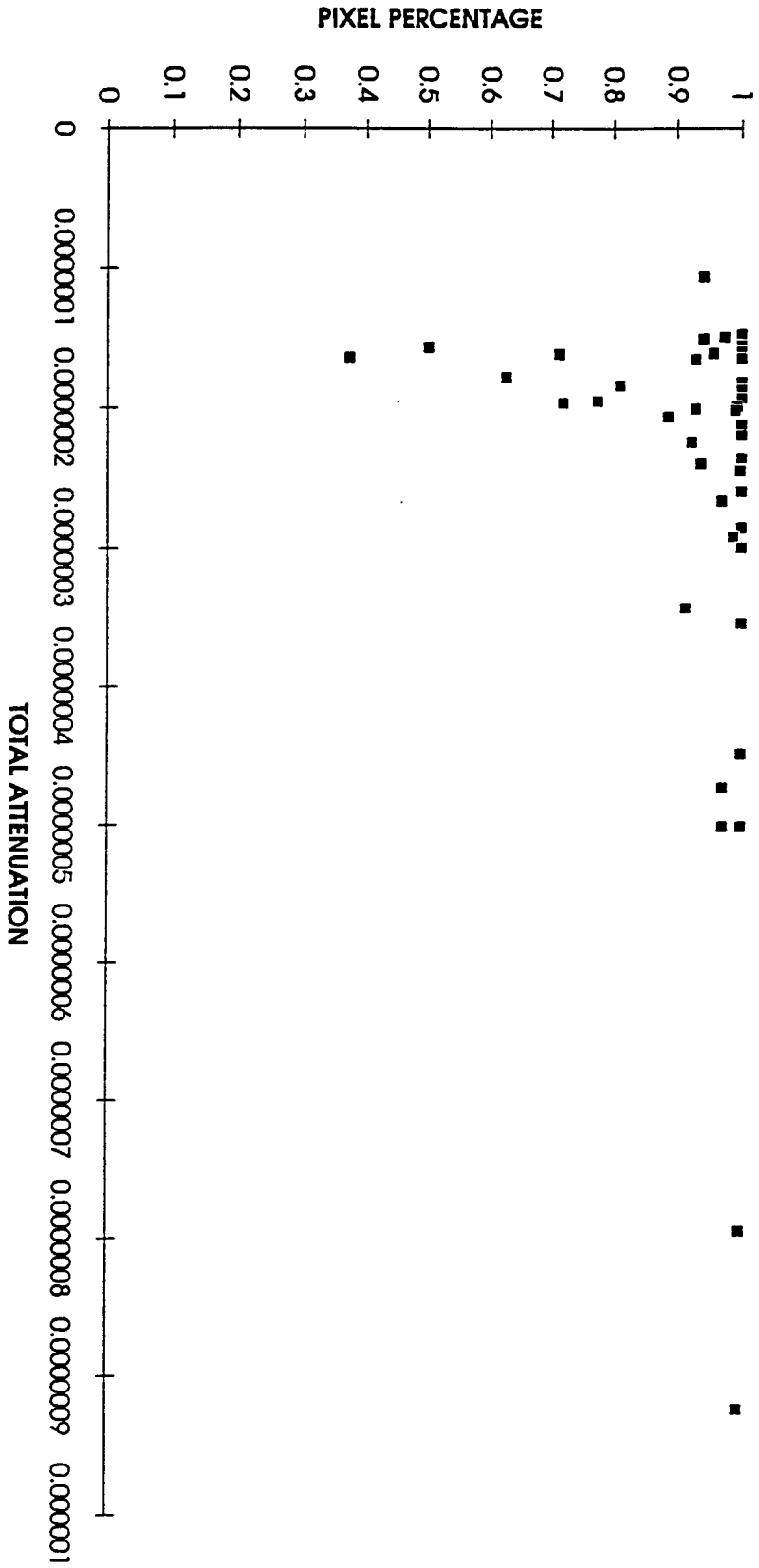
After all attenuation factors and pixel percentages were recorded, the formula for total reflectance was entered into the spreadsheet and calculated. A graph was made with the total attenuation as the x axis and the pixel percentage as the y axis. The graphs produced are merely a series of points that show the general trend in the images. This is appropriate since the graph is not meant to be a perfect line but merely a indicator for the behavior of the image.

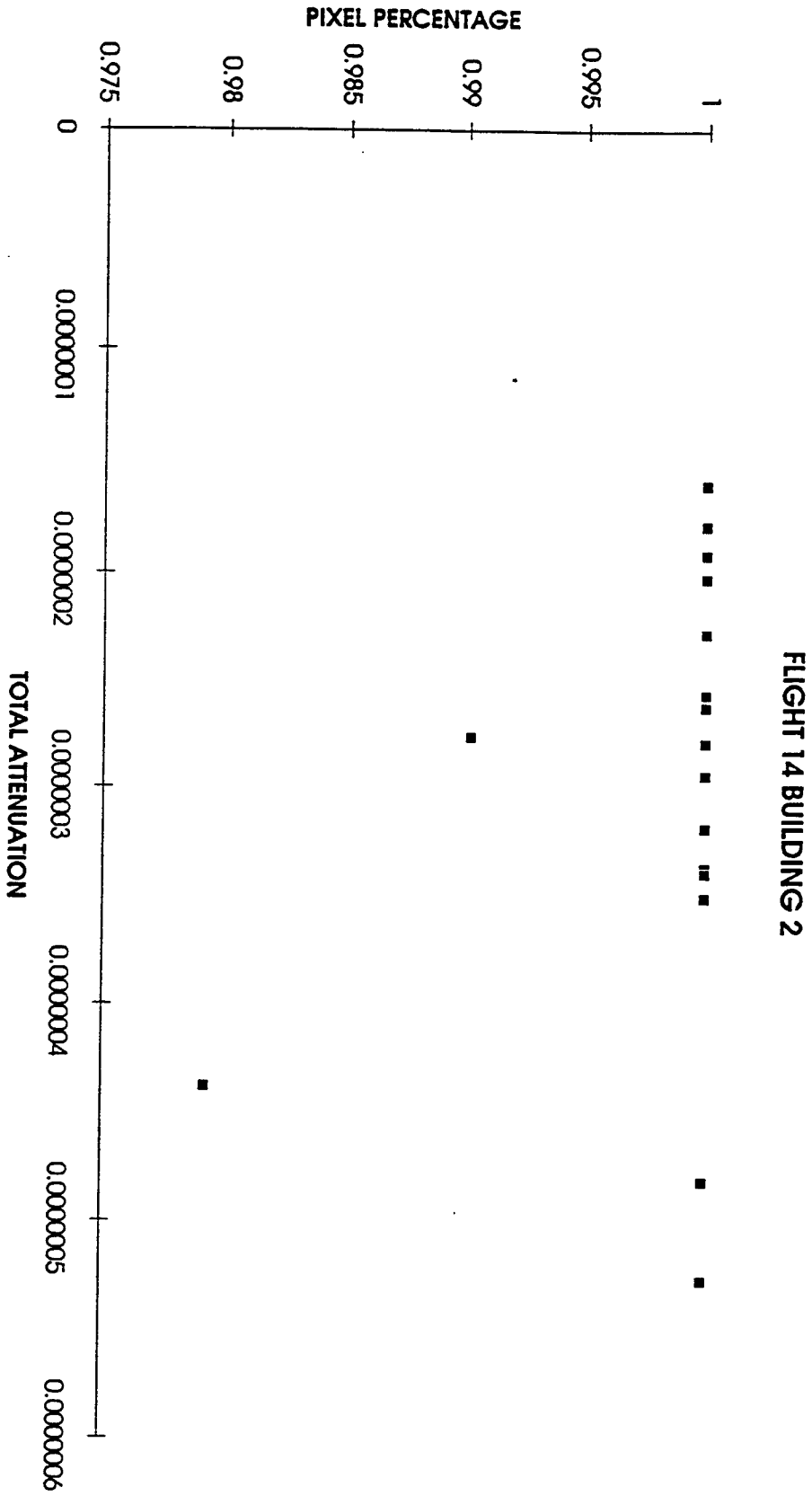
Results

The graphs came out a little bit differently than expected at first. A somewhat regular curve was expected that approached 1 as the attenuation coefficient increased. Instead, there was a wide range of values when the attenuation coefficient was low but this range decreased to 0 as the coefficient increased. This is not too discouraging since a definite trend can be seen on the graphs. Listed is the series of graphs produced this summer.

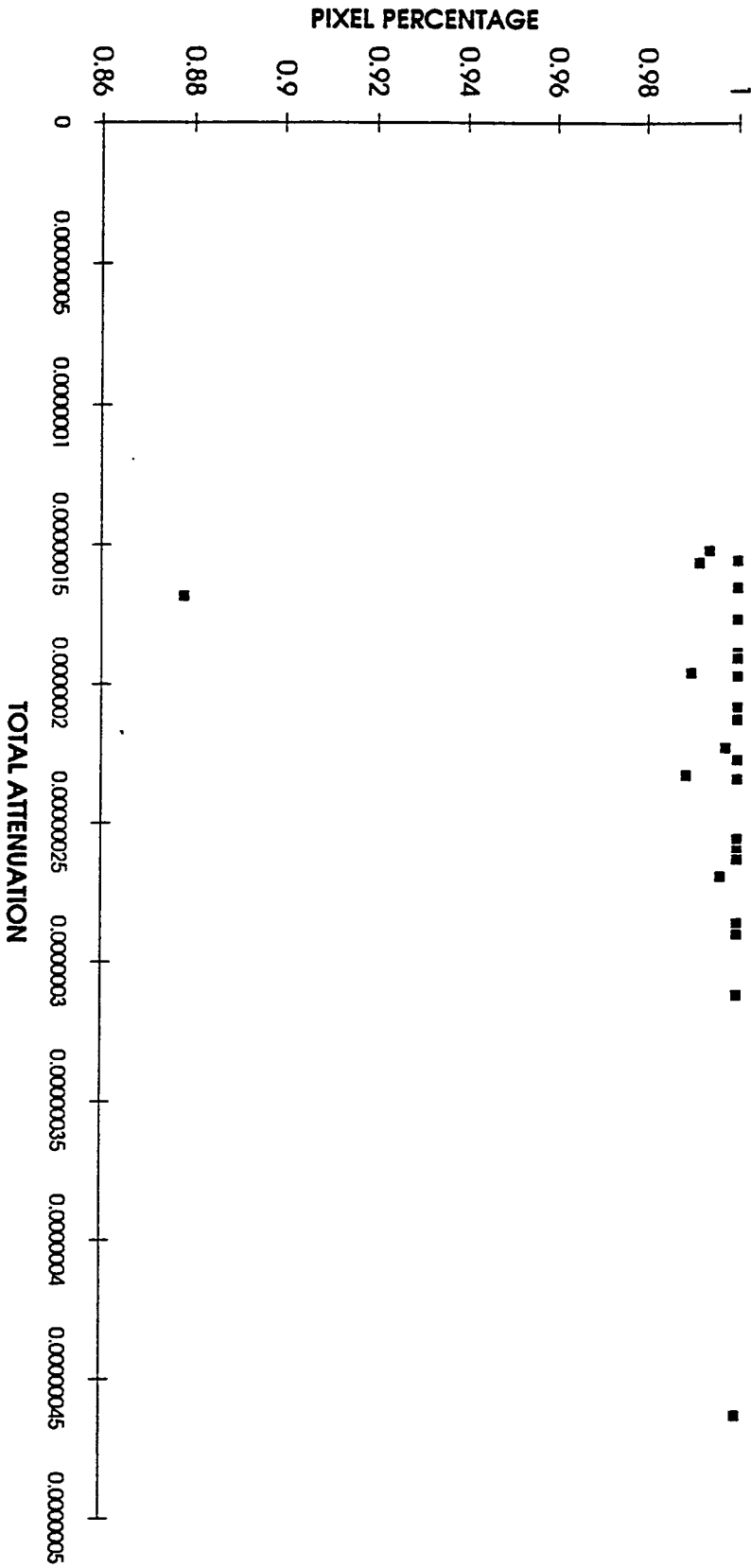


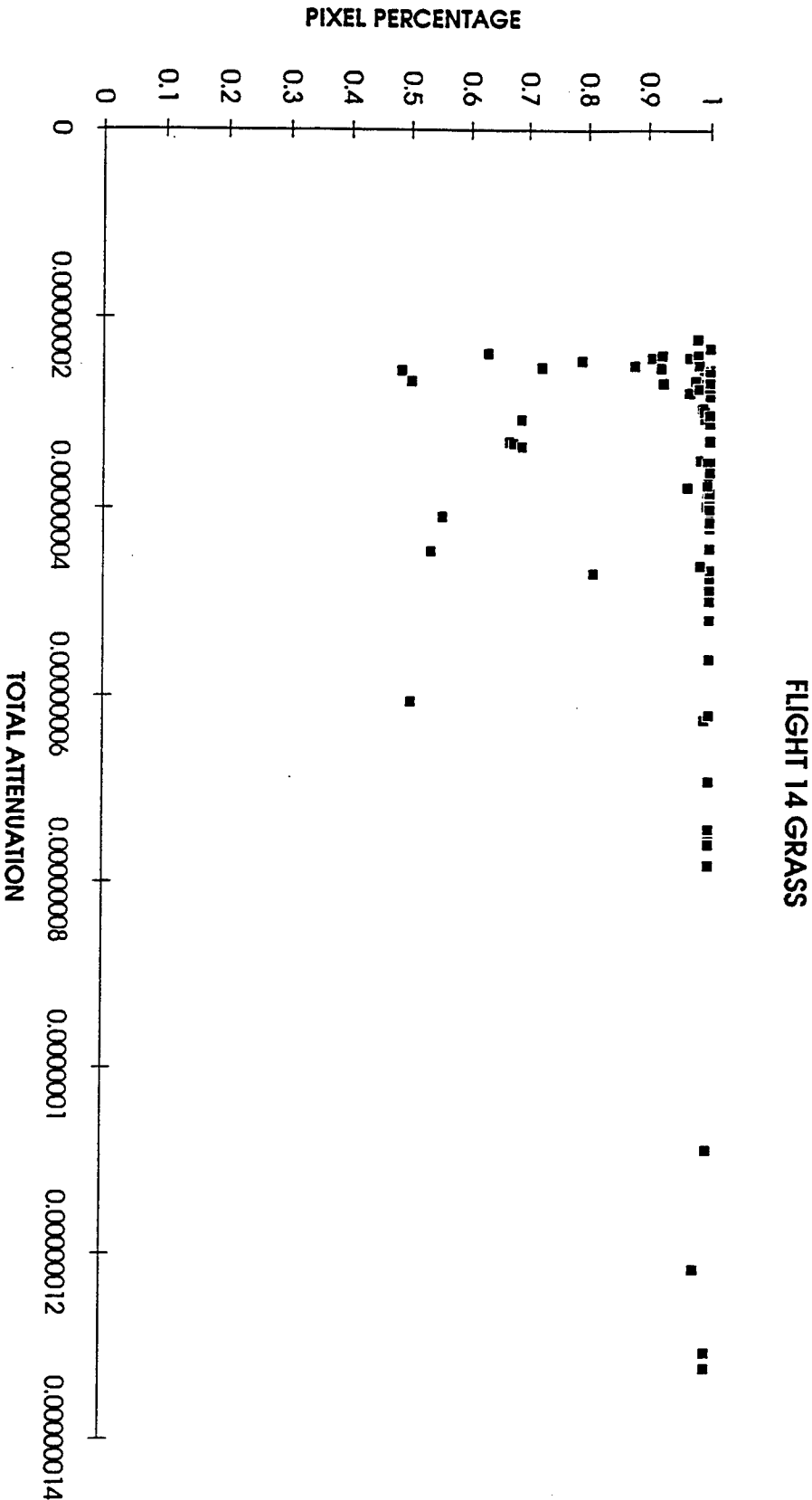
FLIGHT 14 HANGERS



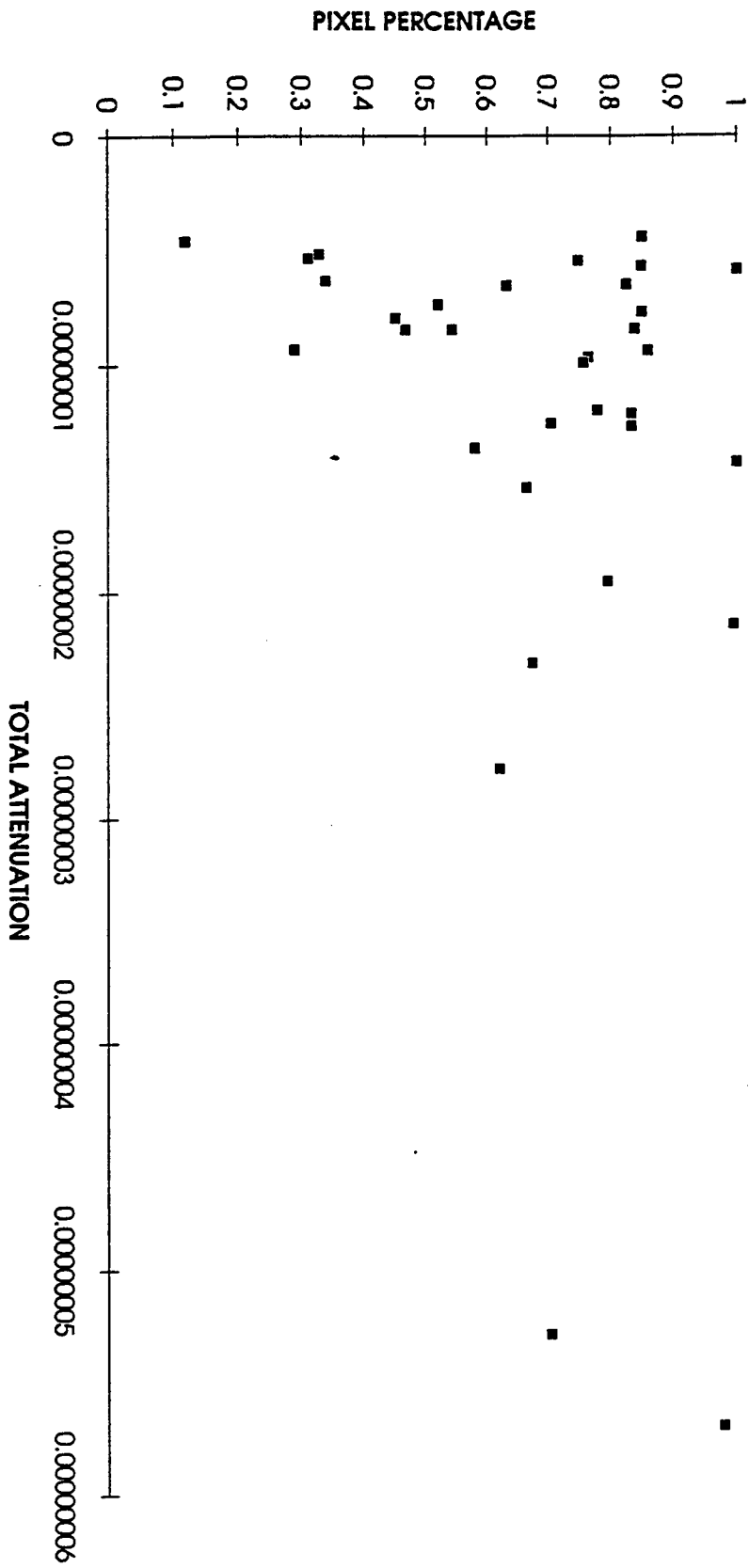


FLIGHT 14 BUILDING ABOVE HANGERS

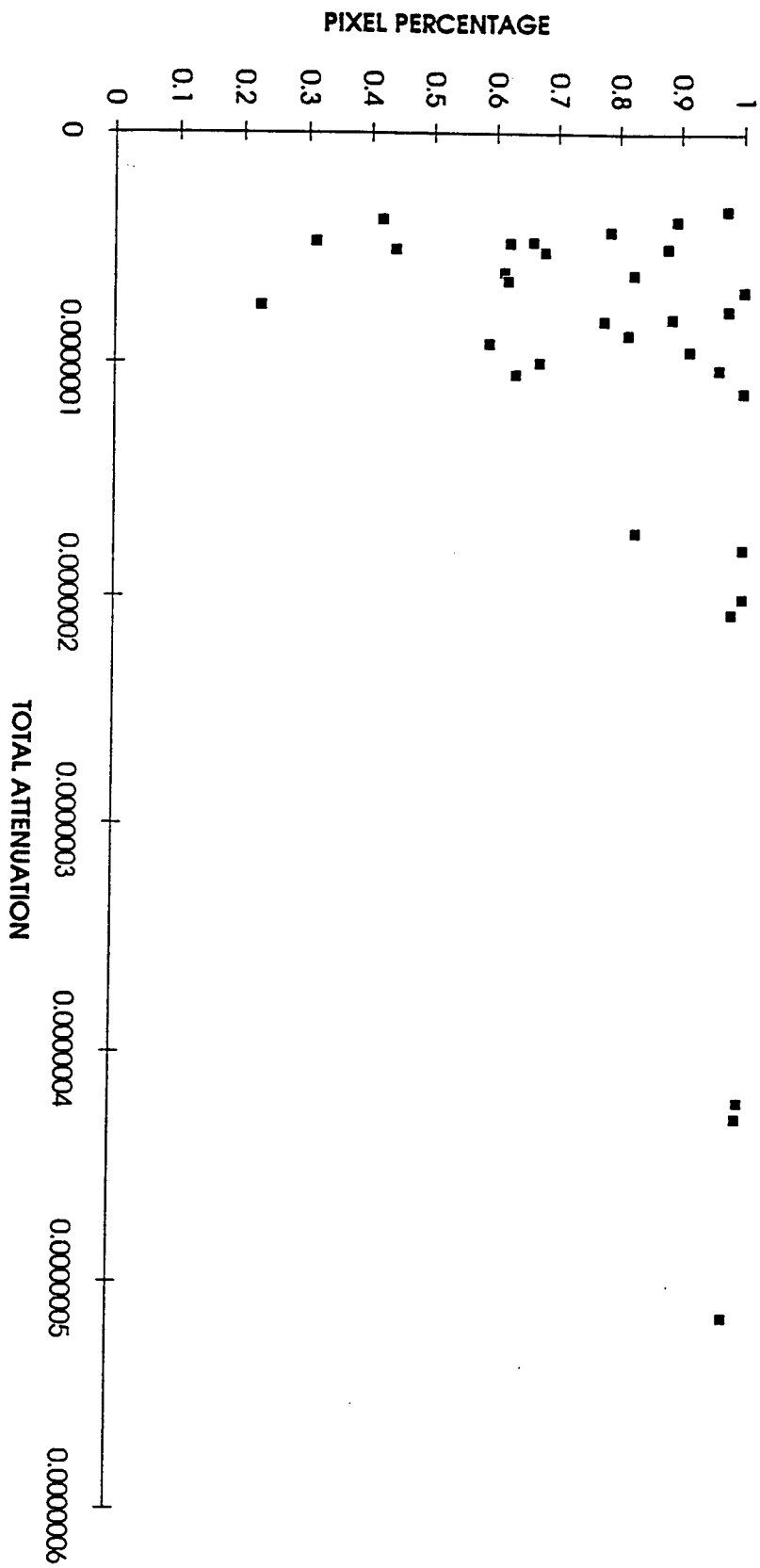




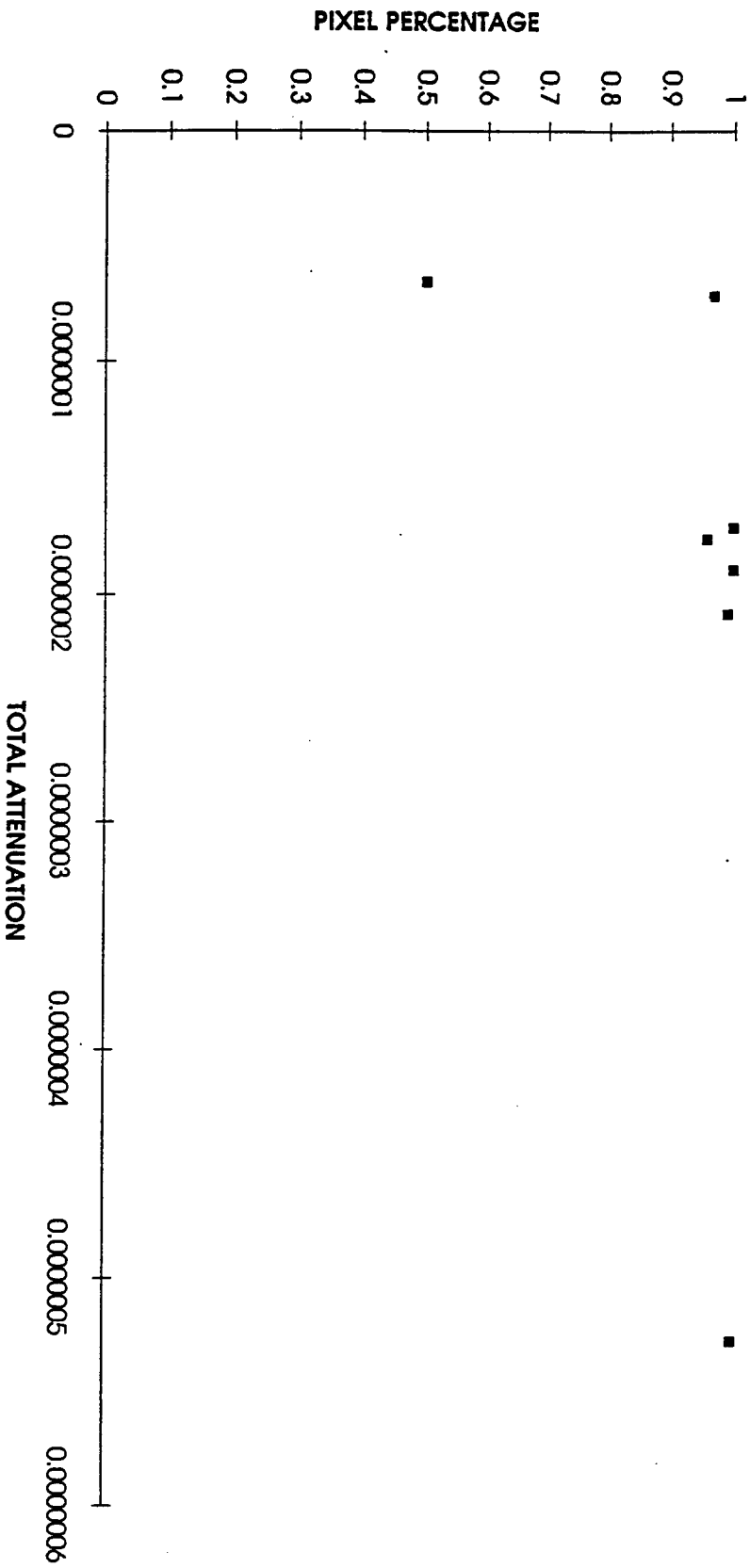
FLIGHT 16 B-6 FIRESTATION



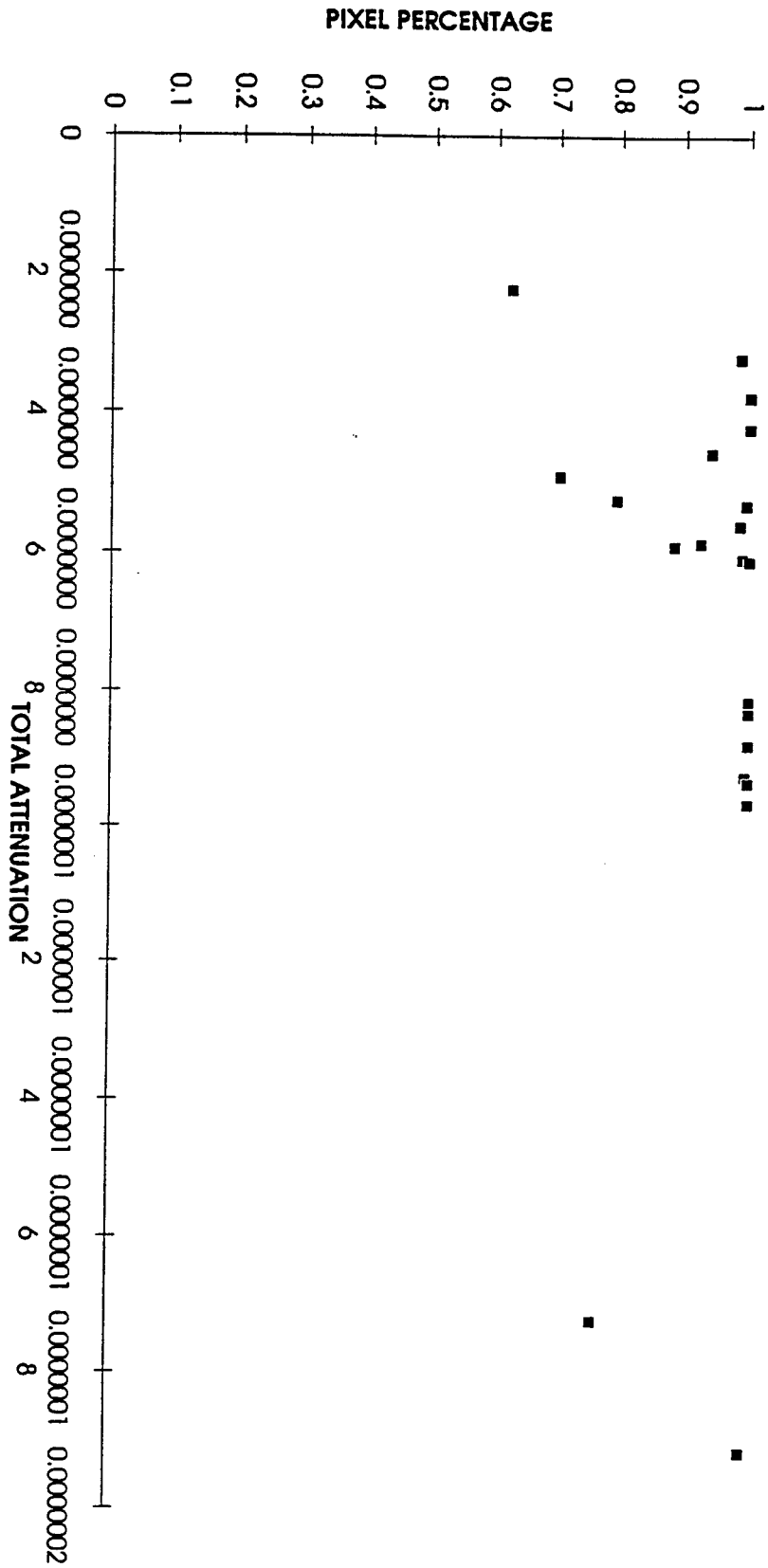
FLIGHT 16 HANGERS



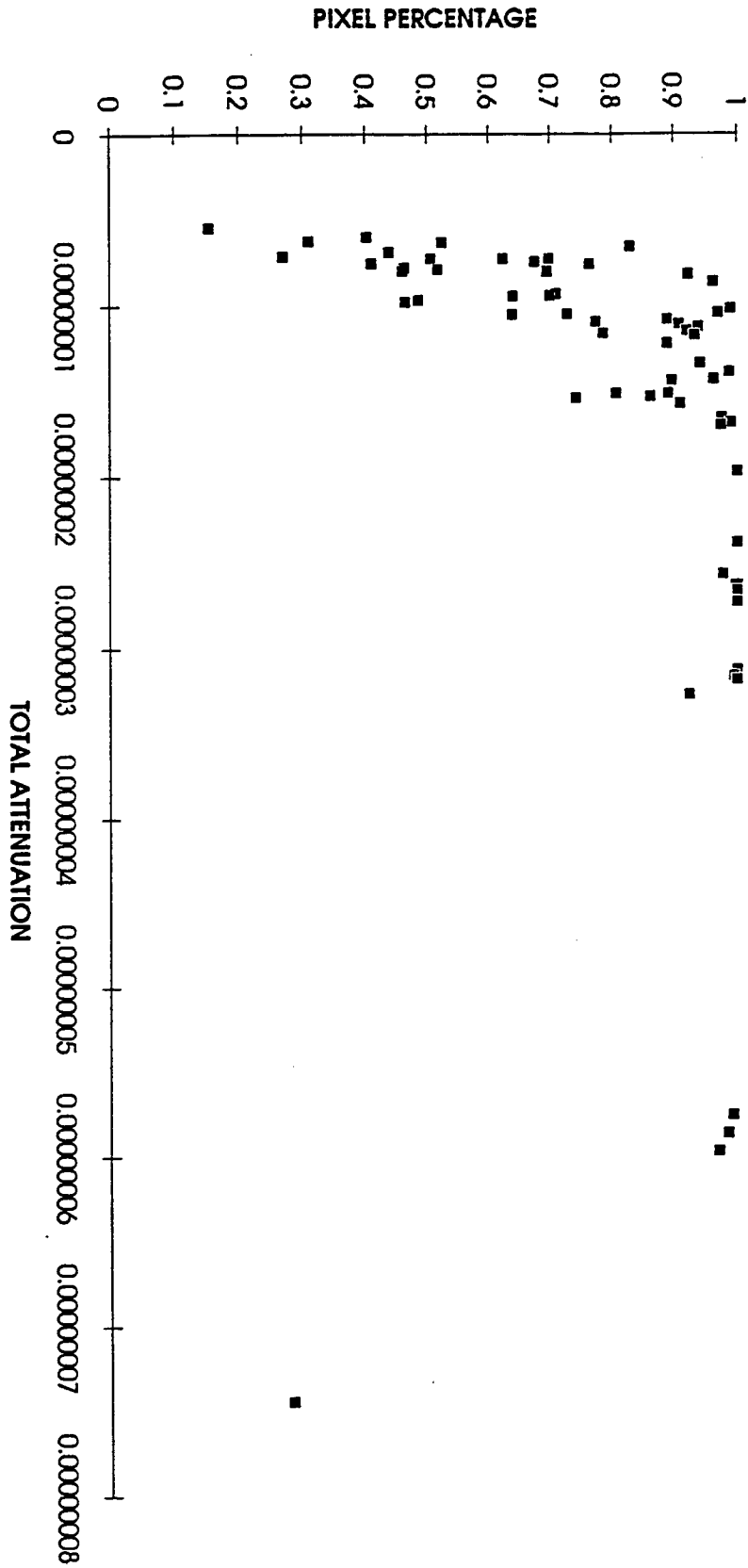
FLIGHT 16 BUILDING 2



FLIGHT 16 BUILDING X



FLIGHT 16 GRASS



Conclusion

Since no synthetic image graphs have been made for comparison, no real conclusions about the similarity can be given. A greater amount of points on the graphs would improve the accuracy of the relationship between pixel percentage and total attenuation. From the graphs produced, this method appears to be an orthodox strategy for proving similarity between real and synthetic imagery.

Bibliography

Hitran PC Database, University of South Florida, 1991

University Physics, Sears and Zemansky, Addison-Wesley Publishing Company, 1957

Acknowledgments

I'd like to thank all the following people for making this paper possible.

Steve Whyte for being such a great mentor and friend.

Lynn Deibler for his advice with this project.

Mike Welfare for his instruction and crash course instruction on synthetic imagery.

Todd

Mike Deiler and Don Harrison for running the program

Col. Pletcher for his support of the HSAP program.

Dr. Klausidus for his support of the HSAP program

Entire MNGA branch for their support

Glenda Apel for helping out with the pay vouchers

All the other High School Apprentices for their fellowship

Daniel R. Pfunder

Centerville High School
500 East Franklin Street
Centerville, Ohio 45459

Final Report for:
High School Apprentice Program
Wright Laboratory

Sponsored by:
Air Force Office of Scientific Research
Bolling Air Force Base, DC

and

Wright Laboratory

August 1994

35-1

INTEGRATED GENERATOR TECHNOLOGY

Daniel R. Pfunder
Centerville High School

Abstract

Several tasks were attempted and completed during the weeks between June 13, 1994, and August 5, 1994. These tasks all centered around the research of high speed gas turbine generators for aircraft power supply. These tasks covered a wide range of disciplines. These disciplines include: graphical analysis, computer aided design, text research, spreadsheet applications, computer programming, and lab work. This report will follow the work of the Wright Laboratory Electromechanical Technology Section Engineers on the Integrated Power Unit (IPU) generator concept, and whenever possible, explain my contributions to the project.

INTEGRATED GENERATOR TECHNOLOGY

Daniel R. Pfunder

Introduction

The Integrated High Performance Turbine Engine Technology Initiative (IHPTET) is a joint project between the Army, Navy, Air Force, NASA, DARPA, and industry working together to accomplish the goal of doubling the propulsion capability of gas turbine engines by the turn of the century. In order to accomplish this goal, advanced materials, innovative structural designs, and advanced computational methods need to be developed and incorporated into all aspects of the turbine engine and its support systems (Oxley, Thomson 2-3). It is theorized that if an aircraft's accessories such as inlet guide vane actuators, fuel and lube pumps, and inlet particle separators could be powered electrically rather than the current mechanical method of running gearboxes with the main turbine engine, then a significant amount of weight could be saved when these gearboxes are eliminated. Engineers at the Wright Laboratory are working with the idea that an internal generator, powered by a small, non propulsion gas turbine engine, might someday power all of the aircraft's main and secondary systems. Current technology is not at the level of advancement where a "More Electric Aircraft," (MEA), will soon be a complete reality but small steps forward are taking place every day.

Discussion of Problem

In most aircraft in use today, including civilian and military aircraft, both main and secondary power for most systems is supplied by the main propulsion engine. Engine adjustments, such as inlet particle filtration, and fuel and lubrication pumping, are taken care of via a system of gearboxes attached to the main propulsion engine's drive shaft. Electrical power is also produced with this method. The rotor of a generator is turned with a gearbox from the main propulsion engine. Due to the ongoing quest for improvement of current aircraft systems, industry has been searching for a better, lighter, and more reliable alternative to the traditional system of gearboxes for the operation of aircraft systems. The answer is the More Electric Initiative. The More Electric Initiative is a joint endeavor between the Department of Defense, and industry to focus research and development efforts in the field of electrical powered subsystems for aircraft applications. The motive for this switch is the fact that the bulky gearbox, and hydraulic systems can be eliminated in exchange for compact, electrical versions of fuel pumps, brakes and other systems. As more electrical power is utilized on the aircraft, new methods of power generation are discussed to meet these growing needs. One popular new concept in generator configuration is the idea of spinning a generator rotor directly with a turbine engine. The turbine could either be the main turbine engine, or a separate, non propulsion engine located in the fuselage. Either configuration poses new problems in the areas of heat dissipation, and extreme angular velocities because generators typically are not designed for continuous use at fifty-thousand revolutions per minute inside a turbine compression chamber. Further research needs to be done on the effects of such high speeds and temperatures on electric generators so that as

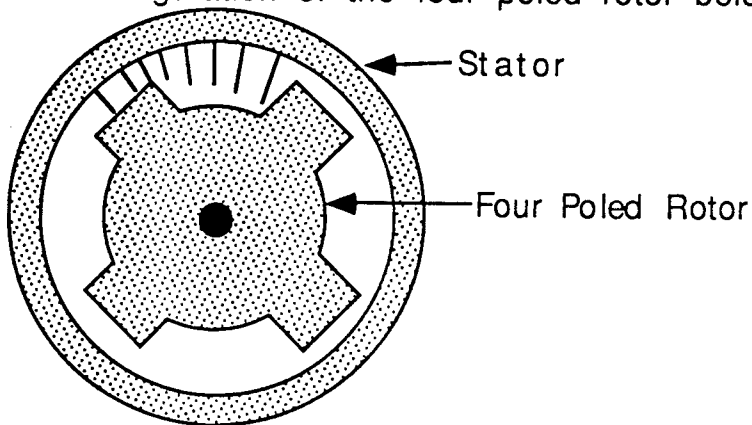
other More Electric Initiative components become flight ready, an effective power supply will be there, ready to power these new technologies in an aircraft situation. At Wright Laboratory, work is being done to find the effects of windage losses and heat extremes on the high speed generators designed for use inside turbine engines.

Methodology

Several different tests were completed in order to discover the separate contributions of the different types of losses making up the total windage loss on the generator. The basic test consisted of spinning up a generator in a vacuum chamber up to around fifty-five thousand revolutions per minute and measuring the deceleration rates of the rotor when allowed to "spin down" freely without any interference from the air. Then the same generator was spun back up to an angular velocity of around fifty-five thousand revolutions per minute, and allowed to "spin down" in an ambient air pressure environment. The difference in deceleration rates leads to the values of air friction affecting the system and the total amount of energy lost due to this friction. Instantaneous deceleration rates at five specific angular velocities were found by taking a time versus angular velocity graph and finding the tangent line to that graph at the desired velocity given that $\Delta\omega / \Delta t$ is an instantaneous angular deceleration value.

One of the first tasks I worked on during my tour at Wright Laboratories was finding these deceleration values for the tests ran in the lab up to date, and organizing the data into a spreadsheet format that could easily be followed by any reader. After some experience with the test, I was able to realize when the chart was not doing what it was supposed to, and what type of rotor configuration was used just by inspection of the concavity of the curves.

As the generator is exposed to higher speeds, the effects of wind friction become very significant. There were four types of windage losses that affect the generator in the tests performed which add up to the total windage loss on the generator. Each of these losses can be singled out by adjusting the rotor and stator configurations inside the generator. The first of these windage types is disk windage. Disk windage is the effect of spinning a circular disk in the presence of air. In this case, disk windage occurs on the end of the rotors where the circular surfaces of the roughly cylindrical rotor are exposed to air as they rotate. The overall losses contributed to this particular type of windage loss is relatively small, only about half a horsepower compared to the total windage loss of around seventeen horsepower. The second type of windage loss affecting the generator is viscous windage. This type of windage is generated by two parallel surfaces moving past each other. In case of the generator, viscous losses occur in between the rotor and the stator where there is only a small gap of about two hundredths of an inch between the rapidly moving surfaces. As would be expected, the losses are smaller in a four poled rotor design compared to a smooth rotor design because there is less rotor surface within close proximity to the stator surface on a poled rotor compared to a smooth rotor. There is around a half horsepower loss with the poled rotor design compared to approximately a one and a half horsepower loss in the smooth rotor design. Another type of windage loss that affects the generator is mixing windage. Notice the configuration of the four poled rotor below. If it is imagined



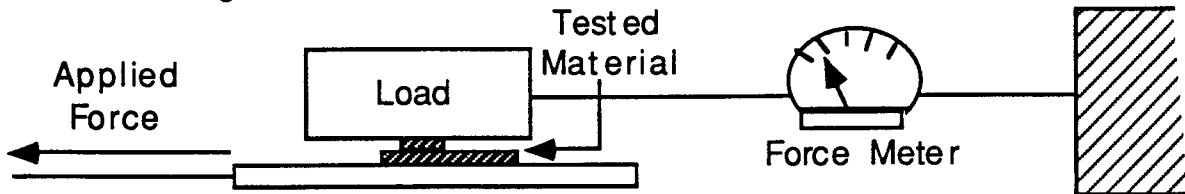
that the stator is moving around a stationary rotor, it best illustrates the idea that as the air being pulled through the gap between the pole and the stator, it is exposed to the larger volume of air between the poles, the moving air is diffused and strikes the side of the next pole. This torque is the source of some windage loss. In the tests done in the Wright lab these losses were calculated to be around 3.8 horsepower. Mixing losses also occur when there are slots cut into the stator inner surface. The final source of windage loss noted in this study is known as pumping loss. The generator being developed is air cooled because of the desire to dramatically improve reliability and simplicity over the traditional oil cooling approach. Air is pumped through the gap in between the poles of the rotor. While rotor spins, it takes energy to get the air to stop moving in a straight line, and to rotate with the rotor. This transmission of energy results in a loss of energy in the generator, and is a form of windage. Tests continue in order to further understand the basics of how the integrated power unit generator should work.

As tests continue, new pieces of test apparatus need to be fabricated. In order to make sure that the new pieces will fit the old pieces that were constructed earlier, I took on the task of taking accurate measurements of the bearing housings on the generator. The bearing housings are the end caps which hold the rotor in place and hold the stator just outside the spinning rotor. Measurements were taken with a straight edge ruler, inside micrometers, and a vernier calipers. Accuracy was kept to the thousandth of an inch. The final results were presented in an actual sized computer aided drafting sketch of the cross section with all of the measurements included. For some of the results, a Microsoft Excel spreadsheet was used to take several measurements over a two-week span and average the results to find the most accurate measurements. If in the future changes need to be made to the housings, the diagrams will be useful in making these changes

In addition to information on the physical properties of the generator, the Electromechanical Technologies Section Engineers were also interested in the materials used for the rotor. Rotors are generally comprised of a thin magnetic material that is cut into sheets in the shape of the rotor cross section. Hundreds of these laminates are bolted together with two thousand pounds of force. It is this stack of laminates which makes up the rotor body. In order to work correctly, each of the individual laminates must be insulated from the others. This is accomplished by quickly oxidizing the outside surface of the laminate. This oxide layer is a very effective insulator. This type of process works very well for most low speed generator applications, but it is not known what effect running this type of generator at close to sixty thousand revolutions per minute will have on the rotor and its laminates.

The gap between the rotor and stator is approximately two hundredths of an inch thin, any motion of the laminates might result in a condition that would destroy the generator. Tests have shown that the laminate material is very brittle and does have a tendency to fracture due to the stresses placed on the generator rotor. This raises the question of whether or not these laminate pieces have the ability to slide out of place, possibly destroying the generator. I was asked to build an apparatus to find the coefficient of static friction between the laminate pieces. After completing some research, it was found that the official method of discovering the static coefficient of friction of a material is to find the relation of the force required to set the test sample in motion with respect to the other sample, over the force applied to the sample perpendicular to the direction of motion. The method I had in mind was to secure the load attached to a piece of test sample to a wall or other rigid barrier. A force measuring device, such as a spring balance, would be in between the load and the wall. The load would be resting on a "cart" that had a piece of test sample attached to it. By recording

the force shown on the force meter as the "cart" begins to slide and dividing it by the load placed on top of the sample, the static coefficient can be found. The diagram below shows the basic set up of the test rig.



As time passed, the apparatus changed shape a bit. the loads I was asked to work with were in the neighborhood of fifty to one-hundred pounds per square inch on the test sample. If possible, larger loads would be used. In order to pull these larger weights, a crank drive system was built. The largest change in the apparatus, was the addition of a load cell as the force measuring device. A load cell is a mechanical device which changes resistance proportionally to the force applied to the cell. because of this electrical aspect of the test rig, computer interaction became a reality. A Hewlett Packard 34401A multimeter was attached to the output of the load cell. This multimeter has the capability to take and record it's own readings. A ZEOS 386 laptop computer was then programmed to tell the Hewlett Packard multimeter when to start to take readings of the voltage output of the load cell. The computer then was programmed to convert the voltage readings into the equivalent force values. The benefit of having the computer in the test rig is that it can graph the recorded data at a moment's notice. After many hours spent debugging the computer program, data towards finding the static coefficient of friction of the laminates of the proposed generator was taken.

Results

Acceptable data was obtained for all of the tasks I attempted to complete during my summer tour at Wright Laboratories. The deceleration rates I obtained from the windage tests were matched up against a set of deceleration rates a computer configured from a graph of the data, and the values were very close for the most part. The deceleration rates of different tests which were run on different days with the same apparatus were very similar. This also is a positive sign that the information was coming out accurate. The measurements of the bearing housings were also successful. The instruments I had at my disposal were not of the finest accuracy at the thousandth of an inch increment. But because of repeated measurements, I am confident that an accuracy of ± 2 thousandths of an inch holds true for most measurements. The results of the coefficient of friction rig were both encouraging and disappointing. I expected the graphs of the different trials to have a sharp spike in the beginning representing the higher static coefficient values, and then fall down to a horizontal line representing the kinetic coefficient while sliding. In the actual graphs, there is rarely a sharp static spike. When there is one, it is usually small. Because of this, a good value for the coefficient of static friction was not obtained. I am quite pleased with the value for kinetic coefficient. Most of the graphs agree with the value found within a twelve percent deviance. I also performed a different coefficient test to see if the value found in this test would be close to the value found with the rig. The values did check out. I obtained a new value for the coefficient that was within four percent of the value I was checking. Given the restricted time I had to complete these separate projects, I am quite happy with the results.

Conclusion

I was not sure what to expect from this summer project, nor what I would learn during my tour. But now looking back on it, I have learned quite a lot in such a short amount of time. The projects were interesting, they made me want to go to work and finish the projects just to see what was planned for me next. I especially enjoyed the freedom to work on my own during the coefficient of friction rig. I would have loved to see a spike but no luck.

I think that there is not a spike because the rig may have had just enough vibration in it to break the static coefficient before it could be broken by the force applied to it. I tried to keep the machine's vibration down to a minimum, but I guess it was not enough. If I had more time to concentrate on this particular aspect of the tour, I would try to solve the vibration problem to see if this is why I do not have a static coefficient spike. Of course there is always the possibility that there is not a significantly high static coefficient of friction. I assume that there is, because most materials have a static coefficient that is one and a half of two times the value for kinetic friction. But the oxide coating might be a substance that is different. Only further research will tell for sure. The fact that the values I obtained for the kinetic coefficient of friction for each trial were so close together reassures me that the apparatus does work the way it is supposed to, but something is not letting the static value be a factor in the test. I know that I learned a lot this summer just by being exposed to the Wright Laboratory and how it works, and I think I helped the Electromechanical Technologies Section get one step closer to the development of the Integrated Generator by working on these tasks this summer.

Chemical Characteristics of the Rocky Creek System

Mary F. Pletcher
High School Apprentice
Environmental Assessment Branch

Wright Laboratory Armament Directorate
WL/MNSE
Eglin AFB, FL 32542-5434

Final Report for:
High School Apprenticeship Program
Wright Laboratory Armament Directorate

Sponsored by:
Air Force Office of Scientific Research
Bolling Air Force Base, Washington DC.

August 1994

Chemical Characteristics of the Rocky Creek System
Mary F. Pletcher
High School Apprentice
Environmental Assessment Branch
WL/MNSE

Abstract

Etheostoma okaloosae, commonly known as the Okaloosa darter, is considered to be an endangered species. In order to prevent the extinction of this fish, toxicity tests are being performed by contractors on the very similar *Etheostoma edwini* (brown darter). To conduct these experiments, the conditions of the habitat of both fish must be known. Thus the purpose of this project was to determine the chemical characteristics of the Rocky Creek system.

To determine the chemical characteristics, water samples were taken from five different locations on two different dates to compare normal conditions versus those present after heavy rainfall. Tests were conducted to determine volumetric flow rate, temperature, dissolved oxygen content, pH, conductivity, alkalinity, nitrate nitrogen composition, and turbidity.

The tests showed that an increase in volumetric flow rate after heavy rainfall was dependent on location, temperature changes were only slight with the mean temperature change being 0.68 degrees Celsius, and dissolved oxygen content is higher under normal conditions. The tests also indicated that the Rocky Creek system was acidic with the pH at all locations tested falling between the range of 4.1 to 5.3 under normal conditions and after heavy rainfall. Conductivity tests indicated that the total ionic concentration was lower under normal conditions than after heavy rainfall. Alkalinity generally increased after heavy rainfall as did nitrogen nitrate composition. Finally, turbidity tests showed that the quantity of particulate present was dependent on the location.

Contents

Introduction.....	4
Background.....	4
Procedure and Results.....	5
Miscellaneous.....	8
Acknowledgements.....	8
Appendix.....	9
References.....	11

Chemical Characteristics of the Rocky Creek System

Mary F. Pletcher

Introduction

Etheostoma okaloosae, commonly known as the Okaloosa darter, is a small fish found in freshwater creeks and streams near Eglin AFB testing sites. Federal agencies have determined that the Okaloosa darter is an endangered species. In an effort to prevent the extinction of this fish, contractors are conducting toxicity tests on the very similar brown darter (scientifically referred to as *Etheostoma edwini*). However, before accurate tests can be designed and performed the water conditions of the Rocky Creek system, the common habitat of both fish, must be known. Thus the purpose of this project was to determine the chemical characteristics of the Rocky Creek system. To determine the chemical characteristics of the Rocky Creek system eight tests were conducted: volumetric flow rate, temperature, dissolved oxygen, pH, conductivity, alkalinity, nitrate nitrogen composition, and turbidity.

Background

Eglin AFB Reservation and the Rocky Creek system Eglin AFB reservation is located in Northwest Florida and extends through Walton, Okaloosa, and Santa Rosa counties. The Rocky Creek system begins in the northeast section of the Eglin reservation and transverses south to Rocky Bayou. A relatively large amount of land has remained undeveloped on the reservation. The exceptions are scattered test areas, installations, roads and reforestation areas. Soils on the reservation are primarily yellow brown sand of the Lakeland association with a slightly acidic pH. Lakeland association soil makes up around 78 percent of the Eglin AFB reservation. The other 22 percent is composed of St. Lucie-Paola association (2 percent), Troup-Lakeland association (10 percent), Chipley-Lakeland-Rutledge association (4 percent) and Dorovan-Pamlico association (6 percent). The most significant impact on water quality at the reservation results from the production and movement of sediment

through land-use practices. The primary sediment source is from clay and sand transported by runoff during heavy rains on the many clay roads that cross streams, including the Rocky Creek system, in the reservation. During very heavy rains, washouts have occurred thus causing large amounts of sediment to be carried downstream, eventually settling downstream. (Crews, 2-3).

Dissolved Oxygen Oxygen enters water by diffusion from the atmosphere and from the photosynthesis of green plants in the water. The quantity that is retained in the water is dependent on the velocity, and the amount of pollution and decomposition occurring in the stream. Generally swift water contains more dissolved oxygen than slowly moving or stagnant water (Knots, 23). Dissolved oxygen is also dependent on temperature, with more oxygen being present in cold than in warm water (Schwoerbel, 23). Dissolved oxygen is imperative to the survival of fish and other aquatic life, it also aids in the the natural decomposition of organic matter. Oxygen content is important to determine because the levels of dissolved oxygen in natural waters often indicates the quality.

pH pH is the abbreviation of *potentia hydrogenii*, it indicates the concentration of hydrogen ions. pH values are expressed as the negative logarithms of the hydrogen ion concentrations. pH 7 indicates neutral water, pH 7-14 alkaline, and pH below 7 acid. Naturally occurring water varies around pH 7. Extreme values are a pH 12 in the basic range and a pH of three in the acidic range (21). The pH value of water sources is measured to study the natural conditions of wildlife and it also assists in determining the extent of stream pollution.

Nitrate Nitrogen Nitrate is the final state in the nitrogen cycle, and is the safest form of nitrogen for aquatic life. Since nitrate is the final form of the cycle, and can not easily be changed further, any nitrate which is used by the plants as a nutrient accumulates in the water. Although nitrate has not been found to be harmful to fish, it is recommended that levels be maintained below 20 ppm nitrate nitrogen.

Procedure and Results

To determine the surface chemistry of the Rocky Creek system, testing was conducted at five different locations. One location was at the top of Rocky Creek, Range 74C (R 74C), two were in the middle to lower part of Rocky Creek, Range Road 200 (RR 200) and Range Road 201 (RR 201), and two were at tributaries off of the main creek that crossed Range Road 200, 1st Bridge and 2nd Bridge. Water samples were taken on two

different dates. The first date samples were taken was July 18, 1994. These water samples were used to assess the conditions of the creek system after heavy rainfall. The second date water samples were taken was August 2, 1994 when the creeks were at relatively normal conditions. The samples to determine normal conditions were taken after those used to assess conditions after heavy rainfall due to the record amounts of rainfall Northwest Florida received in the summer of 1994. It was fortunate that water samples to discover normal conditions could be taken at all.

Eight tests were conducted to determine volumetric flow rate, temperature and dissolved oxygen, pH, conductivity, alkalinity, nitrate nitrogen composition and turbidity. Three tests were conducted in the field: flow rate, temperature and dissolved oxygen. The remaining five were conducted in the lab on the water samples that were collected in large plastic jugs and brought back to the main base.

Volumetric flow rate Volumetric flow rate was the first test conducted in the field to determine how fast the water at each location was flowing. Flow rate was determined by inserting a flow probe into the center of the creek at each site. The probe gave the average velocity of the creek. The results indicate (results annotated in Appendix) that the flow rate was lower under normal conditions at three of the locations. However at the RR 201 site, the flow rate doubled under normal conditions from 1.1 feet per second to 2.2 feet per second.

Temperature and Dissolved oxygen Temperature and dissolved oxygen were tested at the same time using the Ciba Corning handheld dissolved oxygen meter. Though the meter is portable thus allowing tests to be conducted in the field, on the first day of testing the meter was not used in the field due to difficulties in calibrating the probe. Instead water samples were collected underneath the surface of the water, ensuring that no oxygen in the air would contaminate the water sample, thus distorting the results. Upon return to the lab on July 18, 1994 calibration of the probe was successful and accurate results were obtained. On August 2, 1994, the probe was used in the field. The results indicated (see appendix) that dissolved oxygen is much higher under normal conditions than after heavy rainfall. The lower amount of dissolved oxygen present after heavy rainfall is probably due to an increase in the amount of aerobic bacteria involved in the decomposition of oxygen. The larger amount of bacteria caused the oxygen to be used up more rapidly, thus causing the drop.

Temperature varied only slightly between the samples with the only significant variation occurring at RR 201 where the temperature dropped 8.9 degrees Celsius from July 18 to August 2. The mean temperature

difference was 0.68 degrees Centigrade. Generally temperature was found to be between 23.5 to 25 degrees Celsius.

pH The first test conducted upon return to the lab was pH. pH was determined with the Accumet pH meter 915. The Accumet pH meter 915 has internal calibration and is user friendly, providing fast results. It was determined (see Appendix) that Rocky Creek is very acidic under normal conditions and after heavy rainfall. One cause of this acidity is that the soil on the Reservation has a slightly acidic pH as noted earlier. Another cause could be the presence of many pine trees which are very acidic in nature.

Conductivity Conductivity is the ability of a solution to pass current. The conductivity measurement indicates the total ionic concentration within the sample solution. Conductivity was assessed by using the Ciba Corning portable conductivity meter. Results (see appendix) which are in microsiemens show that conductivity is lower under normal conditions than after heavy rainfall. However at the second bridge, there was a higher ionic concentration under normal conditions.

Alkalinity Alkalinity indicates the quantity of soluble salts in a water sample. To assess the alkalinity the Lamotte Fresh Water Aquarium Combination Outfit was used. The Lamotte system is capable of testing six different water conditions. Alkalinity (see Appendix) is higher after heavy rainfall. However, though there were higher levels of soluble salts at four of the five locations, there was a slightly higher amount (2 ppm) at normal condition.

Nitrate Nitrogen To determine the nitrate nitrogen content, the Hach DR/3000 Spectrophotometer was used. The spectrophotometer has three different tests to determine nitrate nitrogen composition depending on whether the sample has high, medium or low amounts of nitrate nitrogen. Test procedure are different for each range. A high level is considered to be above 5.0 mg/L. Medium range samples have between 0.5 to 5.0 mg/L nitrate nitrogen. Low range samples have less than 0.5 mg/L. The results indicate (see appendix) that after heavy rainfall, three of the five sites had a composition in the medium range. Two of the sites had low range levels of nitrate nitrogen. Under normal conditions, all of the water samples contained only a low level of nitrate nitrogen.

Turbidity The final test conducted determined turbidity. A turbidity test indicates the amount of particulate present in a water sample. In order to test turbidity, the Hach Ratio Turbidimeter was used. The meter has the capability to measure up to 199 Nephelometric Turbidity Units (NTU). Turbidity (see Appendix) was

significantly lower at normal conditions at RR 200 and the second bridge. At RR 201 and R 74C there was a slightly higher level of particulate in the water under normal conditions. Under both normal conditions and after heavy rainfall, the turbidity measurement was the same at the first bridge.

Miscellaneous

Besides determining the chemical characteristics of the Rocky Creek system, I also accomplished a few other noteworthy activities this summer. One of the biggest accomplishments of the summer was assisting in the chemical inventory of the chemical storage room, the chemistry lab, and the microanalysis laboratory. I also assisted in preparing close to 2000 chemicals for disposal for Amnesty day. Other activities included helping fellow students gather field samples helping contractors seine brown darters. I also learned how to use Charisma2.0 and Microsoft Word with greater proficiency. Finally I gained a greater appreciation of nature. While collecting water samples I had the opportunity to see snakes, insects, and an alligator. It was very rewarding to be able to see animals in the wild, that previously I had only seen in zoos.

Acknowledgements

I would sincerely like to acknowledge those individuals who helped make my summer such a memorable one. First I would like to thank my mentor Lt. Brad Noland, whose guidance and assistance was invaluable. Secondly I would like to thank the Eglin HSAP coordinators: Mr. Don Harrison, Mr. Mike Deiler, and Glenda Apel, the program secretary. I would also like to acknowledge all of the other members of the Environmental Assessment branch. Finally I would like to thank Miss Nancy Deibler, Miss Melissa Griffiths and all of my fellow HSAPs for their assistance and friendship. I will definitely miss this program and the people involved in it.

Appendix

In each of the following graphs, the gray bar indicates conditions after heavy rainfall, the black indicates normal conditions.

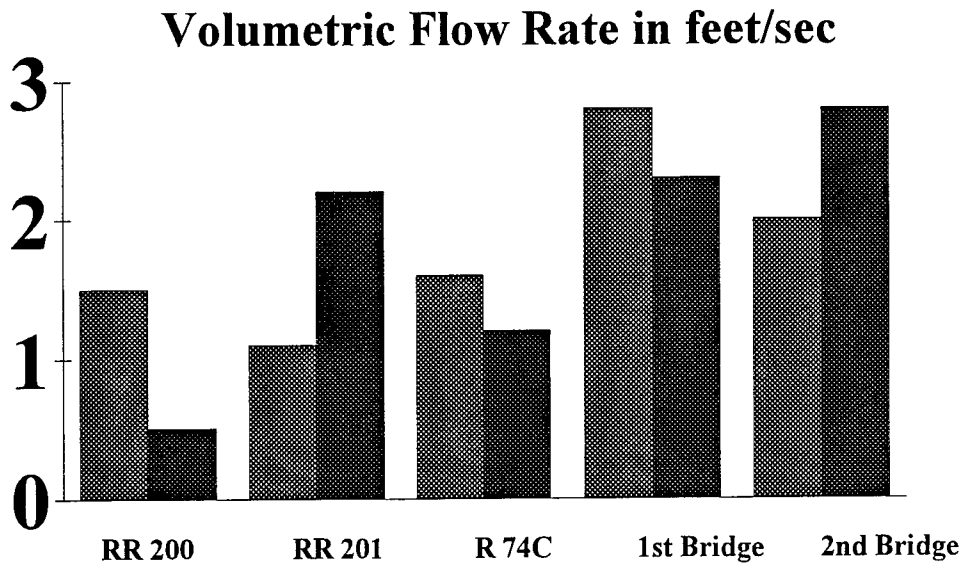


Figure 1- Flow rate results

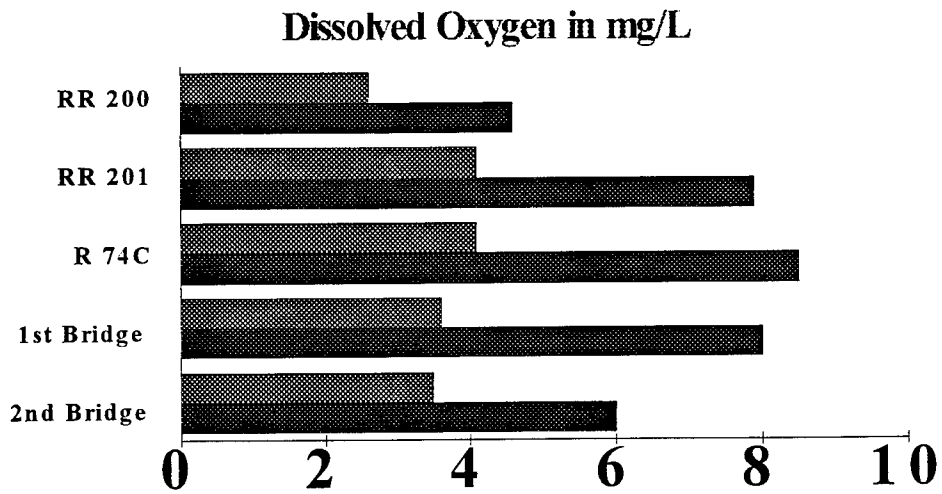


Figure 2- Dissolved Oxygen results

Location	Normal	Heavy Rainfall
RR 200	4.8	4.11
RR 201	4.03	4.19
R 74C	5.29	5.02
1st Bridge	4.67	4.73
2nd Bridge	4.73	4.5

Figure 3- pH results

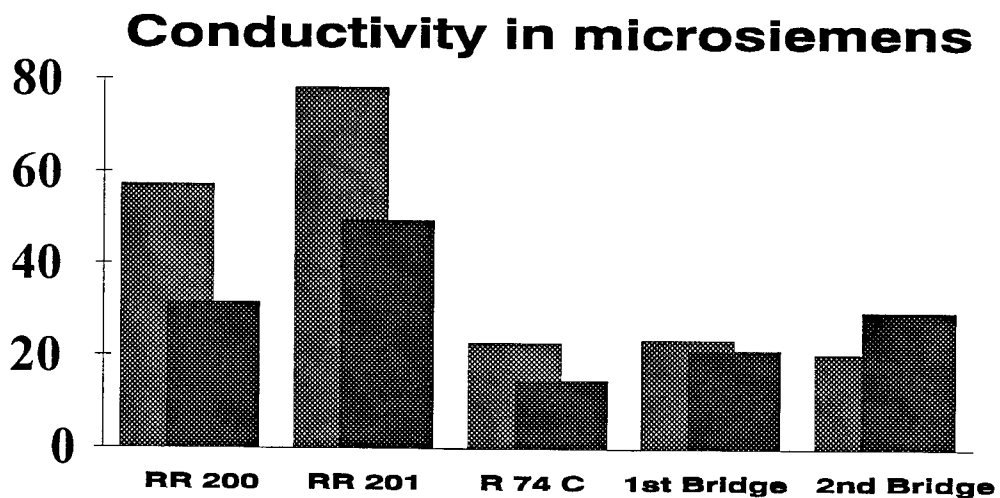


Figure 4- Conductivity results

Location	Normal	Heavy Rainfall
RR 200	16	32
RR 201	12	24
R 74C	20	28
1st Bridge	18	16
2nd Bridge	20	32

Figure 5- Alkalinity results in parts per million

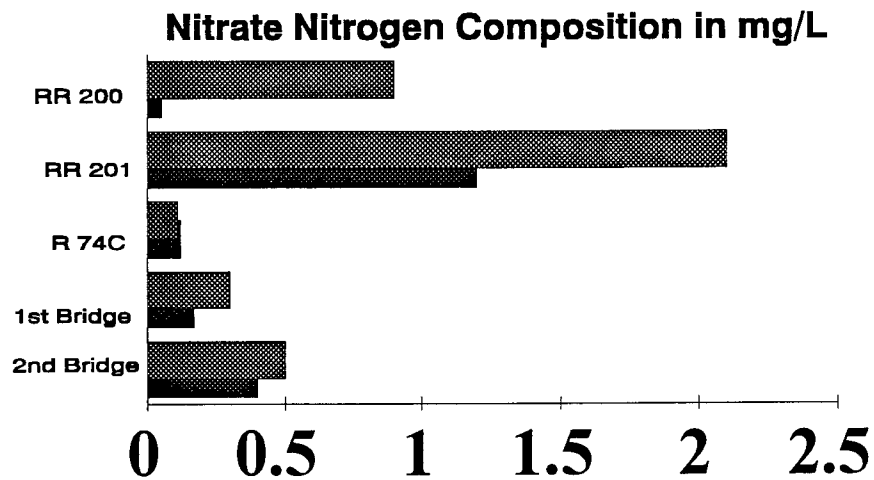


Figure 6- Nitrate Nitrogen results

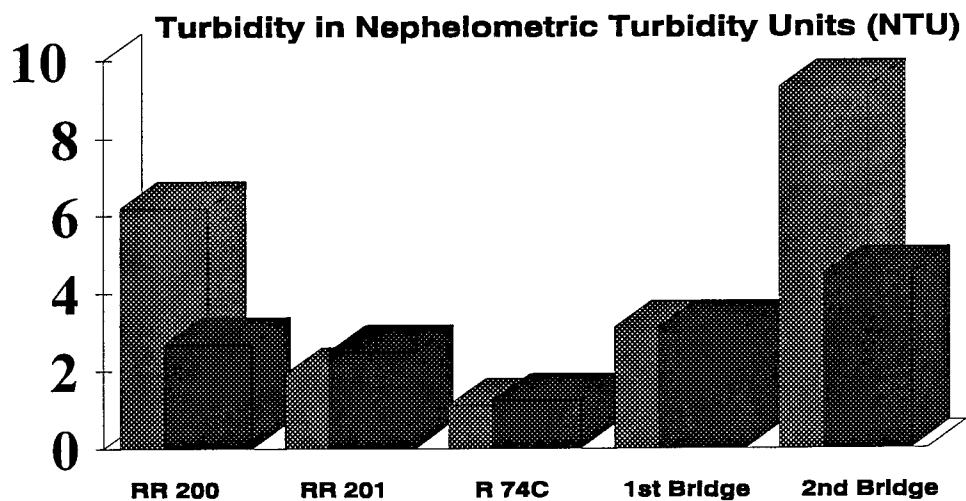


Figure 7- Turbidity results

References

- Crews, Richard C. Lefstad, Sandra M. Miller, Charles I. Wyman, Gary G. Water Quality: Streams and Ponds on Selected Test Areas on Eglin Air Force Base. Air Force Armament Laboratory: 1977. 2-3.
- Klots, Elsie B. The New Field Book of Freshwater Life. Putnam: 1966. 23.
- Schwoerbel, Jurgen. Methods of Hydrobiology (Freshwater Biology). Pergamon: 1970. 21, 23.

PAC vs. Area Methods of Determining "learnability"

Scott E. Sadowski

**Centerville School
500 E. Franklin St.
Centerville, OH 45459**

**Final Report for:
High School Apprentice Program
Wright Laboratory**

**Sponsored by:
Air Force Office of Scientific Research
Bolling Air Force Base, DC**

and

Wright Laboratory

August 1994

PAC vs. Area Methods of Determining “Learnability”

Scott E. Sadowski
Centerville High School

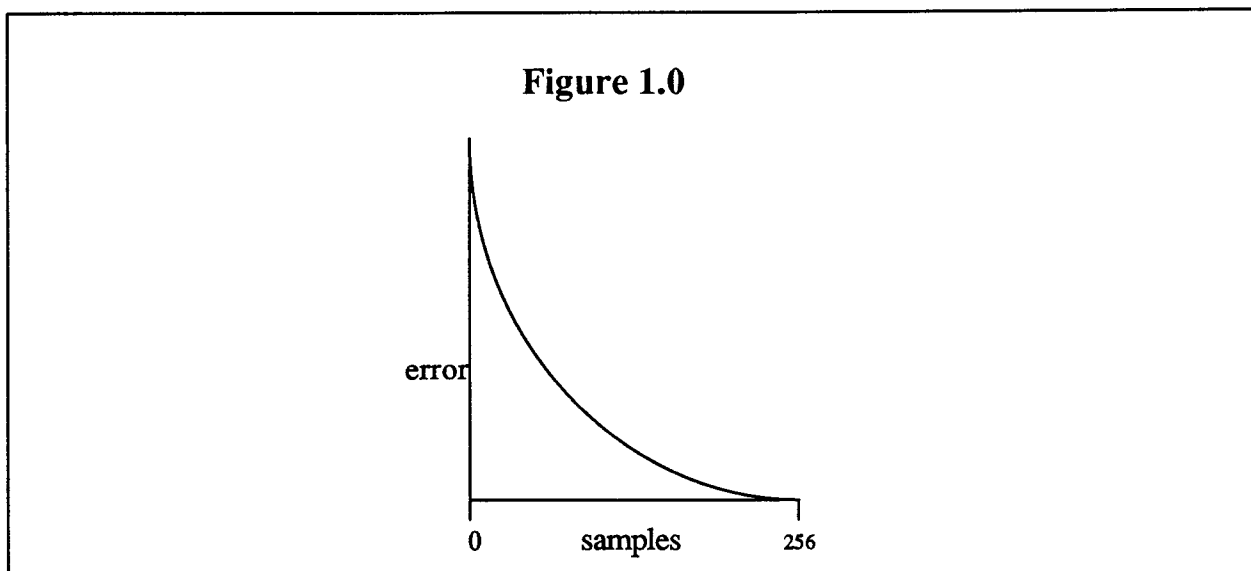
Abstract

This paper reports on creating different ways of awarding merit to learning algorithms. The methods discussed in this paper both have positive and negative aspects. They are not equivalent in performance, except under certain conditions.

Introduction

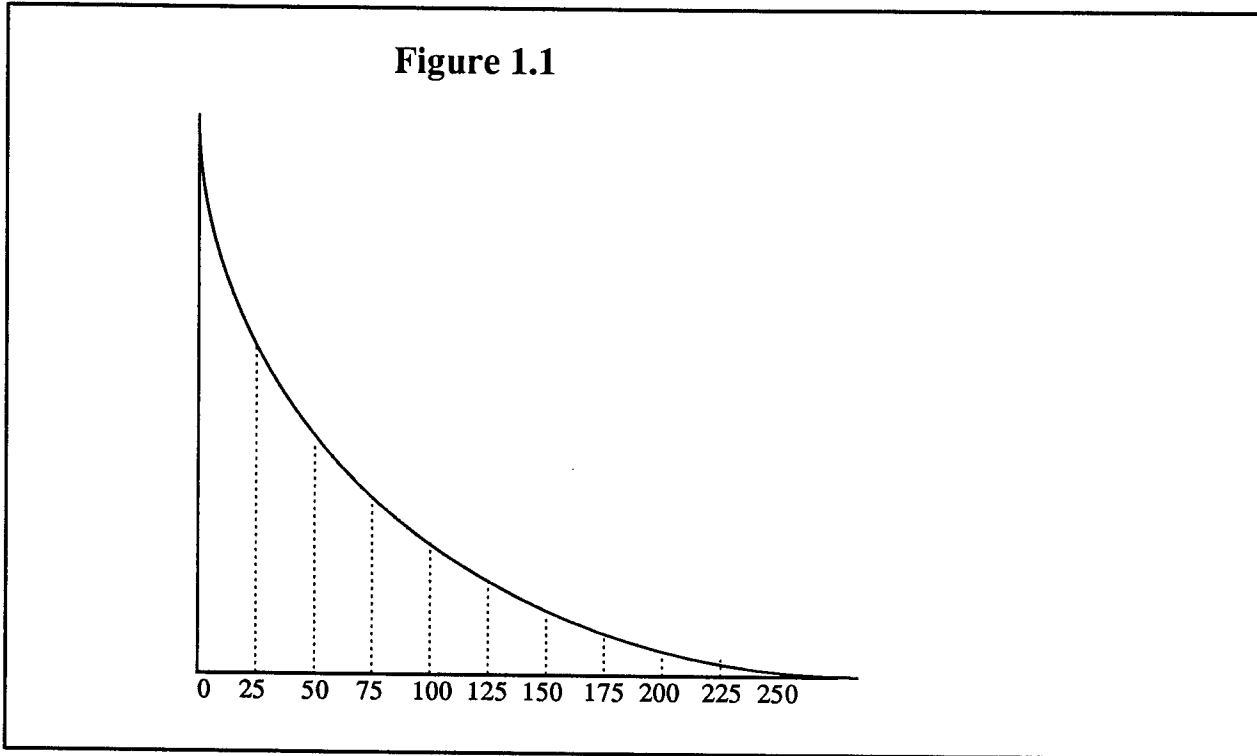
Pattern theory is a concept which involves finding patterns in functions. This process involves decomposing functions or parts of functions in hopes of finding a pattern. Knowing a functions pattern before knowing all the information about the function is the same as learning the function. In order to compare and rank the speed that a function is learned by an algorithm, the "learnability", or merit, of the learning algorithm must be calculated. To make this comparison easy, each function must receive merit of "learnability". The two methods that are shown in this paper are the probably approximately correct(PAC) and area methods. Both of these methods analyze the learning curve of a given function.

A function's learning curve is an error graph for a given number of samples versus the number of samples. The error is the number of samples that are not correctly learned by the algorithm. A function of n variables will have 2^n points.



The graph in figure 1.0 is an example learning curve of an 8 variable function. Since the function has 8 variables it has 256 samples. When the number of samples given is close to 0, the error is large because the computer was expected to learn most of the function based on a small number of samples. When the number of samples are close to 256, the error is very small, if not 0, because most of the function has been sampled

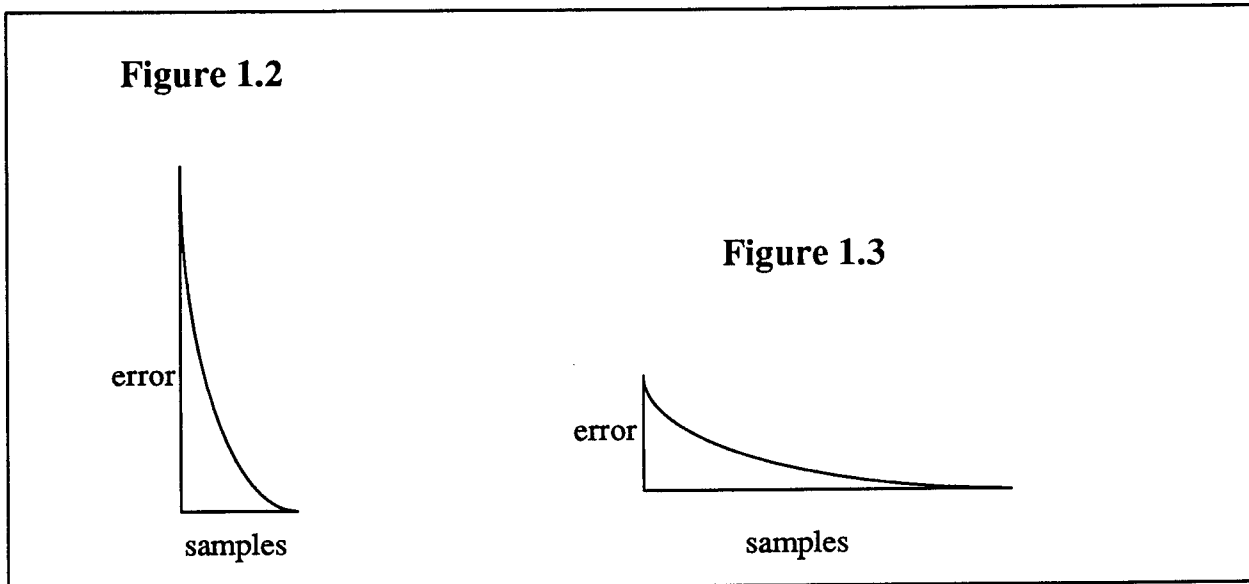
The learning curve in figure 1.1 is also an 8 variable function. It was made by curve fitting data points at each of the intervals of 25 samples. For example, at the 25 sample mark, 25 random samples out of the 256 were given and the error was calculated. This was done 10 times for each interval and then the average was calculated.



Methodology

The PAC method finds the first time that the error is less than epsilon percent, delta percent of the time. Epsilon and delta can be any percentages but we will use 10% and 90% as a baseline. This would mean that 9 times out of 10 the error would be less than 10 percent, or 25.6 for an 8 variable function, at a certain number of samples. Therefore this method doesn't look at the actual learning curve, it looks at the data used to make the learning curve. It looks at all the trials for each bin, or interval of samples. The first time that the error will go under delta percent, epsilon percent of the time will be one point somewhere on the learning curve. The PAC method will find the interval past this point as its figure of merit. For this reason, the PAC method will always return a value that is larger than the exact answer. The error using PAC is always limited to the difference of the number of samples in successive bins. In the graphs shown in figures 1.1 and 1.4 through 1.11 this difference was 25. The accuracy of the PAC method will increase as the difference in the number of samples in successive bins decrease.

The area method uses the area under the learning curve for assigning merit. This allows for a very precise number, but there exists a problem using this technique. The area under the function's learning curve plays an important role in determining the "learnability" of that function, but the location of the area is also important. The location of essentially is the speed in which the computer learns the function.



The area under the learning curve in figure 1.2 is equal to that of figure 1.3. Therefore, using the area method, these two functions would receive the same merit. However, figure 1.2 may be better because it was learned faster.

Data and Analysis

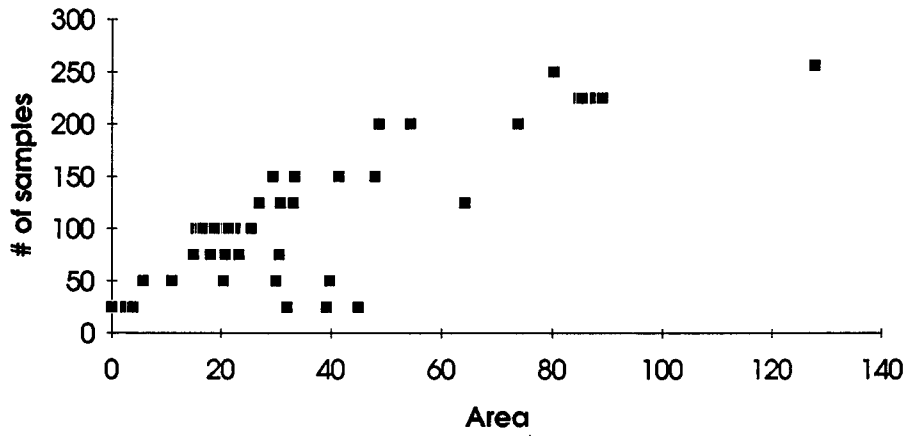
The graphs shown in Figures 1.4 through 1.11 compare the PAC and area methods of giving merit to functions. The X-axis of the graphs in figures 1.4 through 1.11 is the area under the learning curve of a set of functions and the Y-axis is the PAC performance of those functions. Therefore these graphs show one method of giving merit to a function graphed against another. If these graphs shown in figures 1.4 through 1.11 were linear, it would mean that the two methods were equivalent. These two methods are clearly not equivalent as shown by the non-uniform distribution of data points of Figures 1.4 through 1.11. The data for figures 1.5 through 1.11 were generated using the Functional Learning And Synthesis Hotbed (FLASH) algorithm [1]. Figure 1.4 also compares the PAC and area methods but using the C4.5 learning algorithm [2].

Summary and Conclusions

Taking into account the approximation of the PAC method there is still a discrepancy between the two methods as shown by the learning curves in figures 1.4 through 1.11. The learning algorithm was used to compare the PAC and area methods has little, if any, affect on the correlation of the two methods as shown by Figure 1.4. The correlation between the two methods was fairly consistant in all the graphs shown in Figures 1.4 through 1.11 with only two exceptions. These two exceptions were Figure 1.8 and 1.11, which were the most extreme variations from the baseline of epsilon = 10% and delta = 90%. Figure 1.12 also proves that the area and PAC methods are showing two different things. The PAC method is a good technique for assigning merit when the function's learnability is insignificant at a low number of samples. The area method is a good way for assigning merit when the functions performance is important over the complete range of samples. Although the PAC and area methods are not equivalent, they both have their place in determining the "learnability" of a function.

Figure 1.4

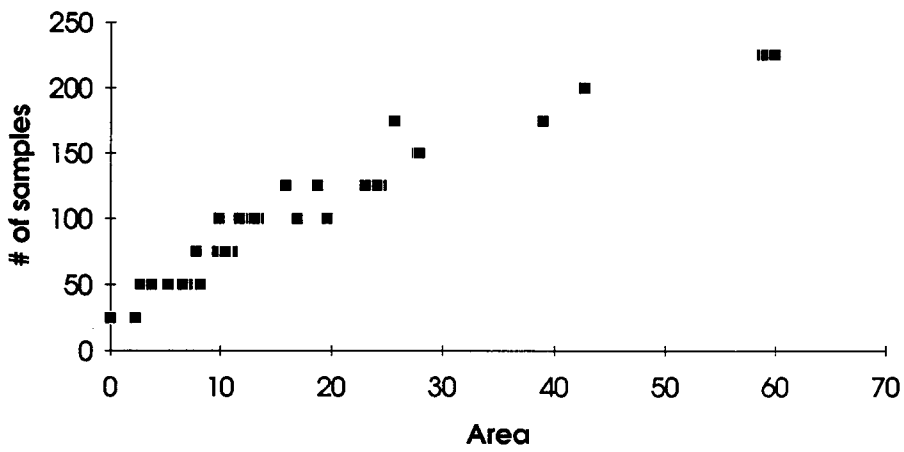
Area vs. PAC(10%,90%) for C4.5



Correlation of Figure 1.4 = .937785779

Figure 1.5

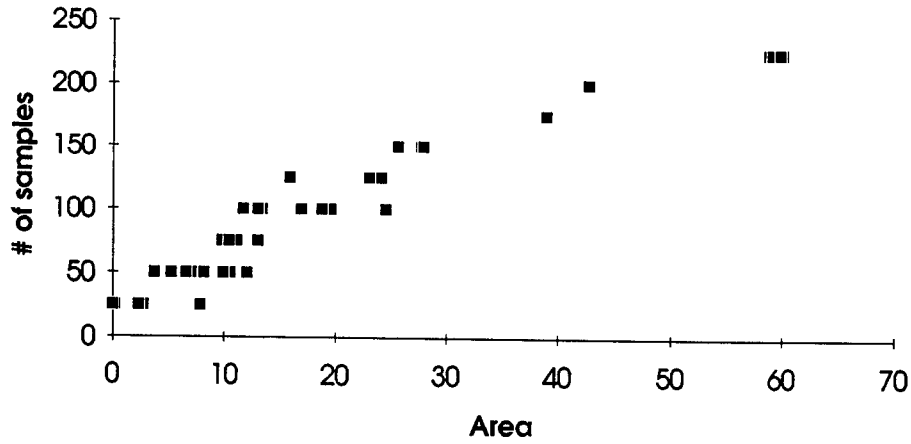
PAC Method (10%,90%) vs. Area Method



Correlation of Figure 1.5 = .965770717

Figure 1.6

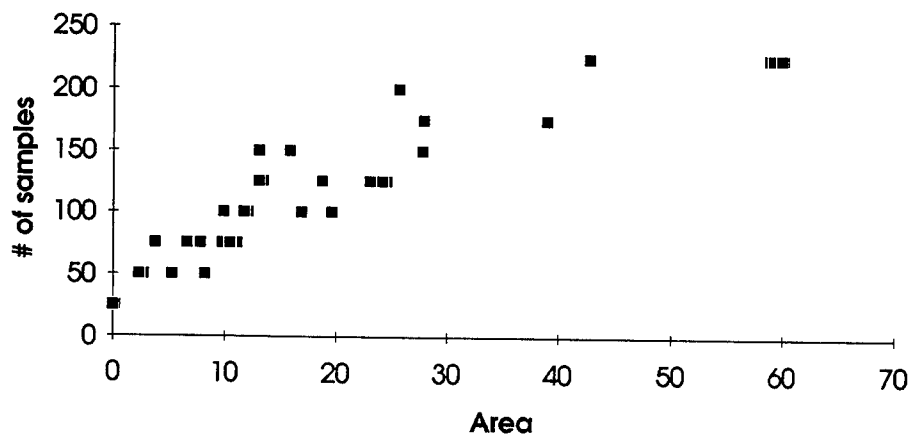
PAC Method (10%,70%) vs Area Method



Correlation of Figure 1.6 = .967267551

Figure 1.7

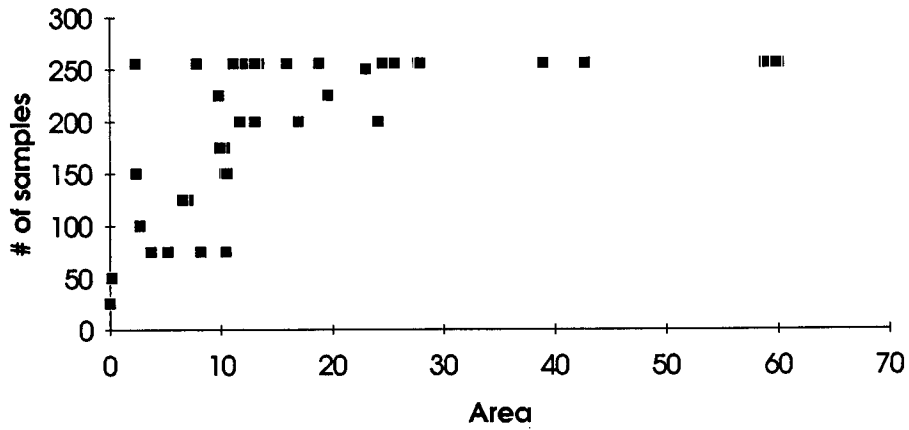
PAC Method (10%,95%) vs. Area Method



Correlation of Figure 1.7 = .963770717

Figure 1.8

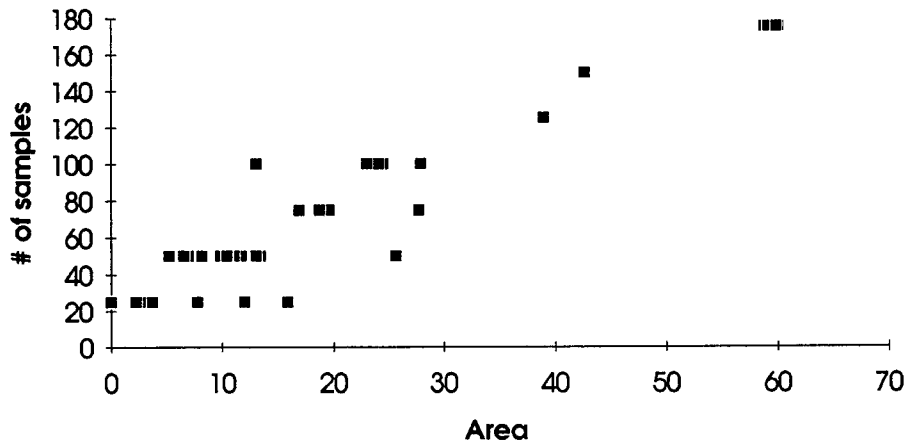
PAC Method (0%,100%) vs. Area Method



Correlation of Figure 1.8 = .634195642

Figure 1.9

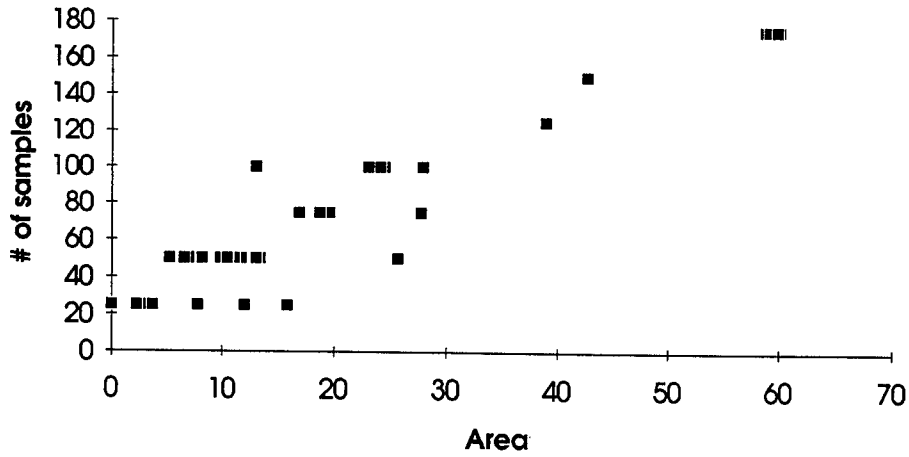
PAC Method (20%,80%) vs. Area Method



Correlation of Figure 1.9 = .952883481

Figure 1.10

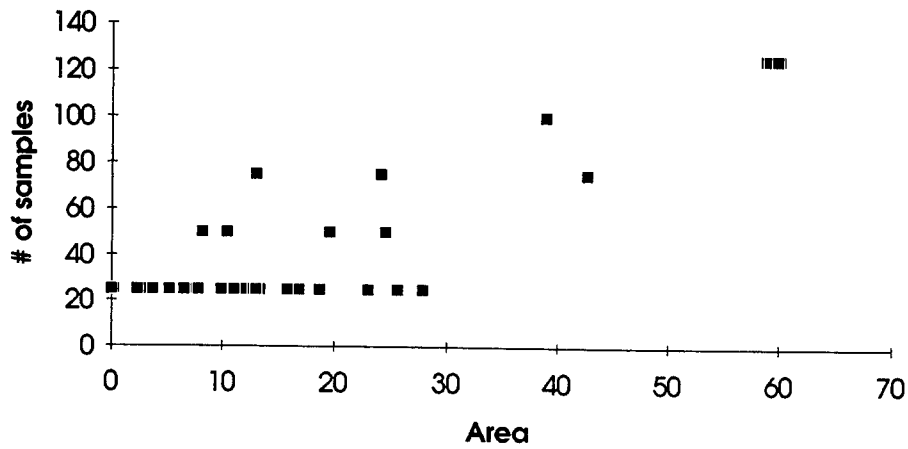
PAC Method (20%,90%) vs. Area Method



Correlation of Figure 1.10 = .952883481

Figure 1.11

PAC Method (30%,70%) vs. Area Method



Correlation of Figure 1.11 = .863780085

Figure 1.12

	PAC FLASH	PAC C4.5	area FLASH	area C4.5
add0	75	100	10.38	22.56
add2	50	125	5.24	64.12
add4	25	50	0	39.72
ch15f0	100	150	19.595	47.96
ch176f0	25	50	0.16	20.54
ch177f0	25	25	0	39.14
ch22f0	50	50	7	29.96
ch30f0	75	75	10.29	18.18
ch47f0	100	125	16.89	33.08
ch52f4	150	125	27.74	30.76
ch70f3	100	100	12.04	15.5
ch74f1	125	100	15.85	20.9
ch83f2	150	150	27.885	33.42
ch8f0	100	75	11.7	20.84
contains	125	250	24.49	80.18
greater_	75	100	9.78	21.36
kdd1	25	25	0	0.64
kdd10	50	100	8.18	25.54
kdd2	25	50	2.4	3.76
kdd3	50	25	2.72	2.56
kdd4	25	25	0	0
kdd5	75	75	11.11	15.02
kdd6	50	50	3.72	3.84
kdd7	75	125	10.53	26.94
kdd8	25	100	0	16.32
kdd9	50	100	6.55	30.56
majority	125	200	18.74	48.68
modulus2	100	100	13.4	16.72
mux8	100	75	13.04	23.28
pd	100	100	9.9	18.8
pd_dbl	175	200	38.94	73.74
pd_outp	225	225	58.79	84.74
parity	75	250	10.45	128
rnd_m1	25	25	2.31	1
rnd_m10	100	50	13.045	11.02
rnd_m25	175	150	25.61	29.34
rnd_m5	75	50	7.815	5.74
rnd_m50	200	200	42.685	54.4
rnd1	225	225	59.125	87.84
rnd2	225	225	60.055	89.04
rnd3	225	225	59.865	85.3
substr1	125	150	24.105	41.44
substr2	125	150	23	33.3
Average:	97.67442	114.5349	16.86337	34.78558

	FLASH wins	C4.5 wins	ties
PAC	18	8	17
area	38	4	1

Bibliography

- [1] Timothy D. Ross, Michael J. Noviskey, Timothy N. Taylor, and David A. Gadd. *Pattern Theory: An Engineering Paradigm for Algorithm Design*. Final Technical report WL-TR-91-1060, Wright Laboratory, USAF, WL/AART, OH 45433-6543, August 1991.
- [2] Jeffery A. Goldman. *Pattern Theoretic Knowledge Discovery*. System Concepts Wright Laboratory, USAF, WL/AART, OH 45433-7408.

**QUANTUM WELL INFRARED
DETECTOR RESEARCH**

Raúl H. Sánchez

**Centerville High School
500 East Franklin
Centerville, OH 45459**

**Final Report for:
High School Apprenticeship Program
Wright Laboratory**

**Sponsored by:
Air Force Office of Scientific Research
Bolling Air Force Base, DC**

and

Wright Laboratory

August 1994

QUANTUM WELL INFRARED DETECTOR RESEARCH

Raúl H. Sánchez
Centerville High School

Abstract

Different infrared detectors for various applications were tested. They underwent different tests such as: spectral response, dark current, blackbody response, and noise measurements. The tests were done at different conditions, with several detectors from each sample tested. The detectors were tested for: a high temperature data study, a dark current study, and a study to determine their quantum efficiency.

QUANTUM WELL INFRARED DETECTOR RESEARCH

Raúl H. Sánchez

Introduction

The Air Force has many labs that aim for the improvement of its airplanes and equipment. The Wright Laboratory consists of directorates for the development of: more efficient engines (Propulsion Directorate), a better airframe (Flight Dynamics), improved aircraft electronics (Avionics), improved materials used in aircraft (Materials), and future electronics (Solid State Electronics). In the Solid State Electronics directorate, there are four divisions. One is the Electro-Optics Division, which is also subdivided into branches. One of the branches is the Detectors Branch. The different detectors they work on are infrared and ultraviolet. Infrared has many uses because it can detect heat. One of infrared's many uses is for nighttime security lights. The lights automatically turn on when someone comes near them because they detect the heat a person gives off. However, most infrared uses are more military-related. Some of infrared's many military uses are: night vision, detecting targets, and heat-seeking missiles.

Methodology

There were four tests done to determine the performance of a detector. The tests were: spectral response, dark current, blackbody response measurements, and noise measurements. Both the spectral response tests and the dark current tests are computer controlled.

In spectral response, an infrared beam is produced using a hot metal bar in a machine called a monochromator. The beam reflects off a special grating, onto the detector being tested. This test is done to determine the relative response wavelengths of the detector. An example of a spectral response curve is shown in figure 1.

In dark current testing, the current flowing through the detector was tested with the detector in the "dark." To the detector, "dark" means that it is looking at something cold. Therefore, the dark current tests measure the current the detector draws when it is cold. The numbers should be low, because there is no heat to detect. In dark current testing, the lower the data, the better the detector. An example of a dark current plot is shown in figure 2.

In response measurements, several detectors were tested. These were tested under different temperatures, different voltages, and with different aperture diameters of the infrared blackbody source. Before the response measurement tests, a machine called a blackbody must be set at a temperature of 527 C. The temperature of 527 C was chosen because it equals 800 K. This blackbody source is what emits infrared waves at various aperture diameters to the detector being tested. The diameters through which the signal is being emitted range from .1 inches, to .6 inches.

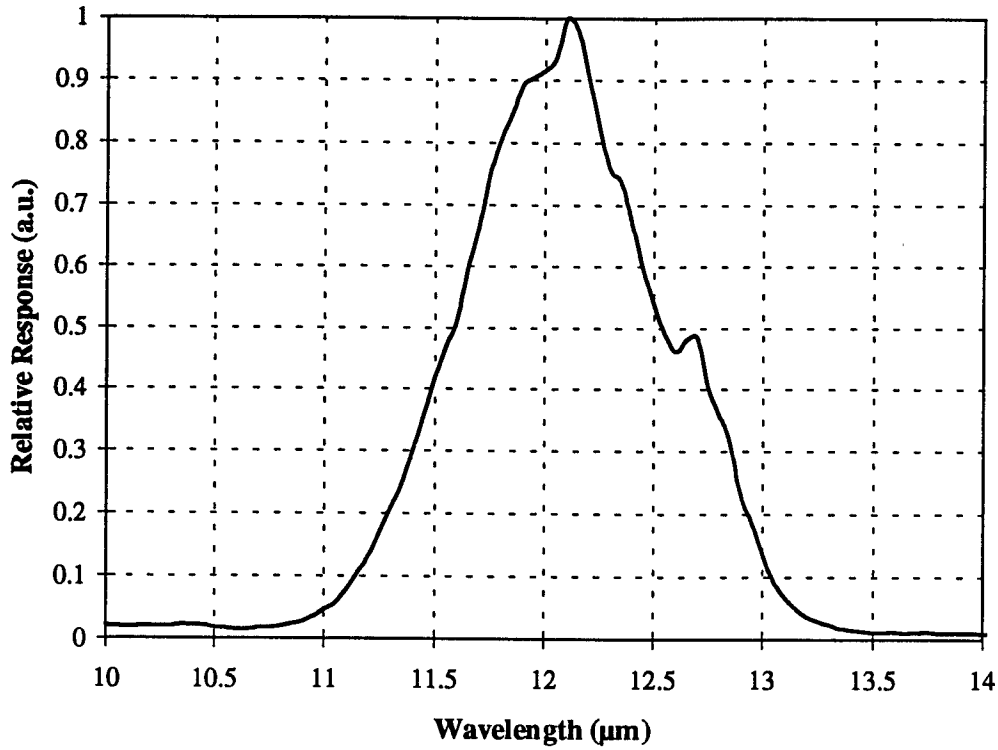


Figure 1. Sample spectral response curve.

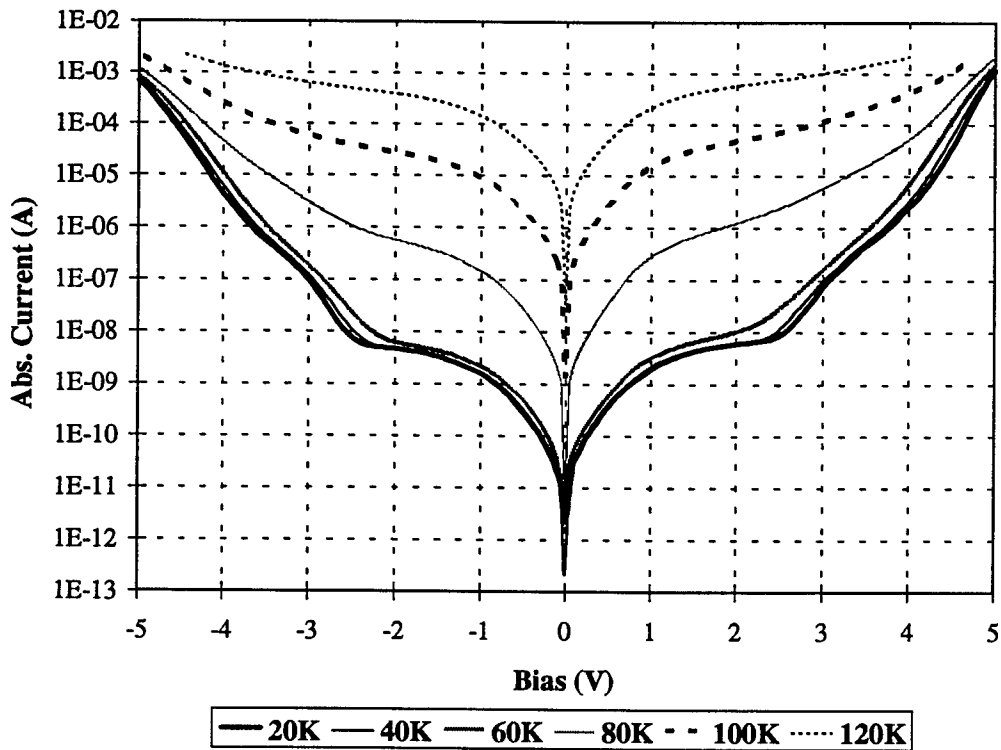


Figure 2. Typical dark current curve.

The temperatures under which the detectors are being tested range from 20 K to 300 K. The voltage bias applied to the detector, ranged from .4 volts to 2.6 volts, with the current amp gain was set at 1×10^8 V/A. Data was read out on a machine called the FFT Spectral Analyzer. The machine took 2,000 averages, and this was repeated five times for each blackbody aperture diameter from .6" to .1." The same testing was repeated for the next detector until all were tested. A sample response curve is shown in figure 3.

The last test is noise measurements, which are used with the other data to determine a performance factor called "detectivity." In this test, the detector was covered and the blackbody was turned away from the detector so that the infrared would not reach it. This test was done to determine the amount of noise each detector had, and was also done at different voltages and temperatures. In this test, the FFT took 2,500 averages, and this was repeated five times for each voltage setting. The same was done to the next detector until all were completed. In the noise tests, the other machines in the room were turned off so they would not raise the noise level. An example of a detectivity plot is shown in figure 4.

Results

After collecting the response and noise data, it was entered into the computer. The computer found the median value of each of the five readings for the different diameters, temperatures, and voltages, under which each detector was tested. After the data was put in tables, it was checked to make sure the ratio between diameters was correct. The reading obtained at .1" diameter should be 1/4 of the reading obtained at .2" diameter. The reading obtained at .2" diameter should be 1/4 of the reading obtained at .4" diameter. Finally, the reading obtained at .4" diameter should be 4/9 of the mean obtained at .6" diameter. If these ratios were not obtained, then the testing was repeated. When the resulting ratios were correct, the data was plotted on graphs and printed.

Conclusions

The graphs were studied to determine which detectors had higher performance than others. For example, in the dark current graph, the lower the coordinates, the better the detector. Data from the graphs will be used in future reports and technical papers to be written by my mentor and his co-workers.

References

- MODEL SR760 FFT Spectrum Analyzer. Sunnyvale: Stanford Research Systems, 1991.
- Instructional Manual Model 428 Current Amplifier. Cleveland: Keithley Instruments, 1990.
- Instruction Manual Model 486 Picoammeter Model 487 Picoammeter/Voltage Source. Cleveland: Keithley Instruments, 1990.

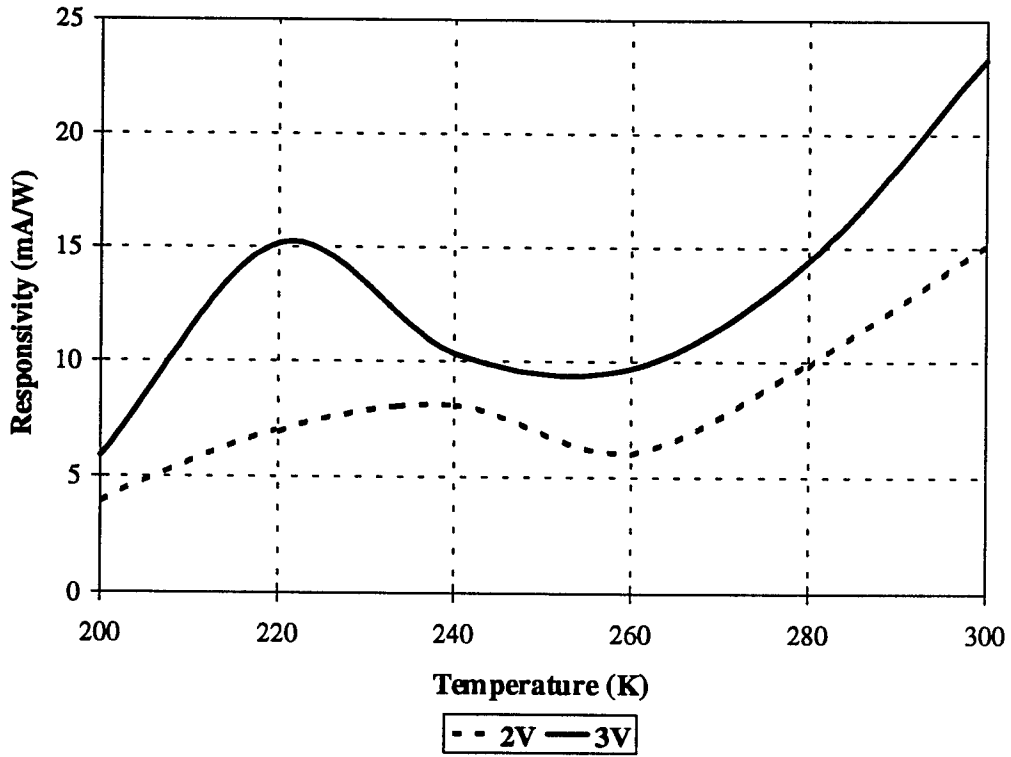


Figure 3. Typical responsivity plot.

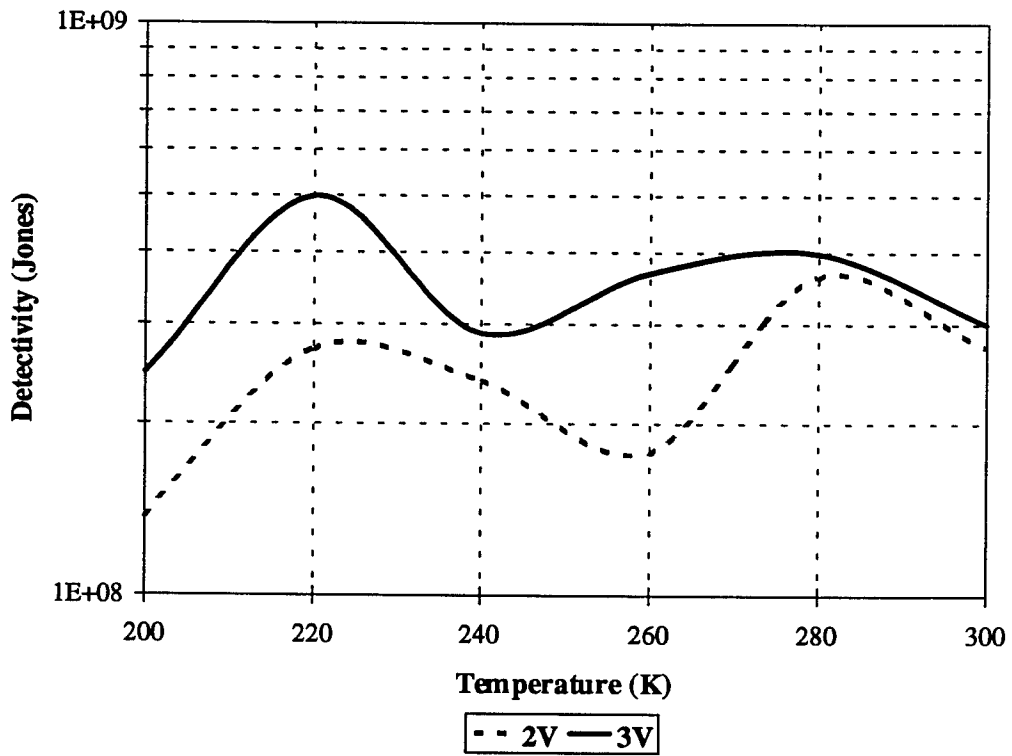


Figure 4. Typical detectivity plot.

A STUDY OF A SINGLE TUBE CATALYZED
HEAT EXCHANGER

Jill M. Schlotterbeck

Fairmont High School
3301 Shroyer Rd.
Kettering, Ohio 45429

Final Report for:
High School Apprenticeship Program
Wright Laboratory

Sponsored by:
Air Force Office of Scientific Research
Bolling Air Force Base, Washington DC

and

Wright Laboratory

August 1994

A STUDY OF A SINGLE TUBE
CATALYZED HEAT EXCHANGER

Jill Schlotterbeck
Kettering Fairmont High School

ABSTRACT

A single tube catalyzed heat exchanger was studied. Wright Laboratory and Technology Development Associates Inc. (TDA) developed the single tube catalyzed heat exchanger, which counter flows hot air through the inner tube and methylcyclohexane through the outer tube. TDA also developed the catalyst, which is coated on the external surface of the inner tube. The catalyst and hot air induce the break up of methylcyclohexane into hydrogen and toluene.

A STUDY OF A SINGLE TUBE CATALYZED HEAT EXCHANGER

Jill Schlotterbeck

Introduction

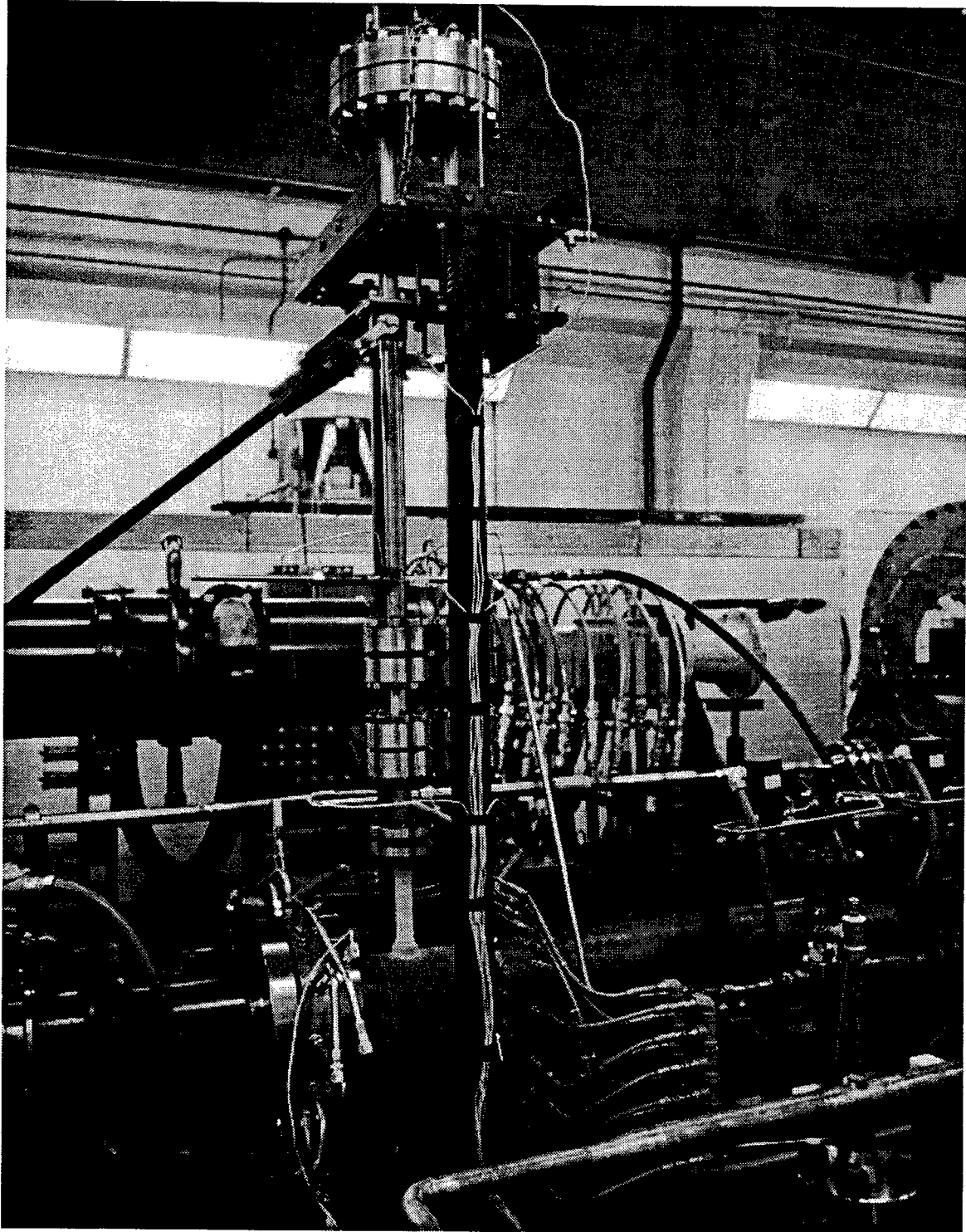
While jet airplanes fly through the skies at speeds up to mach 2 and 3, the temperature of the equipment inside the aircrafts greatly increase. This overheating of equipment greatly reduces the lifetime of the equipment. Putting a catalyzed heat exchanger in a aircraft nearly doubles the capacity to cool the equipment by running methylcyclohexane (MCH) around it, which breaks up into hydrogen and toluene. The life of the equipment is increased, and hydrogen and toluene, are more easily combusted.

Experimental

Wright Laboratories and TDA Inc. designed the experimental method for testing the single tube heat exchanger is tested . A photograph of a section of the test rig is shown on 39 - 4. The single catalyzed tube heat exchanger is designed to test the dehydrogenation of MCH in conditions similar to the conditions a catalyzed heat exchanger would experience in an aircraft. The single tube catalyzed heat exchanger is a .624 inch diameter tube inside a 1.5 inch diameter tube made from 316 stainless steel.

The test rig is composed of two main systems, the reactor heater system and the single tube heat exchanger, and many smaller components. A schematic drawing of the reactor heater system is on 39 -7 and a schematic of the single tube heat exchanger is on 39 -8, followed by a legend on 39 -9. The reactor heater system is composed of the sudden expansion (SUE) heater. The hot air flows into the single tube heat exchange system through a line connected down stream of the SUE heater.

The hot air from the SUE heater flows through the inner tube of the single tube heat exchanger, while MCH counter flows through the outer tube. A model of the single tube heat exchanger reactor is shown in 39-10 figure 1, along with the organic structure of the dehydrogenation of MCH in figure 2. The powder catalyst, created by TDA Inc., is sprayed on the finned external surface of the inner tube with a thickness of 75 microns. The fin length is .235 inches and they are .015 inch thick. The fins not only hold the catalyst, but they also increase surface area for heat transfer. As the MCH flows over the catalyst



Test Cell 22

and absorbs the heat from the inner tube, the MCH breaks up into hydrogen and toluene.

Down stream of the heat exchanger a sample line leading to the gas chromatograph (GC) taps into the main fuel line. The gas chromatograph's carrier gas for this test is 98% Helium and 2% Hydrogen. The gas sample is introduced into a heated chamber by a two position, hexport sampling valve. The carrier gas carries the sample through the column where the components separate and pass through the detector one after the other. Then a signal is sent from the detector to the recorder. The analyst must know the characteristics of the expected gases.. The GC measures the species concentrations and determines reactor performance.

RESULTS

Below are data from two test runs with the predicted outlet temperatures of the fuel and air and the predicted conversion followed by the actual temperatures and conversions.

Run 1

(actual)	AIR	FUEL
TEMPERATURE IN (Rankine)	1949	557
TEMPERATURE OUT (Rankine)	1458	1404
MASS FLOW (lbs/sec)	.18	.017
PRESSURE (psia)	180	800
CONVERSION		60%

(predicted)

TEMPERATURE OUT (Rankine)	1499.8	1384.9
CONVERSION		66.73%

RUN 2

(actual)	AIR	FUEL
TEMPERATURE IN (Rankine)	2051	559
TEMPERATURE OUT (Rankine)	1498	1449
MASS FLOW (lbs/sec)	.1714	.0167
PRESSURE (psia)	176	798
CONVERSION		69%

(predicted)

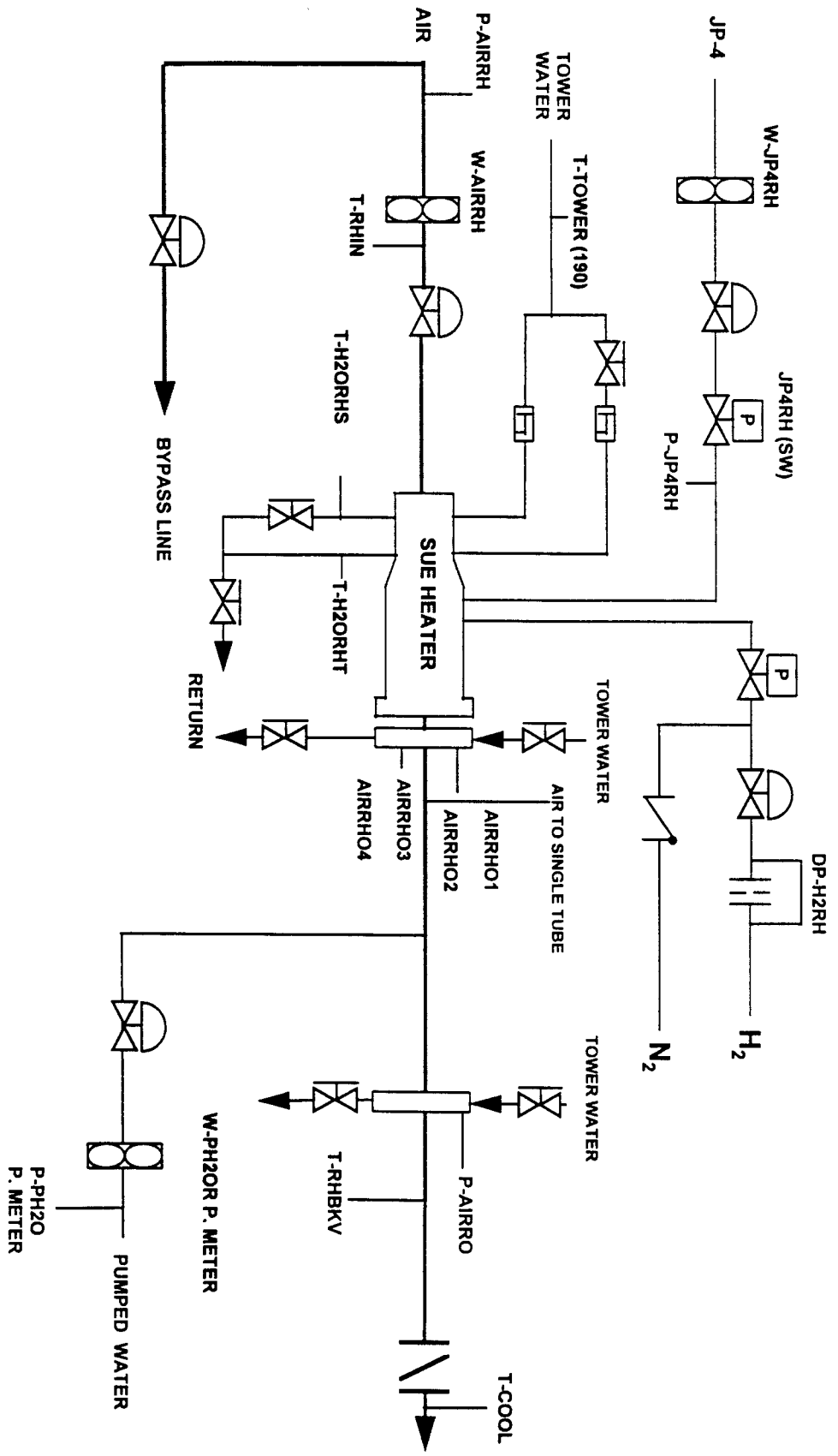
TEMPERATURE OUT (Rankine)	1546.6	1475.8
CONVERSION		76.01%

In both test runs the predicted conversion was higher than the actual conversion. In test run 1 the predicted air temperature out was higher than the actual and the predicted fuel temperature was lower than the actual. In test run 2 the both the predicted air temperature out and the fuel temperature out were higher than the actual temperatures out.

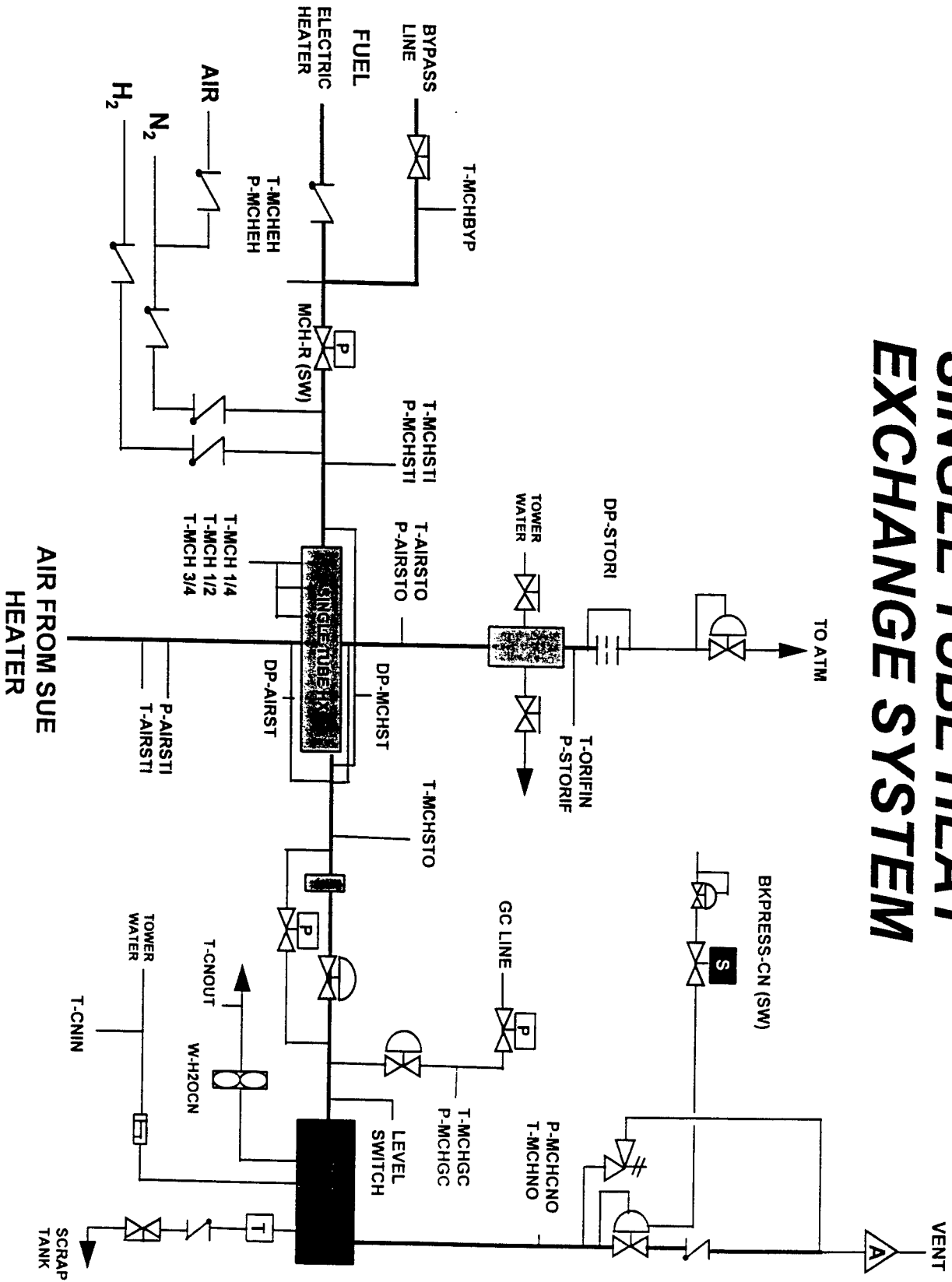
CONCLUSIONS

Methylcyclohexane is an easily stored fuel because it has properties similar to ordinary jet fuel or kerosene. Once MCH is run through the heat exchanger and the dehydrogenation occurs the products, hydrogen and toluene, can easily combust and propel the aircraft. The dehydrogenation nearly doubles the ability of the fuel to cool the engine and aircraft components. Wright Laboratories and TDA Inc. have finished testing the catalyst developed by TDA Inc. and will start testing a different catalyst in the same type of single tube heat exchanger. The results will be compared and the catalyst with a better conversion of MCH into hydrogen and toluene will be used in future testing in a full scale test rig. In the future TDA Inc. and Wright Laboratory hope to employ this type of heat exchanger in an aircraft.

REACTOR HEATER SYSTEM

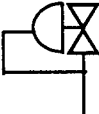


SINGLE TUBE HEAT EXCHANGE SYSTEM



LEGEND

	Butterfly Valve
	Flow Switch
	Control Valve
	Flame Arrestor
	Filter
	Flow Meter
	Flow Switch

	Hand Valve
	Orifice Plate
	Pneumatic ON/OFF Valve
	Pressure Regulator
	Relief Valve
	Solenoid Valve

SINGLE TUBE REACTOR MODEL

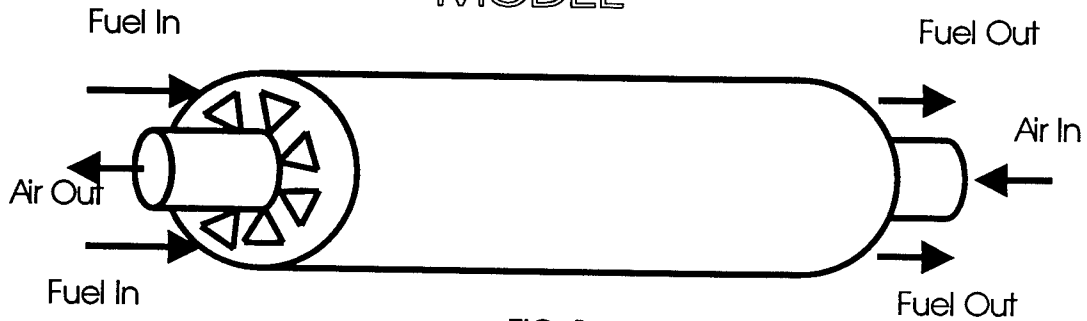


FIG. 1

DEHYDROGENATION OF METHYLCYCLOHEXANE

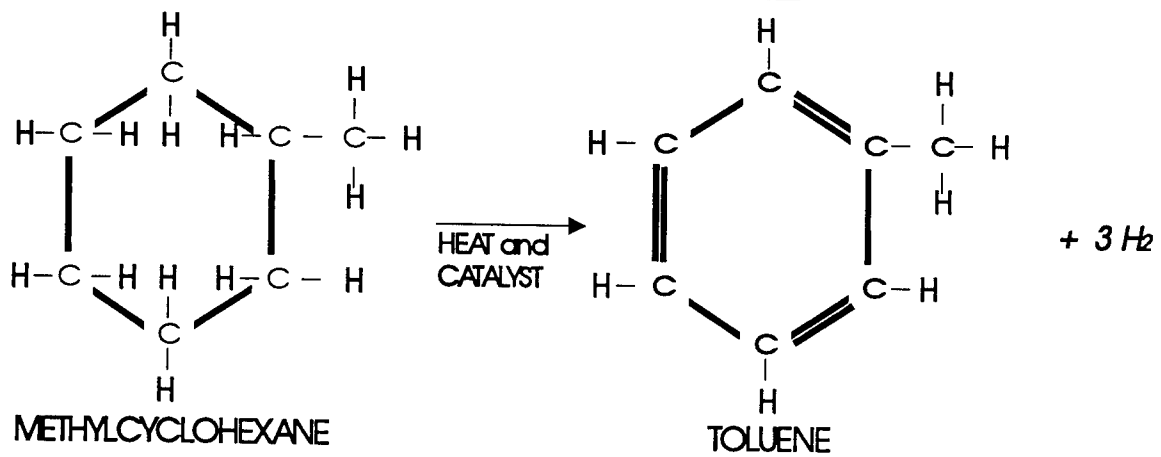


FIG.2

**THE EFFECT OF HUMIDITY ON FRICTION AND WEAR FOR M50 STEEL BEARINGS
IN THE PRESENCE OF A LINEAR PERFLUOROPOLYALKYL ETHER LUBRICANT**

Robert J. Skebo Jr.

Beavercreek High School
2940 Dayton-Xenia Rd.
Beavercreek, OH 45434
(513) 426-1522

Final Report for:
High School Apprentice Program
Wright Laboratory

Sponsored by:
Air Force Office of Scientific Research
Bolling Air Force Base, DC

and

Wright Laboratory

August 1994

**The Effect of Humidity on Friction and Wear for M50 Steel Bearings
in the Presence of a Linear Perfluoropolyalkyl Ether Lubricant**

Robert J Skebo Jr.
Beavercreek High School

Abstract

The effectiveness of a commercial perfluoropolyalkyl ether lubricant (Fomblin Z) was investigated in a controlled environment by maintaining varying temperature and relative humidity using a Cameron-Plint High Frequency Friction Machine. Data was obtained for 50 C, 100 C, and 150 C degree runs with relative humidities ranging from 5% to 100%. Experimental results indicate that lower relative humidities (<20%) in the surrounding bearing environment causes an increased coefficient of friction and an exponentially larger amount of wear to occur. Friction and wear tend to be relatively low and constant at medium and high humidities.

The Effect of Humidity on Friction and Wear for M50 Steel Bearings in the Presence of a Linear Perfluoropolyalkyl Ether Lubricant

Robert J. Skebo Jr.

Introduction:

Members of the perfluoropolyalkyl ether (PFPAE) chemical family have exhibited potential as effective lubricants for high performance applications. PFPAE lubricants currently are being used in conjunction with high speed scanning mechanisms, solar arrays, slip rings actuators, and gyroscopes for satellites. The success of PFPAE lubricants has sparked interest for their use in new high temperature jet engines. Fomblin Z (a patented name) is one PFPAE currently being studied for possible use in future aerospace programs.

During previous boundary lubrication experiments with Fomblin Z using either the Cameron-Plint Machine or four ball rigs, it has often been observed that friction and wear results occasionally seem to be erratic. A possible cause for this chaotic behavior is the percent of relative humidity surrounding the experimental bearing environment. The objective of this research project was to determine if humidity was indeed the source of erratic results and therefore increase the reproducibility of tests. In order to accomplish this task the relative humidity was monitored and controlled.

Procedure:

All trials utilized M50 an steel cylinder (6 mm diameter, 6 mm length) and an M50 steel disc pre-polished to a mirror finish. (The disc should not be polished with a diamond paste as this tends to abrade the surface). The cylinders were stored in petroleum oil and the discs were kept in a calcium sulfate dessicator to prevent oxidation.

Prior to each experiment the cylinder was cleaned with hexane in an ultrasonic bath for 1 minute. Then both the cylinder and the disc were cleaned together under methanol in an ultrasonic bath for 1 minute. The experimental results may be very sensitive to the initial conditions of sanitation. In order to insure maximum cleanliness the substrates should be washed 3 times with their respective reagents. The substrates were then dried off using a hot air blow gun with a setting of 5 for 1 minute.

The clean and dry substrates were then clamped into the Cameron-Plint High Frequency Friction Machine to simulate the sliding boundary lubrication conditions found in engines that start up under high loads and low speeds. The disc layed flat in a secure cavity while the cylinder was stationed on a movable mechanical arm. Approximately 1 mL of Fomblin Z was added between the disc surface and the cylinder. The arm and cylinder were lowered to achieve contact with the disc. A 250 N load was then placed on the mechanical arm. All trials were carried out with a 6 Hz frequency with a 9 mm stroke for a 5 hour duration.

The atmosphere of the bearing environment was controlled with a small, clear plexiglass box placed over the apparatus. All visible openings were covered with scotch tape to prevent unwanted circulation with room air. In order to control relative humidity inside the box, a dry air tank, wet paper towels, water bubbler, and steam bath were individually connected to the box via a rubber tube as needed. The relative humidity inside the box was monitored using a small digital humidity probe.

* One may note that all of these wear studies deal with the scar area. However it may be beneficial to record scar volume since that measurement increases linearly with time. Since volume can be calculated given the cylinder radius and scar area, it may be possible to stop the run at set intervals, remove the cylinder, measure the scar area, and place the cylinder back precisely to continue the run..

The Cameron-Plint Machine has electronic devices that monitor temperature (in degrees C), friction, and electrical resistance throughout the 5 hour experiment while a record is printed out on a data versus time chart. These experiments were run at either 50, 100, or 150 degrees Celsius. Electrical resistance is monitored because it is a way of indirectly measuring the thickness of surface film being produced between the metal cylinder and disc (i.e. high electrical resistance implies a thick film and perhaps low wear). Before the load was increased to the 250 N capacity a 5 minute "run in" time at 20 N was employed with the motor at the normal 6 Hz frequency to rub remove any surface films.

Following the experiment the disc and cylinder were unclamped. Excess Fomblin and wear debris was wiped off with a lintless paper towel. Next the cylinder was placed under a light microscope set at 100X with a conversion factor of 150 microscope units = 1 mm. The cylinder's wear scar length and average width were measured and multiplied to give an overall area. The substrates were then labeled and placed in the dessicator for additional future analysis. The residual Fomblin was extracted from the disc cavity using a Pasteur capillary pipet and stored in a glass vial to be analyzed later.

A print out from the machine's chart recorder was used to determine the average friction by measuring data values every 8 minutes, adding them together, and dividing by the number of values taken. The average friction in volts was then converted to an average coefficient of friction by multiplying by 50 N/volt and dividing by the 250 N load. Data is recorded in Table 1.

Discussion of Results:

At 50 C the average coefficient of friction tends to be a linear inverse function of relative humidity although there may be a slight drop in friction around the 15%-20% humidity range (**Graph 1**). Low humidities yield high friction while high humidities yield low friction. This data indicates that water vapor in the air will reduce the amount of friction generated during boundary lubrication.

At 50 C the wear scar area can be viewed as an exponential function of relative humidity (**Graph 2**). From the 0% to 20% a very steep slope illustrates high wear for this amount of moisture. The curve levels out and becomes nearly flat from 30% up to 100% relative humidity. It should be noted that high wear rates often resulted in a very shiny wear scar on both the cylinder and the disk whereas low wear rates yielded black wear scars due to production of a film. Cloudy, murky or grey lubricant was retrieved from the cavity following the high wear runs.

At 100 C the average coefficient of friction drops from a high value at 5% humidity to a relatively low and stable value at 20% humidity (**Graph 3**). There may also be a gradual decrease in friction for values up to 100% relative humidity. The solid square data points on this graph represent data compiled by myself and my mentor, Dr. Larry Helmick (LH Data). The open squares symbolize data gathered by a previous researcher Dr. Bulent Cavdar using the same technique (BC Data).

At 100 C the wear scar area appears on the graph as an even steeper curve than that seen at 50 C. Between 5% and 10% relative humidity the substrates experienced astronomical amounts of wear. The wear area then settled down to a normal constant level from 15% on up to 100% humidity (**Graph 4**).

At 150 C the average coefficient of friction also appears to decrease dramatically with an increase in humidity (**Graph 5**). This data is consistent with the 100 C runs. From 0% to 20% there is a sharp decrease in friction which levels off from 30% to 100%. A strong correlation is evident between Cavdar's data and our own.

At 150 C the wear scar area is again inordinately high for humidities between 0% and 20% with a sharp drop and leveling out from 30% to 100% relative humidity (**Graph 6**). This graph also includes Bulent Cavdar's values that once again fit in very congruently with our wear scar areas.

Conclusion:

The percent relative humidity of the experimental environment has a significant effect on the coefficient of friction and wear scar area for Fomblin Z at 50, 100, and 150 degrees. This may explain why Fomblin exhibits erratic behavior from day to day as room humidity changes. (In the winter room humidity has been recorded around 15% yet in the summer it can reach 70%). This means it is possible to have environmental room humidities across the range where wear rates are strongly affected by humidity.

1. At humidities less than 20%, an exponential amount of wear damage occurs on the cylinder. Wear values between 30% and 100% remain fairly low and constant.
2. There is a noticeable trend of gradual linear decrease in friction with increase in humidity at 50 C. This decrease occurs at a more rapidly and at lower humidity (between 5% and 20%) for 100 C and 150 C runs. After the initial drop off, friction stays at a normal, constant value from 30% to 100%.

In order to insure reproducibility of tests, future studies with Fomblin Z using the Cameron-Plint Machine or four ball rig should treat the percent relative humidity as a condition that needs to be controlled. A predetermined value (preferably between 30% and 100%) should be selected, monitored, and controlled throughout the experiment.

Acknowledgements:

I would like to express my sincere thanks to Dr. Larry Helmick, my mentor, of Cedarville College, and Mr. Shashi K. Sharma, Dr. Peter John, and Dr. Jim Liang of Wright Laboratories for giving me the opportunity to work with them on this research project.

References:

1. Lancaster, J. K., "A Review of the Influence of Environmental Humidity and Water on Friction, Lubrication and Wear," Tribology International, (1990), pp.371-389.
2. Mercer, A.P. and Hutchins, I.M., "The Influence of Atmospheric Humidity on the Abrasive Wear of Metals," Wear, 103 (1985), pp. 205-215.
3. Larsen-Basse, J. and Sokoloski, S.S., "Influence of Atmospheric Humidity on Abrasive Wear - II. 2-Body Abrasion," Wear, 32 (1975) pp. 9-14.
4. Campbell, W.E., Boundary Lubrication: An Appraisal of World Literature, ASME (1969), pp.87-117.
5. Snyder, C.E., Jr., Gschwender, L.J., and Tamborski, C., "Linear Polyperfluoroalkylether-Based Wide-Liquid Range High-Temperature Fluids and Lubricants," Lubr. Eng., 37 (1981), pp. 344-349.
6. Snyder, C.E., Jr., and Dolle, R.E., "Development of Polyperfluoroalkylethers as High Temperature Lubricants and Hydraulic Fluids," ASLE Trans., 19 (1976), pp.171-180.
7. Fusaro, R.L., and Khonsari, M.M., "Liquid Lubrication for Space Applications," NASA TM-105198, July 1992.

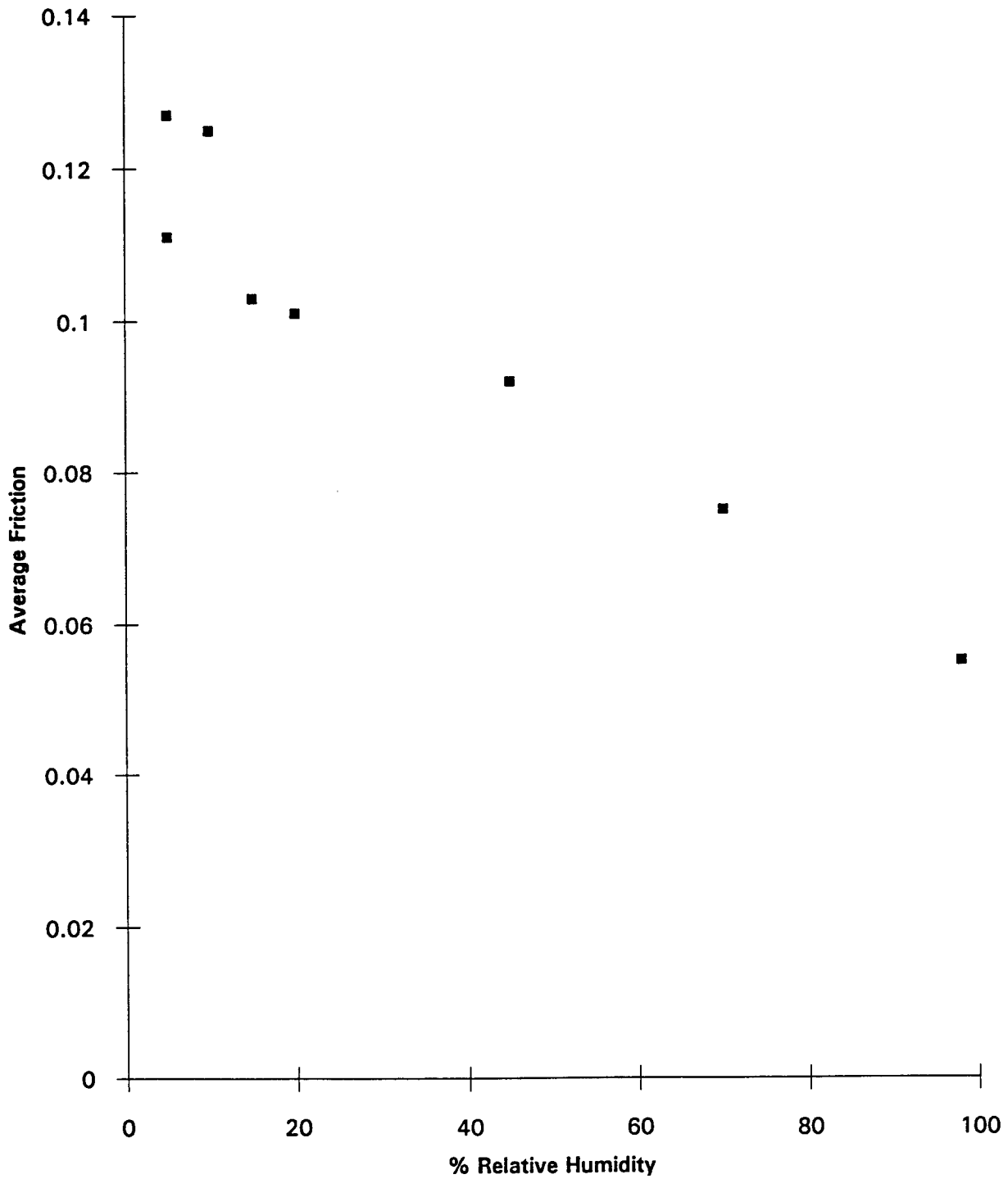
Table 1

FRICTION AND WEAR DATA

Trial #	Temp (C)	Box Hum (%RH)	F-Average	Scar Length (msu)	Scar Width (msu)	Wear Area (mm ²)	Wear Volume (mm ³)
LH-15	50	5	0.127	781	98.4	3.416	0.030714
LH-19	50	5	0.111	782	98.9	3.437	0.031225
LH-22	50	10	0.125	756	71.1	2.389	0.011200
LH-23	50	15	0.103	728	45	1.456	0.002732
LH-21	50	20	0.101	573	28.5	0.726	0.000546
LH-13	50	45	0.092	523	23.5	0.546	0.000279
LH-14	50	45	0.092	498	17.7	0.392	0.000114
LH-24	50	70	0.075	525	19.6	0.457	0.000163
LH-17	50	98	0.055	553	25.5	0.627	0.000377
LH-39	100	5	0.129	775	109.3	3.765	0.041799
LH-28	100	5	0.13	778	114.4	3.956	0.048130
LH-31	100	10	0.099	545	20.6	0.499	0.000196
LH-38	100	10	0.106	595	25.5	0.674	0.000406
LH-29	100	20	0.103	532	20.2	0.478	0.000180
LH-30	100	70	0.097	535	20.7	0.492	0.000195
LH-40	100	98	0.095	511	18.3	0.416	0.000129
LH-16	150	5	0.092	578	33.9	0.871	0.000927
LH-36	150	5	0.148	788	146.1	5.117	0.101803
LH-32	150	10	0.112	766	73.3	2.495	0.012435
LH-34	150	10	0.124	775	77.2	2.659	0.014701
LH-35	150	10	0.114	771	80	2.741	0.016277
LH-37	150	15	0.096	550	20.7	0.506	0.000201
LH-25	150	20	0.092	540	25.44	0.611	0.000366
LH-18	150	56	0.101	562	28.4	0.709	0.000530
LH-33	150	70	0.099	752	46.3	1.547	0.003074
LH-20	150	99	0.096	500	19.2	0.427	0.000146

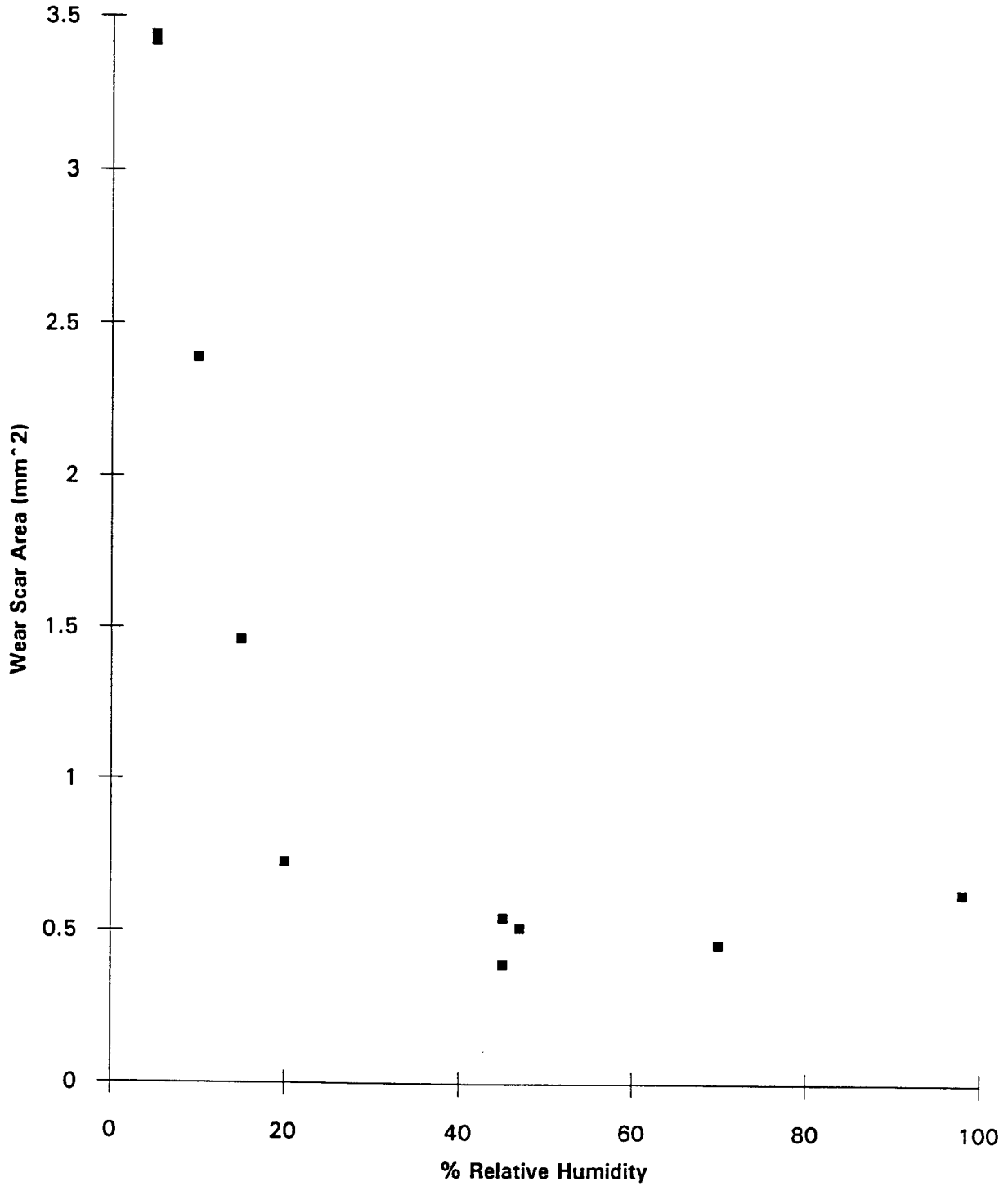
Graph 1

Average Coefficient of Friction Versus Relative Humidity at 50 C



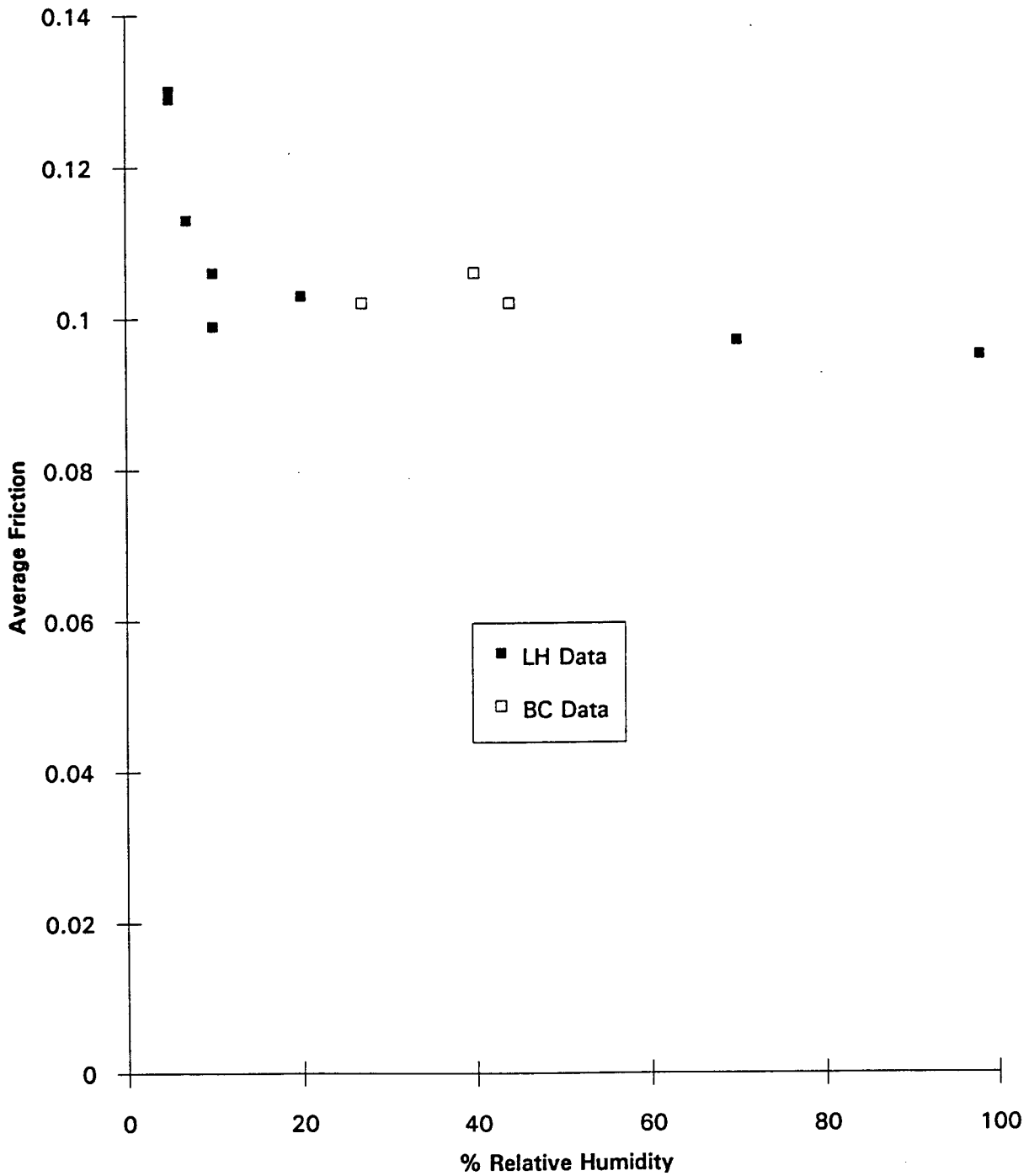
Graph 2

Wear Scar Area Verses Relative Humidity at 50C



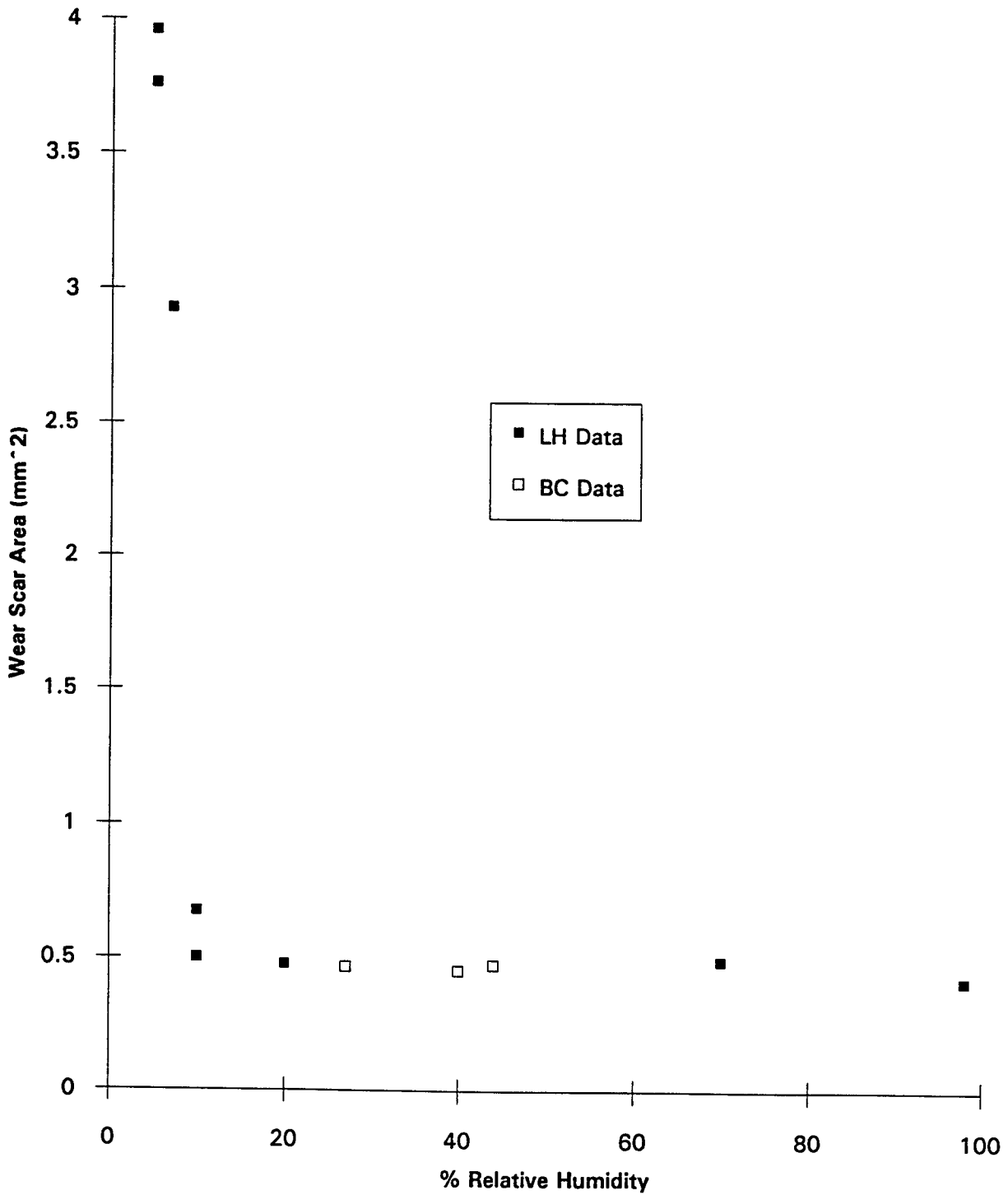
Graph 3

Average Coefficient of Friction Versus Relative Humidity at 100
C



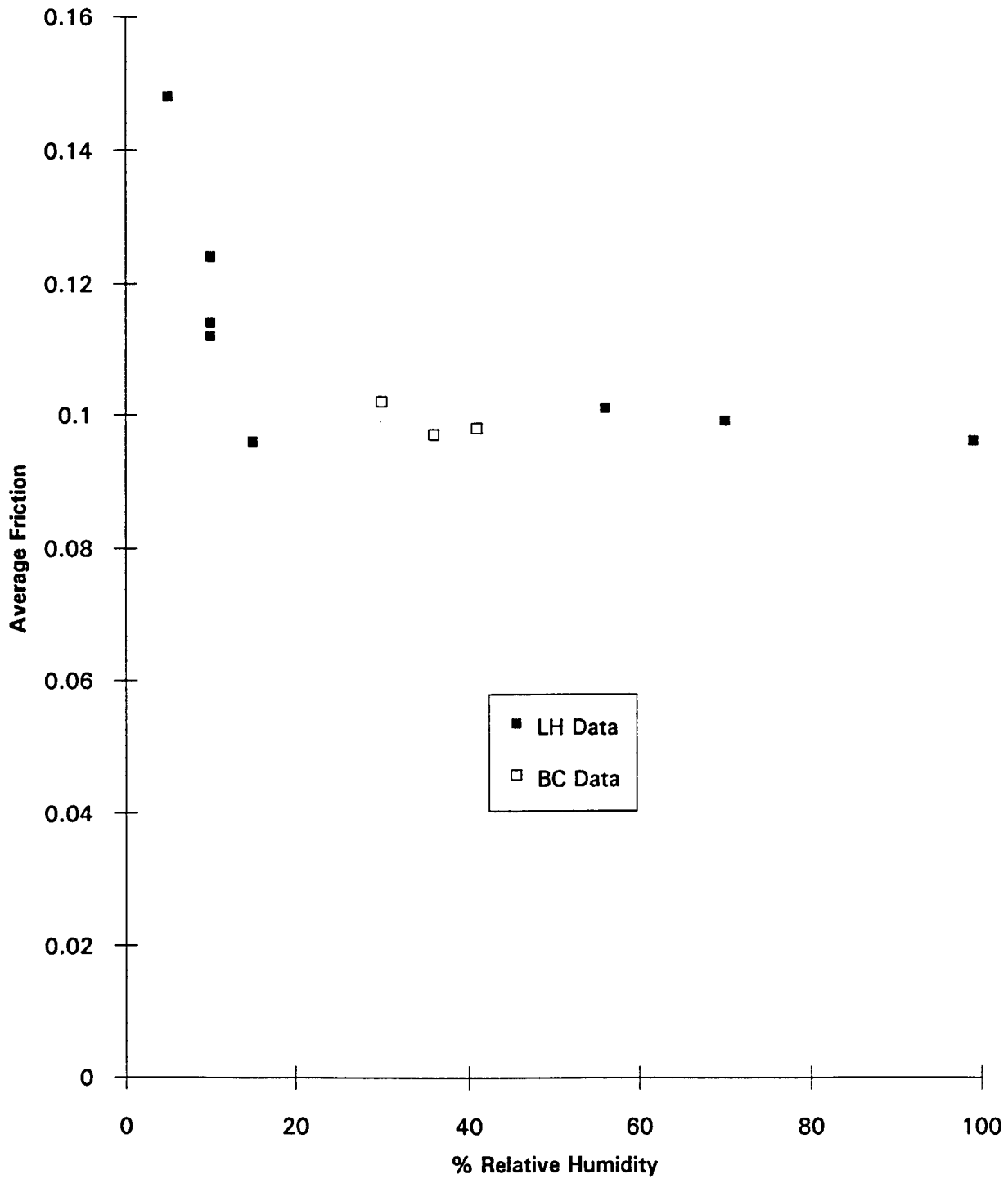
Graph 4

Wear Scar Area Versus Relative Humidity at 100 C



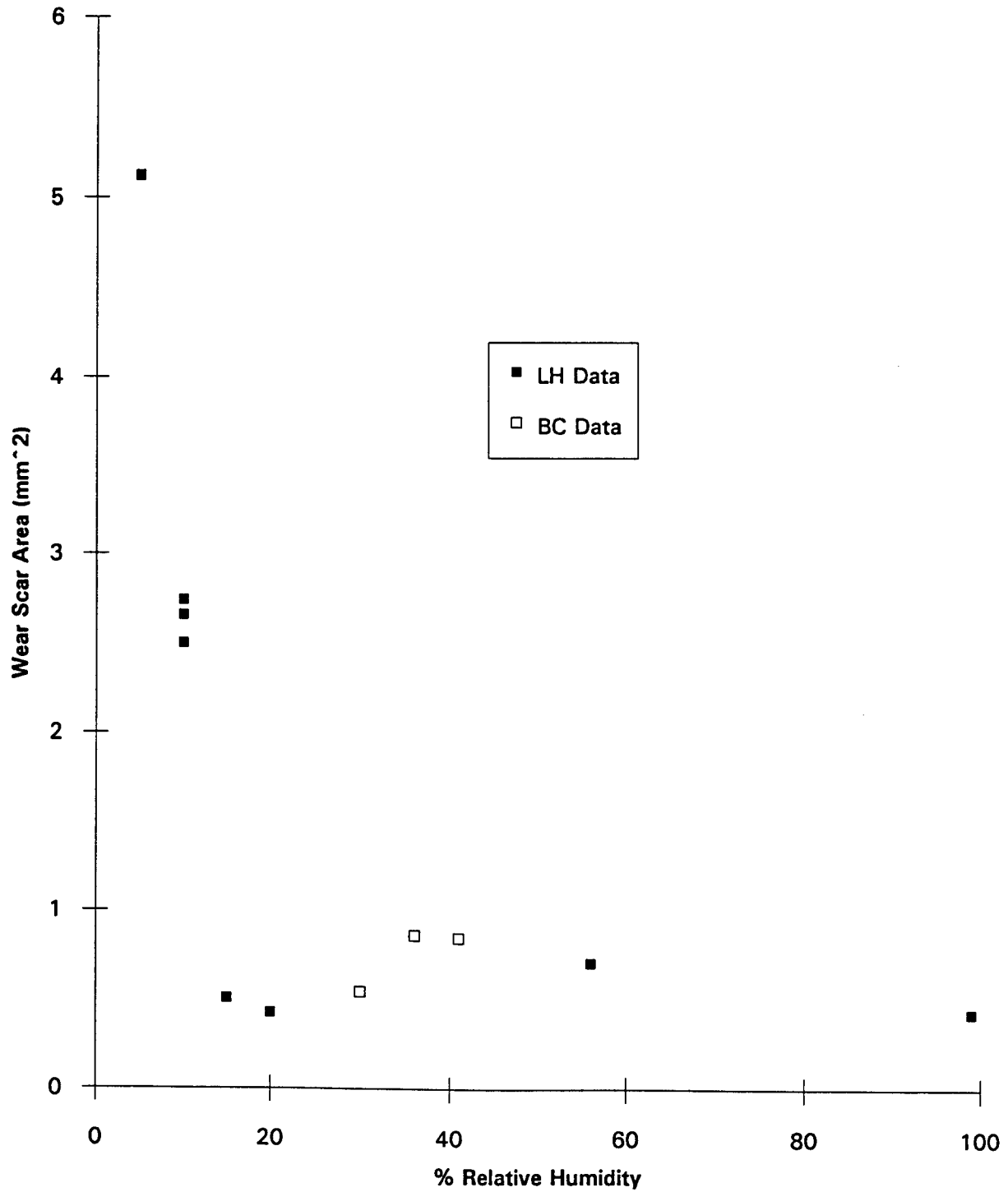
Graph 5

Average Coefficient of Friction Versus Relative Humidity at 150 C



Graph 6

Wear Scar Area Versus Relative Humidity at 150 C



MY INTRODUCTION TO THE INTERNET

Jennifer A. Starr
student
Trotwood Madison Sr. High

Final Report for: AFOSR Summer Research Program

Wright Laboratory

Sponsored by: Air Force Office of Scientific Research

Boiling Air Force Base, Washington, D.C.

July 1994

MY INTRODUCTION TO THE INTERNET

Jennifer A. Starr
student
Trotwood Madison Sr. High

ABSTRACT

This report will explain the knowledge obtained, while working at Wright Patterson Air Force Base. It will explain the information acquired about Internet, and its useful functions. In addition, this report will discuss my experience with Internet.

MY INTRODUCTION TO THE INTERNET

Jennifer Starr

INTRODUCTION

RDL has enabled me to get paid for researching useful things about today's technology. Through my employment, I have obtained knowledge about computers. This information will prove useful to me, upon entering a institution for higher education this fall. A great deal of my summer was spent learning as much as possible about the Internet and its useful functions.

METHODOLOGY

One of the interesting things I learned this summer was how to use the computer network called Internet. Internet is the world's largest computer network. All the networks, using the IP protocol, combine to form a seamless network for their collective users. This includes federal, regional, campus, and some foreign networks. All these networks combined are only part of what makes up the Internet because now other non IP networks are connected. There is no single authority figure for the internet as a whole. Everyone pays for their part of the internet, it isn't one big bill. I thought it was interesting how you could send one message all around

the world's computer networks and receive a reply from all the computers with information on that one message. This process is called E-mail (electronic mail). The internet is an extensive information retrieval and vending system that allows those that are "connected" access to information on almost endless subject matters. With so much information that can be accessed, you would assume someone had to be a computer genius to use the system, but, that is not true. Although the system operates with the use of complex network configurations, operating the system was simplified so that those versed only in basic computer literacy could access the system, gather and send information. That is what makes the Internet a valuable tool.

Even with the simplest programs there are certain words that you must know to help things run smoothly. The first of those is a program called "gopher". The "gopher" is a good point to start at when looking for information. There are many "gopher" clients for just about any computer you or your institution may be using. In essence you tell the "gopher" what you seek and it goes to the home sever and asks for its main menu. After you select the main topic, the "gopher" asks for more information on that subject, such as (text files, directory, charts, etc.).

When searching through indexed material and finding articles based on what they contain, the internet provides WAIS, which allows you to search the Internet archives looking for articles containing certain groups of words to assist you in the search.

Another service which is very useful but limited is "archie" , which allows you to search files by filename or file description. You can also search for useful resources through the World Wide Web (the Web or WWW). The web is a great way to search for useful resources because it has its own

resources and allows you to use the other searching services mentioned previously. With the Web you are able to use hypertext which is a method of getting information, where selected words in the text can be expanded at any time to provide more information. Those words are "links" to other documents which may be helpful. They might consist of, text, files, pictures, charts, etc.

MOSAIC is another tool to navigate on the Internet. MOSAIC is based on the WWW technology. It uses the WWW common client library for most of its low-level communication layers. MOSAIC relies on a server to provide access to documents containing formatted text and graphics on the Internet. These documents are stored in a specific format called HTML (hypertext markup language). HTML is a markup language used in the formatting process for WWW. A portion of my time with MOSAIC was spent using HTML to format documents into smaller files. The HTML files contained WWW address for various categories (government, education, foreign, etc.) for which I broke down into separate files.

At first glance you might assume that the "web" and "gopher" are the same. Although they have similarities they are fundamentally different. The only real similarity in the two is the fact that they both are used for searching, but there is a greater difference. The "web" is using the hypertext format which links to other pages of the hypertext. There are no rules on where documents point. For example, you research automobiles highlight tires in the text and see what kind of tires were first used, the compositor of the tire etc. The search could be endless. The "gopher" just isn't as flexible because it doesn't have a link between files it only knows what is written under the main topic.

There are many more services that are provided by the Internet but the ones discussed in this report are what I became familiar with this summer. I highly recommend working with the Internet, it is just as useful as any library would be; If your not familiar with the Internet, then I would also suggest going through a user's guide to familiarize yourself with the network.

THE EFFECT OF TEMPERATURE
UPON Ho:YAIO₃ FLUORESCENCE

Todd Stockert

Centerville High School
500 W Franklin Street
Centerville, OH 45459

Final Report for:
High School Apprentice Program
Wright Laboratory

Sponsored by:
Air Force Office of Scientific Research
Bolling Air Force Base, DC

and

Wright Laboratory

August 1994

THE EFFECT OF TEMPERATURE
UPON Ho:YAlO₃ FLUORESCENCE

Todd Stockert
Centerville High School

Abstract

The trends and mechanisms of temperature variant Ho:YAlO₃ upconversion were studied. The crystal was pumped with a chopped Ti:sapphire laser beam and the emissions were monitored with a spectrometer. The temperature of the crystal was varied from 19 to 325 K. Previous work with holmium crystals indicates mechanisms of two step upconversion with phonon emission. The present studies conducted with Ho:YAlO₃ followed the same pattern. Temperature effects upon spectral excitation, excitation time, and relaxation time indicated a strong influence of temperature. Findings were attributed to the Boltzmann effect. The studied trends suggest maximized intensity for Ho:YAlO₃ 543.5 nm emission at around 250 K.

THE EFFECT OF TEMPERATURE UPON Ho:YAlO₃ FLUORESCENCE

Todd Stockert

Introduction

The laser is a relatively new tool¹, with numerous unexplored regions of thought. Much research is put into discovery and development of new laser crystals. Ho:YAlO₃ is a crystal at such a stage. When optically pumped, the Ho:YAlO₃ crystal emits at green wavelengths in the 540 nm region². This property makes it a prospect for possible use as a solid state visible laser. Research is being conducted on the viability of Ho:YAlO₃ within that role. The upconversion mechanism is not completely understood. Excitation lifetime, relaxation lifetime, and spectral response are properties which will be reported on in this paper. Temperature is also an important variable in these properties. By measuring the trends with temperature, an optimum temperature for the crystal could be ascertained and lasing efficiency of the crystal would be increased.

Procedure

The crystal observed is on loan from Prof. Steve Rand at The University of Michigan. It nominally has 1% holmium concentration. When pumped at 965 nm, the crystal emitted wavelengths in the regions of 540 nm(green) and 660 nm(red). These were the wavelengths used to find trends for the Ho:YAlO₃ fluorescence. The measurements were made between 19 and 325 K. The lab setup (see figure 1, p 42-8) consisted of a pump laser, a chopper, a cooling assembly, the crystal, a monochromator, a photomultiplier, and an oscilloscope. The pump laser consisted of a Coherent Model 300 argon continuous wave laser. It pumped a Coherent Model 899 Ti:sapphire laser which generated a tunable laser beam in the 910-980 nm region. A stepper motor allowed computerized control of the pump wavelength. The laser's power was then controlled with and monitored with a variable attenuator and a power meter. The continuous wave laser beam was then cut into observable segments by a mechanical chopper. The chopper ran at 120 Hertz and had a 50 percent duty cycle. With a repeating segment, the rise and decay of the pumped Ho:YAlO₃ crystal could be consistently observed. After the chopper, the beam entered the crystal holding chamber. The Air Products Displex DF-202 "cold finger" allowed temperature control of the crystal without hindering the optical path. A Balzers turbo-molecular vacuum pump provided a vacuum for the cooling unit. The average variation in temperature was ± 1 K. Optical emissions collected from the pumped Ho:YAlO₃ crystal were directed into a SPEX 1269 1.26 m monochromator. This isolated the separate wavelengths emitted by

the crystal. A chosen wavelength was then sent to the photomultiplier and fed into a LeCroy 9310 oscilloscope for analytical study. The data was then converted, manipulated, and graphed on computer.

Observations

The first trends studied were those of excitation spectrum changes. These were obtained by scanning the crystal with different pump wavelengths and monitoring the fluorescence response. The spectra did not remain constant relative to temperature. They translated along different wavelengths and transformed in shape and size with temperature (see Figs. 2+3, p. 42-9 and 42-10).

The features of the low temperature spectra were sharper than those at high temperature. These characteristics made rise and fall time observations more difficult, as the spectra changed with temperature. The excitation intensity would have to remain relatively constant throughout the thermal range 19 to 325 K. The pump wavelength of 965.0 nm met this criterion.

The excitation spectra show excitation in the range between 960 and 975 nm. The transmission measurements for Ho:YAlO₃ show downward fluctuations in transmittance in the region (see Fig. 4, p. 42-11). This shows that a ground state absorption is leading to 662 or 543 nm upconversion. However, the details of the process remain unknown. Note that the 970 nm and 1500 nm absorption features in this crystal do not correspond to Ho³⁺ absorption; they are characteristic of Er³⁺ absorption. The possibility of erbium contamination and doping needs to be considered when interpreting the results reported here.

Another variable affecting the observation of the Ho:YAlO₃ was pump intensity. Through the initial stages of this study, the upconversion mechanism was taken to be independent of the pump beam intensity. If this were true, an increase in pump power would result in a quadratic increase in emission intensity assuming each green or red emission photon required two pump photons for its creation. As shown by the Emission Intensity vs. Pump Power graph (Fig 5, p. 42-12), this was not the case. The reason for this deviation could not be determined, but since the intensity decreased from the quadratic pattern at increased power, it was assumed that saturation effects were occurring. Pump power was consequently held constant in the quadratic region throughout the lab procedure.

Excitation lifetimes were also studied. The mechanical chopper effectively chopped at the rate of 120 Hertz at a 50 percent duty factor. This created square pulses 4.17 ms long with edge transition times of about 60 μs. The observed emission waveforms were not square. Instead they exhibited a gradual rise. The traces of the waveforms revealed an exponential growth function (Fig. 6, p. 42-13).

These waveforms were then fit to:

$$I_r = I_0^r [1 - e^{-(t-t_0)/\tau_r}]$$

This was done through conversion of the data into Sigmaplot and then running a Marquardt-Levenberg algorithm based curve fitter with I_0^r representing the asymptotic intensity; τ_r representing the effective excitation risetime; and I_r representing the resultant intensity at time t with time shift t_0 .

This excitation is at least a two-step process of upconversion. A possible model for green upconversion includes four energy levels n_0 , n_1 , n_2 , and n_3 . For upconversion an electron is excited by a photon to cause a transition from the ground state (n_0) to n_2 . The electron then decays with non-radiative emission to reach n_1 . It is then excited by a second photon to bring the electron to n_3 . The electron then relaxes with photon emission at the green wavelength (see Fig. 7 p. 42-14). The monitored excitation lifetime τ_r was a combination of τ_{02} , τ_{21} , and τ_{13} . These effective rise time constants were plotted against temperature, and it was determined that they varied with temperature.

The trends found for excitation were different between the two emission wavelengths (543.5 nm and 662 nm). For the green wavelengths (543.5 nm), the rise times start low--about .7ms--then consistently increase to a point above 1.2 ms at around 125 K. The rise times then decreased from that point for the remaining temperatures (see Fig. 8 p. 42-15). At red wavelengths (662 nm), the trend was not quite the same. The general trend was a decrease in excitation rise time with temperature (see Fig. 9 p. 42-16).

A possible explanation for the observed changes with temperature includes interaction of the trivalent holmium ion's energy levels with the electric field of the surrounding ions. At absolute zero the ions are as close to each other as possible. This makes their effect upon the holmium energy levels maximal. At this same point (0 Kelvin), all electrons are in their ground state. The energy difference for the pump wavelength intersects at, above, or below some excited state energy level. If the energy difference equals the photon energy, the system has the maximum possible number of electrons being excited and therefore has the shortest excitation time. If the difference lies above or below the mean, then very few electrons will have the opportunity to become excited and the rise time will be extremely long. As the crystal warms and expands, the ions surrounding the holmium ion move away. This shifts the energy levels in a certain direction, either up or down. The distribution also changes, with the mean of the Boltzmann distribution rising through various manifolds. With this change, the energy difference from the upper level to these manifolds changes and the opportunity

exists for a higher or lower probability of excitation. If the excitation probability increases, a shorter excitation lifetime results. If less electrons are excited, then an increase in lifetime results. In addition, nonradiative relaxation is known to increase with temperature. These temperature dependent effects combine into the observed changes in rise times.

The relaxation stage was another observed and studied characteristic of Ho:YAlO₃. Relaxation lifetime was studied in the same manner as excitation. The chopper allowed a consistent look at the relaxation lifetimes. The relaxation process, like the excitation was found to be gradual. The waveforms for the green emission were consistent with a single exponential decay. To study these decays and their reliance on temperature, the green data was fitted to:

$$I_f = I_0^f e^{-\frac{t}{\tau_f}}$$

Where I_0^f is the intensity constant, τ_f is the effective relaxation lifetime constant, and I_f is the resultant intensity at time t . The curves fit well and verified that the decay was in fact single exponential (see Fig. 10 p. 42-17). Therefore a single relaxation lifetime and consequently a single energy level transition is responsible for the actual 543.5 nm emission.

The red emission was not as simple. The data indicated that a single exponential decay was not adequate for the higher temperature relaxation traces. When fit to a double exponential decay, they did fit (see Fig. 10a p. 42-17). The double exponential fit indicates two different relaxation stages are responsible for the 662 nm emission. A possible explanation for this effect arises from the presence of the 543.5 nm energy levels. The upper green level may, in part, be decaying to the red level which effectively creates additional red emission. Under this model, when the laser pumping is stopped, the normal decay of the red level occurs. While this happens the level is effectively repopulated through the green decay, lengthening the decay and bringing in a second set of parameters to the relaxation. More experimentation and modeling may be necessary to isolate this process and to determine its complete origin (see Fig. 7a p. 42-14).

Temperature trends for the green emission relaxation were studied through comparison of the lifetime constants τ_f from the fitted exponential curves. Temperature was found to affect the relaxation lifetimes of Ho:YAlO₃. A general decline in lifetime with temperature was observed. Other trends may be within this, but the small magnitude of the data makes further interpolation unreliable (see Fig. 11 p. 42-18). The slight decrease in relaxation lifetime with increasing temperature can be explained in terms of non-radiative relaxation. The decay process has two possibilities, phonon emission and the

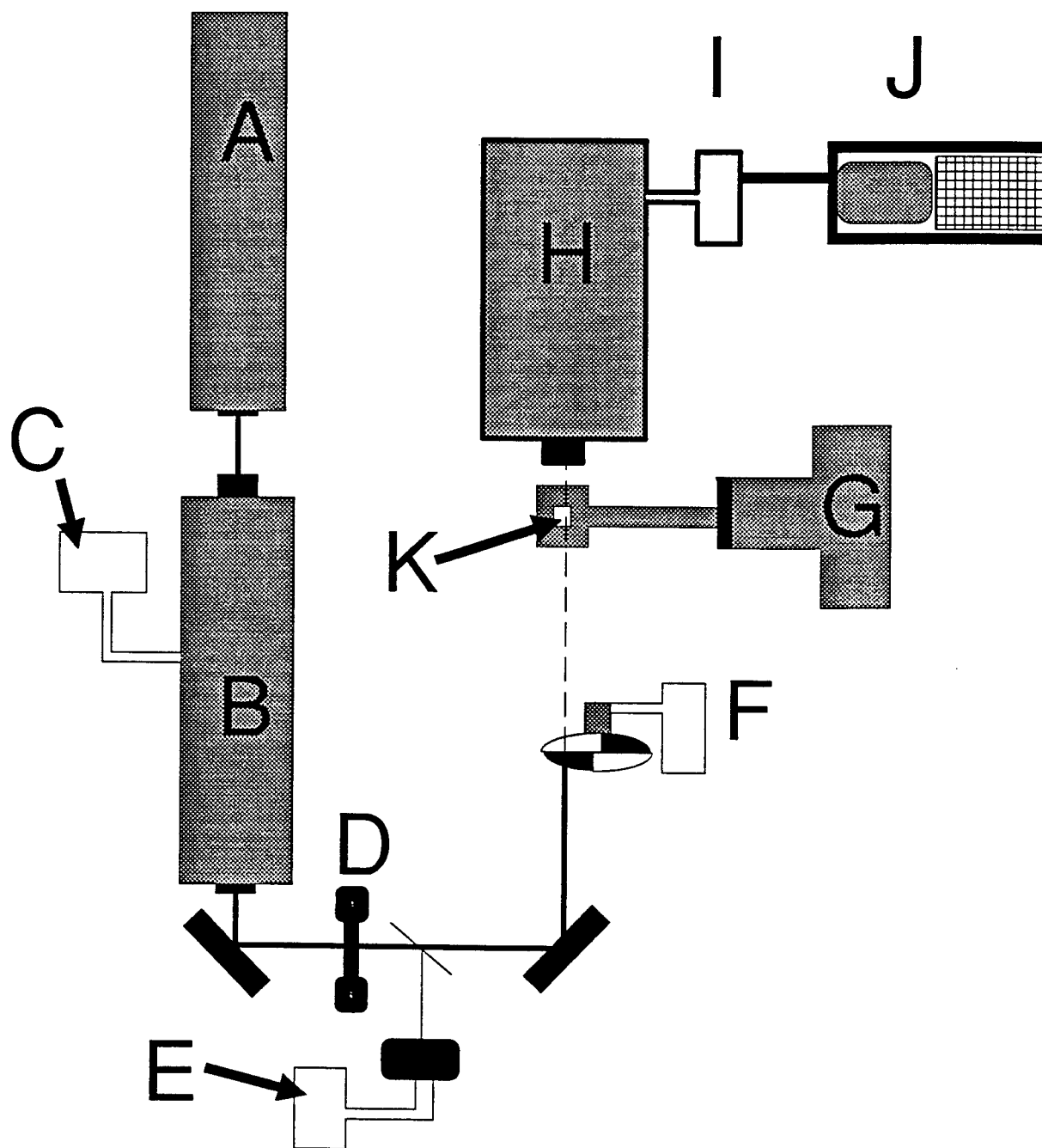
radiative 543.5 nm photon emission. The relaxation rate is then equal to the radiative and non-radiative rates summed. The non-radiative relaxation is known to increase with temperature. Phonon emission occurs between two very close energy levels. Thus, when the temperature rises, the total relaxation rate increases. This explains the increased rate and decreased lifetime with increased temperature.

From the observations on excitation rise times, a general trend on efficiency can be determined. The steady state intensity of the holmium emissions are equal to the calculated constants for I_0^f . The measurements for this data were taken at constant power. Therefore, the greater the intensity, the greater the efficiency of converting pump photons to green emission (Fig. 12 p. 42-19). The maximum efficiency for the 543.5 nm emission is around 250 K.

Conclusions

The study of the temperature affects upon the Ho:YAlO₃ crystal properties has resulted in a number of trends. The excitation spectra were determined to change with temperature. The excitation rise time of the 543.5 nm wavelength emission was determined to increase then decrease in duration with temperature. The cause of this trend was attributed to the Boltzmann effect and nonradiative relaxation. The 662 nm emission rise time was also studied and determined to have a general downward trend with temperature. The relaxation lifetimes of the 543.5 and 662 nm wavelengths were also studied. The green emission relaxation rate was determined to be singular in nature. This holds true with the modeled mechanism of upconversion. The relaxation lifetime of the green emission was determined to generally decrease with temperature. The red emission was determined to have a double decay model for relaxation. The specific origin of the secondary relaxation was not conclusively determined, but is suspected to be a result of decay from the 543.5 nm emission energy level. All of the above conclusions help delineate the actions within the pumped Ho:YAlO₃ crystal and should help further studies of the upconversion mechanism within Ho:YAlO₃.

Ho:YAlO₃ Lab Layout



A Argon cw Laser
B Ti:Sapphire Laser
C Stepper
D Var. Attenuator
E Light meter
F Chopper

G Cold Finger+Vacuum Pump
H Monochromator/Photomultiplier
I Amplifier
J Oscilloscope
K Ho:YAlO₃ Crystal

FIGURE 1

Ho:YAlO₃ Excitation Spectrum

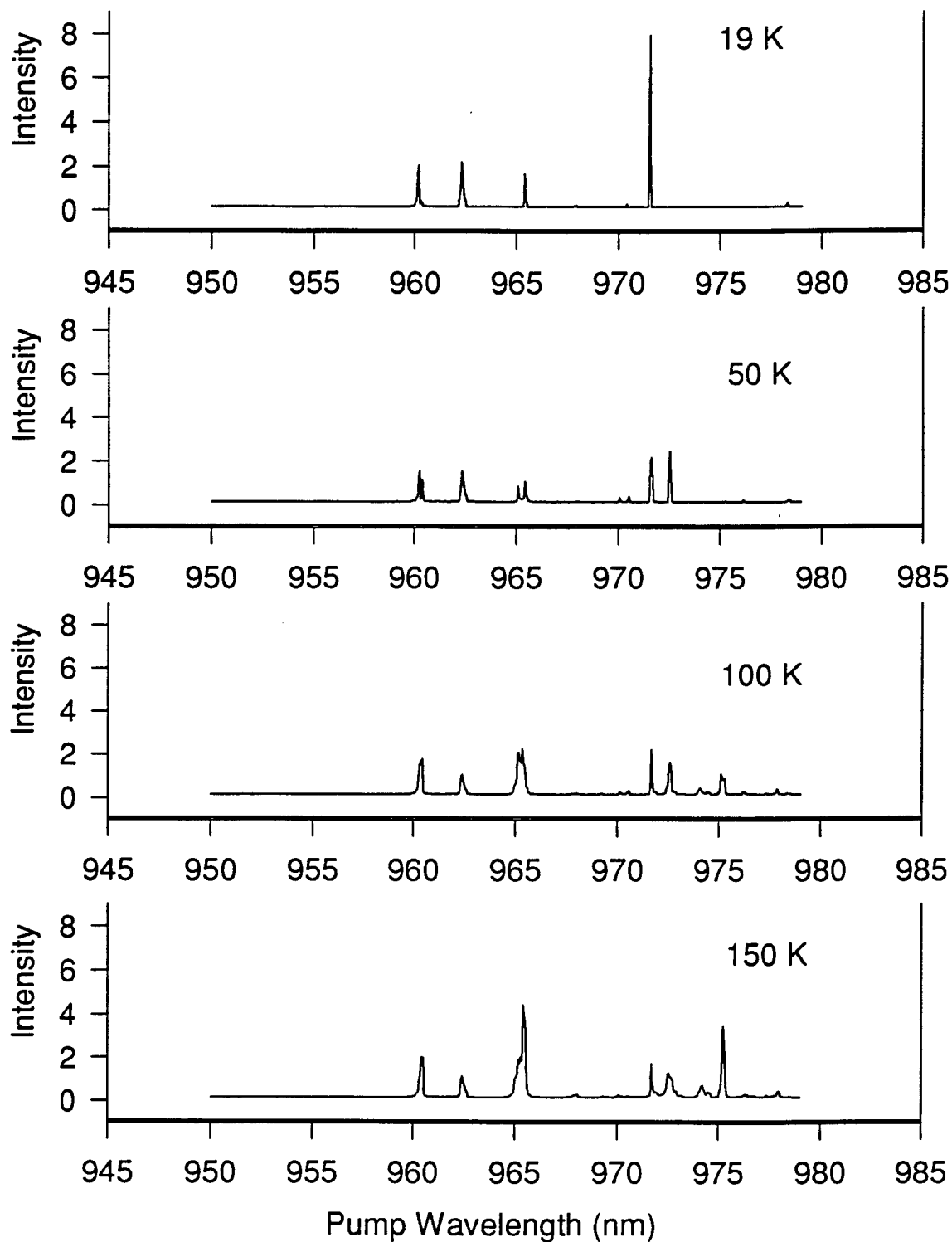


FIGURE 2

Ho:YAlO₃ Excitation Spectrum

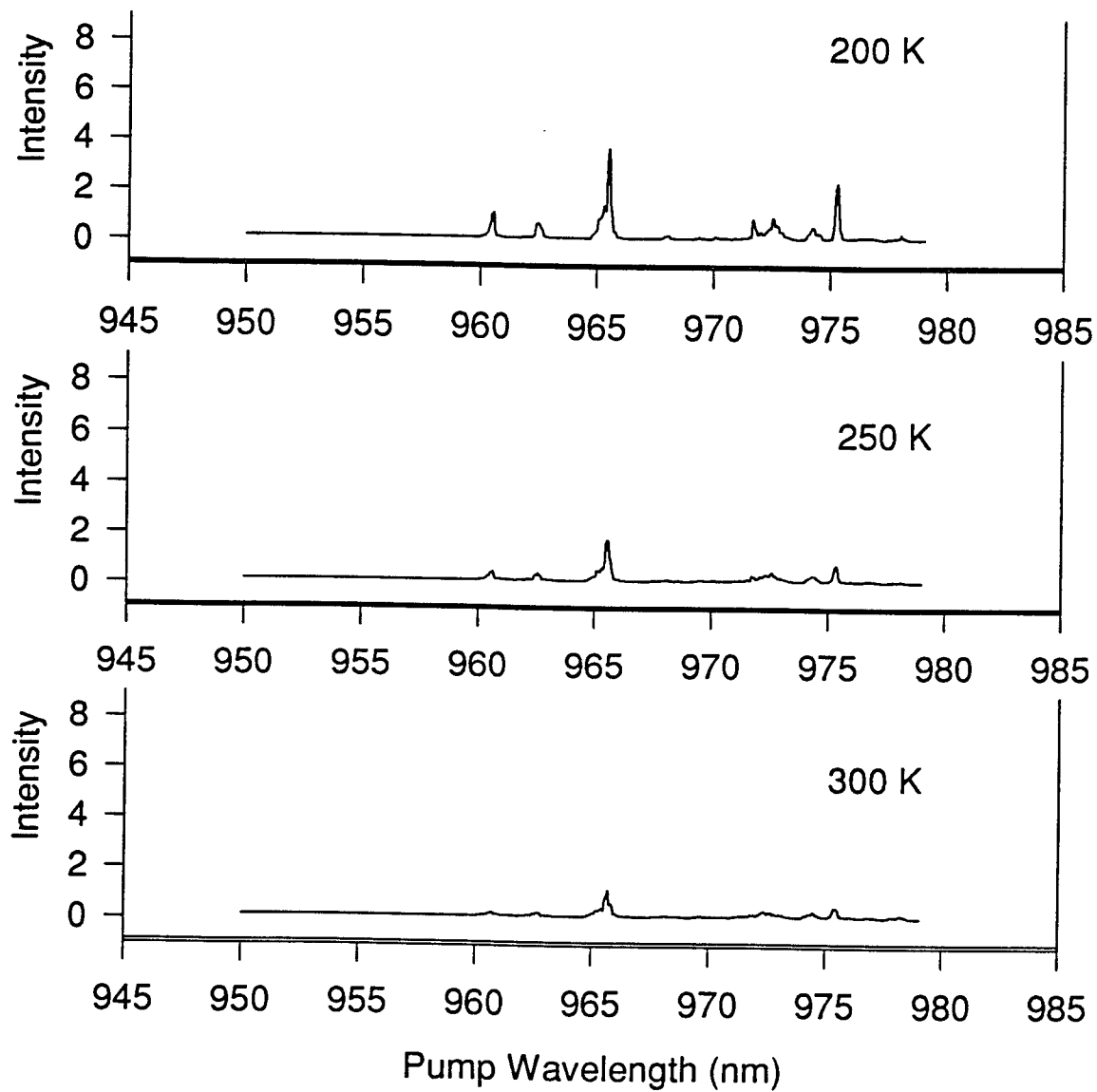


FIGURE 3

Ho:YAlO₃ Transmission Spectrum

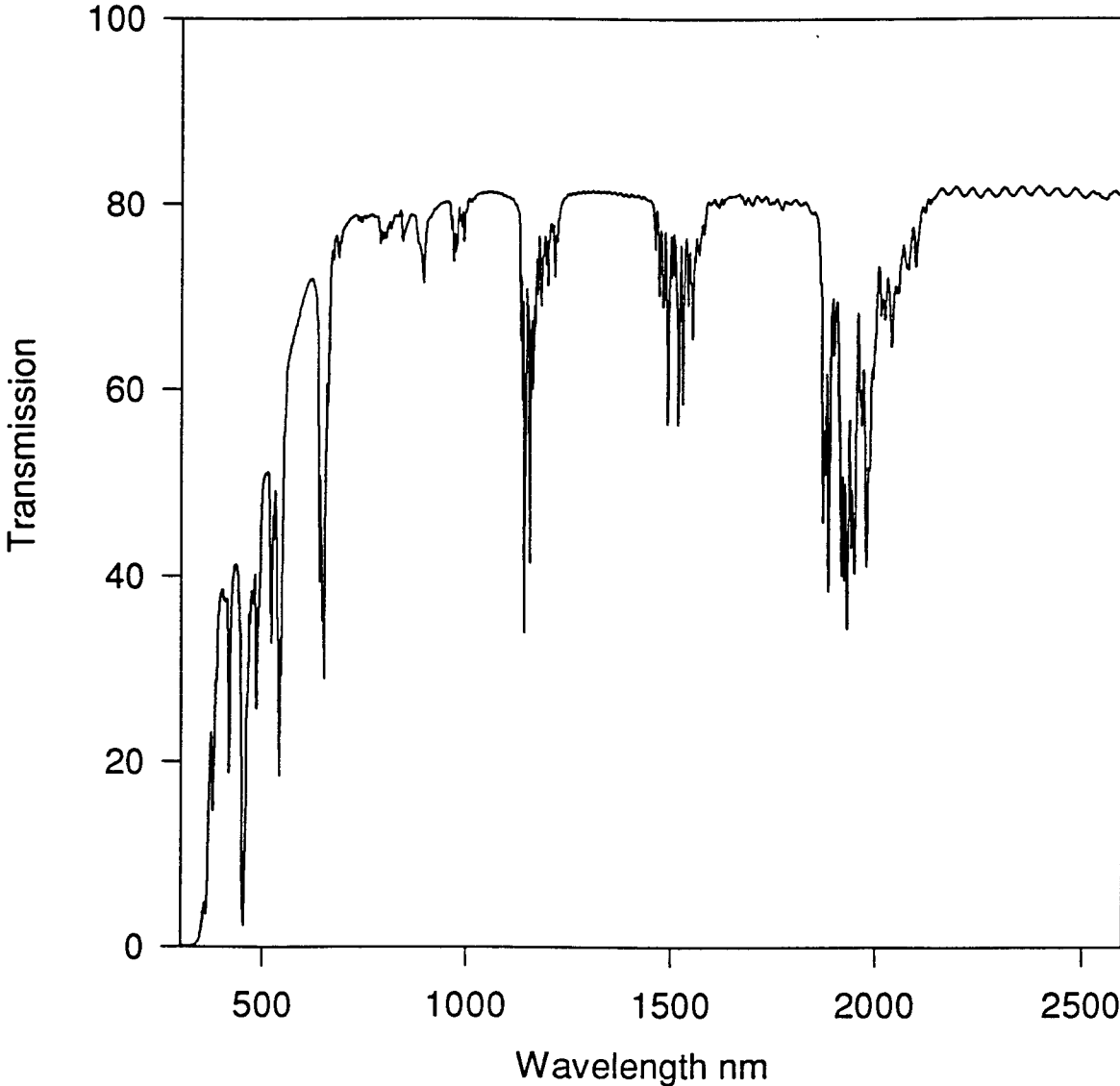


FIGURE 4

Ho:YAlO₃ Intensity vs. Power @50K @543.5nm

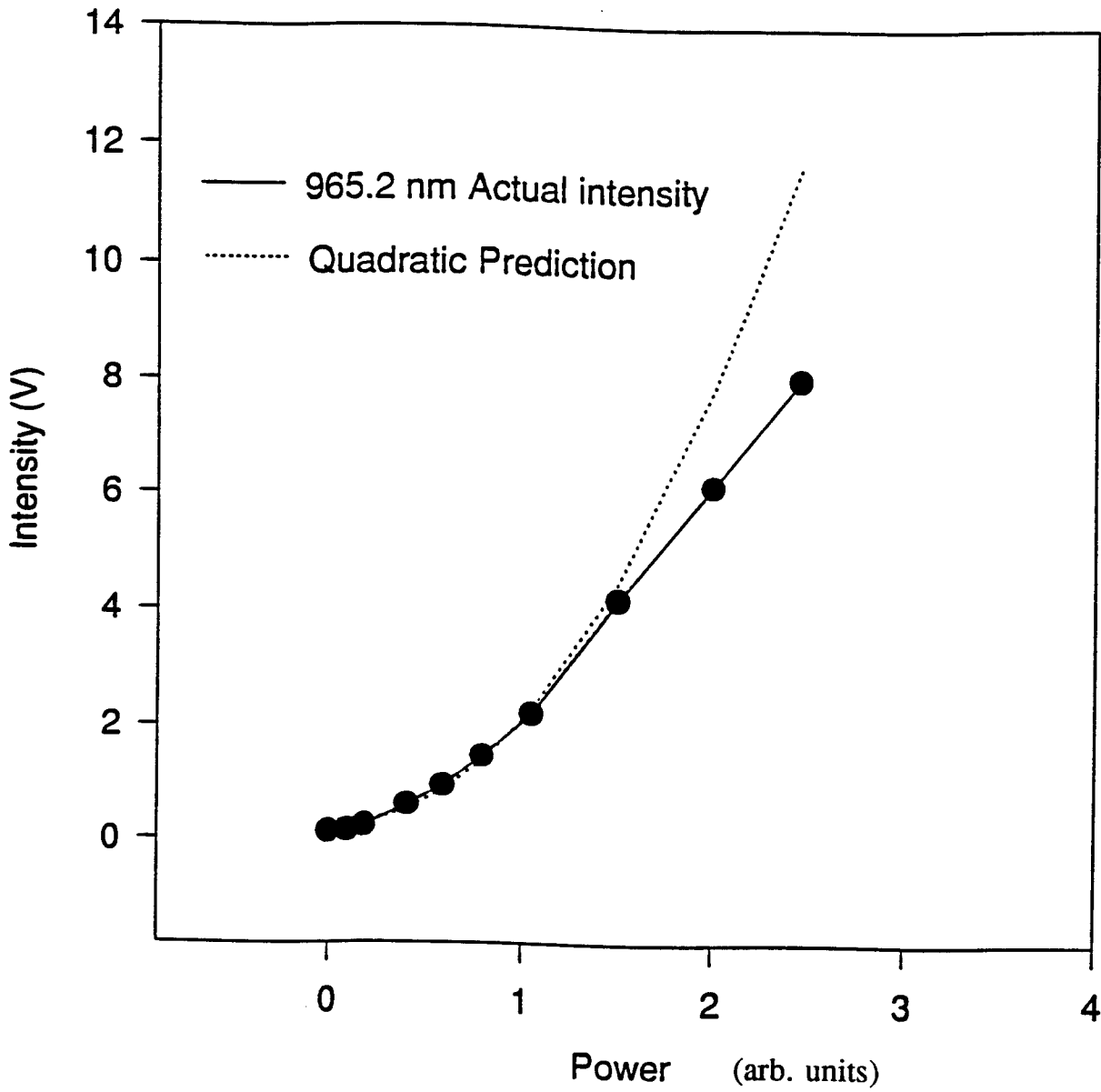


FIGURE 5

Ho:YAIO₃ 543.5nm Rise comparison at 175K

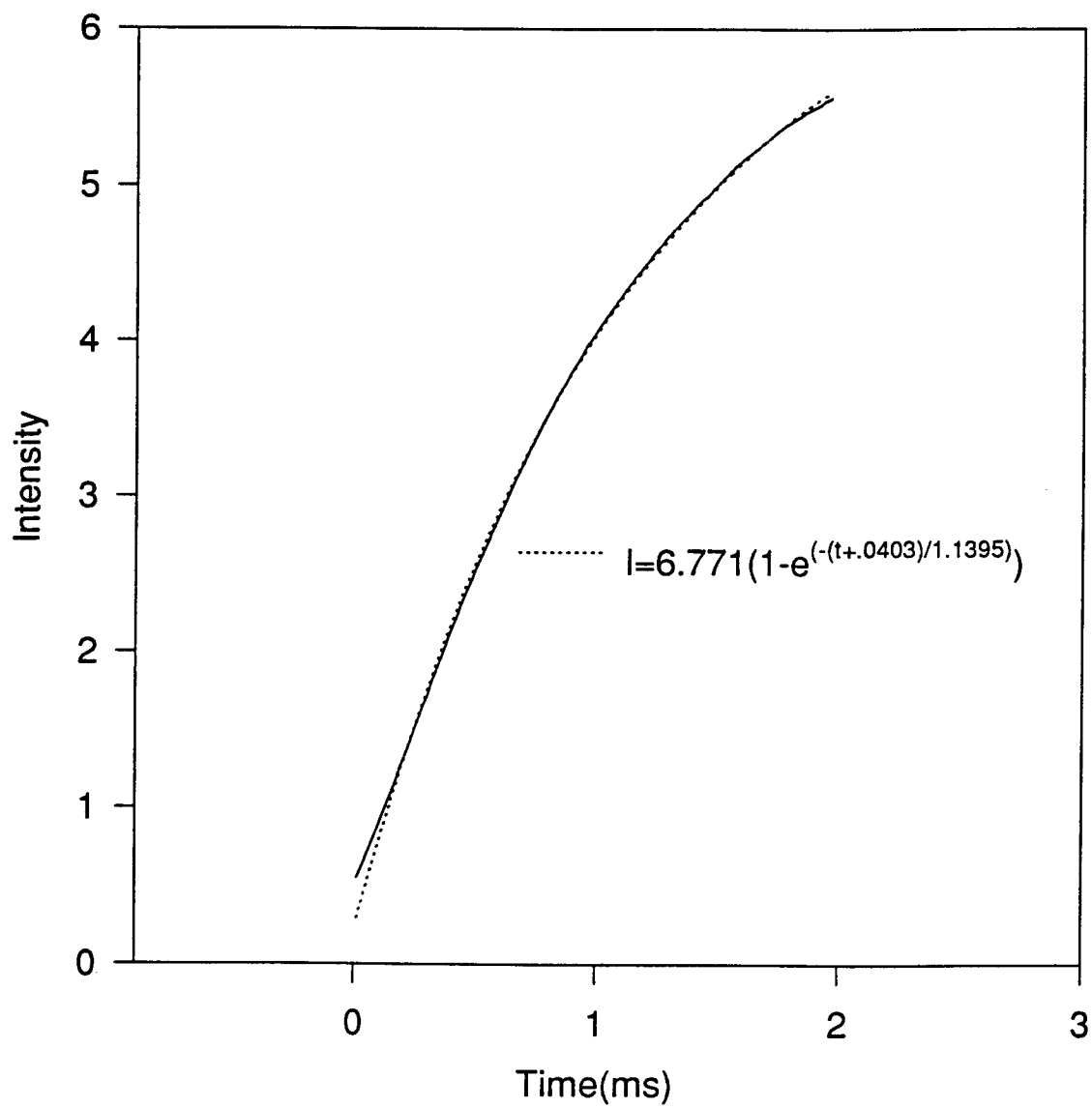


FIGURE 6

Proposed 543.5 nm Upconversion Mechanism

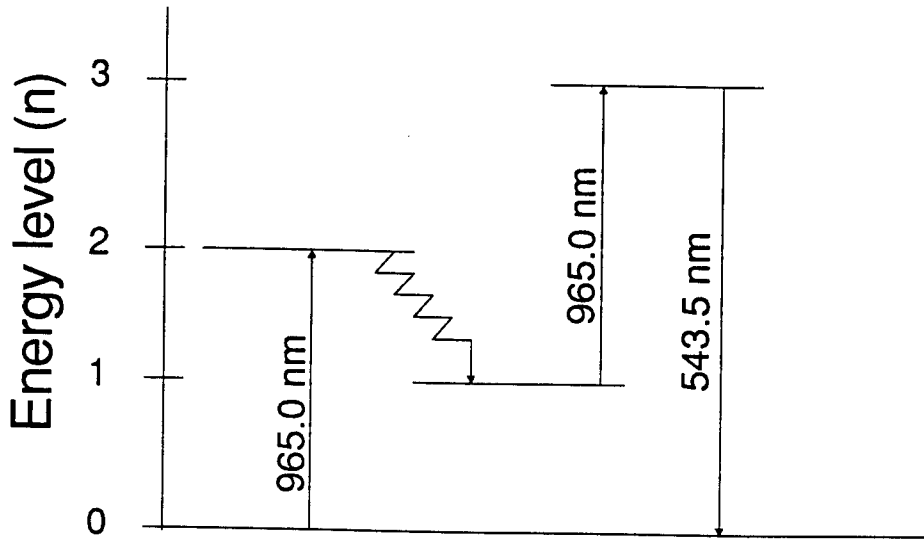


FIGURE 7

Proposed 662.0 nm Upconversion Mechanism

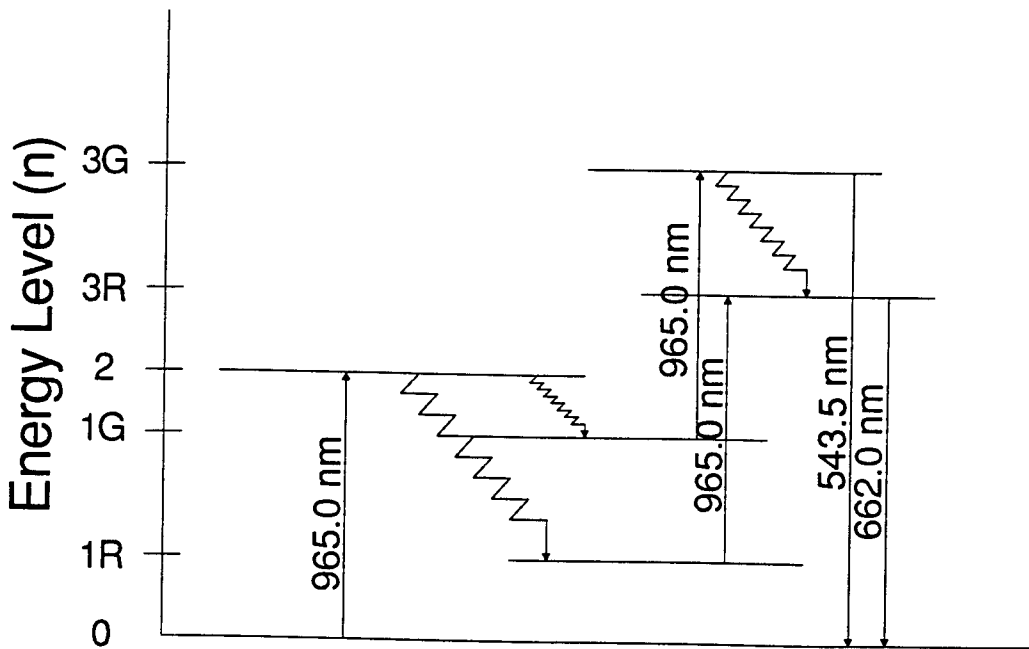


FIGURE 7a

Ho:YAIO₃ Rise Lifetimes vs. Temperature @543.5nm and Constant Power

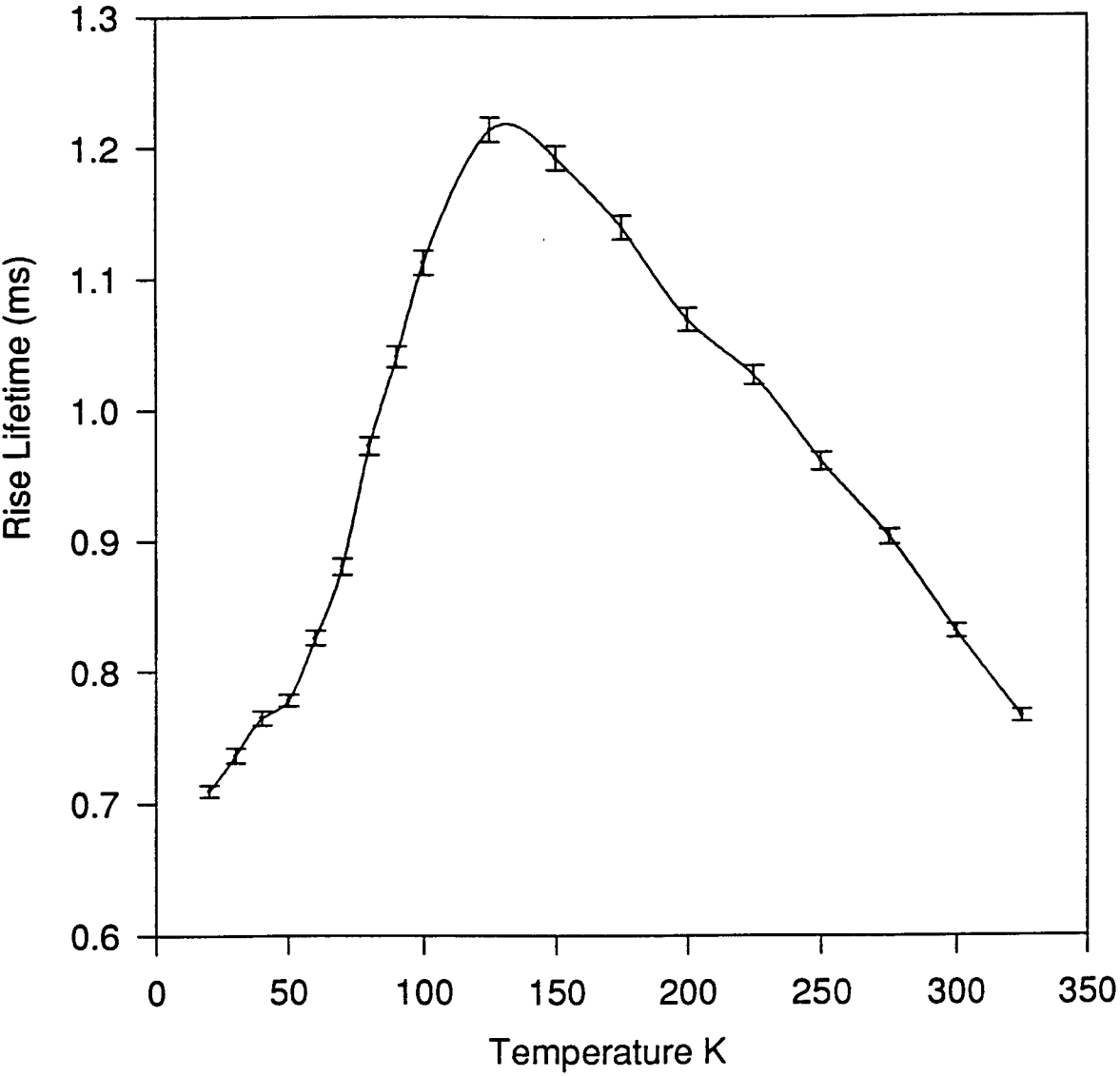


FIGURE 8

Ho:YAIO₃ Rise Lifetimes vs. Temperature @662nm and constant Power

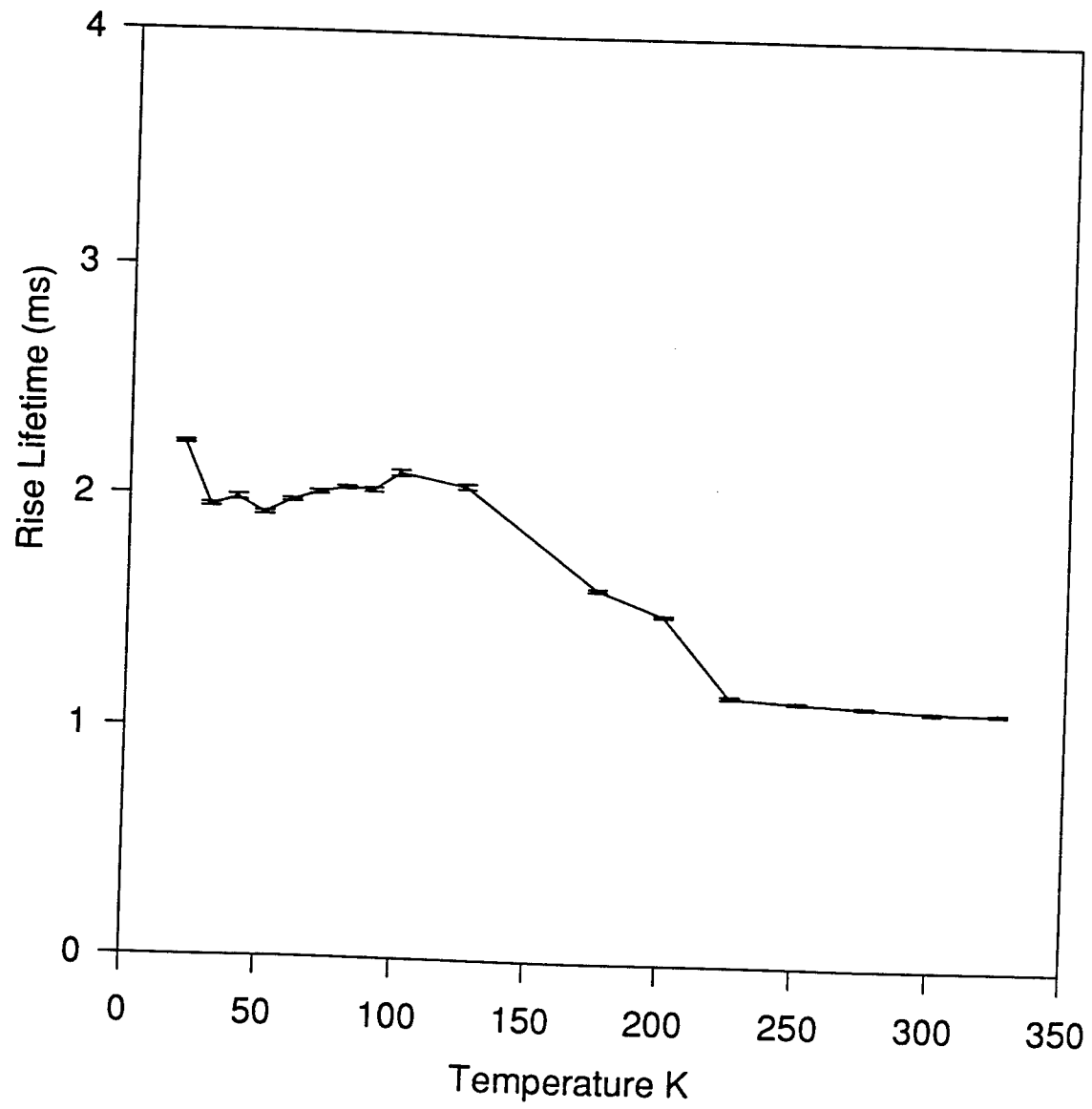
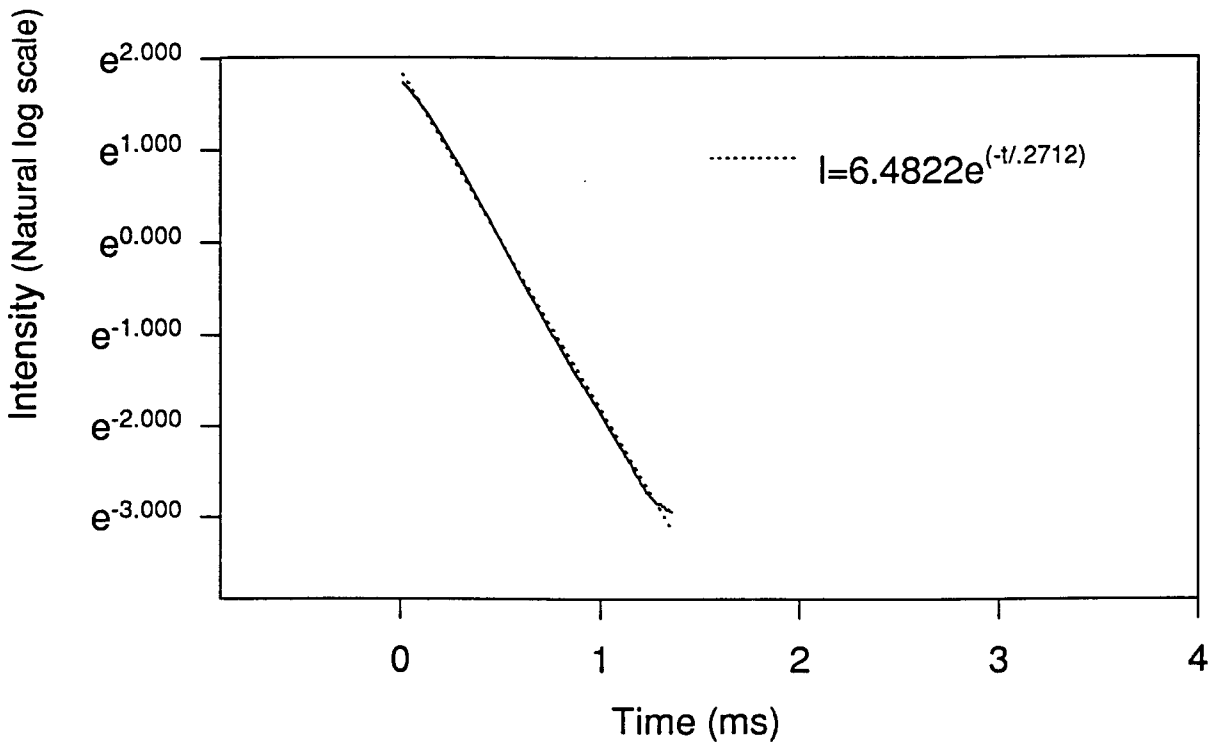


FIGURE 9

Ho:YAIO₃ 543.5 nm Decay Comparison at 175 K

FIGURE 10



Ho:YAIO₃ 662 nm Decay Comparison at 200 K

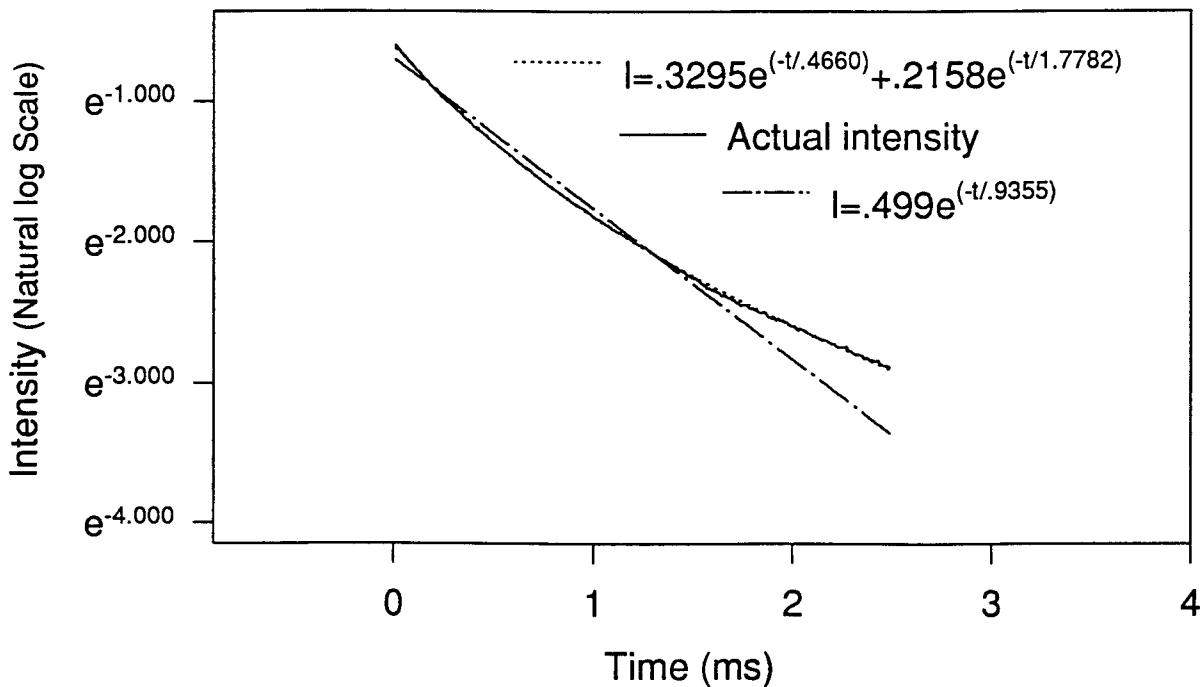


FIGURE 10a

Ho:YAlO₃ Decay Lifetimes vs. Temperature @543.5nm and Constant Power

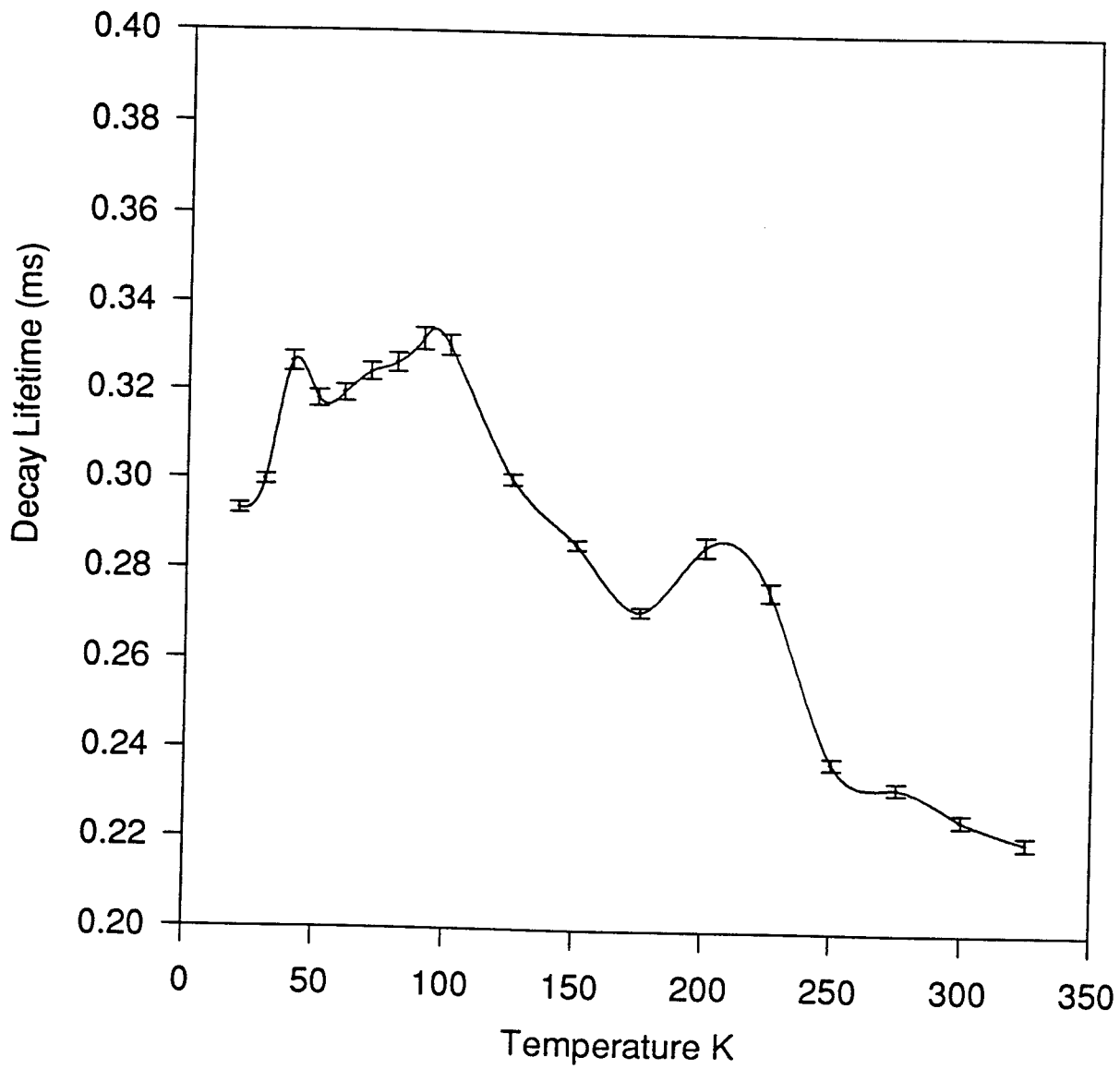


FIGURE 11

Ho:YAIO₃ Maximum Intensity vs. Temperature @543.5nm

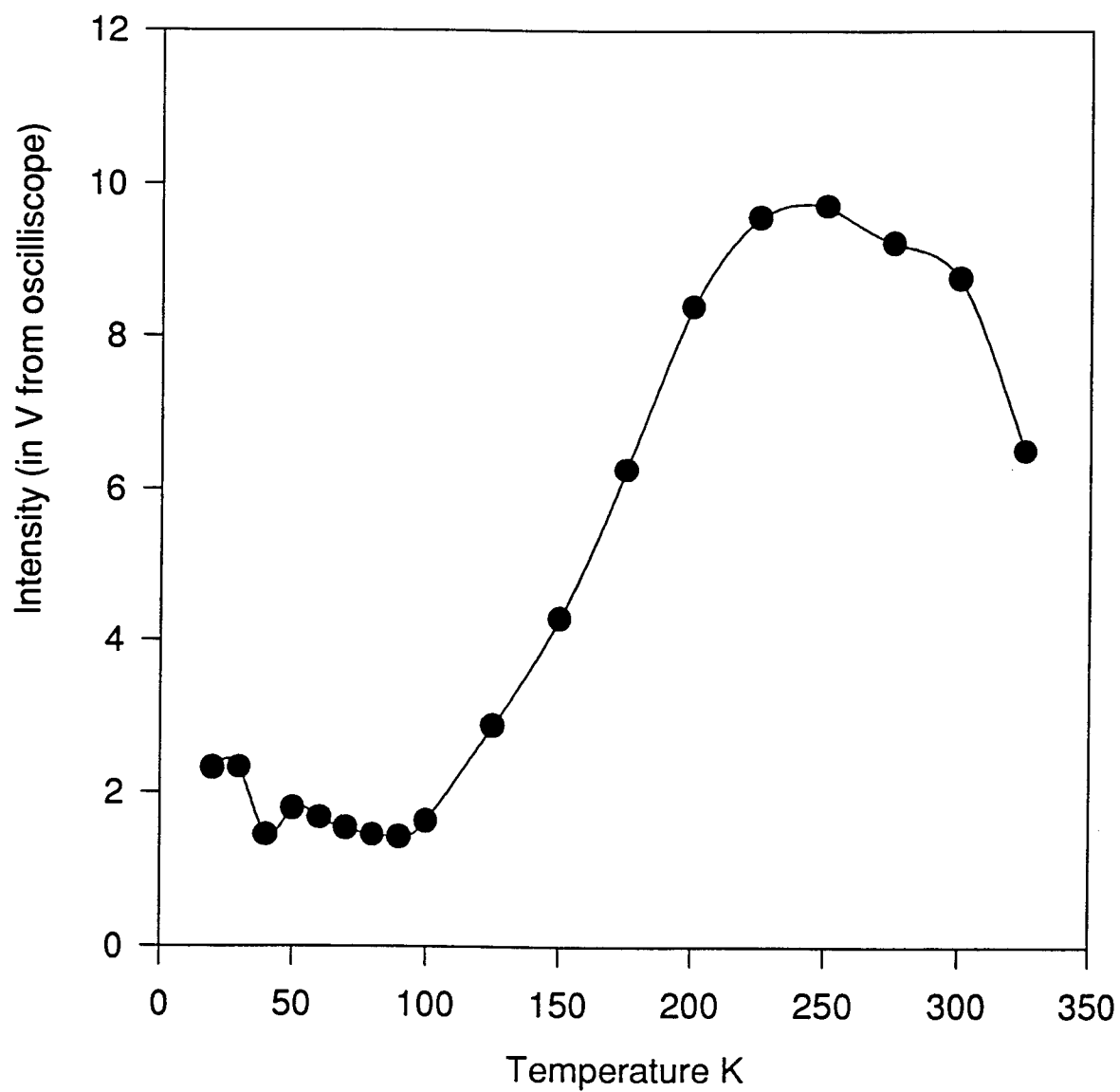


FIGURE 12

References

1. T. Maiman, Nature **187**, p. 493 (1960).
2. B. R. Reddy, S. Nash-Stevenson, P. Venkateswarlu, "Near-infrared-to-blue energy upconversion in $\text{LaF}_3:\text{Ho}^{3+}$," J. Opt. Soc. Am. B **11** 923-927 (1994).

HIGH TEMPERATURE / HIGH SPEED LASER PROJECT

David B. Storch

**Beavercreek High School
2660 Dayton-Xenia Rd
Beavercreek, OH 45434**

**Final Report for:
High School Apprentice Program
Wright Laboratory**

**Sponsored by:
Air Force Office of Scientific Research
Bolling Air Force Base, DC**

and

Wright Laboratory

August 1994

HIGH TEMPERATURE / HIGH SPEED LASER PROJECT

David B. Storch
Beavercreek High School

Abstract

Experiments were conducted into the fabrication of a semiconductor laser device for use in an all-optical backplane. Semiconductor material was grown by Molecular Beam Epitaxy (MBE) and then patterned with an optical lithographic process. Numerous variations in growth procedures and in the patterning process were made to develop a laser that would meet the specified requirements.

HIGH TEMPERATURE / HIGH SPEED LASER PROJECT

David B. Storch

Introduction

Originally motivated by the System Avionics Division (AAA) this project was initiated to fulfill the system requirements for an all-optical Avionics backplane. In a modern day fighter, millions of bits of information are processed every second. Since all this information is vital to the plane's operation, the faster this data can be assimilated, the better. Computer chip technology has reached a point where the chips can process data faster than their connecting wires can transmit. A faster mode of chip to chip communication is thus required. Semiconductor lasers patterned on the chip itself and linked to each other via fiber optics, appears to be the ideal solution. The average semiconductor diode laser (used in compact disc players for example) is not subjected to the harsh environment experienced in a modern fighter. Therefore it is necessary to develop a new laser that can withstand the radical environment. The laser should have a bandwidth of approximately 10 GHz, be capable of uncooled operation at temperatures around 150°C, be able to generate 25 milliwatts of Continuous-Wave optical power, operate for 100,000 hours between failures and above all, have a bit-rate (on/off), fast enough to keep up with the plane's computer.

Problem

Because of the unusual requirements, and small demand, little or no research is being done in the private sector into the area of high temperature/high speed lasers. In order for such research to be done there are two choices: Either pay a company large amounts of money for them to develop a device for which there would

be nearly no commercial market, or conduct all research for such a device in-house. The latter of these two being the most ideal. Unfortunately there were many other problems left to solve. An ideal growth recipe must be found to give the most efficient laser. The optimum laser dimensions must also be decided. A shorter lasing cavity has a faster bit-rate, but a longer cavity provides more gain, which makes it more energy efficient. The width of the cavity varies how the light waves propagate, so an ideal width must also be found. Finally the structure would have to be made out of materials that would not vaporize or delaminate at the extreme operating temperatures. Because there are so many variations to explore, a large number of lasers must be made.

Methodology

Such devices were fabricated on Gallium Arsenide wafers through the use of Molecular Beam Epitaxy (MBE) and optical lithographic procedures. The process begins with a 2" disc of Gallium Arsenide (GaAs). Different layers of material are coated on the GaAs disc to form the basic laser diode structure (fig. 1). The actual lasing cavity is the Indium doped GaAs quantum well.

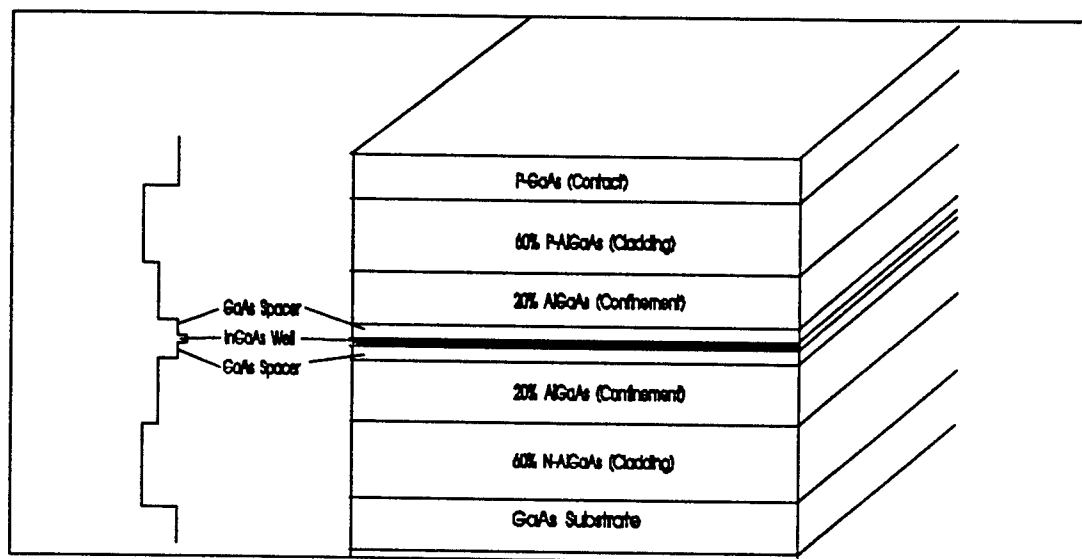


Figure 1 -laser diode structure

When the wafer has completed the growth phase it then goes through a series photolithographic patterning, followed by chemical or plasma etching. All work done on the wafer during the growth and fabrication phase is done by hand in the class 100 cleanroom facility. This unique laboratory, filters all the air until there are fewer than 100 particles .5 microns or larger per cubic foot of air. This allows the devices to be made in a relatively sterile environment. Because all work is done by hand, it can take more than a week to completely fabricate the structures on a single chip.

Once completed the chip is removed from the cleanroom and taken to a different laboratory where, the wafer is scribed and cleaved into multiple bars a few hundred microns in width. Each bar contains dozens of individual laser devices running perpendicular to the cleaved edges (fig. 2). The cleaved edges of the diode act

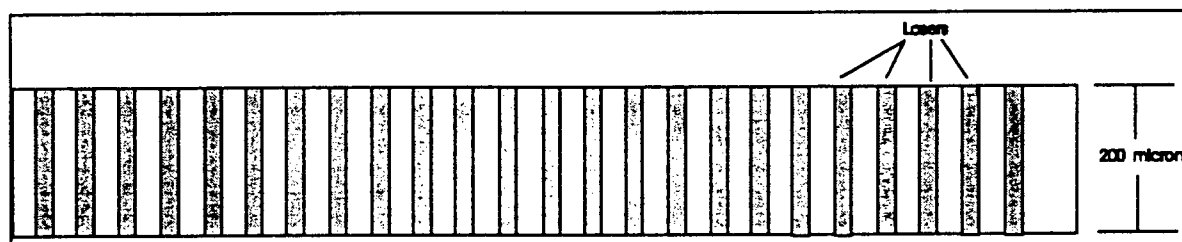


Figure 2 -a single bar from a wafer showing individual laser structures

as the reflecting mirrors for the laser. The difference in the indices of refraction between air and the GaAs creates a set of mirrors that are 30% reflective. Once cleaved, the individual lasers must be tested. A single bar (which may contain up to 40 lasers) is vacuum clamped to a copper block, hooked to the negative terminal of a power supply. A probe tip is gently lowered on to the top surface of a laser. The probe tip is linked to the positive terminal of the power supply. The power supply is connected to a computer. Also connected to the computer is an infra red detector which measures the optical power output from the laser. The computer turns on the power supply and gradually increases the DC current through the diode. The laser light is read by the detector and plotted on a graph in relation to the electrical current (fig. 3). From the graph of the data, it is possible to calculate the threshold current density. This is the point at which the laser "turns on", or begins emitting laser light. Ideally the threshold current density should be a low number, in that it would require less power to activate the laser. Each laser must be tested individually, and in order to get an accurate representation

of the data a large number of lasers must be tested. On a two inch wafer quarter, it is possible to fabricate 10,000 or so lasers, only 300 of these lasers may be tested, but to do so takes the better part of a day. Based on the efficiency and integrity of the laser, as determined by the tests, it is then possible to construct the optimum high temperature / high speed laser.

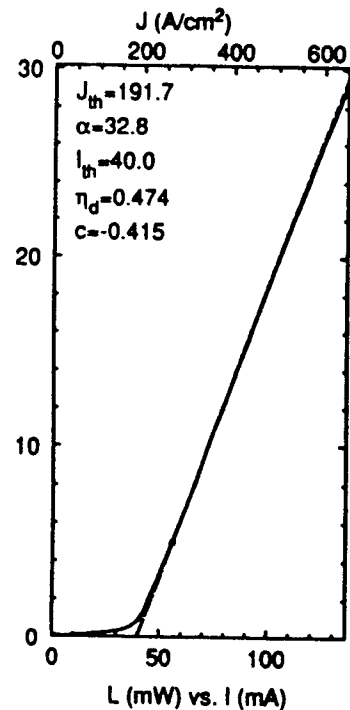


Figure 3 -laser test output

Results

As the experiment is still underway, and probably will be for at least another year there is little data to show. There have been a number of set backs along the way. In addition to the numerous power outages caused by near by construction, there have been problems with the chemical distribution companies as well. The power outages result in lost time as all equipment is reset, and often the spike in the power as it comes back on damages equipment which then costs time and money to repair. To date it, it appears that an ideal growth recipe has been found. A test setup has been devised to evaluate the lasers, and a high-yield cleaving method is in use to isolate the structures. All that remains to be done is to exhaust each experimental variable in order to find the best combination.

Conclusions

Although the finished product is still a ways away early results indicate that the goal is achievable. Only hard work and time will show whether the all-optical backplane is possible.

DYNAMIC TESTING of COMPOSITES

Christopher Sutton
High School Apprentice
Methodology Section

Jefferson High School
2989 South Union Road
Dayton, OH 45418

Final Report For:
High School Apprenticeship Program

Sponsored By:
Air Force Office of Scientific Research
Bolling Air Force Base, Washington DC

August 1994

DYNAMIC TESTING of COMPOSITES

Christopher Sutton
High School Apprentice
Jefferson High School

Abstract

During my apprenticeship data was collected from targets that were tested at a gun range to see how different structural composites react to various weapons. The resulting damage to the composites was recorded in pictures and Cscans. Over 650 composites were tested. Part of my responsibility was to accumulate and record the new data and make sure everything was correct. This gave me access to new tools, state of the art technology and software, an engineering atmosphere, and an experience unique to any high school student in the world. It was an honor to participate in this apprenticeship program.

DYNAMIC TESTING of COMPOSITES

Christopher Sutton

The Flight Dynamics Directorate at Wright Patterson Air Force Base frequently tests composite panels ballistically. The composite panels simulate materials on aircraft and other military vehicles currently in use. It is important to test composites so that the vulnerability of these vehicles can be determined accurately and then minimized. By using the data that the Flight Dynamics Directorate accumulates, new military vehicles will gradually become less vulnerable in any given compact situation.

Wright Patterson Air Force Base has four highly equipped gun ranges scattered around the base. One of the gun ranges has engines that help to simulate airflow before a target is shot at. The ranges have many different types of guns that are used to simulate enemy weapons.

Before testing occurs the composite panel and the projectile are weighed and measured so that after the shot comparisons can be made. The panel is tagged so everything can be identified after impact. The composite panels are shot at with various projectiles. Almost everything that happens during a test shot is recorded. Impact and residual velocities are recorded by various sensors set up before the shot. Cameras precisely record the action that the human eye might miss. The cameras help to show the length and size of fireballs that occur when the projectile impacts the composite.

After the shot, lots of data is ready to be recorded. If the projectile scatters when it hits the panel, all of the individual pieces are collected and weighed. The panel is retrieved and ready for measurements to be taken. The visual damage is what you can see. Calipers are used to determine the dimensions of the area that is damaged on the panel. But visual damage is not enough. Each panel must be Cscanned to see the damage that is not seen by the human eye. The damage that the Cscan shows can be seen by using an image analysis program from which measurements can be taken. Every panel and

projectile is photographed at a high tech photography studio located on the base. The cameras in this studio can accurately record the damage digitally or on film for later use. By reviewing the data from past shots the next test shot can almost be predicted.

All of the information that was recorded before and after the test shots are recorded in a database. When reviewing the shots on the database sometimes patterns can be found. This helps to determine valuable equations and theories that are used in the future.

This apprenticeship was a valuable way to continue my education after school. I also learned many things that I would not have learned in high school. I was taught how to use powerful software packages and use scientific tools. I was also introduced to an engineering atmosphere that is lacking in a school setting. The people at the Flight Dynamics Directorate took the time to explain to me what they were doing and how to use their equipment.

THOMAS R. SUTTON

REPORT

UNAVAILABLE

Development and Testing of a Two-Dimensional Finite Element Hydrocode

Randy Thomson
High School Apprentice

WL/MNSA
Eglin Air Force Base, Florida

Final Report for:
High School Apprenticeship Program
Wright Laboratory/Armament Directorate

Sponsored by: Air Force Office of Scientific Research
Bolling Air Force Base, Washington, D.C.

August 1994

Development and Testing of a Two-Dimensional Finite Element Hydrocode

Randy Thomson

High School Apprentice

Abstract

One of the tasks of Wright Labs Armament Directorate, including MNSA, is to design and improve hydrocodes for use in modeling a variety of impact phenomena. One of the main ways that this is accomplished is by adding new material models, failure models, and equations of state. Normally, these models under development must be inserted into a large hydrocode such as EPIC for examining the models' validity. However, this has inherent difficulties. The sheer size, modularization, vectorization, and similar attributes of the EPIC hydrocode make this problematic. Additionally, the EPIC architecture was made highly parallel, which leads to greater efficiency on vectorized supercomputers, but efficiency is drastically reduced when the program is run on a computer of lesser power that is not highly parallel. In fact, it is incredibly difficult and sometimes impossible to run these programs on a x86 personal computer. A need was seen for a smaller, simpler, portable, user-friendly and easily customizable program to use in testing new models. During the summer of 1994, research was conducted to fulfill these requirements, and the resulting hydrocode is the basis for this report.

Development and Testing of a Two-Dimensional Finite Element Hydrocode

Randy Thomson

BACKGROUND

One of the tasks of Wright Labs Munitions Division, including MNSA, is to design and improve hydrocodes for use in modeling a variety of impact phenomena. One of the main ways that this is accomplished is by adding new material models, failure models, and equations of state to existing hydrocodes. Normally, these models under development must be inserted into a large hydrocode such as EPIC (Elastic-Plastic Impact Code) for examining the models' validity. However, this has inherent difficulties. The EPIC hydrocode is huge, consisting of approximately 100,000 lines of code. This sheer size makes it difficult to find the desired subroutine for modification. Also, EPIC is modular, that is, broken into a number of subroutines, each of which may contain one or more subroutines, and so on. Errors in one subroutine will propagate through all of the other subroutines in a highly nonlinear fashion, which can make it difficult to change one subroutine of a hydrocode. Additionally, the recent versions of EPIC have been made highly vectorized and parallel. In vectorization, the program is broken down into many small blocks, which are then executed in parallel. This makes it difficult to go into the code and obtain a holistic view of the problem at any point in time. This also makes loops very difficult to follow, because the vectorization makes many of the loops no longer linear. While this parallelization makes the EPIC architecture highly efficient on vectorized machines such as a Cray Y-MP, efficiency is drastically reduced when the program is run on a computer of lesser power, such as a one- or two-processor Silicon Graphics workstation that is not highly parallel. In fact, it is incredibly difficult and sometimes impossible to run these programs on common machines such as a x86 personal computer. A need was seen for a smaller, simpler, portable, user-friendly and easily customizable program to use in testing new models. Thus this researcher worked on the development of a hydrocode that would meet these needs.

2D-FLASH-OVERVIEW

2D-FLASH, or Two Dimensional Finite Element Lagrangian Axisymmetric Hydrocode, is the resulting hydrocode. The program was limited to two-dimensions to increase computational speed and efficiency.

However, instead of a plane strain model, in which a two-dimensional slice of a problem is modeled, an axisymmetric model was used for 2D-FLASH. An axisymmetric model, as used in this code, allows any three-dimensional problem with symmetry around a single axis to be modeled as a two-dimensional problem without significant loss of accuracy. Instead of modeling the problem in Cartesian rectangular coordinates (xyz space), 2D-FLASH models the problem in cylindrical coordinates ($r\theta z$ space), with r and z being defined by the problem and calculation based on an implicit rotation of this 2-D slice about the z axis. A Lagrangian finite element formulation was chosen to allow for enhanced material models and to increase computational efficiency. Two basic categories of hydrocodes exist, Lagrangian and Eulerian, plus various hybrid codes intermediate between the two formulations. The basic premise of a finite element code is to create a finite grid to overlay the computational region of interest. The problem is only considered at the vertices of the grid, or nodes, and in the grid spaces themselves treated as units, or elements. Thus, calculations made at one point in space are allowed to represent an entire region, sometime with polynomial interpolation to smooth the functions of interest between nodes. Lagrangian codes define the material and mass of nodes and elements and then allow the elements and nodes to move as stresses are applied. This models the problem by mesh deformation and preserves material boundaries, for material is not allowed to flow between cells. This is in contrast to Eulerian codes, which leave the mesh fixed in space, but allow the materials to flow between mesh cells according to conservation equations. This models the problem by material deformation and motion independent of the fixed mesh. Material boundaries quickly become obscure and are measured by mixed material cells intermediate between cells on either side of the boundary. This makes Eulerian codes inherently superior for codes where there will be large material deformation and extensive material mixing, such as hypervelocity impacts involving melting and/or vaporization. However, this can cause nonphysical effects, such as mixing of materials at much lower velocities in the plastic deformation range. Advection routines exist in Eulerian codes to reduce this problem, but Eulerian codes are still inferior in this regime. On the other hand, this is the regime where Lagrangian codes excel. Maintaining explicit material conservation and material boundaries, as well as the capability of including element load history effects

and a wide range of sophisticated fracture, failure, and fragmentation models, makes Lagrangian codes ideal for problems in the elastic and plastic regimes. Because this is the regime that these new material models were needed for, a Lagrangian code was chosen. However, this particular type of finite element code as used in this project, like EPIC, is different from many past finite element codes. Past finite element codes were limited to static boundary value problems. They were normally not intended for advancement through time. This created difficulties when the problem needed to be advanced in time and nonlinearities or discontinuities were involved (such as across a shock propagating through a material) due to the iterative nature required for convergence with this solution technique. 2D-FLASH, like EPIC and several other recent finite element codes, is different. In this code, the problem is meshed and divided into many regions, but the conservation equations and related equations governing the problem are explicitly integrated in time, bringing in aspects of a finite differencing scheme. This increases accuracy and efficiency and allows the problem to be advanced forward in time, one increment at a time. Also, with a correctly defined initial mesh and correct explicit equations applied to individual elements and nodes, there is no need for repeated iteration at each time step for the mesh to accurately represent the solution at that point in time.

TRAINING

First, understanding of hydrocode methods was enhanced by studying a short course in hydrocode design and by researching various numerical methods schemes for background on their application to hydrocodes. Course notes for a short course in penetration mechanics were also studied for further insight into the theoretical background involved. Experiments were done to model simple partial differential equations through a variety of differencing schemes to gain further understanding of hydrocode techniques. Finally, study and experiments were conducted with a greatly simplified one dimensional finite element hydrocode, based on simplified routines taken from EPIC, provided by Dr. William Cook of WL/MNMW. This allowed examination of a primitive working hydrocode and its structure. With this established knowledge base for the task at hand, the code development proper could begin.

2D-FLASH CODE STRUCTURE

2D-FLASH begins with a simple dimensioning of arrays to set aside storage space for the variables needed in the solution of the problem. Next is the material data section, that contains all of the necessary parameters for modeling materials in the code. Additional materials may be added fairly easily by adding extra data lines in this section. After the material database, the code interactively reads in the necessary parameters to set up the problem from standard input. Next is the mesh generation routine that creates the nodes and elements for use in the problem. The nodes are set up in a crossed triangle configuration through a simple iterative procedure. After the nodes have been placed in the appropriate positions, the nodes are written into an array that associates global nodes with local nodes of elements. Once the mesh has been generated, the mesh is then initialized; that is, masses and velocities are assigned to the nodes and appropriate parameters assigned to the elements. First an element loop is set up. The initialization process begins by calculating twice the area of the element under consideration:

$$2A = \begin{vmatrix} 1 & x_1 & y_1 \\ 1 & x_2 & y_2 \\ 1 & x_3 & y_3 \end{vmatrix}$$

The radius from the axis of symmetry to the centroid of the element is then calculated:

$$\bar{r} = \frac{x_1 + x_2 + x_3}{3}$$

The initial volume of the element under consideration is found by a theorem of Pappus to be:

$$V_0 = 2\pi\bar{r}A$$

In a finite element hydrocode, elements are treated as if they have all of their masses concentrated at the nodes. To perform this, the mass of element is apportioned as follows:

$$m_{1i} = m_{1i} + \rho_i V_i \frac{\frac{1}{4} + x_{1i}}{12 \bar{r}_i}$$

$$m_{2i} = m_{2i} + \rho_i V_i \frac{\frac{1}{4} + x_{2i}}{12 \bar{r}_i}$$

$$m_{3i} = m_{3i} + \rho_i V_i \frac{\frac{1}{4} + x_{3i}}{12 \bar{r}_i}$$

Next, the initial velocities and boundary conditions are assigned to the nodes. The nodes are assigned their user-defined initial velocity in the y direction, unless a boundary has been violated, in which case the node is placed on the boundary and the component of the velocity normal to the boundary is zeroed. Finally, the initial kinetic energy is calculated for comparison with later steps.

$$E_k = \sum_{i=1}^{\# \text{ of nodes}} \frac{m_i v_i^2}{2}$$

Having completed the initialization loop, the main loop begins, which will be iterated once per time step until the final time is reached. First, the program checks to see if it is time to output information. If this check is true, a header is printed to standard output and state plot information is written to a file. After the data has been output if necessary, the program checks to see if a problem stop time has been reached; that is, if the desired amount of time has elapsed, if the minimum time step for stability has excessively degenerated, or if an energy check indicates instability. If this is true, then the program jumps to the ending routine. Otherwise, the nodal, or equations of motion loop, is begun. Velocities and displacements are updated using basic principles:

$$\begin{aligned}\dot{x}_i &= \dot{x}_i + \frac{F_{x_i} \cdot d\bar{t}}{m_i} \\ \dot{y}_i &= \dot{y}_i + \frac{F_{y_i} \cdot d\bar{t}}{m_i} \\ x_i &= x_i + \dot{x}_i \cdot dt \\ y_i &= y_i + \dot{y}_i \cdot dt\end{aligned}$$

Next, the boundaries are checked. If any node violates a boundary as a result of this displacement, the node is placed on the boundary and the component of the velocity in the direction of the boundary zeroed. Next, the kinetic energy is updated based on the new velocities:

$$E_k = \sum_{i=1}^{\text{\# of nodes}} \frac{m_i v_i^2}{2}$$

Then the radius to the centroid, twice the area of the element, and current volume are updated as before:

$$\begin{aligned}2A &= \begin{vmatrix} 1 & x_1 & y_1 \\ 1 & x_2 & y_2 \\ 1 & x_3 & y_3 \end{vmatrix} \\ \bar{r} &= \frac{x_1 + x_2 + x_3}{3} \\ V &= 2\pi\bar{r}A\end{aligned}$$

Volumetric strain, alternative volumetric strain, and volumetric strain rate are then calculated:

$$\begin{aligned}\varepsilon &= \frac{V}{V_0} - 1 \\ \mu &= \frac{-\varepsilon}{\varepsilon + 1} \\ \dot{V} &= \frac{\varepsilon_{t+1} - \varepsilon_t}{dt}\end{aligned}$$

After calculating the volumetric strain rate, the average volumetric strain is calculated using the formula:

$$\bar{\epsilon} = \epsilon - \frac{\dot{V} \cdot dt}{2}$$

Next, a series of geometric constants is calculated. These geometric constants are equal to the projections of the lengths of the sides of the element triangle onto the x and y coordinate axes:

$$b_i = y_1 - y_3$$

$$b_j = y_3 - y_2$$

$$b_m = y_2 - y_1$$

$$c_i = x_3 - x_1$$

$$c_j = x_2 - x_3$$

$$c_m = x_1 - x_2$$

For stability purposes, the minimum altitude of the element triangle must be determined. This is accomplished by means of the following formula:

$$l_j = b_j^2 + c_j^2$$

$$l_m = b_m^2 + c_m^2$$

$$h_{\min} = \frac{2A}{\sqrt{\max(l_1, l_2, l_3)}}$$

Next is one of the most critical sections of the code. The strain rates in each direction are calculated by using the geometric constants defined earlier and the velocities of the nodes:

$$\dot{\epsilon}_x = \frac{b_i \cdot \dot{x}_2 + b_j \cdot \dot{x}_1 + b_m \cdot \dot{x}_3}{2A}$$

$$\dot{\epsilon}_y = \frac{c_i \cdot \dot{y}_2 + c_j \cdot \dot{y}_1 + c_m \cdot \dot{y}_3}{2A}$$

$$\dot{\gamma}_{xy} = \frac{b_i \cdot \dot{y}_2 + b_j \cdot \dot{y}_1 + b_m \cdot \dot{y}_3 + c_i \cdot \dot{x}_2 + c_j \cdot \dot{x}_1 + c_m \cdot \dot{x}_3}{2A}$$

$$\dot{\epsilon}_z = \frac{\dot{x}_1 + \dot{x}_2 + \dot{x}_3}{3\bar{r}}$$

Having calculated these strain rates, the average normal strain rate is calculated, and then this result is used to find the strain rate deviators. These deviators are then used to find the equivalent strain rate and then the plastic strain is updated based on the previous plastic strain rate.

$$\begin{aligned}\bar{\dot{\epsilon}}_1 &= \frac{\dot{\epsilon}_x + \dot{\epsilon}_y + \dot{\epsilon}_z}{3} \\ \dot{\epsilon}_x &= \dot{\epsilon}_x - \bar{\dot{\epsilon}}_1 \\ \dot{\epsilon}_y &= \dot{\epsilon}_y - \bar{\dot{\epsilon}}_1 \\ \dot{\epsilon}_z &= \dot{\epsilon}_z - \bar{\dot{\epsilon}}_1 \\ \dot{\epsilon} &= \sqrt{\frac{2}{9} \left((\dot{\epsilon}_y - \dot{\epsilon}_x)^2 + (\dot{\epsilon}_y - \dot{\epsilon}_z)^2 + (\dot{\epsilon}_x - \dot{\epsilon}_z)^2 + \frac{3}{2} (\dot{\gamma}_{xy})^2 \right)} \\ \bar{\epsilon}^{t+1} &= \bar{\epsilon}^t + \dot{\epsilon}_p^t \cdot dt\end{aligned}$$

The average normal stress is calculated, and used to determine the previous deviator stresses in a manner analogous to the calculations for the strain rates:

$$\begin{aligned}\bar{\sigma}_1 &= \frac{\sigma_x + \sigma_y + \sigma_z}{3} \\ S_y &= \sigma_y - \bar{\sigma}_1 \\ S_x &= \sigma_x - \bar{\sigma}_1 \\ S_z &= \sigma_z - \bar{\sigma}_1\end{aligned}$$

The actual temperature is calculated based on internal energy, and then used to calculate the dimensionless homologous temperature:

$$\begin{aligned}T &= T_1 + \frac{E_i}{C\rho} \\ T^* &= \frac{T - T_{room}}{T_{melt} - T_{room}}\end{aligned}$$

The maximum flow stress is then calculated based on the Johnson-Cook constitutive model, ignoring thermal softening, but including work hardening:

$$\sigma_{\max} = [A + B\varepsilon^n] [1 + C \ln(\dot{\varepsilon}^*)]$$

If thermal softening is included for the material under consideration, the flow stress is revised to account for thermal softening:

$$\sigma_{\max} = \sigma_{\max} (1 - T^{*m})$$

If the calculated maximum flow stress is less than zero, it is set to zero, making the material behave like a fluid. Next trial stress deviators and shear terms are calculated based on strain rate data:

$$S_x^{t+\Delta t} = S_x^t + 2G\dot{\varepsilon}_x \cdot dt$$

$$S_y^{t+\Delta t} = S_y^t + 2G\dot{\varepsilon}_y \cdot dt$$

$$S_z^{t+\Delta t} = S_z^t + 2G\dot{\varepsilon}_z \cdot dt$$

$$\tau_{xy}^{t+\Delta t} = \tau_{xy}^t + G\dot{\gamma}_{xy} \cdot dt$$

The Von Mises maximum flow stress is calculated:

$$\bar{\sigma} = \sqrt{\frac{3}{2} [(S_x)^2 + (S_y)^2 + (S_z)^2] + 3(\tau_{xy})^2}$$

If the Von Mises maximum flow stress is exceeded, the material will flow plastically, and the deviator and shear stresses must be decreased proportionally so the Von Mises flow stress equals the previously calculated maximum flow stress:

$$\beta = \frac{\sigma_{\max}}{\bar{\sigma}}$$

$$S_y = \beta \cdot S_y$$

$$S_x = \beta \cdot S_x$$

$$S_z = \beta \cdot S_z$$

$$\tau_{xy} = \beta \cdot \tau_{xy}$$

Next, the internal energy from stresses must be accounted for, so the internal energy is calculated based on the previous cycle's stresses.

$$E_{dev} = \frac{[(\sigma_x + S_x) \cdot \dot{\epsilon}_x + (\sigma_y + S_y) \cdot \dot{\epsilon}_y + (\sigma_z + S_z) \cdot \dot{\epsilon}_z + (\tau_{xy} + S_{xy}) \cdot \dot{\gamma}_{xy}] \cdot (1 + \bar{\epsilon}) dt}{2}$$

2D-FLASH now converts the strain rates into plastic strain rates, calculates the equivalent plastic strain rate, and updates the plastic strain.

$$\dot{\epsilon}_{xp} = \dot{\epsilon}_x - \frac{S_x - \sigma_x}{2Gdt}$$

$$\dot{\epsilon}_{yp} = \dot{\epsilon}_y - \frac{S_y - \sigma_y}{2Gdt}$$

$$\dot{\epsilon}_{zp} = \dot{\epsilon}_z - \frac{S_z - \sigma_z}{2Gdt}$$

$$\dot{\gamma}_{xyp} = \dot{\gamma}_{xy} - \frac{\tau_{xy} - \sigma_{xy}}{Gdt}$$

$$\dot{\epsilon}_p = \sqrt{\frac{2}{9} \left((\dot{\epsilon}_{yp} - \dot{\epsilon}_{xp})^2 + (\dot{\epsilon}_{yp} - \dot{\epsilon}_{zp})^2 + (\dot{\epsilon}_{xp} - \dot{\epsilon}_{zp})^2 + \frac{3}{2} (\dot{\gamma}_{xyp})^2 \right)}$$

$$\bar{\epsilon}^{t+1} = \bar{\epsilon}^t + \dot{\epsilon}_p \cdot dt$$

For purposes of the artificial viscosity and the Courant time step routine, the square of the sound speed must be calculated for the material using the current condition of strain and variables solved for in the the Mie-Gruneisen equation of state routine.

$$c^2 = \frac{K_1(1 - \Gamma\mu) + K_2 \left(2\mu - \frac{3}{2}\mu^2 \right) + K_3(3\mu^2 - 2\mu^3) + E_i\Gamma + \frac{\Gamma|\bar{\sigma}_\perp|}{1 + \mu}}{\rho_0}$$

if $\mu < 0$:

$$c^2 = \frac{K_1 + E_i\Gamma + \Gamma|\bar{\sigma}_\perp|}{\rho_0}$$

To spread the shock across several zones to maintain the accuracy of the calculation an artificial viscosity routine is needed. A combination of quadratic and linear artificial viscosity is used to reduce numerical oscillations.

$$Q = Q_2 \rho_0 (1 + \mu) [h_{\min} \dot{V} (1 + \mu)]^2 - Q_1 \rho_0 (1 + \mu)^2 c \cdot h_{\min} \dot{V}$$

if $\dot{V} \geq 0$:

$$Q = 0$$

Next is the equation of state routine. A Mie-Gruneisen equation of state is used and trial values are used to solve the simultaneous equations. There are two different routines, based on whether the volumetric strain is positive or negative. In the case of volumetric strain greater than or equal to zero:

$$P_{\text{trial}} = (K_1 \mu + K_2 \mu^2 + K_3 \mu^3) \left(1 - \frac{\Gamma \mu}{2}\right)$$

$$E_{\text{new}} = \frac{E_{\text{old}} + \frac{\bar{\sigma}_1 - P_{\text{trial}} - Q}{2} \dot{V} dt + E_{\text{dev}}}{1 + \frac{\Gamma(1 + \mu) \dot{V} dt}{2}}$$

$$P = P_{\text{trial}} + \Gamma E_i (1 + \mu)$$

If volumetric strain is less than zero and pressure is greater than P_{\min} :

$$P_{\text{trial}} = K_1 \mu \left(1 - \frac{\Gamma \mu}{2}\right)$$

$$E_{\text{trial}} = \frac{E_{\text{old}} + \frac{\bar{\sigma}_1 - P_{\text{trial}} - Q}{2} \dot{V} dt + E_{\text{dev}}}{1 + \frac{\Gamma(1 + \mu) \dot{V} dt}{2}}$$

$$P = P_{\text{trial}} + \Gamma E_{\text{trial}} (1 + \mu)$$

If, instead, volumetric strain is less than zero and P_{\min} has been exceeded:

$$P = P_{\min}$$

$$E_{\text{new}} = E_{\text{old}} + \frac{\bar{\sigma}_{\perp} - P - Q}{2} \dot{V} dt$$

Now the total normal stresses must be recalculated and the stresses must be transformed from deviators into total stresses:

$$\bar{\sigma}_{\perp} = -P - Q$$

$$\sigma_x = S_x + \bar{\sigma}_{\perp}$$

$$\sigma_y = S_y + \bar{\sigma}_{\perp}$$

$$\sigma_z = S_z + \bar{\sigma}_{\perp}$$

To maintain stability in this computational scheme, the time step must not exceed a certain value. The modified Courant stability criterion is used:

$$B_2 = \frac{Q_2 \cdot Q}{\rho_0(1 + \mu)}$$

$$dt_{\text{Courant}} = k \left(\frac{h_{\min}}{\sqrt{B_2} + \sqrt{B_2 + c^2}} \right)$$

If this determined time step is less than the currently set next time step, the time step is forced to comply with the Courant condition. Before the forces can be updated, the hoop stress must be calculated:

$$\sigma_{\text{hoop}} = \frac{-2\pi A \sigma_z}{3}$$

Now the forces on each local node of the current element must be updated. The stresses are combined with the geometric constants to obtain components of the force in both the x and y directions:

$$\begin{aligned}
F_{x1} &= F_{x1} - \pi \bar{r} (b_j \cdot \sigma_x + c_j \cdot \tau_{xy}) + \sigma_{hoop} \\
F_{x2} &= F_{x2} - \pi \bar{r} (b_i \cdot \sigma_x + c_i \cdot \tau_{xy}) + \sigma_{hoop} \\
F_{x3} &= F_{x3} - \pi \bar{r} (b_m \cdot \sigma_x + c_m \cdot \tau_{xy}) + \sigma_{hoop} \\
F_{y1} &= F_{y1} - \pi \bar{r} (c_j \cdot \sigma_y + b_j \cdot \tau_{xy}) \\
F_{y2} &= F_{y2} - \pi \bar{r} (c_i \cdot \sigma_y + b_i \cdot \tau_{xy}) \\
F_{y3} &= F_{y3} - \pi \bar{r} (c_m \cdot \sigma_y + b_m \cdot \tau_{xy})
\end{aligned}$$

Finally, the total energy is incremented, closing the element loop.

$$E_{tot} = E_{tot} + E_i \cdot V_0$$

Before the next time step begins, the code internally reorganizes itself to prepare for the next time step. The last time step is set equal to the current time step, the cycle counter is incremented, time is incremented, and the new time step is set. If the new time step is greater than the limiting maximum time step size, the time step is set to the maximum time step size. The time integration loop finally repeats. After one of the flags at the beginning of the time integration loop has been set to true, the program jumps to the final routine. An appropriate message is written to standard output, and a final state plot is written to a file. The program then ends.

USERS GUIDE TO 2D-FLASH

If you are not working with a compiled version of the code, begin by compiling the code. 2D-FLASH is written in standard FORTRAN 77 and uses no extensions, so the code is highly portable. Set the compiler and linker to the highest level of optimization that functions on your system. For the Silicon Graphics UNIX f77 compiler this program was developed on, syntax would be:

```
f77 -O3 -mips2 -o 2D-FLASH 2D-FLASH.f
```

or

```
f77 -O2 -o 2D-FLASH 2D-FLASH.f
```

If you run 2D-FLASH in another environment with a different compiler, check the manual for your compiler to find the syntax for higher levels of optimization. The increased computational speed and efficiency should be well worth it.

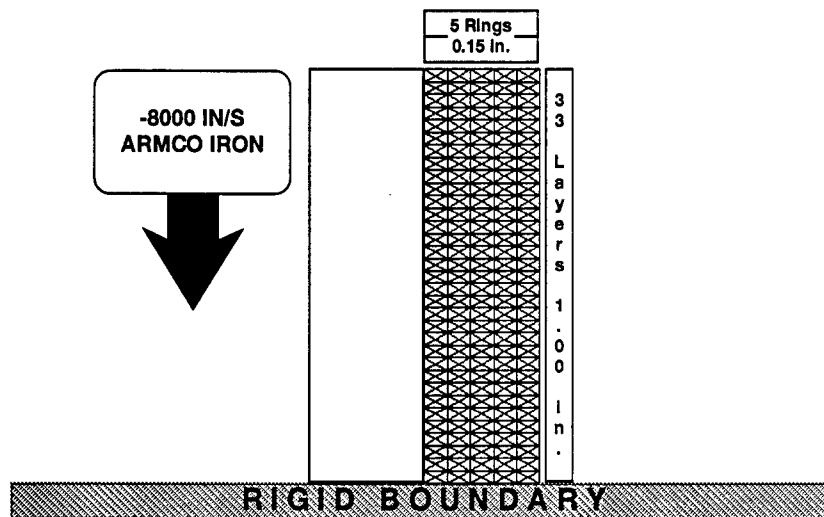
Once the code is compiled, execute 2-DFLASH. The program will ask for a series of parameters from standard input. For batch execution, you can create a script file with the appropriate parameters and redirect it to 2D-FLASH:

```
2D-FLASH < your_file_name
```

First, the program will ask for the radius of the cylindrical projectile, in inches. Next 2D-FLASH will ask for the length of the projectile, also in inches. The program will then ask for the number of layers and rings, respectively. This is for determining the mesh resolution for the problem. See the diagram for an example of layers and rings. The program will then ask for material type by number. The currently supported materials are OFHC copper, ARMCO iron, and 2024-T351 aluminum. Other materials may be added by simply updating the materials database. Next, the program will ask for the initial velocity of the projectile. This velocity should be in inches per second and must be negative, due to the coordinate system as currently set up. A non-negative velocity will never impact the boundary. 2D-FLASH then requests the shock speed factor for the time step. This is the factor on the Courant condition as mentioned earlier. This factor must be positive for convergence and less than or equal to one for stability. Increased accuracy and smoother time history curves are generally achieved with smaller factors. 0.9 is a sufficient value for most problems; however, 0.5 produces smoother curves in particularly noisy problems. Experiment with this factor to optimize the program for the task at hand. 2D-FLASH will then ask for the time to run the simulation out to, provided other factors do not prematurely end the simulation. Values are multiplied by 10^{-6} in the code, so enter "50" to run the problem out to 50 microseconds. The program will next ask for the time interval for printing, also in

microseconds. State plot data will be output at this time, as well as a header showing the status of the problem. Finally, the code asks for a time to begin printing, also in microseconds. Usually, this is set to zero, but in some circumstances where late time effects are of importance, a later time may be desired.

Figure 46-1



USERS GUIDE TO THE 2D-FLASH POST-PROCESSOR

2D-FLASH creates an output file called "meshplot.out." This file is for use with the 2D-FLASH postprocessor, MESHPlot. MESHPlot is a routine written in Microsoft QBasic for use on an MS-DOS personal computer. The MESHPlot source code can also be compiled with QuickBasic for increased computational efficiency. To run the post-processor, you must have meshplot.out and MESHPlot in the same directory. The program will then ask for the number of cycle dumps. This is the number of frames the program is to read from the input file. The total number of frames in the file is equal to [maximum computation time/printing time step] + 1. The program will then ask what type of plot is requested. Plots of pressure, internal energy, and Von Mises stress are available, as well as blank mesh plots, useful for simply watching projectile information. The program will then display a series of mesh plots. The color scales are modified logarithmic scales, as can be seen by examining the code. On the

legend, values corresponding to colors increase from bottom to top. To get another plot, simply rerun the program. The sample plot above is an annotated and modified version of a MESH PLOT graph.

PROCEDURES AND RESULTS

Once 2D-FLASH was completed and in good working order, it was time to benchmark the code against a known entity. The 1992 research version of the EPIC hydrocode was chosen due to its extensive validation and ready availability. EPIC example problem 2 was chosen and the input files modified to correspond with the algorithms in place for 2D-FLASH. A series of time history plots was created using the POST2 postprocessor for EPIC and Microsoft Excel for 2D-FLASH. As can be determined from the sample graph, there is excellent correlation between the two curves. Similar results were obtained for the other time history plots. The projectile deformation, as compared with state plots in both MESH PLOT for 2D-FLASH and POST1 for EPIC, also showed excellent correlation. This was to be expected, but the real proof was in the computational efficiency comparisons. For both example 2 and a similar problem that merely quadrupled the number of elements, there was more than a fivefold decrease in elapsed time between 2D-FLASH and EPIC. This showed that 2D-FLASH was indeed living up to its expectations of being fast running and accurate.

Figure 46-2

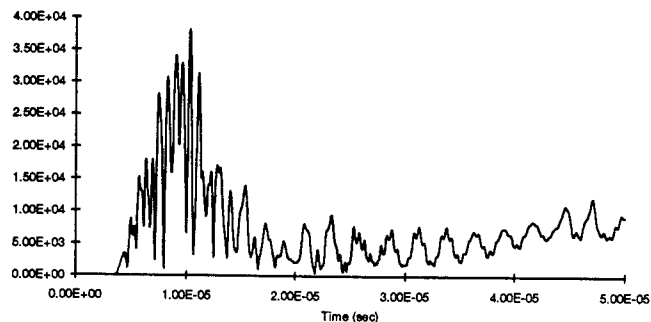
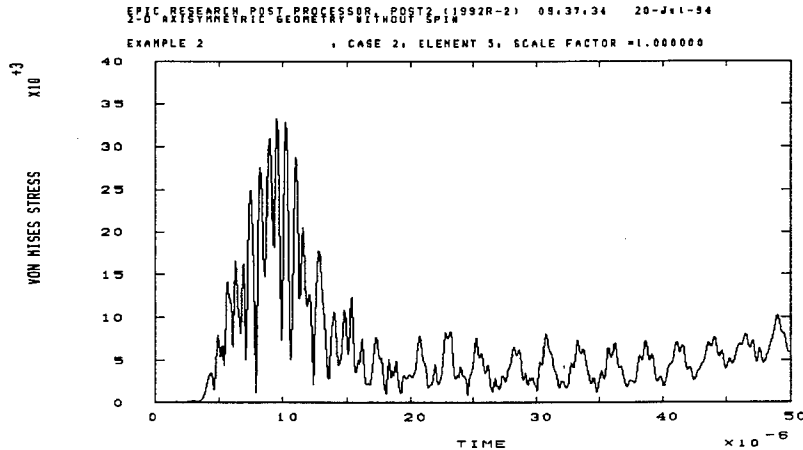


Figure 46-3



CONCLUSIONS

On the basis of the results of this summer's research, it would seem that if used properly, 2D-FLASH in its present incarnation does fulfill many of its design requirements. It is very fast running compared to EPIC, and with appropriate parameters, gives accurate results. It provides a simple post-processing capability with MESH PLOT, which allows a user to see the effects of new material models being tested. It is much shorter than EPIC (<900 lines of code, including MESH PLOT, versus 80,000 for the EPIC92 code and 110,000 for EPIC94), having no unneeded routines to slow the computations down. The biggest problem is lack of a multi-material algorithm incorporating slidelines, for modeling collisions between two nonrigid bodies. The author is currently finishing a more sophisticated version of the code, where this option is implemented, along with additional materials to choose from. In the meantime, 2D-FLASH gives a useful shell for the design and implementation of new material models, is fast running compared to EPIC, and is much more user customizable due to the decreased code length. It should only improve as further experimentation is performed with it.

ACKNOWLEDGEMENTS

The author would like to thank Research & Development Laboratories (RDL) for sponsoring this program and the Wright Laboratory/Armament Directorate for serving as a host site for the 1994 HSAP. Thanks are also in order for Mr. Don Harrison, Mr. Mike Deiler, and Ms. Glenda Apel for running the local aspects of the program smoothly. This project could not have been accomplished without Mr. Bruce Patterson, who served as a mentor for the author and provided guidance for the past two summers. These people also gave assistance from a supervisory perspective: Lieutenant Colonel Paul Coutee; MNSA Branch Chief, Mr. Ron Hunt and Mr. John Bailey; MNSA Section Chiefs, and Mr. Walt Maine, MNS Division Chief. Other people who gave the author assistance included Dr. William Cook of WL/MNMW, who provided the initial one dimensional hydrocode and gave suggestions for 2D-FLASH during its development. Mr. Dan Brubaker (MNSA) gave much needed assistance with the debugging process of 2D-FLASH, and also helped with preparing outbriefings and the final report. Mr. Brian Peterson (MNSA) helped with too many little things to possibly mention, especially providing some additional insight into the EPIC hydrocode. Everyone else in MNSA also deserves thanks for assistance rendered and for suffering through the past two summers with this apprentice. Thank you all for your support, for this project could not have been done alone.

CHARACTERIZATION OF OPTICAL FILTERS BUILT USING SYNTHETIC IMAGERY

John W. Vest

**Niceville Senior High School
800 E. John C. Sims Parkway
Niceville, FL 32578**

**Final Report for:
High School Apprentice Program
Armstrong Laboratory**

**Sponsored by:
Air Force Office of Scientific Research
Bollin Air Force Base, DC**

and

Wright Laboratory

August 1994

CHARACTERIZATION OF OPTICAL FILTERS BUILT USING SYNTHETIC IMAGERY

John W. Vest
Niceville Senior High School

Abstract

This research project had two primary goals. The first of these goals was to become familiar with the Irma modeling software to prove that it could be used by someone with little or no engineering experience. The second goal was to make two test sequences of images that can be used to make optical filters. To accomplish the first goal, a "movie" was made using Irma and a F-16 facet model. These images were animated at real time speed and transferred to video tape for viewing. Two sets of images were also created for the optical filter test sequences. T-62 and a F-16 facet models were used to make these images. All of these images were made around a 360 degree rotation at a 20 degree elevation. These images were also animated and transferred to video tape.

CHARACTERIZATION OF OPTICAL FILTERS BUILT USING SYNTHETIC IMAGERY

John W. Vest

Introduction

The current method of optical filter generation is both time consuming and costly. This method involves assembling scale models of the target objects. These models must be bought and then constructed by hand. Then, for each angle of elevation and rotation, a motorized camera must take a picture. When all is done, this amounts to over eleven thousand images. This process takes an extreme amount of time, even when assuming everything goes smoothly. Even more time is required if there are any technical problem with either the model or the camera.

A synthetic modeling program called Irma is capable of creating realistic simulations of infrared sensor images. If this program could be utilized to create images like those required for optical filter design, the filter making process could be greatly improved. The time involved in taking pictures of scale models would be drastically cut and the cost of fabricating scale models would be eliminated. The filters might even be more realistic since Irma can accurately reproduce infrared images that would be taken in real battlefield situations.

Methodology

The first part of this summer's project involved becoming familiar with the Irma modeling software. To accomplish this, a "movie" was to be made utilizing Irma and a F-16 facet model. The first step, of course, was to read the Irma 2.2-2 S User's Manual. The Irma 2.2 simulation consists of three main programs, many associated data files and numerous supplementary programs. The ENVIRO model calculates the radiometric characteristics of the backgrounds and targets necessary for the subsequent image's generation of the scene. The SSG (Scene and Sequence Generator) generates the passive infrared signature of the user specified scene as observed by a passive IR sensor. Numerous utility programs are provided for data format conversions and the analysis of output data. The Irma User Interface assists users in setting up input files, executing jobs, and examining the generated output.

To create images, Irma uses facet models. Facet models of a T-62 tank and a F-16 airplane were used for this project. Appendix A contains images of these facet models created by Irma. These images are 512x512 pixel resolution, which was used for the F-16 "movie." The 512x512 images provided make the facet models very clear and detailed and in some places the facets can actually be seen.

When entering the data for the creation of the images, there was little concern with backgrounds or weather conditions because the images for the optical filters would not use these factors. Therefore, the main point of interest was the Eyepoint and Motion files Irma uses. To create an image, Irma reads several files, usually text files that tell it to perform certain operations and provide the necessary information for the modeling. The Eyepoint and Motion files were the most important for this project since these were the files that would need to be manipulated in order to create the optical filter image sequences.

The Sensory Trajectory File, or Eyepoint File, specifies the sensor position and look direction desired by the Irma user. This file also determines the total number of frames to be rendered. There are several different formats that can be used to create an Eyepoint File. The format picked to make these images was

the LALFLU format. LALFLU stands for "Look At, Look From, Look Up." This format is used when the user wants to look at some specific point in the world. The "Look At" and "Look From" parts of this format are 3D world coordinates. "Look At" is the coordinate the sensor is looking at, and "Look From" is the sensors location. The "Look Up" part is a vector. Its projection onto the image plane specifies which direction is "up" in the viewing transformation.

A Motion File is used if the "gmotion" keyword is specified in the Model File. A Motion File is used for animating objects throughout a generated sequence of images. There must be a one to one correspondence between the motion specifications in a Motion File and the eyepoint specifications in an Eyepoint File. A motion specification has two parts, a rotation transformation and a translation. The rotation transformation consists of three angles defining roll, pitch, and yaw. There are as many different formats for this file as there are permutations of roll, pitch and yaw. For simplification, "yaw, pitch, and roll" was used. The translation is an XYZ coordinate defining the targets location in the 3D coordinate plane. The Motion File translation and the "Look At" part of the Eyepoint File must be the same.

Nine-hundred images were created for the F-16 "movie." Therefore, nine-hundred lines of data had to be created for both the Eyepoint and Motion Files. Sample Eyepoint and Motion Files from the actual "movie" can be found in Appendix B.

Once Irma created these nine-hundred images, they were converted to byte format using the Byte program included with Irma. A program was written for IDL, an image viewing program, that animated these images. Unfortunately, it could not animate them at real time speed. To solve this problem, all of the byte files were transferred to a Datacube that was capable of animating them in real time, 30 frames per second. The Datacube setup used was also able to record the animation to either VHS or U-Matic.

After the "movie" had been created and a better understanding of Irma had been developed, two test sequences of images for optical filter generation, one of a T-62 tank and one of a F-16 airplane, were to be

made. Again, for these images, a background was not needed. Only the Eyepoint and Motion Files needed to be manipulated. To conform with the optical filter image requirements, the images had to be in a 128x128 pixel resolution and at specific elevations and rotations. Images are required for all elevations between 20 degrees and 50 degrees inclusive and for a complete 360 degree rotation and each elevation. For these test sequences, images were only created at the 20 degree elevation. See Appendix C for illustrations describing the elevations and rotations for optical filter design.

Again, after the sequences of images were created by Irma, they were converted to byte format and animated on IDL. For viewing purposes, they were also transferred to the Datacube and animated at real time. The results were recorded on video tape.

Results and Conclusions

A F-16 "movie" and two image sequences capable of being made into optical filters were produced. Initial inspection indicates that these images will indeed be usable by optical filter design software to generate optical filters. Before the actual filters can be built, images will need to be made at the other elevations between 20 degrees and 50 degrees. These filters will then be compared to filters built using scale models, and the validity of the filters built using synthetic images will be assessed. Once these comparisons have been made, it will be determined whether or not this process will be useful for optical filter generation. At this point, though, it can be said that the actual image generation using Irma is indeed more cost efficient and less time consuming.

Bibliography

IRMA 2.2-2 S User's Manual, Nichols Research Corporation, May 21, 1993.

Acknowledgments

I sincerely wish to thank several people who assisted me in this project:

NRC: Leslie Love, Noel Oshea, and Karen McCarley.

Sverdrup/TEAS: Larry Neal, Steve Halprin.

WL/MN: Otto Martinez, Captain Eric Augustus, Darryl Huddleston, Captain James Grimm,

Emily Martinez.

HSAP: Don Harrison, Mike Deiler, Glenda Apel, Jennifer Bautista, Kyle Perry, and the rest of the 1994

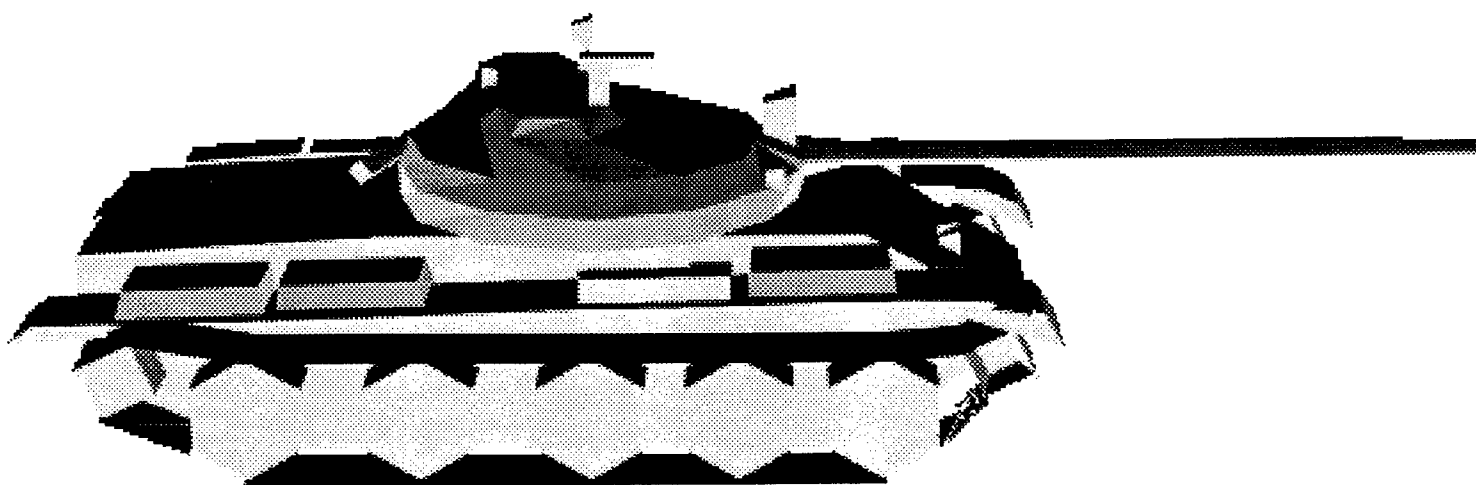
Apprentices

Appendix A

Facet Models

T-62: 512x512

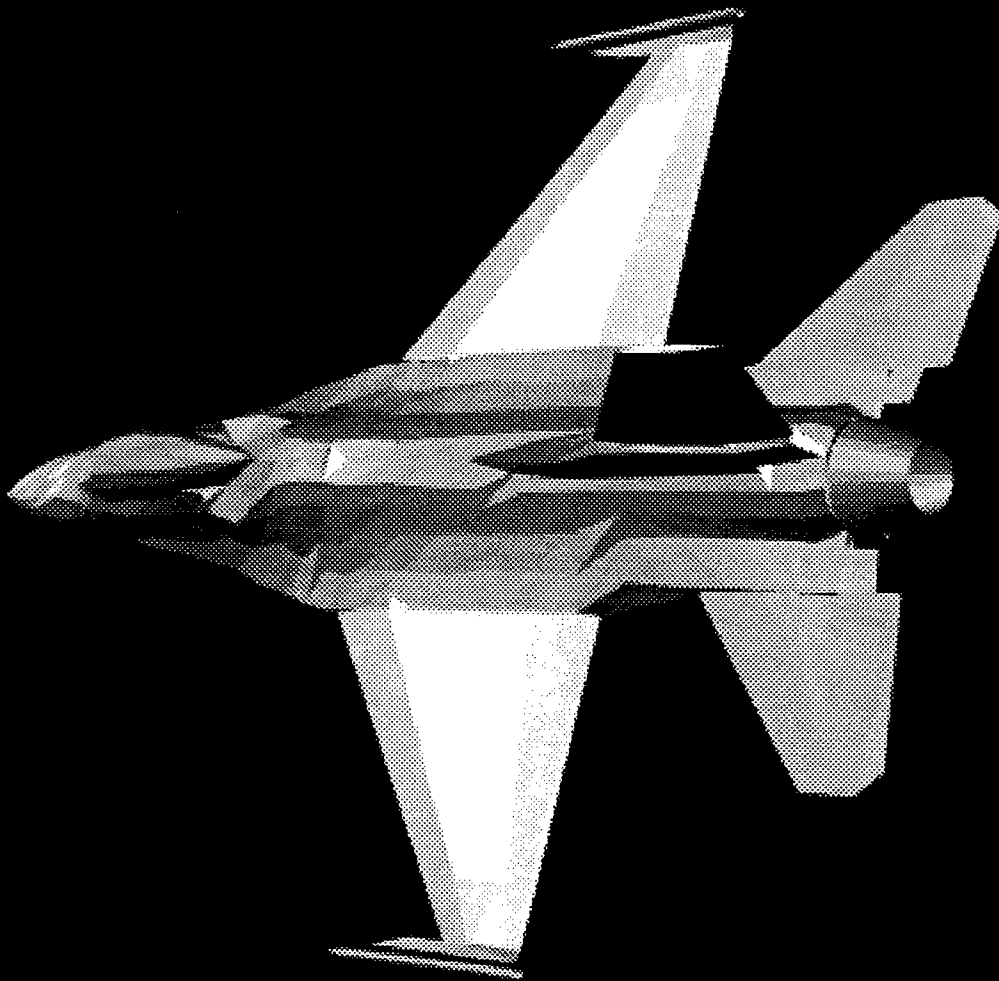
Gray range : 587.3 588.9



File: /home4/student/vest/irma/interface/ssg/output/images/ir/vest_plane-a.ir_508

F-16: 512x512

Gray range : 587.1 588.9



Appendix B

Sample Eyepoint and Motion Files

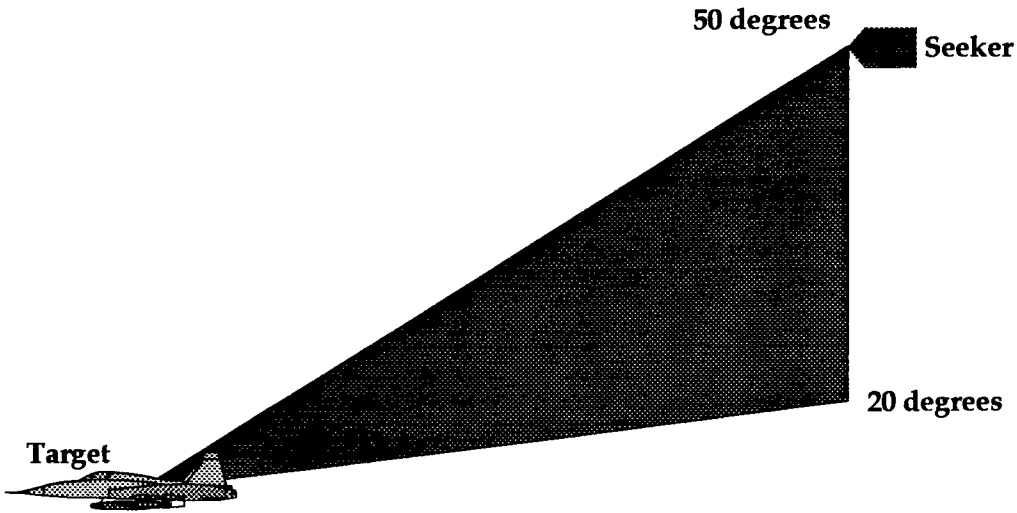
-1000.0	1087.35005	3420.0	0.0	1087.35005	5000.0	0.0	1.0	0.0
-1000.0	1087.35005	3405.0	0.0	1087.35005	5000.0	0.0	1.0	0.0
-1000.0	1087.35005	3390.0	0.0	1087.35005	5000.0	0.0	1.0	0.0
-1000.0	1087.35005	3375.0	0.0	1087.35005	5000.0	0.0	1.0	0.0
-1000.0	1087.35005	3360.0	0.0	1087.35005	5000.0	0.0	1.0	0.0
-1000.0	1087.35005	3330.0	0.0	1087.35005	5000.0	0.0	1.0	0.0
-1000.0	1087.35005	3315.0	0.0	1087.35005	5000.0	0.0	1.0	0.0
-1000.0	1087.35005	3300.0	0.0	1087.35005	5000.0	0.0	1.0	0.0
-1000.0	1087.35005	3285.0	0.0	1087.35005	5000.0	0.0	1.0	0.0
-1000.0	1087.35005	3270.0	0.0	1087.35005	5000.0	0.0	1.0	0.0
-1000.0	1087.35005	3255.0	0.0	1087.35005	5000.0	0.0	1.0	0.0
-1000.0	1087.35005	3240.0	0.0	1087.35005	5000.0	0.0	1.0	0.0
-1000.0	1087.35005	3225.0	0.0	1087.35005	5000.0	0.0	1.0	0.0
-1000.0	1087.35005	3210.0	0.0	1087.35005	5000.0	0.0	1.0	0.0
-1000.0	1087.35005	3195.0	0.0	1087.35005	5000.0	0.0	1.0	0.0
-1000.0	1087.35005	3180.0	0.0	1087.35005	5000.0	0.0	1.0	0.0
-1000.0	1087.35005	3165.0	0.0	1087.35005	5000.0	0.0	1.0	0.0
-1000.0	1087.35005	3150.0	0.0	1087.35005	5000.0	0.0	1.0	0.0
-1000.0	1087.35005	3135.0	0.0	1087.35005	5000.0	0.0	1.0	0.0
-1000.0	1087.35005	3120.0	0.0	1087.35005	5000.0	0.0	1.0	0.0
-1000.0	1087.35005	3105.0	0.0	1087.35005	5000.0	0.0	1.0	0.0
-1000.0	1087.35005	3090.0	0.0	1087.35005	5000.0	0.0	1.0	0.0
-1000.0	1087.35005	3075.0	0.0	1087.35005	5000.0	0.0	1.0	0.0
-1000.0	1087.35005	3060.0	0.0	1087.35005	5000.0	0.0	1.0	0.0
-1000.0	1087.35005	3045.0	0.0	1087.35005	5000.0	0.0	1.0	0.0
-1000.0	1087.35005	3030.0	0.0	1087.35005	5000.0	0.0	1.0	0.0
-1000.0	1087.35005	3015.0	0.0	1087.35005	5000.0	0.0	1.0	0.0
-1000.0	1087.35005	3000.0	0.0	1087.35005	5000.0	0.0	1.0	0.0
-969.7	1087.35005	2985.0	0.0	1087.35005	5000.0	0.0	1.0	0.0
-939.4	1087.35005	2970.0	0.0	1087.35005	5000.0	0.0	1.0	0.0
-909.1	1087.35005	2955.0	0.0	1087.35005	5000.0	0.0	1.0	0.0
-870.8	1087.35005	2940.0	0.0	1087.35005	5000.0	0.0	1.0	0.0
-848.5	1087.35005	2925.0	0.0	1087.35005	5000.0	0.0	1.0	0.0
-818.2	1087.35005	2910.0	0.0	1087.35005	5000.0	0.0	1.0	0.0
-787.9	1087.35005	2895.0	0.0	1087.35005	5000.0	0.0	1.0	0.0
-757.6	1087.35005	2880.0	0.0	1087.35005	5000.0	0.0	1.0	0.0
-727.3	1087.35005	2865.0	0.0	1087.35005	5000.0	0.0	1.0	0.0
-697.0	1087.35005	2850.0	0.0	1087.35005	5000.0	0.0	1.0	0.0
-666.7	1087.35005	2835.0	0.0	1087.35005	5000.0	0.0	1.0	0.0
-636.4	1087.35005	2820.0	0.0	1087.35005	5000.0	0.0	1.0	0.0
-606.1	1087.35005	2805.0	0.0	1087.35005	5000.0	0.0	1.0	0.0
-575.8	1087.35005	2790.0	0.0	1087.35005	5000.0	0.0	1.0	0.0
-545.5	1087.35005	2775.0	0.0	1087.35005	5000.0	0.0	1.0	0.0
-515.2	1087.35005	2760.0	0.0	1087.35005	5000.0	0.0	1.0	0.0
-484.9	1087.35005	2745.0	0.0	1087.35005	5000.0	0.0	1.0	0.0
-454.6	1087.35005	2760.0	0.0	1087.35005	5000.0	0.0	1.0	0.0
-424.3	1087.35005	2775.0	0.0	1087.35005	5000.0	0.0	1.0	0.0
-394.0	1087.35005	2790.0	0.0	1087.35005	5000.0	0.0	1.0	0.0
-363.7	1087.35005	2805.0	0.0	1087.35005	5000.0	0.0	1.0	0.0
-333.4	1087.35005	2820.0	0.0	1087.35005	5000.0	0.0	1.0	0.0
-303.1	1087.35005	2835.0	0.0	1087.35005	5000.0	0.0	1.0	0.0
-272.8	1087.35005	2850.0	0.0	1087.35005	5000.0	0.0	1.0	0.0
-242.5	1087.35005	2865.0	0.0	1087.35005	5000.0	0.0	1.0	0.0
-212.2	1087.35005	2880.0	0.0	1087.35005	5000.0	0.0	1.0	0.0
-181.9	1087.35005	2895.0	0.0	1087.35005	5000.0	0.0	1.0	0.0
-151.6	1087.35005	2910.0	0.0	1087.35005	5000.0	0.0	1.0	0.0
-121.3	1087.35005	2925.0	0.0	1087.35005	5000.0	0.0	1.0	0.0
-91	1087.35005	2940.0	0.0	1087.35005	5000.0	0.0	1.0	0.0
-60.7	1087.35005	2955.0	0.0	1087.35005	5000.0	0.0	1.0	0.0
-30.4	1087.35005	2970.0	0.0	1087.35005	5000.0	0.0	1.0	0.0
0.0	1087.35005	2985.0	0.0	1087.35005	5000.0	0.0	1.0	0.0

0 180 -90 -1000 1087.35005 3420
0 180 -108 -1000 1087.35005 3405
0 180 -126 -1000 1087.35005 3390
0 180 -144 -1000 1087.35005 3375
0 180 -162 -1000 1087.35005 3360
0 180 -180 -1000 1087.35005 3330
0 180 -198 -1000 1087.35005 3315
0 180 -216 -1000 1087.35005 3300
0 180 -234 -1000 1087.35005 3285
0 180 -252 -1000 1087.35005 3270
0 180 -270 -1000 1087.35005 3255
0 180 -288 -1000 1087.35005 3240
0 180 -306 -1000 1087.35005 3225
0 180 -324 -1000 1087.35005 3210
0 180 -342 -1000 1087.35005 3195
0 180 -360 -1000 1087.35005 3180
0 180 -18 -1000 1087.35005 3165
0 180 -36 -1000 1087.35005 3150
0 180 -54 -1000 1087.35005 3135
0 180 -72 -1000 1087.35005 3120
0 180 -72 -1000 1087.35005 3105
0 180 -72 -1000 1087.35005 3090
0 180 -72 -1000 1087.35005 3075
0 180 -72 -1000 1087.35005 3060
0 180 -72 -1000 1087.35005 3045
0 180 -72 -1000 1087.35005 3030
0 180 -72 -1000 1087.35005 3015
0 180 -72 -1000 1087.35005 3000
0 185.5 -72 -969.7 1087.35005 2985
0 191 -72 -939.4 1087.35005 2970
0 196.5 -72 -909.1 1087.35005 2955
0 202 -72 -870.8 1087.35005 2940
0 207.5 -72 -848.5 1087.35005 2925
0 213 -72 -818.2 1087.35005 2910
0 218.5 -72 -787.9 1087.35005 2895
0 224 -72 -757.6 1087.35005 2880
0 229.5 -72 -727.3 1087.35005 2865
0 235 -72 -697 1087.35005 2850
0 240.5 -72 -666.7 1087.35005 2835
0 246 -72 -636.4 1087.35005 2820
0 251.5 -72 -606.1 1087.35005 2805
0 257 -72 -575.8 1087.35005 2790
0 262.5 -72 -545.5 1087.35005 2775
0 268 -72 -515.2 1087.35005 2760
0 273.5 -72 -484.9 1087.35005 2745
0 279 -72 -454.6 1087.35005 2760
0 284.5 -72 -424.3 1087.35005 2775
0 290 -72 -394 1087.35005 2790
0 295.5 -72 -363.7 1087.35005 2805
0 301 -72 -333.4 1087.35005 2820
0 306.5 -72 -303.1 1087.35005 2835
0 312 -72 -272.8 1087.35005 2850
0 317.5 -72 -242.5 1087.35005 2865
0 323 -72 -212.2 1087.35005 2880
0 328.5 -72 -181.9 1087.35005 2895
0 334 -72 -151.6 1087.35005 2910
0 339.5 -72 -121.3 1087.35005 2925
0 345 -72 -91 1087.35005 2940
0 350.5 -72 -60.7 1087.35005 2955
0 356 -72 -30.4 1087.35005 2970
0 360 -72 0 1087.35005 2985

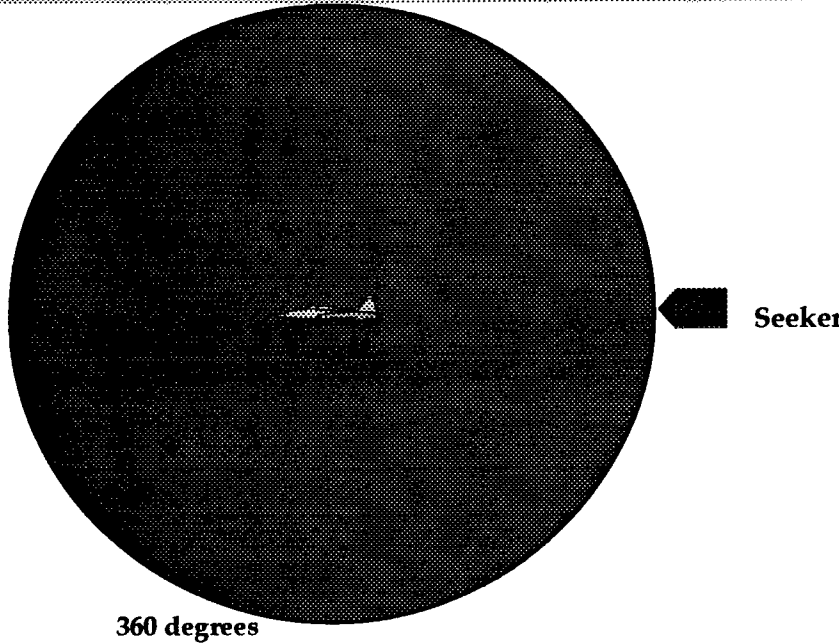
Appendix C

Optical Filter Elevations and Rotations

Elevation Range For Optical Filter Images



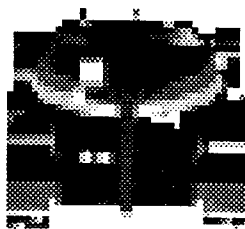
Rotation for Optical Filter Images



File: /home4/student/vest/irma/interface/ssg/output/images/byte/tank_four

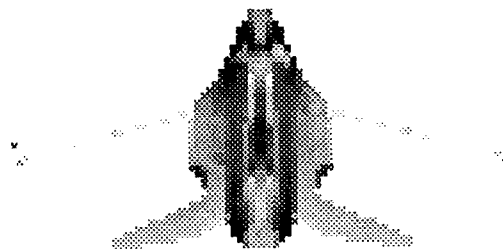
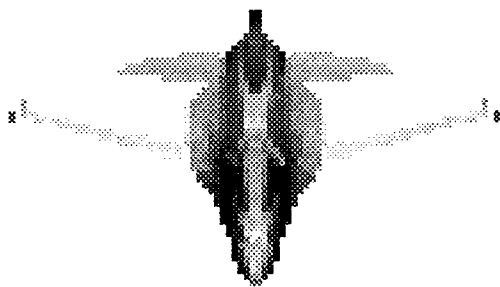
tank.001,tank.091,tank.181,tank.271

Gray range : 0. 231.0



File: /home4/student/vest/irma/interface/ssg/output/images/byte/plane_four
plane.001,plane.091,plane.181,plane.271

Gray range : 0. 231.0



Data Acquisition, Reduction, and Storage Using LabVIEW and the Tektronix RTD 720A
Digitizer

Jon R. Ward
High School Apprentice
Instrumentations Branch

Wright Laboratory Armament Directorate
WL/MNSI
Eglin Air Force Base, FL 32542-5434

Final Report For:
High School Apprenticeship Program
Wright Laboratory Armament Directorate

Sponsored By:
Air Force Office of Scientific Research
Bolling Air Force Base, D.C.

August 1994

Data Acquisition, Reduction, and Storage Using LabVIEW and the Tektronix RTD
720A Digitizer

Jon R. Ward
High School Apprentice
Instrumentations Branch
WL/MNSI

Abstract

A virtual instrument (VI) created using LabVIEW was created which automates data acquisition, data reduction, and data storage. Current data acquisition must be done by manually setting digitizers. Using the program created, the computer communicates with the digitizer via GPIB card and can set vertical mode, channel settings, trigger settings, and data acquisition settings. Then the virtual instrument acquires the data, which may be read and/or stored onto disk. This program was used in the evaluation of a prototype fiber optic air blast pressure sensor and in polyvinylidene fluoride stress sensor validation experiments.

Introduction

Data Acquisition and Storage is an important part of research and development testing. Much of the current software for data acquisition saves only raw and header files which are stored and aren't even usable until they are reduced using other software. This process is very time consuming and inefficient, especially for large files. Using LabVIEW, a graphical programming development application, a virtual instrument was created which not only acquires and stores data files in usable, already reduced, data, but may also be used to reduce and store (in usable form) large raw files that would normally take much more time to reduce. Also, using LabVIEW, I modified and debugged an existing dysfunctional VI used to communicate via GPIB card to a stepper motor rotary table to move in increments of degrees instead of steps.

Background

LabVIEW is a program development application different from most programming applications (such as C or BASIC) in respect to that it uses a graphical programming language, G, instead of a text-based language. LabVIEW creates programs (called virtual instruments, or VI's) in block diagram form. LabVIEW is a multi-purpose programming application with extensive libraries of functions and subroutines for any programming task. LabVIEW also has application specific libraries for data acquisition, GPIB instrument control, data analysis, data presentation, and data storage. LabVIEW programs are called virtual instruments because their appearance and operation imitate actual instruments. However, they are identical to functions from conventional program language programs.

The Tektronix RTD 720A digitizer is a state of the art high bandwidth, fast sample rate, long record length digitizer designed to accurately capture fast transient events. The input amplifiers provide accurate gain, excellent transient response, wide bandwidth, low reflections, and rapid overdrive recovery. A single analog signal path is maintained even at highest acquisition rates, for high performance in all vertical operating modes. The RTD 720A supports pre-trigger capture to nearly 100% of the user selected record length. Control of the RTD720 is either via GPIB card or from the optional front panel display unit. Its extensive GPIB command set provides complete programmability and control. The RTD 720A has sample rates as high as .5 nanosecond using one channel, 1 nanosecond using 1 channel, and 2 nanoseconds using four channels. The RTD 720A's slowest sample rate is 200 nanoseconds. For slower sample rates, the RTD 710A must be used.

Methodology

The first step in acquiring data from the RTD 720A was to be able to communicate with it. To begin, I was given several VI's from National Instruments that communicated via GPIB to the digitizer. Their VI's included most controls needed to acquire the data from the digitizer, but they all had too many bugs to work properly. The first VI I modified was one that set the vertical mode and channel settings. This VI only operated in channel one mode or dual mode and it didn't even include channel settings for channels three and four. After duplicating the front panel settings of channels one and two to create controls for channels three and four, the block diagram had to be modified to allow for a quad mode and channel three and four settings to be communicated to the digitizer via GPIB. The Select and Append String command in the block diagram had to be changed to an Index and Append String command because with three possible vertical settings a Boolean control couldn't be used to select the vertical mode. Therefore the string constants CH1, DUA, and QUA had to be put into an array which was indexed and sent either CH1, DUAL, or QUAD mode. Next, the sequence structure had to be changed to add two frames for channel three and channel four settings. The following diagrams of the two VI's front panels shows the difference between the original (TEK RTD 720 Vertical.vi) and the modified VI (TEK RTD 720 Vertijon.vi).

The next VI that I worked on was actually a sub-VI, or one used in another VI. It reads waveforms and stores the data in a binary file after acquisition. The following diagram is a copy of the finished product. It communicates via GPIB card to get information such as vertical mode, channel settings, record count, starting record, starting point, the Y multiplier, the Y zero, and the X increment by using the GPIB Read and Write subroutine VI's that came with LabVIEW. It takes all the raw points in the file and subtracts 128 from each point and multiplies it by the Y multiplier, and adds the Y zero to

TEK RTD 720 Vertical.vi

channel 1

GPIB address

range

offset

vertical mode dual channel 1

offset units % volts

coupling (AC:1) DC AC off

BW limiting (full:0) 100MHz 20 MHz full

channel 2

range

offset

offset units % volts

coupling (off:0) DC AC off

BW limiting (full:0) 100MHz 20 MHz full

TEK RTD 720 Vertijon.vi

channel 1

GIPIB address: 20

range: 0.00

offset: 0.00E+0

offset units: % / volts

coupling (AC:1): DC, AC, off

BW limiting (full:0): 100MHz, 20 MHz, full

channel 2

range: 0.00

offset: 0.00E+0

offset units: % / volts

coupling (AC:1): DC, AC, off

BW limiting (full:0): 100MHz, 20 MHz, full

channel 3

range: 0.00

offset: 0.00E+0

offset units: % / volts

coupling (AC:1): DC, AC, off

BW limiting (full:0): 100MHz, 20 MHz, full

channel 4

range: 0.00

offset: 0.00E+0

offset units: % / volts

coupling (AC:1): DC, AC, off

BW limiting (full:0): 100MHz, 20 MHz, full

QUAD -

DUAL -

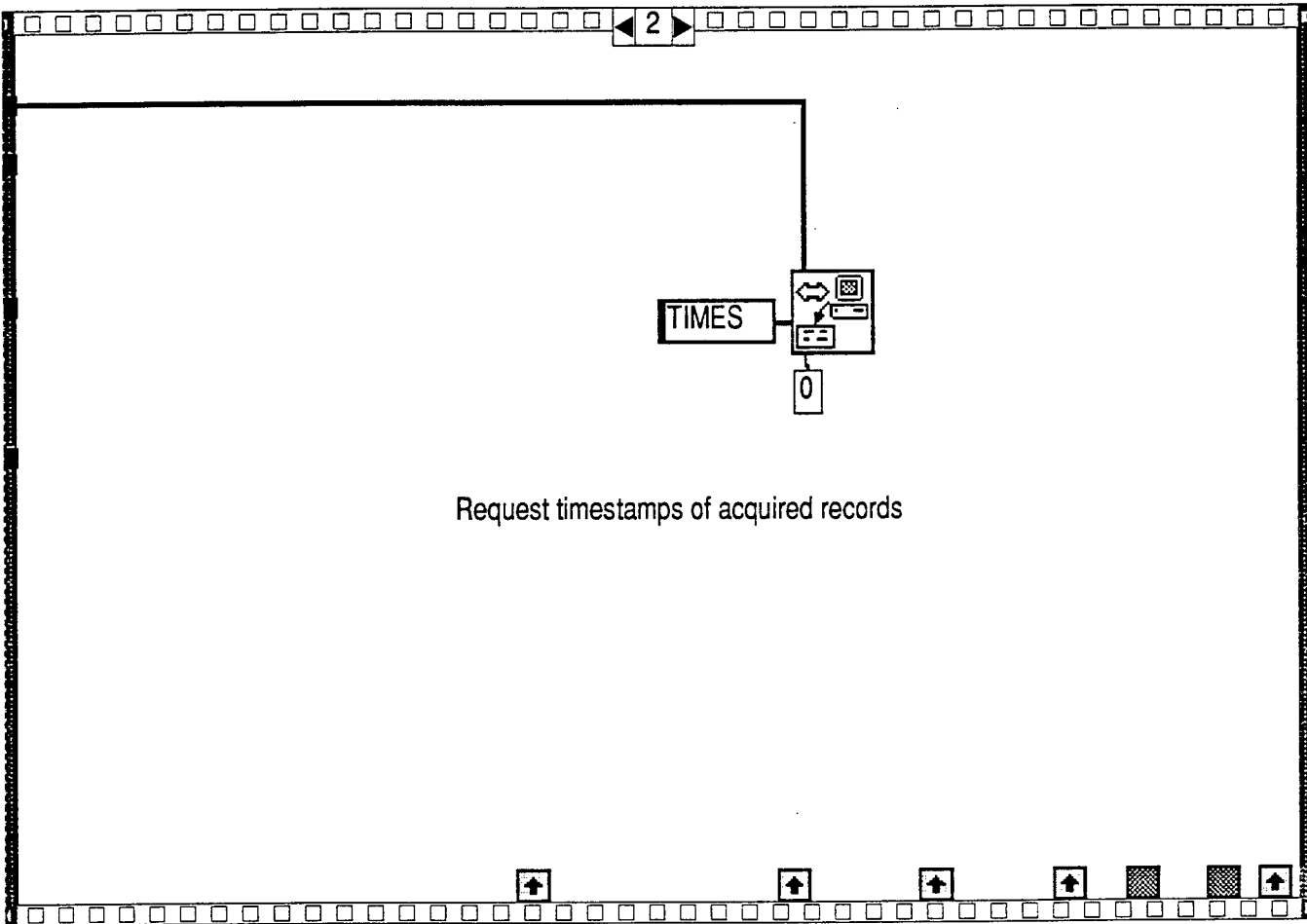
CH 1 -

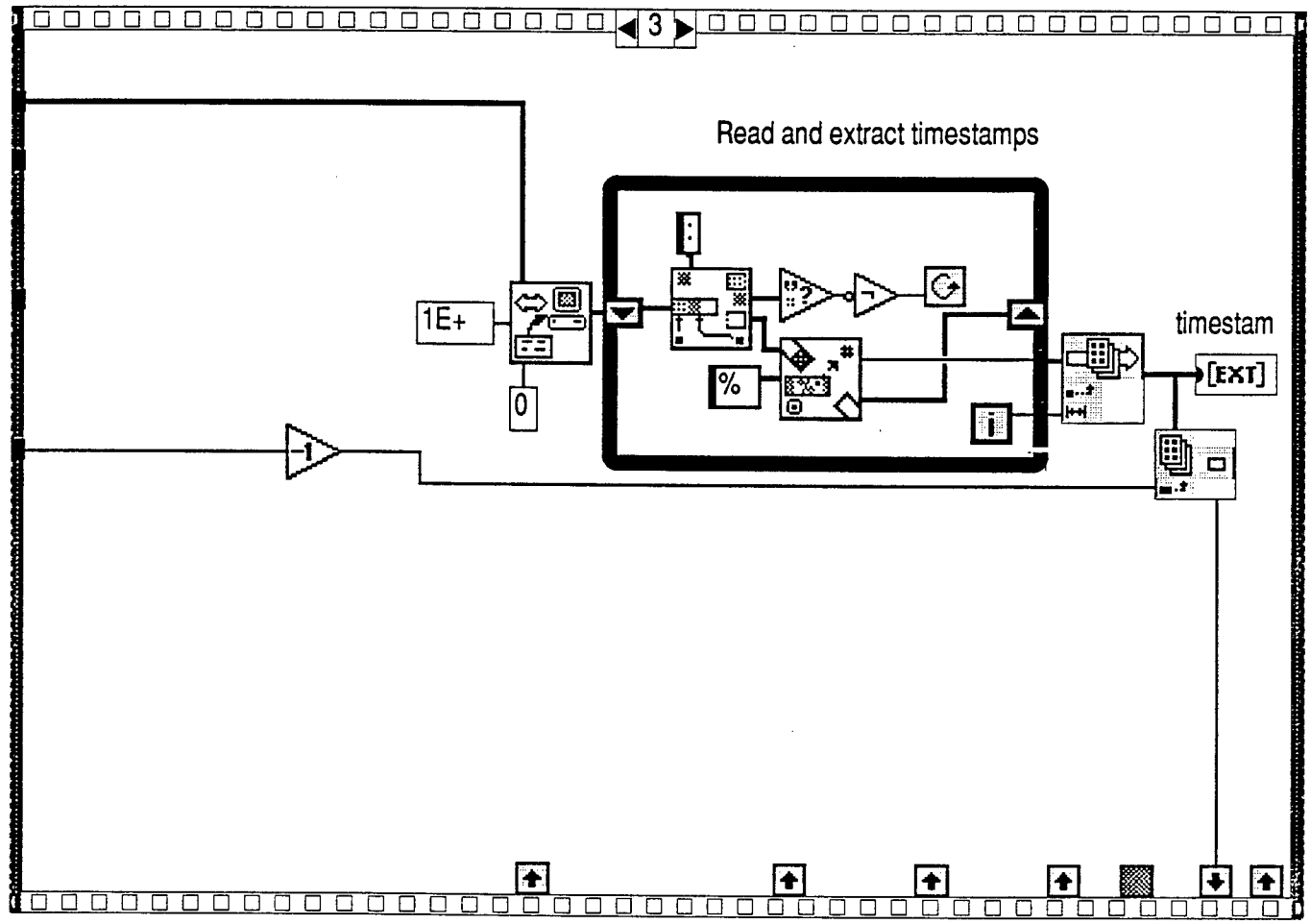
Vert. mode: CH 1

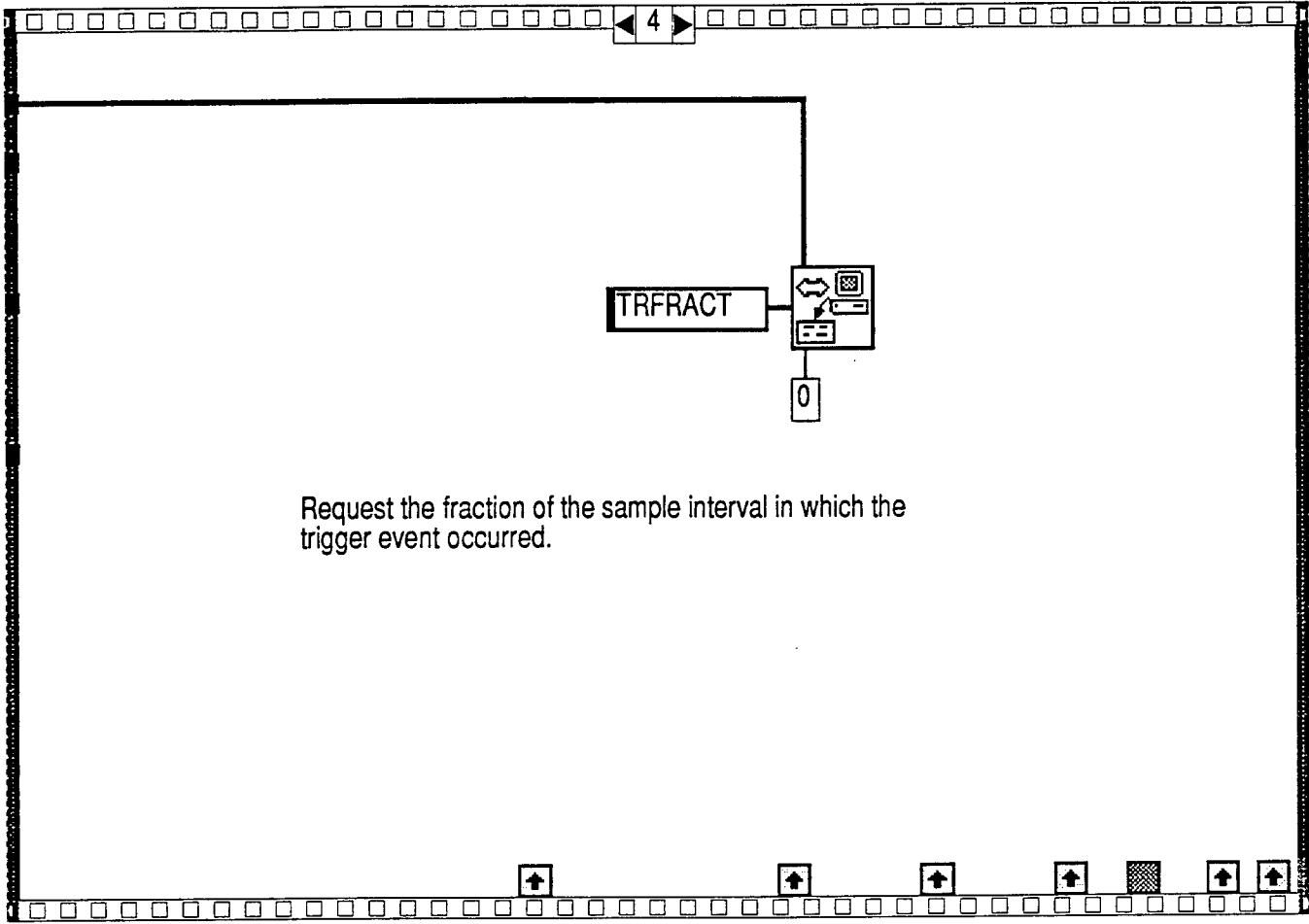
each point. This array plus the X increment (time scale) is put into a cluster array which is sent to a graph in the main VI on its front panel and saves those numbers in a file which can be retrieved later using another VI. A modified version of this VI saves the numbers to a spreadsheet file.

According to record length, the VI used to run the Read Waveform sub-VI can either graph and save one, two, or four channels at once. If the record length is greater than one megabyte then the graph and save program must do one channel at the time due to memory requirements. At 520 kilobytes, data from two channels can be graphed and saved at once. At 262 kilobytes, all four channels' data may be graphed and saved.

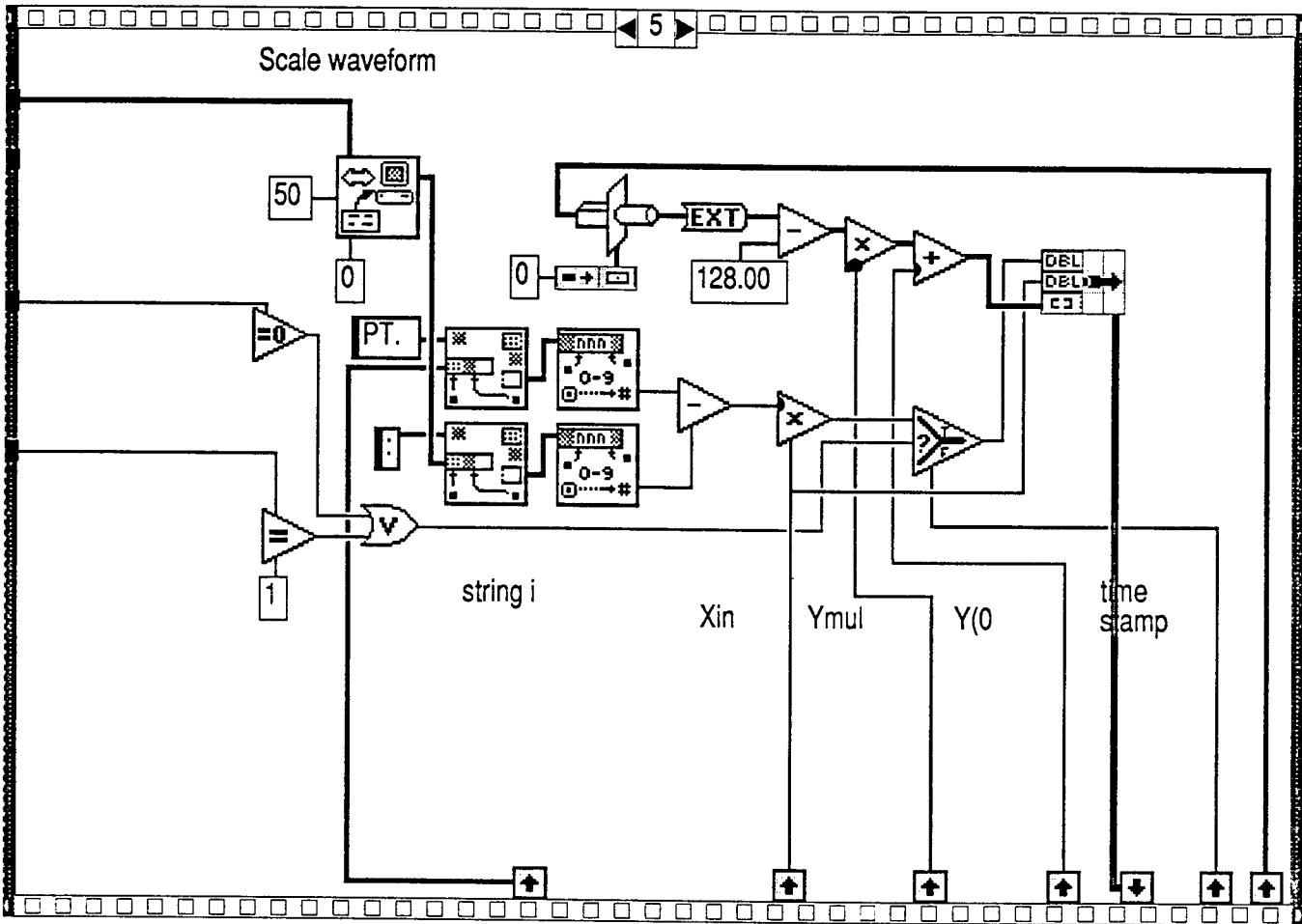
If data wasn't acquired using the VI's mentioned before, then it must be reduced. LabVIEW's commands for writing data reduction VI's are efficient and saves many man hours in the long run. To reduce much-needed test data from past polyvinylidene fluoride stress sensor testing I created a VI based on much of the same concept as the Read Waveform sub-VI. The Read Waveform sub-VI obtained the X increment, Y zero, Y multiplier, and other important information from the GPIB. All of this information needed for the raw data to be reduced is located in the header files of each raw file. So instead of using GPIB Read and GPIB Write VI's, read and write to and from file commands could be used. That in combination with the Match String Pattern command provides the same information as the GPIB Read and Write did in the Read Waveform sub-VI. The reduced data then can be graphed and/or saved to a file for later retrieval. In LabVIEW's analysis package a command to run a Fast Fourier Transform (FFT) on the data is included. It is wired in the block diagram in this VI and, if desired an FFT of the reduced data may be run.

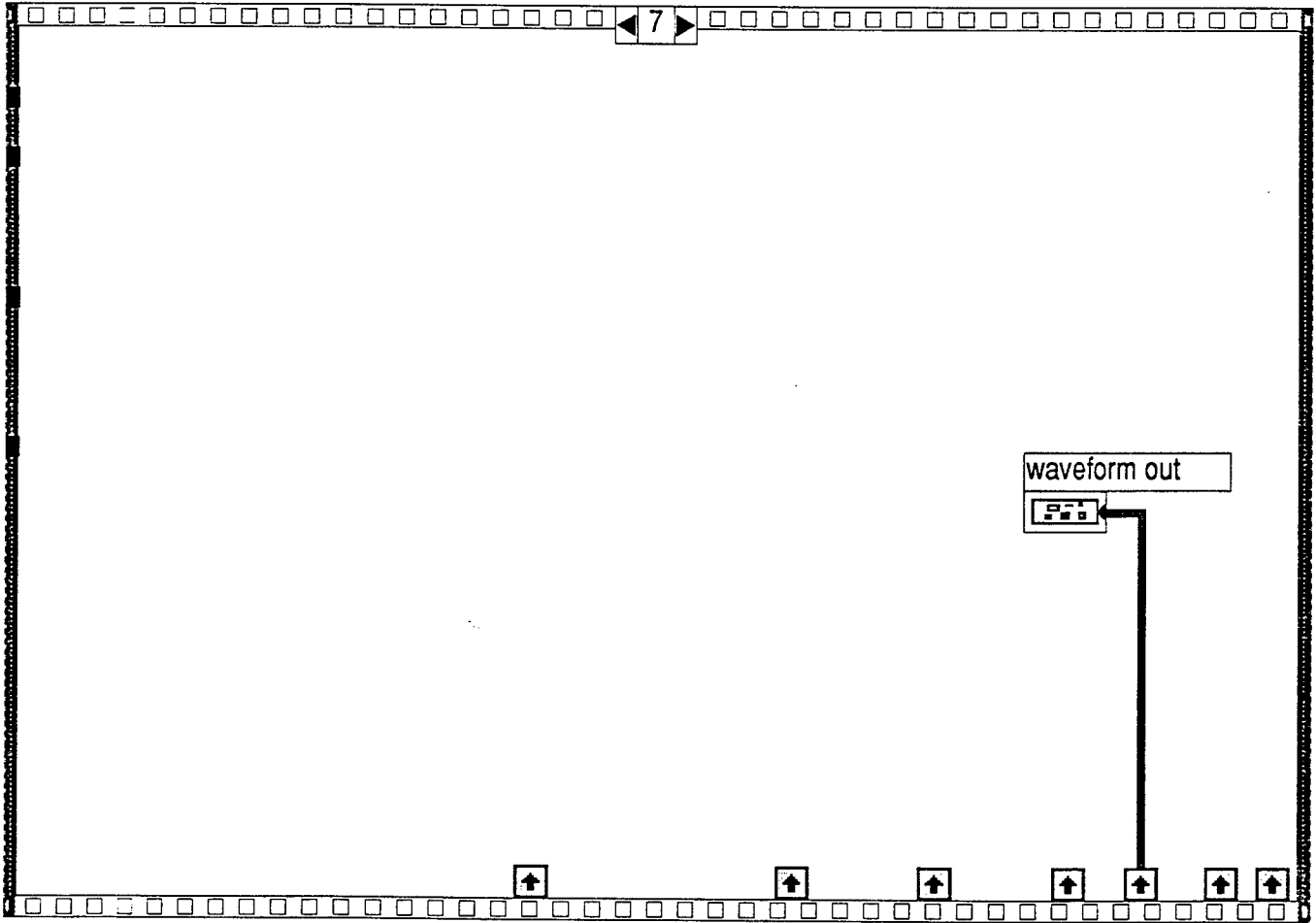
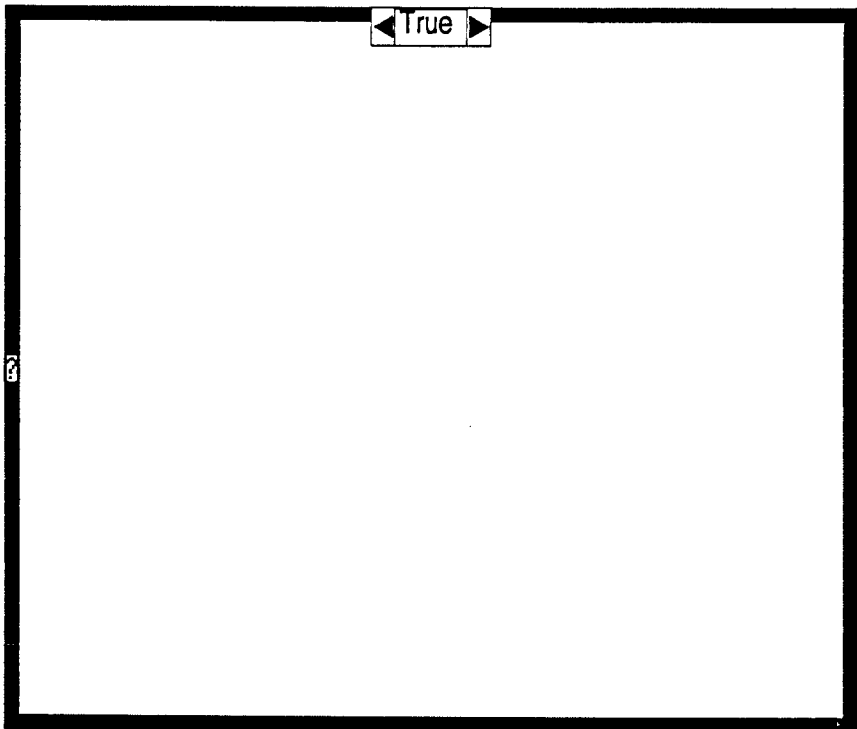






Request the fraction of the sample interval in which the trigger event occurred.





Acknowledgements

I would like to thank the many people who have made this summer research program an enjoyable and enlightening experience. First, I would like to thank Mrs. Glenda Apel who seemingly could handle any problem that came up. I would like to thank Mr. Mike Deiler and Mr. Don Harrison for directing the program again. I would like to thank Mr. Mike Van Tassel, Mrs. Voncile Ashley, and Mr. Dave Onuffer for helping me with any technical problems my equipment would often give me. I thank Mr. Joseph Gordon for being my mentor this year. I would especially like to thank Mr. David Watts who guided me this year in completing several difficult tasks this year that when I began thought were nearly impossible. And last, I would like to thank all the other H.S.A.P.'s for being there when the computer screen annoyed me to much to look at.

COMPUTER RESOURCE TEAM

Jeffrey D. Warren

Fairborn High School
900 E. Dayton-Yellow Springs Rd.
Fairborn, Ohio 45324

Final Report for:
High School Apprentice Program
Wright Laboratory

Sponsored by:
Air Force Office of Scientific Research
Bolling Air Force Base, DC

and

Wright Laboratory

August 1994

COMPUTER RESOURCE TEAM

Jeffrey D. Warren
Fairborn High School

Abstract

The Computer Resource Team at building 450, Wright-Patterson Air Force Base, Ohio maintains the computational environment for the scientists and engineers who work in the Aeromechanics Division (FIM) of the Flight Dynamics Directorate. The team also obtains the computers and associated resources necessary for the fulfillment of the Division's missions.

COMPUTER RESOURCE TEAM

Jeffrey D. Warren

Introduction

The computer resource team plays an important role in all of the work performed by the Aeromechanics Division of the Flight Dynamics Directorate. The team must maintain and improve upon the Local Area Network (LAN) and all of the computer resources associated with that network. This includes PCs, SGI workstations, Sun workstations, IBM workstations, MicroVax systems, and a Prime system.

Discussion of Problem

The computer resource team consists of four individuals who maintain a large number of PCs, workstations, and network servers. They administer and maintain the computer systems and improve upon them when the need arises. They also must educate the users on the correct way to operate each system and correct any mistakes made by these users.

Methodology

In order to make completion of their task possible, each individual specializes in particular areas of the overall task. The network manager specializes in the administration and maintenance of the LAN. The PC manager specializes in PC hardware installation and maintenance and PC software. The maintenance of backup

tapes for the Prime and many of the workstations is one of the responsibilities of the inventory manager. The inventory manager is also in charge of the record keeping for all of the computational resources possessed by the Aeromechanical Division of the Flight Dynamics Directorate. The team leader is in charge of the continued operation of the Prime system. The team leader is also in charge of the procurement of new computer supplies and parts to repair existing systems, the functioning of the MicroVax and SGI systems, and administrating the computer resource team.

The everyday jobs are the most important ones performed by the team members. For the network manager this involves periodic checks to make certain that the network is functioning as it should. When the network does become inoperable, the network manager must find what is wrong and fix it. This must be done in minimum time to minimize the effect to the operations of the division. The network manager must also attempt to find the cause of the malfunction and, if possible, to prevent the same problem from occurring again.

The PC manager often has to solve user caused malfunctions in the personal computers. These can range anywhere from lost or misplaced files to a complete system failure. The later is not common, but does occur occasionally. The PC manager typically must deal with programs operating abnormally or hardware malfunctions of varying nature. A relatively common problem that the PC manager must deal with is a worn out battery. The battery must be replaced and the computer must be reconfigured to make the PC usable again. The PC manager must also move systems and exchange systems for the users.

The inventory manager makes periodic backups of the primary operating systems to prevent large losses of data. Maintaining the records of all the resources is also one of the manager's responsibilities. This involves the hardware and software used by each system and includes the location and users of these systems.

The team leader must deal with requests from the users for new computational supplies. The team leader also sees to the successful operation of the MicroVax and SGI systems. The team leader monitors the operation of the Prime operating system. The team leader maintains the supplies necessary for the everyday operation of the computer resource team. Furthermore, the team leader works with the other members of the team to ensure that the necessary tasks are completed.

The assigned areas of these team members often overlaps which creates the need for teamwork among them. Most of the tasks that are performed by members of the computer resource team involve all or most of the members at some point.

One such instance is the procurement of a personal computer. The team leader must obtain the money to make the purchase. The computer must then be configured for use by the PC manager. This manager must load the software and configure the hardware so the computer can operate on the LAN. The network manager must then make sure that network connectivity is available to the computer at its destination. The inventory manager must keep records of what hardware and software are being added, where the system will be placed, and who will be using it. All this is necessary to insure the introduction of a new system which is properly configured and will not upset the previously installed systems.

Even though the procurement of a new PC is not by any means an everyday event, the members of the computer resource team constantly work together. This teamwork is often in the form of theorizing together in an attempt to find a solution to a problem. This method allows the team members to use their different perspectives to find a solution to the problem that faces the computational environment.

Also necessary to the smooth operation of the computational resources is the upkeep of accurate records. These concern the location, types, associated hardware, and associated software of the computers used by the Aeromechanics Division. The records must be kept current to avoid various difficulties concerning the computational environment.

The most recent record of the tools used in the environment is the Contingency Report. One of the subjects that this report outlines is the types of problems that could affect the computational environment adversely and how each of these threats would be dealt with if it would occur. Guidelines for the solving of the everyday problems of the computational environment are also included in the Contingency Report. A third subject addressed by the report is the present operation of the in-building and out-of-building communications. The report also addresses possible improvements either in the planning stages or for use sometime in the future. This report also contains detailed descriptions of the hardware and software used by the division. In addition to this listing, there is also a copy of the configuration files for the Prime system. There are also listings of cabling, air conditioning, power supply, and network specifications. These listings are presented in case one of the possible catastrophes does occur and records of the destroyed

systems and their associated hardware and software are required for the rebuilding of the computational environment.

Conclusion

The Aeromechanical Division of the Flight Dynamics Directorate has a solid computational environment that is well maintained. Additions to the computer resources are being made and will allow for the further development of the division's work. This environment is supported by individuals who can respond to problems quickly and efficiently.

References

Warren, Jeffrey D., Contingency Report, Computer Resources Team, Wright-Patterson Air Force Base, Ohio, printed 1994

MOMENTS AND OTHER PC UTILITIES

Josh A. Weaver
High School Apprentice
Warheads Branch
WL/MNMW
Mentor: Mr. Mike Nixon

Wright Laboratory Armament Directorate
WL/MNMW
Eglin AFB, FL 32578-5434

Final Report for:
High School Apprenticeship Program
Wright Laboratory Armament Directorate

Sponsored by:
Air Force Office of Scientific Research
Bolling Air Force Base, Washington DC.

August 1994

MOMENTS AND OTHER PC UTILITIES

Josh A. Weaver
High School Apprentice
Warheads Branch
WL/MNMW
Mentor: Mr. Mike Nixon

Abstract

Over the course of my first summer working at Wright Labs, I completed three main projects under the mentorship of Mr. Mike Nixon. The first task that I was given dealt with the rewriting of a program by the name of MOMENTS, making it easier to use and more suited for today's computing capacity. The second project that I was assigned was the development of a computer program that displays a 3D graphical representation of an converted PATRAN neutral file using simple 2D graphics commands. The third and final project of the summer was developing a finite element mesher for the eventual testing of EPIC's evaluation of structural data.

MOMENTS AND OTHER PC UTILITIES

In the summer of 1982, a program was written as a computational utility for axisymmetric projectiles. This program, titled MOMENTS, gave the user the power to design a complex penetrator composed of numerous materials and calculate key information about the given penetrator, such as the transverse and polar moments of inertia, location of the center of gravity, and the overall mass of the projectile. Although the first use of the program was to supply additional input to the PENCO2D program, the MOMENTS program was found useful enough to merit reconstruction for easier use and enhanced compatibility with today's computers. To make MOMENTS better suited for today's computers, it was apparent that MOMENTS would have to be translated into a more modern language. Also, to increase the user friendliness of the program, it was decided to create a Graphical User Interface (GUI) to MOMENTS in the popular Windows programming language, Microsoft Visual Basic. This would combine the editing, viewing, and calculating stages of the original MOMENTS into one easy to use package in a computing environment designed for ease of use among novice users.

The task of revitalizing MOMENTS was divided into three steps. First, a copy of the original MOMENTS program code was obtained and translated into Lahey Fortran. Once this was completely debugged, it was translated into Microsoft Quick Basic, which is very similar to Visual Basic. Research was done on the proper correlation between specific function calls in Lahey Fortran and their match in QBasic. When this task was completed, the actual GUI was designed for MOMENTS and the QBasic code was copied directly into the Visual Basic program with only two slight modifications.

To test the new MOMENTS program, a projectile of known values was mapped into the MOMENTS editor. During the course of the data input, situations arose that

could be more easily solved with short generic utilities. Accordingly, a nose generation utility and a body generation utility were developed. Once the projectile was mapped in to MOMENTS, the program was run, and the results recorded. When compared to the results of EPIC and EPIC-Pro, MOMENTS generated the same results to an equal, or greater level of accuracy.

In the world of Computational Mechanics, almost all of the most effective tools for projectile development are designed to run on the SGIs or other workstations. This presents a problem when all of the computers are in use, or the developers want to continue work at home. To help alleviate this problem, a program was developed that would display, on an IBM-PC or clone, a 3D graphical representation of a converted PATRAN neutral file using simple 2D graphic commands that are found on all computers.

The development of this program, called PC-Plot, was divided into five steps. At first, a Fortran program was written to read the converted PATRAN data file into arrays and to plot the individual points on the computer's screen. From there, the program was modified so that it would now display a 3D model of the image, showing how all of the nodes in each element connected. The next step was to display only the surfaces, defined as a set of three points on the exterior of the solid. The first attempt of this was marginally successful; the correct surface areas were displayed, but in the order of specification in the data file. Because of this, surfaces that should have been in the background and were at the end of the data file, were displayed in the foreground. To rectify this problem, the location of the surface vertices, as well as their greatest z-distance, were calculated and loaded into an array. This array was then sorted according to the z-distance so that the surface with the greatest z-distance (the one farthest in the background) was at the top of the array. When the surfaces were again displayed, this time in the order of the sorted array, the surfaces in the foreground were displayed over the images in the background, producing an accurate image. Finally, a menu system was

added so that the program would not have to be recompiled each time a different view was requested. Additionally, an axis system was created, modeling the one in PATRAN, to give the user the proper perspective when looking at the image.

From here, some utilities were also added to PC-Plot. The first, the zoom feature, allows the user to zoom in on any area of the image to whatever magnification is desired. The main feature of the program, image rotation, was added to give the user the ability to view the figure from any required perspective. Finally, the user was given the option to see the image either as a solid view of the surfaces, or a linear view of the connectivity of the overall image.

One of the most used programs in the Computational Mechanics section of Wright Labs is EPIC. It became an interesting question to see how the structure of the data file for this program influenced the computational time and the formation of the final result of the calculations. In order to test this, a program was designed to create a finite element mesh (the normal input into EPIC) of a rectangular parallelepiped, commonly referred to as a brick. What this program would do, is take a brick of the user's dimensions and divide it into a number of smaller bricks using the user's input of the number of sub-bricks allowed along each axis of the original brick.

The program was written in two steps in the F77 Fortran found on the SGI workstations. The first step of the program development was designing the user interface and the logic for finding the individual nodes that represented the vertices of the sub-bricks. After this was completed, the program, known as Bricker, was modified to show the connectivity that made up each sub-brick. To test this data, PC-Plot was rewritten to handle this different data format and used to display the Bricker's output. By using the numerous features of PC-Plot, it was possible to check all of Bricker's computations and

prove its effectiveness. The next step in Bricker's development is to divide each sub-brick into a group of twenty-four tetrahedrons to provide the proper input into EPIC.

Software Assisted Component Testing for the Antenna Wavefront Simulator

Gerad M. Welch

Beavercreek High School
2942 Dayton-Xenia Road
Beavercreek, OH 45434-6151

Final Report for:
High School Apprentice Program
Wright Laboratory

Sponsored by:
Air Force Office of Scientific Research
Bolling Air Force Base, DC
and
Wright Laboratory

August 1994

Software Assisted Component Testing for the Antenna Wavefront Simulator
Gerad M. Welch

Abstract

CNI Concept's Antenna WaveFront Simulator is a complex system with hundreds of components that must be tested to verify that they are in proper working condition. Since this testing is repetitive, several computer programs were written to automate the data collection process. By reading data from the testing device, the HP 8753C Network Analyzer, and storing the results in data files, a faster, more accurate means of component testing is afforded. Two dedicated programs were written to test phase shifters and voltage controlled attenuators, but as a last project for the High School Apprentice Program, a simple scripting language and command line interface were developed as a general purpose interface to the bus.

Software Assisted Component Testing for the Antenna Wavefront Simulator
Gerad M. Welch

Introduction

The Antenna WaveFront Simulator (AWFS) is a project of CNI Concepts Explorations Section of the Wright-Patterson Air Force Base (WPAFB) Avionics Directorate specializing in communications, navigation, and identification. Primarily, the AWFS scans the radio frequency (RF) band and determines the direction of the incoming signals. One immediate application of the AWFS is in the further development and testing of the Navstar Global Positioning System (GPS), also managed by the Air Force. GPS allows the user to determine their planetary position by using several satellites that broadcast the positioning signals. The encoded signals are picked up by a GPS receiver which computes the user's location. Research is being done at CNI Concepts to find an optimal method of filtering noise from the GPS signal using a multiple antenna configuration. The GPS was designed for military use, but has practical applications non-military areas. Some of the uses for GPS include accurate navigation in aircraft (including commercial airplanes), seacraft, and spacecraft; in extremely accurate surveying; and in the much touted navigation computers in automobiles. Improving the implementation of the GPS makes that technology more accessible. Because the GPS uses two specific radio frequencies for broadcasting positioning information, the AWFS is ideally suited for the task of GPS signal detection, enabling research for enhancements to the GPS.

The reception of the AWFS consists of 8 antennas which receive RF signals. As a signal approaches from a given direction, the AWFS detects the slight difference in timing on the reception of the incoming signal at each antenna, from which the AWFS determines the signal's direction. However, the line lengths from the antennas to the equipment may not be the same, and in such timing sensitive operations, the additional time the signal takes in transit can throw off the calculations. Phase shifters are used to equalize the timing by shifting the phase of the signal, thereby causing a delay to compensate for the

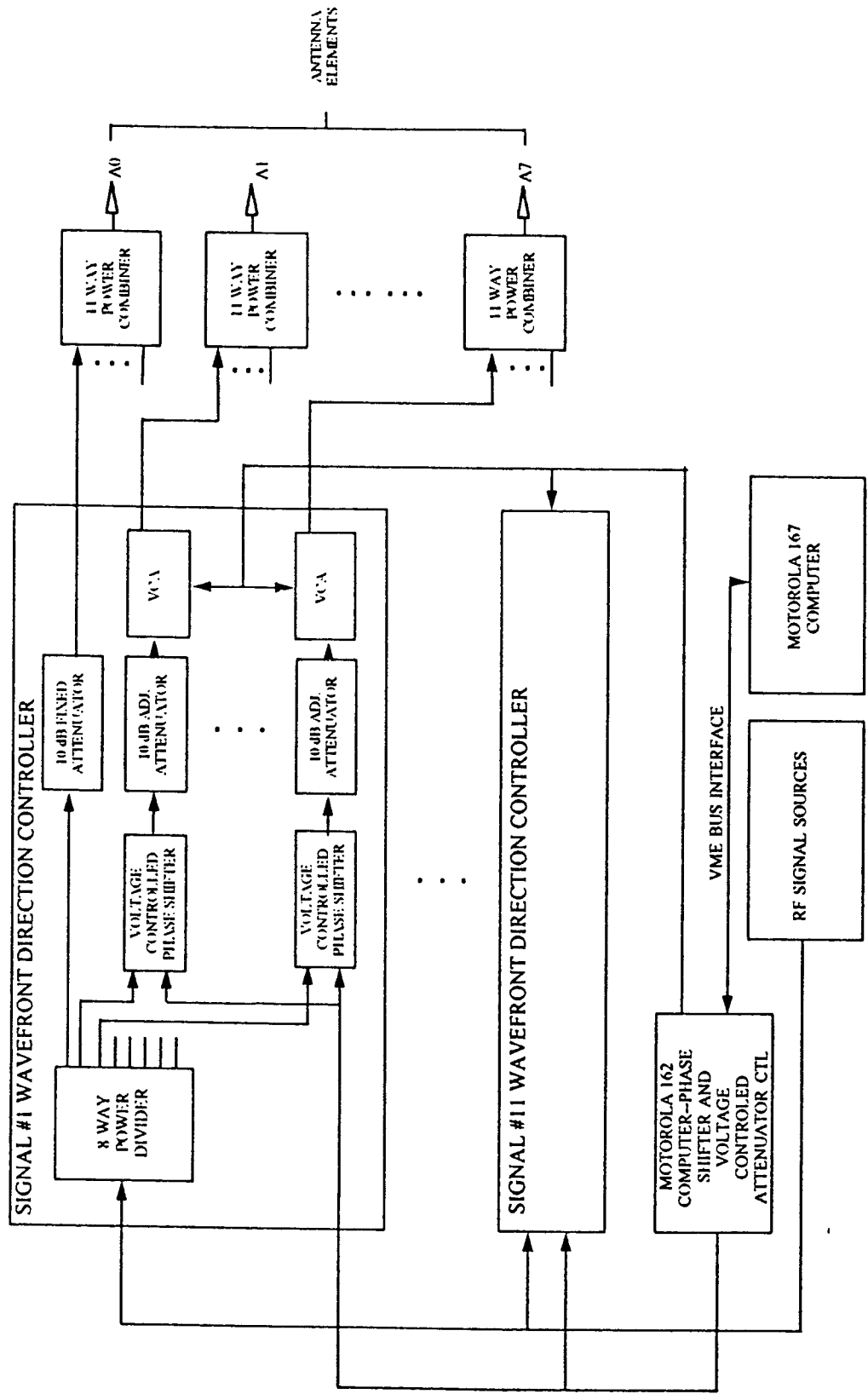
Software Assisted Component Testing for the Antenna Wavefront Simulator
Gerad M. Welch

uneven line length. Because of the fast speed at which the RF travels, the signal's shift need only be slight. Voltage controlled attenuators also modify the signal in the event that the received signal, perhaps being noise, needs to be scaled down. The attenuators normalize a signal by 'attenuating' (truncating) the signal in a uniform fashion, which can be controlled electrically, hence the name 'voltage controlled attenuator'. Quite a few of both of these components are present in the AWFS, all of which must be tested for defects to ensure accurate measurements. Since manual testing of the phase shifters and voltage controlled attenuators is fairly slow and tedious, the production of programs to complete the testing operation faster was necessary. See Figure 1 for a diagram of the AWFS.

The GPS operates by using a technique called time of arrival (TOA) ranging in which the difference in the specific time that the signal was sent out to the later time that it was received. The distance can be found from this by multiplying the TOA by the speed of the signal, called signal propagation speed. Using multiple locations to transmit provides a more accurate means of positioning. There are 21 GPS satellites in near-circular orbit which emit the necessary positioning signals. The GPS provides two basic categories of service: the Standard Positioning Service (SPS) and the Precise Positioning Service (PPS). The Link 1 (L1) frequency, which sends general positioning data for SPS, is 1575.42 MHz and the Link 2 (L2) frequency, which sends specific positioning data for PPS, is 1227.60 MHz. The signals consist of different 'frames' of data which are encoded in using a technique called Phase Shift Keying (PSK). PSK alters both the frequency and phase of the waveform. As an aside, the computer modem, which stands for modulation-demodulation, performs a similar transform on the bitstream before emitting the data on phone lines. Of course this description of the GPS is extremely simplified; there are many more aspects to the GPS system, such as the encoding of the data frame and error correction.

PHASE II

BLOCK DIAGRAM



Software Assisted Component Testing for the Antenna Wavefront Simulator
Gerad M. Welch

For the testing of the AWFS electronics, a Hewlett-Packard 8753C Network Analyzer was purchased, allowing much faster manual tests on the components as well as providing the capability to read the test data over an interface bus. The IEEE-488 interface bus, also known as the Hewlett-Packard Interface Bus (HPIB) and the General Purpose Interface Bus (GPIB), is the particular bus used to connect to the network analyzer. The attenuators' voltage is varied by a Tektronix PS 5010 Programmable Power Supply, which allows a program to alter the voltage across the IEEE-488. In the Communications System Evaluation Lab (CSEL), the network analyzer and the power supply, via the IEEE-488, are attached to the CSEL network, which is called CSEL2. The CSEL network server is a DEC VAX running VMS, so VAX system calls are necessary to communicate with the network analyzer. A menued application called UDOIT (User Defined Operation and Interactive Test) developed by WPAFB contractors was used previously to communicate with the IEEE-488, allowing device drivers to be written per device. However, in the interest of expedience, two dedicated programs were written for the network analyzer; one to test phase shifters and another to test voltage controlled attenuators. The idea for a command line interface to the bus, allowing for script files, was conceived later.

Methodology

Initially, research on the network analyzer was necessary to gain a working knowledge of how to send messages and get data from it. It was necessary to consult the current persons testing the phase shifters and voltage controlled attenuators to determine what features should be incorporated into the programs. In addition to those features, all programs were to be written in the C programming language. However, it was necessary to examine the UDOIT source code in the FORTRAN language to see how to communicate with the IEEE-488 using the VAX device routines. Although UDOIT was

Software Assisted Component Testing for the Antenna Wavefront Simulator
Gerad M. Welch

not used on a user level, the FORTRAN code would be used in messaging with the bus. A port of the bus interfacing routines to C would be fairly time consuming, and since VAX C allows calls to routines in other languages, the UDOIT routines would be used. There are three functions of the UDOIT code called: `udoit_488_init()`, `udoit_488_send_msg()`, and `udoit_488_rcv_msg()`. Using these functions, a basic shell program was written to send and receive messages to the network analyzer in order to test some of the HP commands. Once this preliminary activity was done, the actual coding could begin.

The first program to begin to be coded was for the voltage controlled attenuators, named VCACal for voltage controlled attenuator calibration. Algorithmically, VCACal is relatively simple (Figure 2), but due to the interfacing with VAX FORTRAN code, some additional coding had to be done. This is primarily with the way that VAX FORTRAN passes arguments to functions, which is, by default, by reference, requiring additional variables. The VMS operating system also uses a special structure to output strings called a *descriptor*, effectively nullifying portability because a lot of modifications to the code would be required.

```
Initialize bus;
Recall preset;
Set markers;
While the user wishes to continue {
    Prompt the user to replace the attenuator;
    Prompt the user for a filename to save the data in;
    Open output file;
    Initialize the voltage counter to 0.0;
    While the voltage is greater than or equal to -3.0 {
        Send the current negative voltage to the power supply;
        Read the marker data from the network analyzer;
        Output the marker data to the file;
        Reduce the current voltage by -0.25;
    }
    Close output file;
}
End;
```

Figure 2.

Software Assisted Component Testing for the Antenna Wavefront Simulator
Gerad M. Welch

Initialization of the program is accomplished by calling `udoit_488_init()`, recalling the network analyzer's first preset, and setting the markers in the network analyzer to the two GPS carrier frequencies, 1575.42 MHz and 1227.60 MHz. The HP mnemonic RECA1; recalls the preset, on this setup switching to dual screen mode, and the statements MARK11575.42MHZ; and MARK21227.60MHZ; set the marker positions. Note that the all HP network analyzer commands must be terminated by a semicolon. The user is then prompted to attach an attenuator and enter an output filename. For this program, it was necessary to use a floating point loop counter to maintain the current voltage for the power supply. Since the attenuators are tested using a negative voltage, the power supply command VNEG is sent by calling `udoit_488_send_msg()`. There are two channels on the dual screen display: the first is insertion loss in dB, and the second is phase shift in degrees. Subsequently, each marker is selected for each channel and the command OUTPMARK is issued. This command returns a string of three numbers, read by `udoit_488_recv_msg()`, the first of which is the value of the marker. The phase shift for either marker must be processed however; if the value is less than zero, it is left alone, otherwise it is subtracted from 360 degrees. Finally data is output to the destination file in tabular format, the voltage counter is decremented by 0.25 and the next iteration begins. In debugging the program, a problem was discovered regarding the network analyzer, indicated by a slight deviation in the values output from the program to that of a manually tested attenuator. The network analyzer had to have a little time after the voltage change on the power supply to sweep and get a proper reading; insertion of a two second delay relieved the problem.

The next task was to replicate the program except for operation on the phase shifters. For this, a copy of VCACal was merely modified in the appropriate areas to become PhaseCal. The primary difference in the program is the voltage: the phase shifters are tested with a positive voltage, from zero to twenty-seven volts in increments of one.

Software Assisted Component Testing for the Antenna Wavefront Simulator
Gerad M. Welch

This is only a minor change in the program's algorithm. Later, several revisions were made to both programs to improve their operation. An option to recalibrate the network analyzer was added to the startup, as well as the option to zero the opposite voltage of the power supply (i.e. in VCACal, the positive voltage would be zeroed; in PhaseCal, the negative voltage would be zeroed). Output of the data to the screen was added so that the tester can check the results without having to quit the program. The most recent addition was the generation of data files containing comma separated values in addition to the normal data files for easy importing of the data into a spreadsheet application, specifically *Microsoft Excel*. The user is asked at program startup if these files should be generated. The testers reported that the time in testing of the voltage controlled attenuators alone had been reduced from an estimated 40 hours to 4 hours.

As previously mentioned, the VCACal and PhaseCal programs are very much alike and are completely dedicated to the CSEL testing operation. For example, in order to change the bus address, the program must be altered and recompiled. This, as well as the repetitive nature of the VCACal and PhaseCal programs, spawned the idea of a script interface to the bus for simple operations. A simple scripting language was developed in this interest, such that the functionality of the VCACal and PhaseCal programs could be emulated. Built around this is the command line interface, which allows the user to run scripts and communicate with any bus device.

The implementation of the command line interface, called BusCLI, was a rather interesting problem. The script language itself is not as paramount as the concept of using script files to communicate with the bus, so not an extreme amount of development time was spent designing it. BusCLI was designed with the thought of expansion in mind, which is why it has the capability to have complex structures, such as block statements, added to it. The base program provides the capability to use files, loops with a constant iteration count, and call other scripts. The parser that processes the script before

Software Assisted Component Testing for the Antenna Wavefront Simulator
Gerard M. Welch

execution was the hardest to implement in the program. Without any real prior experience with lexical analysis and parsing, the task of writing the script parser was a bit of a challenge. The actual technique utilized was extremely simple in comparison with the parser of a compiler. Figure 3 illustrates the logic of the parser.

```
Read a line from the script
Scan through a table of commands for the string
If the structure is complex, call that command's build function
Otherwise, call the simple command build function
```

Figure 3.

Notably, the logic is very simple--the parse function had to be reentrant for the use with the *call* statement in the script. The command table is a constant array of structures that contain a numeric identifier, a string representing the command, and a pointer to a function that executes the instruction (Figure 4). When the line is read from the file, it is compared against the commands in the table until there are no more commands (which indicates an invalid command) or a match is found. The ordinal value of the command is returned from the function that compares the strings, which is used later to index the command table. Then the build responsibility is dispatched to either a build function for complex structures or a generic build function for simple structures. The command list is merely a singly linked list of command structures, which consist of the command identifier, a pointer to a string, a pointer to a structure (of the same type as this command structure), and a pointer to the next element. In the command identifier field, the ordinal value of the command is stored. The pointer to string points to a dynamically allocated array of characters that is the line read from the file with the command characters stripped off. Any structures are located in the pointer to structure field, but otherwise are NULL. The pointer to the next structure contains the address of the next element, if there is one.

Software Assisted Component Testing for the Antenna Wavefront Simulator
Gerad M. Welch

```
struct tagCmdTable; /* Necessary because of VAX C */
typedef struct tagCmdTable {
    CmdEnum ceCmd; /* Command ordinal */
    char *szCmd; /* Pointer to command's string */
    BYTE (*pfnCmd)(char *); /* Pointer to handler function */
} CmdEnum;

struct tagCmdStruct; /* Necessary because of VAX C */
typedef struct tagCmdStruct {
    CmdEnum ceCmd; /* The ordinal of the command */
    char *szData; /* ASCIIZ argument string */
    struct tagCmdStruct /* Again necessary because of VAX C */
        *pcsStruct, /* Pointer to a structure */
        *pcsNext; /* Pointer to the next element */
} CmdStruct;
```

Figure 4.

Note that since VAX C is not ANSI, the structure prototype is required. Also note that in the naming of the variables and fields that Hungarian Notation is used. Hungarian Notation, invented by Charles Simonyi, a former *Microsoft* employee, is a naming system which easily identifies the type of a variable and reduces the potential for type-based coding errors.

The command list can have 'sub-command lists' because of the any complex structures such as loops. All of these lists are prefixed with a dummy node in the parse function to make the code cleaner; the build functions allocate the current command's node on the previous node's pcsNext. In the case of the LoopN construct for constant iteration count loops, a node in the first list is identified as being a LoopN, and the pcsStruct field of that node points to the loop's command list. When the executor hits the loop, it calls a function to execute that list. The available commands are listed in Figure 5.

Valid command line instructions:

send	sends a string to the selected bus device
sendq	sends a string and prints the result of a read
init	reinitializes the bus
addr	selects a bus device
status	prints the program/bus status
show	shows the current bus address
cls	clears the screen

Software Assisted Component Testing for the Antenna Wavefront Simulator
Gerad M. Welch

<code>cls</code>	clears the screen
<code>parse</code>	tests the file by parsing it
<code>run</code>	runs the specified file
<code>exit</code>	exits from the program
<code>quit</code>	[same as quit]

Valid script file commands:

<code>!</code>	delineates a comment (beginning of line only)
<code>call</code>	calls another script file
<code>loop#</code>	a loop block (constant number of iterations)
<code>echos</code>	echos a string to the screen
<code>echof</code>	echos a string to the current file
<code>reads</code>	reads from the bus to the screen
<code>readf</code>	reads from the bus to the current file
<code>askfile</code>	queries the a filename and opens the file
<code>open</code>	opens the specified file
<code>close</code>	closes the current file
<code>pressret</code>	waits for the user to press return
<code>wait:</code>	waits N seconds

Invalid commands that are present but print an error message:

<code>raw:</code>	(sends raw binary data to the bus device)
<code>timeout:</code>	(sets the timeout value in seconds)

Figure 5.

The command line instructions are available both on the command line and in scripts (except for *exit* and *quit*). The script commands, however, will only be accepted in script files. Because the UDOIT routines are used, there are two commands in the original design that are present, but not implemented. *timeout* could not be implemented because UDOIT terminated when it times out and also uses a fixed timeout setting. *raw* was not implemented because of the uncertainty whether UDOIT can handle binary data.

After the command list is built, if the script is to be run, it is passed to the executor. The main executor function checks to see if there is a function associated with the command in the table; if there is, executes it; if there is a structure present, a structure execution function is called, and then advances to the next command. The structure execution function identifies the structure and calls the executor for the structure. Finally, the list can be freed by calling a function that deallocates the list.

Software Assisted Component Testing for the Antenna Wavefront Simulator
Gerad M. Welch

Conclusion

While dedicated programs are fine for their limited applications, a more general format is easier to write and maintain. Here, the BusCLI program was written to allow potential users to easily write scripts to interface to the IEEE-488 bus. In the future, the BusCLI program could be modified to suit the user's needs or perhaps get cleaned up codewise. A really elegant solution for the command identification would be to use a trie to search for the command or make a guess at a mistyped command. The parser logic could be cleaned up a bit by someone who is more experienced in parsing, and the command line interface could use a few more commands, such as *dir* to show existing script files, *more* to quickly display text files, and *edit* to edit scripts. Meanwhile, the current program will suffice for not too complex a task.... The BusCLI program is thus presented as the representation of an idea rather than an ideal implementation.

**Laser Speckle MTF Test Automation
and Characterization**

**Gabrielle L. White Wolf
High School Apprentice
Electro-Optics Branch**

**Wright Laboratory Armament Directorate
WL/MNSI
Eglin AFB, FL 32542-5434**

**Final Report for:
High School Apprenticeship Program
Wright Laboratory Armament Directorate**

**Sponsored by:
Air Force Office Scientific Research
Bolling Air Force Base, Washington DC.**

August 1994

Laser Speckle MTF Test Automation and Characterization

Gabrielle L. White Wolf
High School Apprentice
Electro-Optics Branch
WL/MNSI

Abstract

The characterization of a camera is necessary to determine the efficiency of the images to be captured; one of the various ways for characterization is with the use of laser speckle. The camera is set up to receive the image projected by a laser, with the use of an integrating sphere, directed through a double-slit aperture. Certain specifications determine the position of the camera and images are acquired at these specific distances. A Fourier Transform is taken of these images and the FFT graphs are used to create a MTF curve. The slope of the curve, as well as its amplitude, can be examined to determine the accuracy of the camera.

Because of the lengthy mathematical equations and the preciseness required to position the camera at specific distances, automation of this process is extremely beneficial for concise examinations of cameras. Automation is even more advantageous when numerous cameras are required to be characterized. With the use of a supplementary program on LabView and the DCI8000, an automated positioner, a procedure based on automation was developed that characterized a KODAK Megaplus camera, Model 1.4, and has the potential to further accurately characterize additional cameras.

Laser Speckle MTF Test Automation and Characterization

Gabrielle L White Wolf

INTRODUCTION

The accuracy of a camera is desired for professional and recreational uses; several techniques have been discovered to effectively characterize a camera and its abilities, such as imaging bar targets, sinusoidal targets or knife edges. Laser speckle has been determined to be another practical method of characterization. A simple optics system consisting of a Helium-Neon laser directed at a double slit aperture, with the use of an integrating sphere to evenly distribute the intensity, is one such method. The result of the laser-aperture system is recorded onto the CCD (charge-coupled device) of a KODAK Megaplus Camera, Model 1.4. Laser speckle insures that the resulting image consists of a random pattern controlled by the design of the aperture.

The images were taken at various distances determined by the specifications of the laser-aperture system and the individual camera. A fast Fourier transform is taken of these images and a modulation transfer function curve is produced to provide an informational curve that can be examined to determine the camera's ability. This lengthy procedure is automated with the use of a supplementary program on LabView and the use of a DCI8000.

BACKGROUND

The efficiency of a camera can be represented by a MTF curve, the x-axis being frequency representation and the y-axis being amplitude. However, once the frequency reaches a certain point, it doubles back on itself and mirrors previous data. This aliasing can be detrimental to characterization in that the aliased information can throw off accurate results. This point, called the Nyquist point, can be determined by dividing the number of pixels by two:

$$\frac{\text{No. of pixels}}{2} = \text{Nyquist frequency}$$

The Nyquist point corresponds to a certain point on the x-axis; this axis representing frequency will indicate where the point lies and the frequency of the point can be resolved as well. Frequency of the Nyquist point (f) is determined by taking the inverse of the product of the distance between slits in microns (d) and two. (The frequency can be further converted into cycles per millimeter with the multiplication of one thousand.)

$$f = \frac{1}{2 d}$$

This frequency of the Nyquist point also determines the frequency of each individual point on the x-axis; the Nyquist frequency (f) divided by the number of points on the x-axis, or the Nyquist point (N), will produce the frequency of each individual point on the x-axis:

$$\text{individual frequency} = \frac{f}{N}$$

Now that the frequency of each individual point on the x-axis is determined, it must be decided which frequencies to sample. The number of samples is determined by the operator of the system; the Nyquist point (N) divided by the number of samples (s) will give the intervals between the samples. This interval multiplied by 1, progressively incremented until it reaches the number of samples desired, will result in the points at which to sample. These points in turn can be multiplied by the frequency of each individual point determined in equation (3) which will display the frequencies at which to sample.

$$\frac{N}{s} = (\text{intervals } 1 \dots s)(\text{individual frequency })$$

Equation (4) produces "s" numbers of frequencies at which to sample; to convert these frequencies to actual distances (d), it must be multiplied by the wavelength in millimeters (w), inverted and multiplied by the spacing between slits in millimeters (p):

$$\frac{p}{(w)(d)} = d$$

The results given in millimeters represent the distance from the camera to the slits; once manually moved to the corresponding position, the image can be captured and the camera can be moved to the next distance.

A fast Fourier Transform is then performed on each of the samples; these FFT graphs typically contain two peaks---one at (0,1) and a second peak further on the x-axis. The maximum value of this second peak is discovered on each sample and the square of this point is plotted to create a modulated transfer function curve. Examining this MTF curve will provide an idea of the camera's efficiency.

APPARATUS

DCI8000 Multi Axis Motion Control The DCI8000 is a motion control positioner automated by a stepping motor. The automation machine can be controlled directly from the front panel or manually from the computer through a serial port. It moves in units of "steps", 10 000 steps corresponding to one inch, and has an accuracy of up to two microns.

LabVIEW for Windows LabVIEW is a graphical programming language that uses "VI's", or virtual instruments, as programs that imitate actual instruments. These VI's can be built on one another; sub-VI's are used in more complex programming. A VI or program consists of a "front panel" that contains the indicators, controls or graph, much like the front control panel of any instrument, as well as a block diagram---the block diagram uses visual graphing devices to program in almost a flow chart method.

KODAK Megaplug Model 1.4 A 1024 x 1024 pixel array is used on the KODAK Megaplug for characterization. The pixels have a 6.8 micron center-to-center pixel spacing.

Helium-Neon Laser The HeNe laser has a wavelength of 632.8 nanometers, which falls under the red portion of the color spectrum. 543-nm HeNes are also available, but a green beam is emitted instead of red.

Visilog4 Visilog4 is an image acquisition program that receives images and

contains procedures to alter the images; the program was used to capture and export the images to a different directory on the Sun for FFT's and image processing using IDL.

METHODOLOGY AND RESULTS

A previously developed program (DCI.vi) allowed the computer to directly "talk" to the DCI8000 by simple movement commands (moving a certain number of steps in either direction); this program was reduced to a sub-VI which allowed easier manipulation for further programming. A basic outline was set up including the above mentioned equations--stipulations, such as the number of pixels, wavelength, spacing between pixels, and number of samples, were to be indicated on the front panel by numeric controls. Eventually, a graph was created to allow the operator to view the movement of the camera as it approaches the aperture, as well as a display window that indicated and printed the response of the DCI to the given commands.

The final program consisted of a front panel with numeric controls for data specification, a graph to track the camera's movement, a response chart, indicator for the number of movements, a display for the instructions entering the DCI and an initialization boolean control .

The block diagram consisted of an initialization procedure ("true" frame) and a summation of the equations 1-5 ("false" frame). Once the initialization button was pressed and the program was run, the block diagram input a "true" value and ran the "true frame"; this frame consisted of initializing the port and then setting the DCI's movable platform with the camera to an extreme end (180 000 steps or 18 inches away from the laser-aperture system.) The specifications are then set on the front panel and the program is run once more; the "false frame" contains equations 1-5 and produces distances corresponding to that particular data. The distances were then converted into string format so that the computer could read the information, then placed behind the prefix "XM" allowing the DCI to comprehend the instructions (X representing the x-axis, M representing the command "move"). This command was plugged into the sub-VI (DCI.vi) that sent commands directly to the DCI. The automation program then ran itself equivalent to the number of samples desired.

The graphing program was present in the block diagram additionally; the

graph received the data and plotted it on the horizontal fill bar on the front diagram. Conditions to reset values to zero once the program was stopped were set in each of the subprograms present in the block diagram, such as the graphing function, the consecutive iterations and the while loop responsible for the command to the DCI; a case structure (true/false structure) was implemented in each of these subprograms so that once the iterations equaled one, any number stored in the shift register would automatically be multiplied by zero to reset the data. The program also informed the operator in the case of impossible commands---the case loop either directed the correct command to the DCI or it printed a pop-up dialog box on the screen that automatically terminated the program once the DCI could not respond to the movements.

In the case that the program required a distance small enough to run the camera into the laser-aperture system, the distance between the CCD and the front of the camera casing was taken into consideration. The program would stop running once the distance required by the program exceeded the distance from the CCD to the front of the camera.

Once the program was developed, the DCI8000 was set up along with the apparatus; on one end, the laser, integrating sphere, and double-slit aperture were positioned so that the slits were in line with the edge of the DCI. On the second platform, the camera was positioned and lined up along with the laser-aperture system.

Acquiring images was done with the assistance of Visilog4 and the automation program on LabVIEW; the camera's parameters were indicated on Visilog4 and specifications were indicated on the front panel of the Automation.vi on LabVIEW. Once initialized, the program was run and the images were exported over the network to the Sun workstation where an FFT was taken of each image and the MTF curve was determined with the use of IDL .

Major obstacles included reducing the physical manipulation of the DCI to direct access through the program. Resetting the machine was previously thought to be confined to controls on the actual front panel of the DCI, however a new method was discovered to reset the machine by computer and implemented into the program.

Certain frequencies with specified parameters also provide distances that become nearly impossible to achieve once the size of the mount of the base was taken into account; a slimmer mount was built and the size of the mounting plate on the DCI8000 was also reduced to allow the distance from the CCD to the slits

come within 1.75 inches.

The MTF curve taken of this particular camera was not as predicted; MTF curves tend to begin from (0,1) and slope continuously downwards. However, the MTF curve produced on the KODAK Megaplug camera (included diagram) does rise back up and then continue to fall. There are several possibilities for this occurrence: the two points in the valley of the curve could simply be bad data points, changing the gain midway through the process could have affected the curve or the camera could have been saturated. The cause of this fall in the curve needs to be determined and taken into consideration for future characterization.

The AUTO.vi on LabVIEW has proven to be effective in providing accurate results under certain specifications; however, due to lack of equipment and faulty programs, the AUTO.vi has not been used in directly characterizing cameras. Its output commands correspond to results from calculations done manually and once a frame-grabber is incorporated into the system, along with a perfect Visilog4 program, the Automation.vi will be used to fully automate the laser speckle system.

ADDITIONALS

During the course of the program, an automated setup for characterization of CCDs was created. However, experience with computers was a strong accomplishment as well--Visilog allowed acquiring images of laser speckle, LabVIEW's graphical programming languages was used to create automation software and modulation transfer function curves were analyzed with the use of computerized image analysis. Basic principles of optics were covered and later applied through the program.

ACKNOWLEDGEMENTS

Entering this specific area of the lab without a strong background in physics or optics made it difficult to quickly enter actual experimenting; Captain Pat Harrington provided a strong base in these fields, more than sufficient to complete this project--enough to carry into education as well. Lt. Scott Carroll also worked in the Optics Lab was extremely supportive and encouraging throughout the entire apprenticeship. Gratitude is also given to Mr. Mark Manzardo who was helpful in the project and was willing to introduce new ideas.

REFERENCES

1. Boreman, Glenn D. "MTF in Optical and Electro-Optical Systems."
2. Sensiper, Martin; Boreman, Glenn D.; Ducharme, Alfred D.; Snyder, Donald R.
"Use of Narrowband laser speckle for MTF characterization of CCDs." Proc.
SPIE V1683-14 (1992).